NOVEL APPROACHES TO IMPROVING DOMESTIC SOLAR PANEL ENERGY YIELDS IN SUB-SAHARA AFRICA

by

KANT ELIAB KANYARUSOKE

Student No. 209230681

Thesis submitted in fulfilment of the requirements for the degree

Doctor of Engineering: Mechanical Engineering

In the Faculty of Engineering

at the Cape Peninsula University of Technology

Supervisor: Prof J Gryzagoridis

Co-supervisor: Prof G Oliver

Bellville

February 2017

DECLARATION

I, Kant Eliab Kanyarusoke, declare that the contents of this thesis represent my own unaided work, and that the thesis has not previously been submitted for academic examination towards any qualification. Furthermore, it represents my own opinions and not necessarily those of the Cape Peninsula University of Technology.

Signed Date 08 Feb 2017

ABSTRACT

This thesis contains innovations that could help homesteads in sub-Sahara Africa (SSA) to 'harvest' more energy from flat solar energy collection surfaces. The thesis makes the assumption that universal resolution of energy poverty is a long term issue – and may not realistically be achieved using the traditional electrification route of: Fossil fuel/Hydro potential → electricity → transmission/distribution → paid for/free usage. Using a combination of literature search, Transient System Simulation (TRNSYS) modelling and experimental validation, the thesis notes the bi-hemispherical tropical location of most of the region and the abundant solar resource. It therefore advocates extensive use of the resource at home level for both electricity generation, and fluid heating/preheating purposes.

Using mathematical models, the thesis critically examines relationships among energy incidence, transformation and yield from a flat surface for both Photovoltaic (PV) and Solar Thermal (ST) usage. It suggests the first set of innovations for the region: the two azimuths installations. The second set uses TRNSYS and Operations Research (OR) modelling to optimise selection of PV equipment meeting a starter–home's energy loads throughout the region. Recommendations for both sets of innovations are presented in the form of colour coded maps. The third innovation in the thesis is the patented gravity driven, hydro-mechanical solar tracker, a novel solar tracking device in three different operation and control modes. In summary, one patent, 4 journal papers and 5 peer-reviewed international conference papers comprise the work.

ACKNOWLEDGEMENTS

A doctorate study starting as late in one's life as the mid - 50s can only be expected to have been supported by too many people to list here. Extended family; old friends; former schoolmates and workmates; past, current and near future students – all encouraged me along the way. However, the following deserve special mention. Prof Gryzagoridis – my mentor and supervisor. I was particularly touched by his patience and elderly advice whenever I seemed to be going off track. Prof Oliver, my co-supervisor gave constant advice on the institutional post graduate processes. Prof. Kaunda – my Head of Department – constantly encouraged me on and did his best - within the institutional policy limitations - to create an enabling environment for me to complete the studies in the time I did. Colleagues, Messrs. Cletus Magoda, Fareed Ismail, Selbourne Makhomo and Tiyamike Ngonda: these often looked towards my finishing as an indicator of simplifying their own journeys through similar studies. As such, whenever we interacted, they would fire me up to push harder. I cannot leave out my undergraduate studies lecturers in the late 1970s to early 80s at Makerere – especially, Eng. Dr. Paul Ssagala. He introduced me to the very exciting subject of Operations Research, which I have since used both in academic and other work. My best family friends Dr. and Mrs. Mwesigye and family, for all the morale boosting they offered. Lastly, I have to appreciate my children: the younger ones – Georinah and Euler who mostly sacrificed quality time with 'Dad' to avail him chance to earn a title of 'Dr.' Also, at times – during their holidays – they expressed eagerness to help along with day long experiments. The older ones: James and Lenz, helped fill part of the gap in my responsibilities to my old parents in Uganda during these 5 study years and they were never shy to tell their friends how proud they were of their father's continuing studies to try to "invent" something.

BIOGRAPHY

Mr Kanyarusoke started formal education at age 7 in 1965 as a gifted mathematics pupil: thanks to his now 96 year old father – who had been teaching him the 3 '***K***'s in the mother tongue – Rutooro: (***K****ubara* for Arithmetic, ***K****usoma* for Reading and ***K****uhandiika* for Writing) since the age of 4. At secondary school level in Uganda, he developed a keen interest in space science and philosophy. He started questioning the origin of the universe and of life. His teachers and fellow students nicknamed him 'Kant', after the 18^{th}-19^{th} century German philosopher, Immanuel Kant. That is how he became Kant Kanyarusoke or **KK**. At Uganda's premier University, Makerere, he studied Mechanical Engineering, graduating with a first class honours BSc. Eng. degree in 1982. He joined the staff development program and went to the University of Lagos, Nigeria as a UNESCO/ANSTI scholar. He obtained an MSc degree in Mechanical Engineering (Design and Production option) in 1985. He returned to Makerere and taught full time for 2 years. In 1987 he joined industry, first with British American Tobacco Company as a Processing Manager – and then later in 1995 with Unilever Plc. as head of the Technical function in Uganda to 2001. He then went into consultancy on setup of small to medium scale manufacturing enterprises in Uganda and Botswana. In Botswana, he re-joined academics and taught Machine Design at the University of Botswana. In 2008, he joined CPUT as a lecturer in Mechanical Engineering Design and Thermo-Fluids. He then studied and obtained a CPUT cum laude HDHET in 2009. Since August 2011, he has been involved in solar energy engineering R&D for energy-poor homes especially in sub-Sahara Africa. Apart from work in solar engineering, he is a reviewer for several international journals in Engineering Education. He is a member of the American Society of Heating, Refrigeration and Air-conditioning Engineers (ASHRAE) and of South African Society of Engineering Education (SASEE).

DEDICATION

This thesis is dedicated to all sub Saharan Africa peasants who toil every day, using manual labour (amidst plenty of solar resource) to try and add an extra day to their stay here on earth.

PREFACE

Purposeful solar energy utilisation by man is probably as old as s/he is. From the basic fact that s/he used it in senses of sight and warmth to usage in drying of gathered and/or farmed crops and fruits, early man knew the potent power of the sun. It is even no surprise that the sun was worshipped by some communities in later millennia. However, as we see in chapter 2 of this thesis, modern use of the sun's energy - only began to attract attention in 1905 when Albert Einstein published work on the photoelectric effect. In 1958, solar panels were deployed in space exploration vessels. They were very expensive then – at about US$ 100 a Watt. Today, the cost has dropped by a magnitude order in excess of 2. To the extent that even in under developed sub-Sahara Africa, individual rural homes far off from national grid supply lines are beginning to opt for domestic photo electrification.

But in all modern attempts to harness solar energy, the relative motion between the sun and the energy collection surface – whether in space or on earth - plays a major role in determining the efficacy of the harnessing. Consequently, lots of effort have been – and continue to be – made to orient the collection surfaces in such a way as to optimise the harnessing. The optimisation processes however vary depending on location, technical abilities, economics, sizes of surfaces, kind of application, etc. In short, the adopted processes depend on the objective functions consciously or subconsciously set by the users.

Chapters 2 to 5 present discussions on these efforts. Specifically, chapter 2 gives a general review of the theory underlying these efforts with special emphasis on applications in sub-Sahara Africa (SSA). Chapter 3 presents a paper published in the *Turkish journal of Electrical and Computer Engineering* on solar photovoltaic (PV) modelling for electrical energy generation. The confidence built from this modelling is used in a subsequent *Applied Energy* journal paper (chapter 4). It is in this chapter that focus begins to be put on domestic applications in tropical Africa. Addressed are the issues of fixed PV panel installation angles and start-up equipment selection for any place within SSA. Two major reasons underlie such treatment at this stage: One – most beginners in the region start with a fixed slope installation. Therefore any subsequent upgrade to a tracking unit would need to use energy yields, quality and costs from the installation as a basis for comparison. Two – the optimal installation angles of fixed slope units provide the optimal 'fixed' angles for the type of solar tracking developed in the later part of the thesis: the single inclined axis tracking. Concluding the discussions on optimisation efforts in tropical Africa and setting the scene for the next group of chapters is chapter 5. This presents a paper published in the *Journal of Energy for Southern Africa* on whether or not, existing tracking technologies are appropriate for tropical Africa.

While some uniquely own suggestions and contributions on fixed slope panel installations in tropical Africa are made in chapter 4, chapters 6 and 7 develop the conclusions of chapter 5 to present a contribution on solar tracking for domestic applications in the region. An intermittently run bladder – Hooke coupling mechanism operated by weights balanced between gravity and low water pressure forces is designed, constructed and tested. Chapter 6 presents an *ASHRAE Transactions* publication on tracking solar siphons. Chapter 7 first describes the design process for the solar tracker and then gives a comparative performance modelling and experimentation between the designed tracker and an 'optimally' inclined fixed slope PV panel at the university campus. Finally in chapter 8, the thesis concludes with a summary of main contributions, cost considerations and required future developments of the work.

GLOSSARY

A	Area of a surface (m^2)
a	A temperature and manufacturing dependent voltage parameter of a PV panel (V)
ASHRAE	American Society of Heating Refrigeration and Air conditioning Engineers – an association of professionals, registered in the US who are involved in practicing, educating others and advancing the art and science of heating, refrigeration and air conditioning.
AfDB	Africa Development Bank – a financial institution based in Abidjan, whose mission is to promote economic and social development, mainly in member African states.
CPC	Compound Parabolic Collector – A system of two or more paraboloid-curved solar collectors assembled to simultaneously focus the radiation at one target receiver.
CTC	Cylindrical Trough Collector – A solar radiation harnessing unit whose reflected energy receiving surface is a pipe running parallel to the axis of a cylinder of which the primary collection concave surface is part.
CSP	Concentrated Solar Power – A term used to describe systems in which solar radiation is collected on a smaller area than that of the aperture normal to the incoming beam.
DNI	Direct Normal Irradiance - The beam radiation flux intensity on a plane normal to incoming rays at a given place (W/m^2)
DOD	Depth of Discharge – The percentage loss of charge of a battery from its full state.
E	Energy (J; kJ; Wh or kWh) – The ability to cause a change in a physical or a thermodynamic state of matter
E_{annual}	The energy produced or consumed in a period of 1 year
f_g	Minimum Manufacturer-guaranteed %age of rated output of a PV panel in a period of 20 years
G	The intensity of radiation flux at a place in W/m^2
G_b	The beam or direct radiation flux intensity on a plane at a given place (W/m^2)
G_{bh}	The beam radiation flux intensity on a horizontal plane at a given place (W/m^2)
G_h	The total radiation flux intensity on a horizontal plane at a given place (W/m^2)
G_d	The diffuse radiation flux intensity on any plane at a given place (W/m^2)
H	The total solar energy per unit area on a horizontal surface in one day (kWh/m^2)
I	Electric current measured in Amperes or Amps or simply A. (chapters 3, 4 and 8) Hourly solar radiation energy on a unit area of surface (kWh/m^2) (chapter 2)
I_{cc}	The charge controller capacity – which is the peak current the controller will deliver to the battery it is charging.
I_D	The diode current – which is the total instantaneous reverse current being generated at a PV module's cell junctions with or without solar radiation

I_L	The light current – which is the total instantaneous forward current being generated at a PV module's cell junctions as a result of activation by solar radiation.
I_{mp}	The net output current of a PV panel when it is producing maximum power
i	Incidence angle – the angle between a ray from the sun and a normal to a surface being struck by the ray.
IEA	International Energy Agency – An "organisation which works to ensure reliable, affordable and clean energy for 29 member countries and beyond" (www.iea.org/aboutus).
L	• Latitude coordinate of a place in °. This is the angle between the earth's equatorial plane and the vertical plane at the place. With the equatorial plane as datum, if the place is 'below' the latitude is negative. • Life of a component or system in years (Ch. 8)
LDR	Light Dependent Resistor – An active electric element whose resistance varies with intensity of light reaching it. (for many, resistance decreases with radiation intensity in W/m^2)
LFR	Linear Fresnal Reflectors – a close assembly of long thin flat mirrors so assembled and mounted as to focus incoming radiation onto a smaller absorber surface some distance away.
MPPT	Maximum Power Point Tracking – a method of internally adjusting loads in a charge controller so that the PV panel is continuously loaded at the point where it generates maximum power for its setting and radiation reaching its surface.
R	Resistance of an electric circuit element (Ohms or Ω)
R_1	The equivalent series connected resistance of a PV panel's simplified circuit
R_2	The equivalent internal shunt connected resistance of a PV panel's simplified circuit
R_{track}	The ratio of energy yield of a solar tracking panel to that when the same panel is not tracking but optimally tilted and oriented.
R&D	Research and Development – Activities involving a search for new knowledge followed by use of that knowledge to solve a specific problem.
S	The number of sunshine hours on a given day. (hrs).
SHS	Solar Home System – a set of energy usage components and devices assembled together for the purpose of harnessing solar energy at the home level.
Solar collector	A solar energy harvest device in which the primary output is thermal energy.
Solar panel	A solar energy harvest device in which the primary output is an electric current.

ST	Solar Thermal – Describes applications of solar energy which primarily target the heating effect of solar radiation usually using flat collection surfaces.
STH	Solar Thermal Hydraulics – Describes applications of solar energy which primarily target the heating and evaporative effect of solar radiation followed by a condensation for purposes of generating or raising a hydraulic head. (This term is not common in literature. It is introduced in this thesis – Ch. 7).
SMA	Shape Memory Alloy – a material which when in a deformed condition is able to regain its un-deformed shape when a particular stimulating variable (e.g. temperature, magnetic strength) reaches a certain value.
T	Temperature – a measure indicative of average linear kinetic energy of molecules/atoms in a substance. (K or °C) (most chapters)
Tracking	The act of making a solar collection surface change its orientation with apparent movement of the sun in the sky.
Tracking - Active	Ttracking the sun using an electric motor as the primary driver
Tracking-Passive	Tracking the sun using means other than an electric motor as a primary driver.
TRNSYS	Transient System Simulation program – A software package developed by a group of Thermal Engineering Experts at the University of Wisconsin-Madison, USA to model and solve transient and steady analysis problems of Thermo-Fluids systems.
V	Voltage – The electric potential difference between a point and another at a grounded level in Volts (V).
V_{mp}	The output voltage of a PV panel when it is producing maximum power
W	The manufacturer rating of a PV panel in Watts.
z	Solar zenith angle – an angular measure of how far the sun deviates from the vertical at a given moment. (the complement to the elevation angle). (^{o})
α	Sun elevation - the angle between a horizontal plane and a ray from the sun. (^{o})
β	Surface inclination – the angle between the solar catchment plane and a horizontal plane. (^{o})
δ	Sun declination - the angle between the earth-sun centreline and the earth's equatorial plane. (^{o})
Ψ	Surface azimuth – An angular measure of where the solar catchment plane is facing relative to the north-south direction at a given moment. (the angle between two vertical planes: one containing the N-S line and the other, normal to the surface). (^{o})

Ψ_s	Solar azimuth – an angular measure of how far - east or west - the sun is from the north-south direction at a given moment. (The angle between two vertical planes: one through the sun and the other, containing the earth's N-S line). (^{o})
τ	Transmittance – the ratio of transmitted radiation through a medium to that incident on it (chapter 2).

CONTENTS

CHAPTER ONE
INTRODUCTION

1.1 Background

Sub-Sahara Africa (SSA) (Figure 1.1) is the African region south of Sahara desert. It comprises 48 countries with a mid-2015 population of about 949 Million (Population Reference Bureau, 2015:12). In energy terms, it is reported to be the least electrified inhabited region – with 76% of the population having no access to grid supply (World Bank and Energy in Africa Fact sheet, 2015). The region can further be divided into two sub regions: the tropical and the temperate areas. The latter, extending to 34°S, consists mainly of South Africa and the kingdom states of Lesotho and Swaziland – giving a combined population of 59 Million at an average electrification rate of about 83% (International Energy Agency (IEA), 2014a:30-33). In Tropical Africa, a Mc Kinsey & Co. report by Castellano et al. (2015:3) gives annual per capita electric energy consumption of 150 against South Africa's 4841 kWh (Index Mundi, 2015). The IEA gives annual per capita consumption values of 250 and 500 kWh as threshold values for rural and urban populations to be regarded as "having access to electricity", and therefore, emerging from "energy poverty".

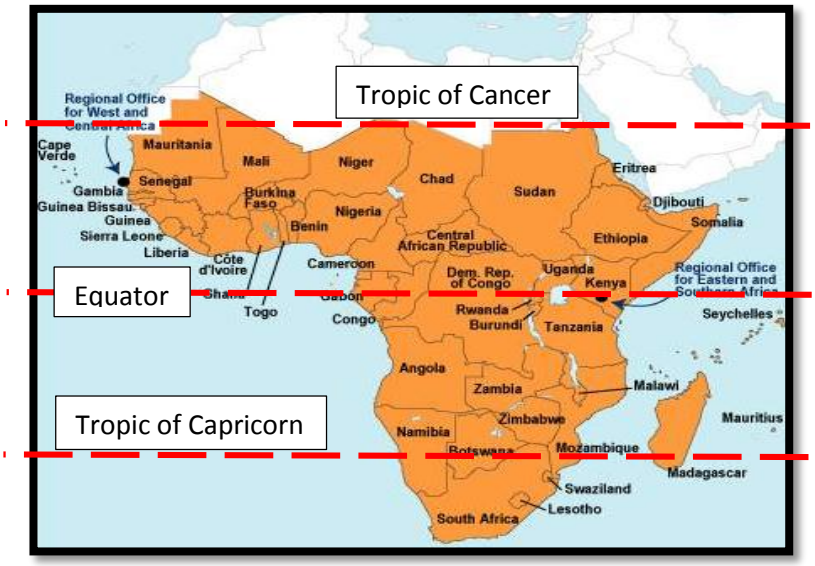

Figure 1.1: Sub-Sahara Africa: the region of interest in this work. Map source: *Exploring Africa*, https://gcps.desire2learn.com/d2l/lor/viewer/viewFile.d2lfile/6605/27261/Unit_3_Map_Skills_SubSaharan_Africa_print.htmlhttps://gcps.desire2learn.com/d2l/lor/viewer/viewFile.d2lfile/6605/27261/Unit_3_Map_Skills_SubSaharan_Africa_print.html

The Castellano report mentioned above, also gives an unutilised solar energy resource in the region, well in excess of 8 TW.

The work reported in this thesis was motivated by two questions that arose mainly from the statistics mentioned above.

First, the energy poverty in presence of a big solar resource led to the question: *Can one make a contribution to reduction of this energy poverty at the home level by suggesting appropriate solar energy harnessing devices for the region?*

The fact of two geographic sub regions presented unexpected issues. For there could be found a reasonable amount of literature relevant to the temperate one as regards approaches to maximising energy yields from solar harnessing devices. But there was not much of the same for most areas in tropical Africa. It was also known that the sun is directly overhead in tropical places twice a year while it is never overhead in the temperate region. A second question therefore arose: *How reasonable was it to rely on solar energy yield improvement efforts in temperate areas for tropical ones*?

1.2 The research problem

The research problem was formulated from the above motivation as: *Investigate and propose novel approaches that would most likely help improve energy yields from flat solar energy panels/ collectors in sub-Sahara Africa's homes*. Flat surfaces were chosen because they were considered to be the simplest to adopt for a start-up home. The issues in this problem were:

- Determining current practices and limitations in harnessing solar energy using flat solar panels/collectors at a home level in the region.
- Developing a framework for comparison between existing approaches and what would be proposed in this work for an area as big as the region in question.
- Designing and testing new approaches in accordance with the framework.

1.2.1 *Research questions*

To resolve the issues stated above, answers to the following questions were sought:

- In such a wide region, how would energy yields from different approaches be reliably compared?
- What are the current solar energy harnessing practices in the region and how can they be improved?
- Have energy yield enhancing methods practiced elsewhere been properly adopted in the region?
- Given answers to the above questions, what novel engineering approaches are feasible?

1.2.2 *Research objectives*

- Develop one or more solar energy harnessing methods that would enable a domestic user in SSA to harvest more energy from her/his existing solar panel/collector at a capital cost that could be justified either from financial considerations or from overall method(s) utility when compared with efforts to acquire equivalent new extra panel/collector area.
- Advance the knowledge on mathematical modelling for harnessing solar energy in tropical Africa specifically.
- Develop a methodology and new hardware for flat solar energy collectors to track the sun.

1.3 Research design and methodology

The work of this thesis covered aspects of research and development (R&D). In the research part, an extensive literature survey on solar engineering in general was undertaken, focused on flat collectors/panels in content and sub-Saharan Africa in geography. Subsequently, mathematical models were derived with a view to maximise energy yields from PV panels in the region. These were complemented by both computer simulations and experimental work. Quantitative methods – using the IBM statistics software – Statistical Package for the Social Sciences (SPSS) were used to compare the results. SPSS was chosen because of the stochastic nature of weather variables during outdoor experimentation.

The engineering development part consisted of two groups of actions. The first was - conceptualising improvements in current PV panel installation practices and making validated TRNSYS simulations recommendations for the region. The second was designing, constructing, and testing a novel solar tracker. The tracker underwent field tests and has been patented for the university. Figure 1.2 summarises the five plan and execution stages of the project as: Literature review → Tools acquisition → Mathematical modelling → Design & construction → Prototype testing. The outputs at various stages are also shown in shaded cells. They consisted of refereed conference and journal papers, a patent and this thesis. Brief explanatory notes on the various aspects of Figure 1.2 follow.

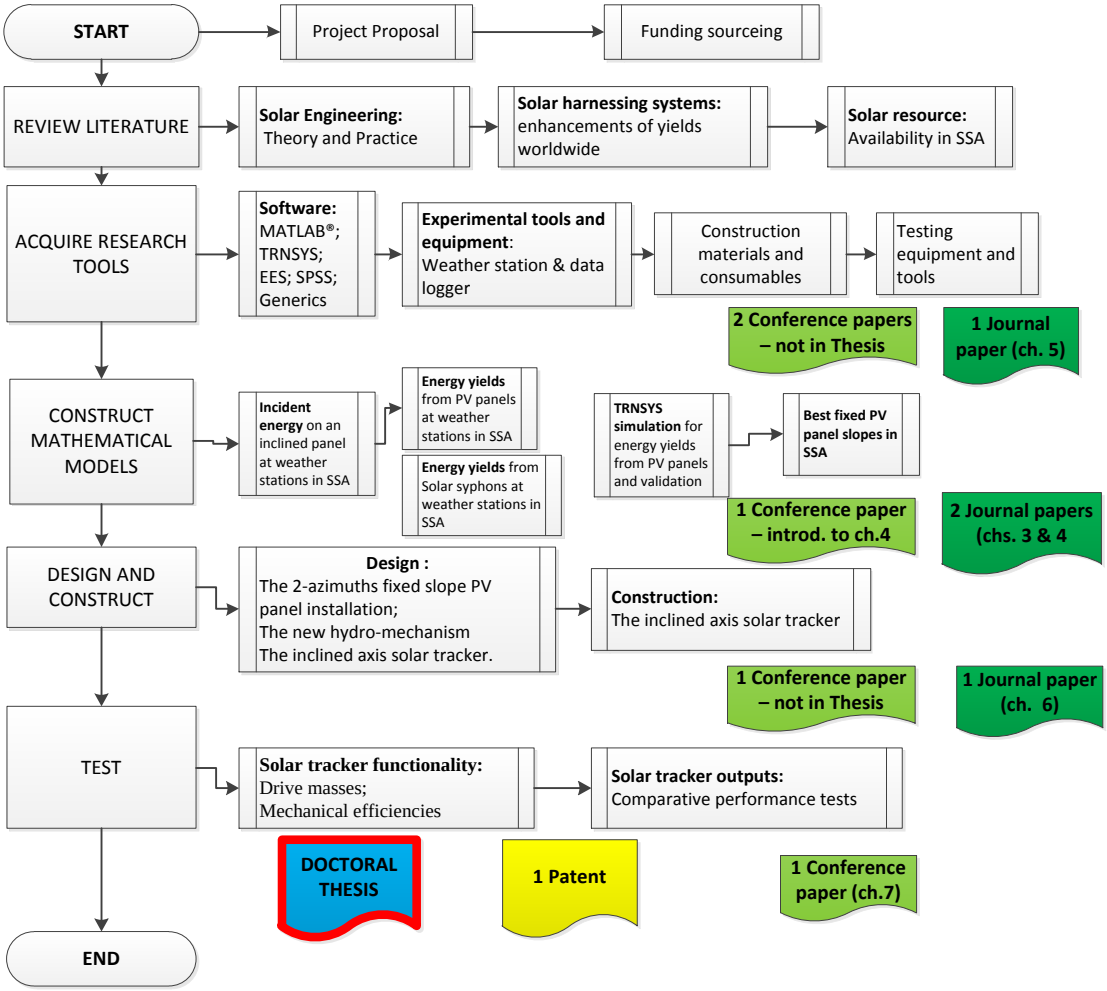

Figure 1.2: Flow chart of project activities: Key milestones are highlighted in shaded boxes.

1.3.1 *Preliminary literature survey*

Prescription of feasible approaches to improve solar energy utilisation required a literature survey on three areas.

- General state of modern energy utility in the region
- Solar energy availability and utilisation in the region
- Methods of enhancing useful energy yields from solar devices – as used elsewhere

This work is mostly covered in chapter 2. Review of work on solar tracking is, however, deferred to chapter 5, where it matches the theme of the chapter on why solar tracking is not common in tropical Africa.

1.3.2 *Acquisition of research tools*

The bulk of the research work was experimental rooted in analytical models and compared with computer simulations. Hence, the following analytical and experimental aids were obtained – and their usage is demonstrated in the thesis as indicated:

- TRNSYS software – Release 17: It is used in chapters 3, 4 and 7.
- MATLAB® and EES software: They are used in chapters 4, 6, and 7.
- SPSS software: It is used in the statistical analyses of chapters 3 and 7.
- A 'Campbell Scientific' weather station and data logger: The data therefrom is used in chapters 3 and 7.
- Assorted engineering materials, components, tools and consumables for the manufacture of prototypes referred to in chapters 3, 4, 6 and 7.

In addition, generic computational, mechanical and electronic design software like MS EXCEL, Auto Desk Inventor, Solid Works and Multisim were used in the analysis and design in parts of the project. Their usage is demonstrated in relevant sections of the thesis and in the appendices.

1.3.3 *Mathematical modelling of different approaches*

Mathematical models were formulated in chapters 4 (PV equipment selection optimisation), 6 (Solar siphons), 7 (PV yields) and 8 (energy costing).

1.3.4 *Design and Construction*

A novel hydro-mechanism was invented and a prototype was constructed.

1.3.5 *Field testing of the prototype*

The mechanism was deployed and thoroughly tested in a single axis solar tracking application using gravity as the immediate source of day-operation power. Communication about the patent of the prototype is found in Appendix A3.1.

1.4 Delineation of the research

The work reported in this thesis is on domestic applications, suitable for rural SSA. The assumptions were that there is no source of grid electricity and that skilled labour for maintenance purposes was scarce. Detailed design was limited to the hydro, mechanical and control work to ensure functionality. Product cost analysis was limited to materials' costing based on those used in the project. In chapter 8, it is explained why at this stage, it would be inappropriate to cost otherwise. Finally, work on solar thermal (ST) systems covered solar siphons in chapter 6. Experimental work on them was short and limited to 'proof of concept'. Other references to ST systems in chapters 4, and 8 are made as frontiers of what has been achieved in the enhancements for energy yield from PV panels.

1.5 Significance of the research

The significance of this research can be assessed from the perspectives of: social-economic; safety, health and environmental; academic.

1.5.1 *Social economic outlook*

In 2011, the African Development Bank (AfDB) reported Africa's middle class had grown to 34% of the population (AfDB, 2011:3). These people needed cheap, reliable, and clean energy in their homes (International Energy Agency IEA, 2014a). Even though most of them worked in the cities, a majority also had rural homes with no grid electricity (Kane & Leedy, 2013: 6-8). The outcomes of this research could help make PV electrification of their rural homes an attractive option.

1.5.2 *Safety, Health and Environment*

Karekezi and Kithyoma (2003:1-27) reported that most people in SSA rely on direct combustion of biomass for their energy sourcing. Ayazika (2002:1-17) reported poor health resulting from incomplete combustion of biomass in poorly ventilated kitchens. Johansson *et al.* (1993:4), Kalogirou (2004b:3075-3092), and Tsoutsos *et al*. (2005:289-296) reported environment degradation to be partly a result of trees destruction for charcoal and firewood during the search for biomass. On safety, (in this thesis, section 2.4.2.1), the fire hazards associated with biomass fuel in rural Africa's grass thatched houses are cited. This research helps reduce the need for biomass fuel. Hence, safety and health risks and threat to the environment would be lessened.

1.5.3 *Technical and academic considerations*

Work in chapter 4 reveals a hitherto ignored influence of the tropical location on fixed slope flat plate installations: the two annual sun crossovers. At the abstract level, this can lead to questioning the prevalent practice of uncritical adoption of technologies and methodologies from elsewhere. Another academic significance is on the generally held view that 'flat plate collectors do not track the sun' (e.g. Duffie and Beckman 2013:236-321). It is demonstrated in chapter 6 that this does not have to be a generality. Nevertheless, for inclined axis east to west tracking, riser fluid flow issues arise if a pump is not used (as in solar siphons) because raised tubes before noon are lowered afterwards – as illustrated in Figure 1.3. These issues require further investigation.

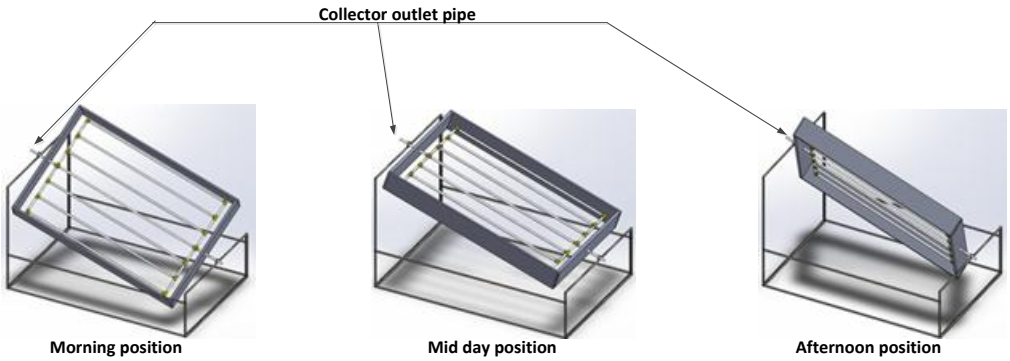

Figure 1.3: Inclined axis solar tracking hot water solar collector: Illustrating tube heights reversal after solar noon

1.6 Outcomes and contributions of the research

The following are the outcomes of this research:

- A novel, patented solar tracker, which enables a PV panel to yield between 5 and 84% (average 34% at the university site in Cape Town) more energy as compared to when installed at an optimal fixed slope.
- An invention of a hydro mechanism with a proven application in solar engineering and with potential for application in industrial systems requiring controlled inter-conversion of linear and rotary motion.
- New science and analysis based outlooks and mapped recommendations on installation of fixed slope PV panels in sub-Sahara Africa
- Four Department of Higher Education and Training (DHET) accredited journal papers about enhancements for energy yields from solar energy.
- Five peer reviewed conference papers (4 international and 1 local – South Africa) on solar energy utilisation in sub-Sahara Africa: three were published – one of which, forms chapter 7).
- An opportunity for current and future researchers and practitioners to re-examine established norms and practices in solar thermal systems design and installations.

In summary, it is hoped that these contributions deepen understanding of the art and science of enhancing solar energy yields from existing devices, especially in sub-Saharan Africa.

1.7 Reading the Thesis

This thesis is principally written as a series of publications. It is a requirement that although the papers should be retyped, as much as possible, the styles of the publishing journals should be left unaltered. Therefore, the referencing and formatting styles from chapter to chapter may vary. However, to facilitate cross referencing, the numbering of sections, tables and figures in a paper normally begin with the chapter's number. The presented papers are self-contained,

complete with their references. They could therefore be read independently of each other. However, it is suggested that they are read in the sequence they are presented. Cross linking has been adopted in the introductory and conclusion parts of the chapters. However, a few unavoidable common facts and/or phenomena within the published papers may occur. For that, the author expresses apologies.

CHAPTER TWO
BIBILIOGRAPHY

2.0 Introduction

The bibliography detailed in this chapter covers areas relevant to this research. These include: general solar energy engineering theory; developments in applications of the theory; and existing work on sub-Sahara Africa's energy crisis. Because submitted, published and conference-presented papers that appear in successive chapters of this thesis contain pertinent literature reviews in their introductions, this chapter restricts itself to aspects which are of importance as background knowledge across the chapters.

2.1 A brief review of the theory of solar energy engineering

2.1.1 *Astronomy Aspects*

Solar energy engineering has its genesis in the fact that the sun is a 1.4 million km diameter sized star, thermally and gravitationally energising a system of eight known planets, several dwarf planets and other space objects within a radius of approximately 2 light years ($18.75X10^{12}$ km) from it (Encrenaz *et al*., 2004: 1). By nuclear fusion of hydrogen atoms into helium, it generates 386 X 10^{24}W of power at its centre in form of gamma rays (Tiwari, 2002: 1). By the time the energy reaches the outer layers - some 700 X 10^3 km away, most of it has dropped in frequency, with some in the visible and infra-red part of the electromagnetic spectrum. This energy leaves what could be called the surface in two forms: as electromagnetic waves across the entire spectrum travelling at 299.8 X 10^3 km/s; and as a solar wind of charged particles travelling at different speeds but averaging about 417 km/s (Schwadron et al., 2005: 3-5). For the harnessing of solar energy on earth, it is the former that is most useful.

The Earth on the other hand is a rocky planet with a gaseous atmosphere spinning once every approximately 24 hours on an axis pointing towards the star Polaris. It has one natural satellite – called the Moon, orbiting it in gravitational gridlock. Gravity causes the combined system of Earth, Atmosphere and Moon to orbit the sun in an elliptical path with the latter at one of the foci. The orbit is in an ecliptic plane inclined at 23.45° to the earth's equatorial plane with the distance from the sun varying between 147.5 X 10^6 km around January 4th and 152.6 $X10^6$ km about July 4th. This gives an approximate average sun-earth distance of 150 X 10^6 km (NASA, 2001). The journey round the sun takes approximately 365.25 days. Figure 2.1 illustrates these relationships.

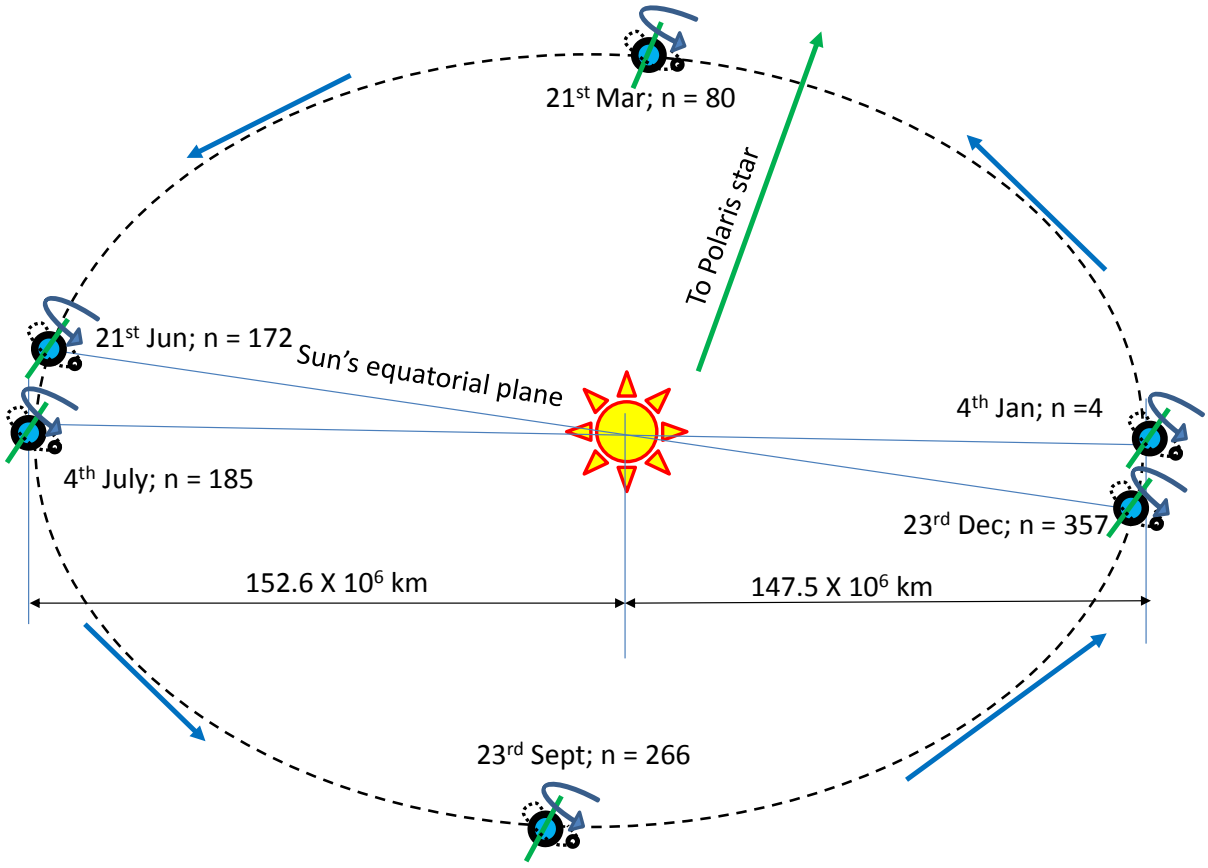

Figure 2.1: The sun at one focus of the spinning Earth's elliptical orbit

The Earth's west to east spin causes variation of direct radiation intensity reaching a particular place on earth to vary between zero at night and a maximum at noon. It also causes the Sun to appear to rise from the eastern horizon, traverse an arc in the sky, reaching a peak elevation at noon, and setting below the western horizon. The curvilinear motion in the ecliptic plane also causes variation of the Sun's radiation intensity at the place because of the variance of distance from the Sun. In addition, the apparent path of the Sun in the sky changes more gradually - ultimately oscillating in a north-south direction. This latter action causes both length of day light and peak elevation of the Sun in the sky to vary. Figure 2.2 illustrates this phenomenon for a point P within the tropics in the northern hemisphere.

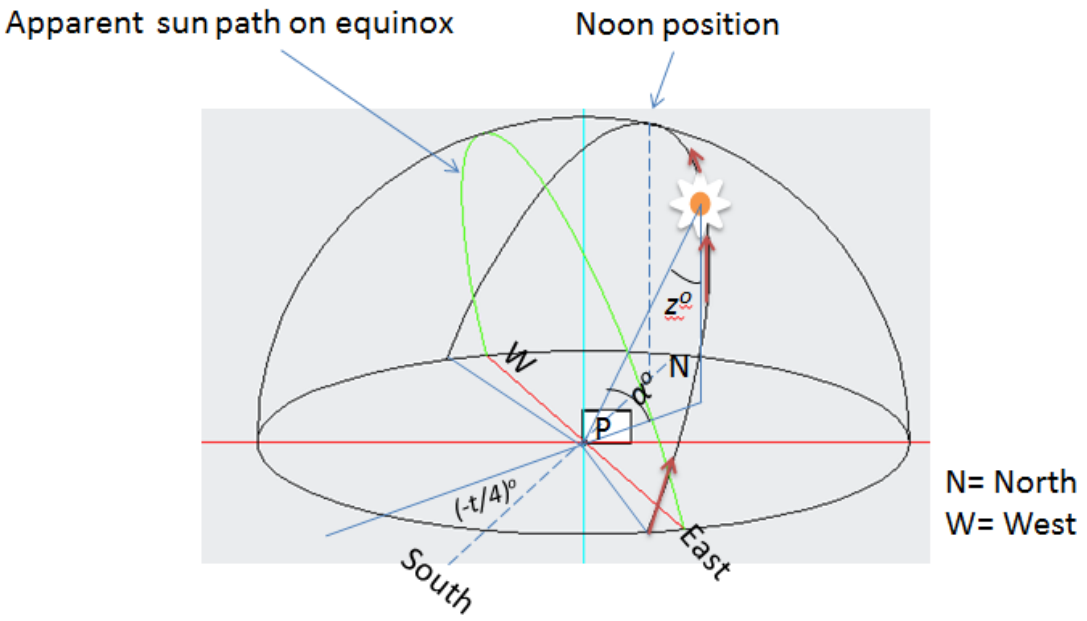

Figure 2.2: Solar angles at 'P': elevation α; zenith z; and time from noon [t (minutes)/4]

2.1.2 *Some relevant atmospheric physics*

Next to astronomy, the most important factors affecting solar energy harnessing at the Earth's surface have to do with the atmosphere and events therein. The atmosphere is a dynamic envelope of gas with suspended small solid and liquid particles whose distribution varies with geographical position (latitude, longitude), depth (converse of altitude, ***h***) and time. Figure 2.3 shows its structure. The elements and events that affect the harnessing of solar energy are briefly reviewed below.

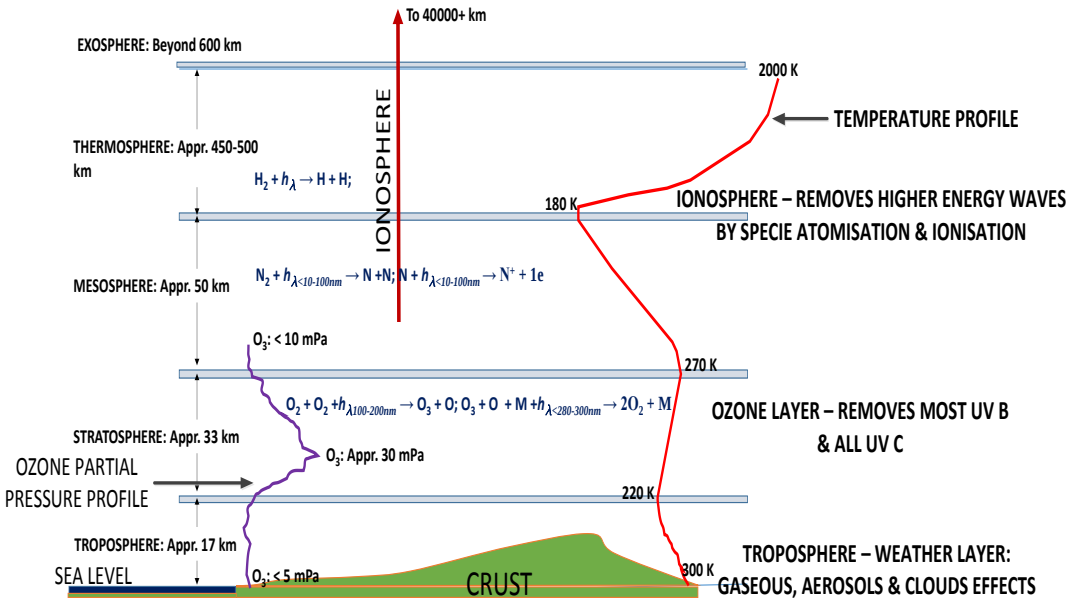

Figure 2.3: The atmosphere and its approximate structure (data adopted from several souces e.g. Yu, nd.; Zell, 2015)

2.1.2.1 *Solar radiation absorption in a 'clean' and dry atmosphere*

A clean and dry atmosphere would be one with zero moisture content and zero suspended solids or aerosols. It would just consist of normal atmospheric gases. It does not exist as a condition on planet Earth but it is a good starting point for discussing the absorption of radiation. It was popularised by Linke in the 1920s (Linke, 1922:91-103).

Extra-terrestrial irradiance $\boldsymbol{G_0}$ arrives at the approximate outer edge of the atmosphere (i.e. physical space-Earth boundary, about 10 000 km from the ground) as a full spectrum of electromagnetic waves from gamma rays of wave lengths shorter than 10^{-13} m to radio waves longer than hundreds of metres. Molecular hydrogen absorbs very short gamma radiation to form atomic hydrogen, some of which in turn absorbs longer waves to form H^+ ions and free electrons as part of the ionosphere. Some hydrogen atoms may recombine before ionisation to reform H_2 molecules. In the mesosphere, shorter waves between 10 and 100 nm first break up nitrogen molecules and then, the longer ones ionise the resulting atoms (Weissler et al., 1952:84-92). This whole range is thus removed from the spectrum. In the stratosphere, some oxygen molecules (O_2) are broken up by waves between 100 nm and 200 nm long (UVC). On absorption of waves between 200 and 300 nm, and in presence of a catalysing molecule (M in Figure 2.3), individual atoms attack more oxygen molecules to form ozone. But the ozone molecule can be attacked by another roaming oxygen atom. This reaction absorbs waves between 200 and about 300 nm (UVB) and regenerates normal oxygen molecules. The cycle continues, effectively filtering out most of the ultraviolet part of the spectrum except for UVA (i.e. longer than 300 nm) - most of which eventually reaches the ground.

Both in the troposphere - and stratosphere, there can be oxides of nitrogen (NO_x) which also absorb different portions of the spectrum to break and remake them, sometimes also affecting the O - O_2 – O_3 equilibrium state in the ozone layer. In summary therefore, the absorption by gases in a dry and clean atmosphere affect the incoming radiation in line with equation (2.1):

$$G_{gas} = G_0 \tau_g \tau_{n-s} \tau_{n-t} \tau_o \qquad (2.1)$$

Where $\boldsymbol{G_0}$ and $\boldsymbol{G_{gas}}$ are the extra-terrestrial and transmitted irradiances respectively; the 'τ's are the fractions transmitted by each gas component: where '*g*' is hydrogen, nitrogen (and any other element in trace amounts); '*n-s*' and '*n-t*' are stratospheric and tropospheric NO_x, respectively; '*o*' is the oxygen-ozone effect.

2.1.2.2 *Solar radiation scattering in a 'clean' and dry atmosphere*

In addition to the absorption of solar energy described above, molecular particles scatter the waves that intercept them. The molecules being small in comparison with the wavelengths encountered (molecular radii ~ 0.1 nm), Rayleigh derived equation (2.2) for the irradiance of

initially unpolarised waves at an angular position $\boldsymbol{\theta}$ from the incident direction and a distance $\boldsymbol{r}$ from the scattering particle as in Figure 2.4 (Rayleigh 1871:447-454).

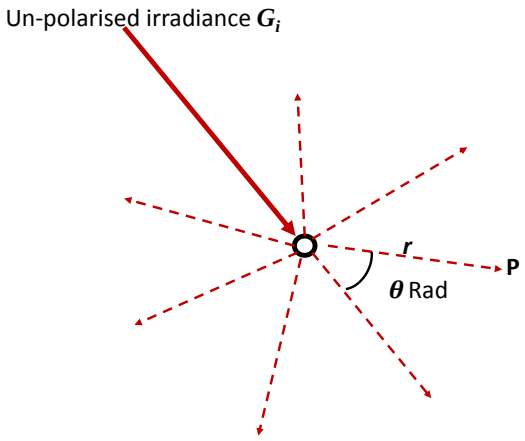

Figure 2.4: Scattering of incident radiation by a particle

$$G_P = G_i\left(\frac{\alpha}{r}\right)^2\left(\frac{2\pi}{\lambda}\right)^4\frac{1+\cos^2\theta}{2} \qquad (2.2)$$

Where $\boldsymbol{\alpha}$ is a space property of the particle ('polarisability') of dimensions $(\boldsymbol{Length})^3$ and may be direction dependent. The variable λ is the wavelength of a particular wave within the unpolarised irradiance $\boldsymbol{G_i}$.

Rayleigh's equation is very important in that it is able to account for many atmospheric observations (e.g. colour of clear sky) and also for the generation of diffuse radiation - which leads to at least two major components of radiation arriving at the surface of the Earth: beam and diffuse radiation. The former is a combination of that radiation propagated in the original direction from the sun uninterrupted plus any that may have been forward scattered in the same direction ($\boldsymbol{\theta}$ = 0). The latter is that which arrives at the Earth's surface from anywhere else, often after multi-direction, multi-scattering. Perez split these majors into 5 components (Perez et al., 1990:111-114). In terms of equation (2.1) for beam radiation, the Rayleigh scattering leads to an additional transmittance term τ_R so that beam radiation through a clean, dry atmosphere is given by equation (2.3).

$$G_{beam-clean-dry} = G_0\tau_R\tau_g\tau_{n-s}\tau_{n-t}\tau_o \qquad (2.3)$$

2.1.2.3 *Effect of water*

Water in the atmosphere can exist in all its 3 thermodynamic phases – and each absorbs different parts of the spectrum depending on the mode of molecular and atomic motion excitation possible. It is the single most important absorber of solar radiation, accounting for up to 70% of all the absorption in the atmosphere (e.g. see:

http://www1.lsbu.ac.uk/water/water_vibrational_spectrum.html). The water molecule is asymmetrical and it has one rotational and three vibrational excitation modes (Mugarza et al., 2009:2030-2036). In addition, hydrogen bonding enables the liquid phase to absorb large quantities of energy with only small changes in translational energy (hence, high specific heat and latent heat of evaporation). These properties enable water to absorb electromagnetic waves as follows:

Water vapour – In the gaseous phase, radiation in the mid infrared range ($2.9 < \lambda < 6$ μm) excites some vibrational modes while 'far' infrared (λ>50 μm) and microwave (1 mm to 1 m) ranges excite rotational modes of the anisometric molecule (Du, *et al*., 2013). Much shorter waves in the ultraviolet range at 65, 115, 125 and 165 nm dissociate the molecule according to the equation:

$$H_2O + hv_{(\lambda=65/115/125/165)} \rightarrow H^+ + OH^- \qquad (2.4)$$

Liquid Water – Absorbs waves in the microwave and in the visible part of the spectrum to create both translational and rotational molecular effects (Pope & Fry, 1997:8710-8723). Vibrational modes are constrained by hydrogen bonding. Most radio waves ($\lambda \geq 1$ m) are also absorbed. In addition to absorption by molecules, aggregated molecules can now reflect and scatter radiation, a phenomenon used in estimations of ground solar radiation using geostationary satellite images.

Ice – exists in clouds as small flakes. Lattice vibrations absorb ultraviolet radiation at 170 nm and lower. Warren found that for the case of snow, scattering dominates and is independent of wavelength in the visible part of the spectrum (Warren et al., 2006:5320-5334).

To summarise, water in its various forms absorbs a great deal of solar radiation as shown in Figure 2.5. The solid state additionally scatters and reflects most radiation, greatly contributing to albedo of the surface and of clouds.

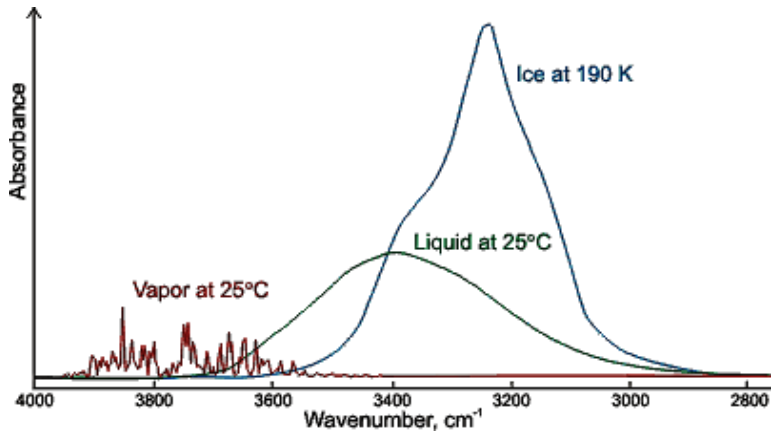

Figure 2.5: Electromagnetic spectrum absorption coefficients of water: source: http://www1.lsbu.ac.uk/water/water_vibrational_spectrum.html

2.1.2.4 *Aerosols*

Aerosols are small solid particles suspended in the atmosphere. According to Allen, three types exist in accordance with their origin: volcanic, desert, and man-made (Allen, 2015). They affect earth bound radiation differently. Volcanic aerosols scatter and reflect radiation back into space, reducing the fraction that reaches the ground. They are reported to remain in the stratosphere for up to 2 years, spreading all-round the globe. Desert aerosols contain small dust particles that scatter and absorb some radiation depending on their composition. In absorbing the radiation, they warm the area below them. Man-made aerosols are products of combustion as in engines, bush fires and also by-products of industrial activity. In the troposphere, earth bound short wave radiation is scattered, producing haze and water vapour condensation sites leading to fog in mornings. Space bound long wave radiation is scattered – and some reflected back to earth causing general warming. In the clouds, they are reported to provide greater surface area for condensation, thus increasing cloud albedo and reducing the short wave reaching the ground. In the stratosphere, they present sites for the ozone depletion reactions.

Because of their sizes (radii exceeding 0.1μm), the Rayleigh scattering equation (2.2) does not apply. Instead, Lorenz (1890:2-62), and Mie (1908:377-445) - cited by Kerker (1982:275-291), suggested equation (2.5) to account for their scattering.

$$G_P = G_i \frac{\sigma_s}{r^2} \frac{f(\theta)}{4\pi} \tag{2.5}$$

Where: $\boldsymbol{f}$ is a normalised phase scattering function of the angle $\boldsymbol{\theta}$ – essentially dependent on nature of the particle;

$\frac{\sigma_s}{r^2}$ is the effective solid angle of the scattering section;

4π is the total solid angle around the particle.

To illustrate the complexity of equation (2.5), Liou (2002:96) cites equation 2.6 as a primary power series equation from which the geometric value σ_s may be obtained.

$$\frac{\sigma_s}{\pi a^2} = c_1 x^4 \left(1 + c_2 x^2 + c_3 x^4 + ----\right) \tag{2.6}$$

Where: '$\boldsymbol{a}$' is the effective radius of the particle;

'$\boldsymbol{x}$' is the ratio $\boldsymbol{2\pi a/\lambda}$;

And the coefficients c_1, c_2, c_3, -- take on forms dependent on the relative air mass m.

From the analysis, it is clear that the theoretical estimation of aerosols' transmittance, τ_{aero} - to be used in a modification of equation (2.3) - is quite difficult. The same is true of τ_{water}. This is perhaps the reason Linke modelled absorption and scattering in the real atmosphere as equivalent to that of an 'artificially' thickened 'dry and clean' atmosphere giving the same total transmittance. This artificial thickening introduced the '*Linke turbidity'* coefficient τ_L in a modification of equation (2.3) to produce equation (2.7).

$$G_{bn} = G_0 \tau_L \tau_R \tau_g \tau_{n-s} \tau_{n-t} \tau_o \qquad (2.7)$$

Where now G_{bn} is the beam irradiance arriving normal to a surface at sea level. Elsewhere, it would be the more common 'Direct Normal Irradiance' or DNI.

2.1.2.5 *Concluding the physics*

Gueymard points out that the Linke turbidity τ_L as in equation (2.7) has since had problems in application because of "its ambiguous dependence on" aerosols and water vapour (Gueymard, 2003:355-379). Consequently many other forms of equation 2.3 have been formulated to account for the two ubiquitous parameters separately. Examples include the Bird equation (Bird & Hulstrom, 1981:182-192), Gueymard's REST and Gueymard's "Multilayer Weighted Transmission" II (MLWT2) models as in equations (2.8) to (2.10) respectively:

$$G_{bn} = 0.9962 G_{0n} \tau_R \tau_g \tau_o \tau_w \tau_{aero} \qquad (2.8)$$

$$G_{bn} = G_{0n} \tau_R \tau_g \tau_o \tau_n \tau_w \tau_{aero} \qquad (2.9)$$

$$G_{bn} = G_{0n} \tau_R \tau_g \tau_o \tau_{ns} \tau_{nt} \tau_w \tau_{aero} \qquad (2.10)$$

The point to note in these - and many other similar models - is that the expressions for the transmittances τ are different in each model. Not even those in the various Gueymard models are the same. Irrespective of the forms however, most transmittances are said to be influenced by the Beer- Lambert extinction law as in equation (2.11). (Tagirov & Tagirov, 1997:664-669).

$$\tau(\lambda) = e^{-\mu(\lambda)x} \qquad (2.11)$$

Where $\mu(\lambda)$ is the wavelength-dependent linear attenuation coefficient; and x is the wave path length in the medium. Because the electromagnetic spectrum covers a wide range of wavelengths, most of the transmittance functions take forms of additive decaying exponential functions of some variable such as relative air mass and/or equivalent column depth. Some

empirical approaches of estimating G_{bn} using some of these models are described in section 2.2.2.3 below.

2.2 Solar Resource availability and estimation

In this section, a short review of literature on the measurement and estimation of solar radiation available at a given location is made. Theoretical methods are given first, and then practical efforts made by different researchers especially in Africa and areas elsewhere with similar climatic conditions are given.

2.2.1 *Solar energy availability on Earth*

Absorptions and scatterings notwithstanding, solar energy is abundantly available on the planet – amounting to an average of 1.367 kW/m^2 of normal projected area just outside the atmosphere (Renné et al., 2007: 19-3). This translates to a total 173 X10^{12} kW of power for the entire planet. After extra-terrestrial reflection, absorption, and a series of exergy destruction processes in the atmosphere, Hermann (2006:1349), estimated that about 53.1% of incident energy reaches the surface of the Earth. This is nearly 5700 more than humanity's energy demand of 141.9 X 10^{12} kWh in 2008 (IEA, 2011). Of the total solar energy reaching the surface, Hermann's study revealed that on average, 75% arrives as beam radiation in the sun-earth direction. The rest arrives as diffuse from different directions after some beam radiation is scattered in the atmosphere. In more rigorous computations and measurements however, Perez, *et al.*, (1990:271-279); Duffie and Beckman (2006:77-97); Goel (2007:A2-1 to A2-21) among many others, show that total radiation and related fractions falling on Earth's surface vary with cloud cover, atmospheric air mass (hence solar time) and aerosol content in the atmosphere. Figure 2.6 illustrates this situation. Thus, diffuse fraction variations between 10% and nearly 100% for completely overcast conditions are possible.

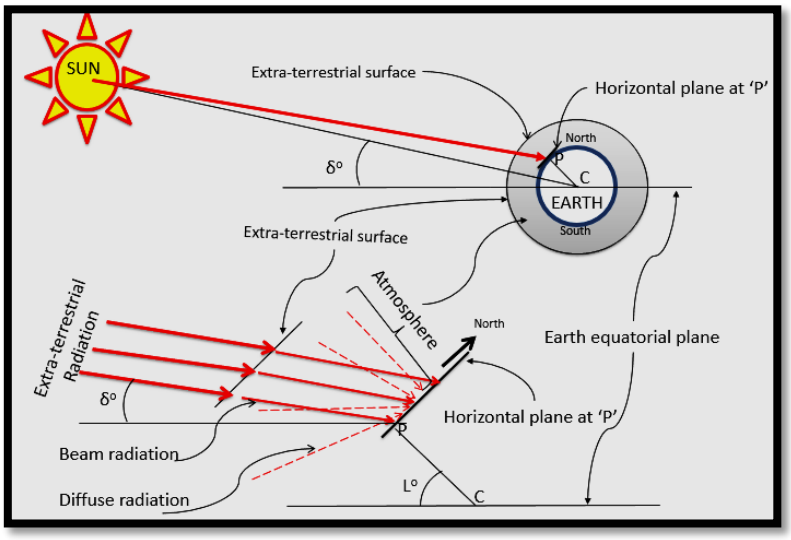

Figure 2.6: Solar radiation incident on a horizontal plane at place 'P' (latitude L) at solar noon

Shafey, *et al.* (1990: 140) showed diffuse radiation to have a lower exergy (75.2%) than that of beam radiation (93.2%). One implication therefore is that systems on earth will derive different energy utility from solar radiation depending on how they are oriented to the sun. In nature for example, sun tracking plants like velvetleaf *(Abutilon Theophrasti)* do orient their leaves to follow the sun during the day so as to maximise the photosynthetic utility (Jurik & Akey, 1994: 93-99). Others like variants of cotton (Ehleringer and Hammond, 1987: 25-35) do track the sun up to a point of radiance saturation, maximising photosynthesis but then stop and begin to increase the proportion of diffuse radiation capture thereby minimising stomata exposure to beam radiation. In this way, they conserve water during hot, bright afternoons.

2.2.2 *Different estimation methods*

2.2.2.1 *Ground based measurements*

Solar radiation at a place may be estimated by measurement in different ways. However, Myers (2013:39) reports that it is very difficult to get accuracies better than within 0.3% - and that most practical instruments give readings within a few percentage points of error margins. This, he explains – is on account of difficulty of conversion of photon energy to a single measurable form and on the labour required for constant calibration and maintenance of measuring equipment. In general however the instrumentation may be classified as in Table 2.1 on page 19.

A pyrheliometer measures beam and circumsolar direct normal irradiation (DNI). Hence, its approximate 5.7° aperture opening tracks the sun disk on two axes. (Duffie & Beckman, 2013:44-47; Myers, 2013:18). A pyranometer on the other hand generally measures global irradiation on a horizontal plane although it could be adapted to measure that on an inclined plane as well. By shading the sun either with a double axes tracking solid ball or with a regularly adjusted ring, it can be used to measure diffuse radiation. Figure 2.7 shows examples of a pyrheliometer, shaded, and unshaded pyranometers.

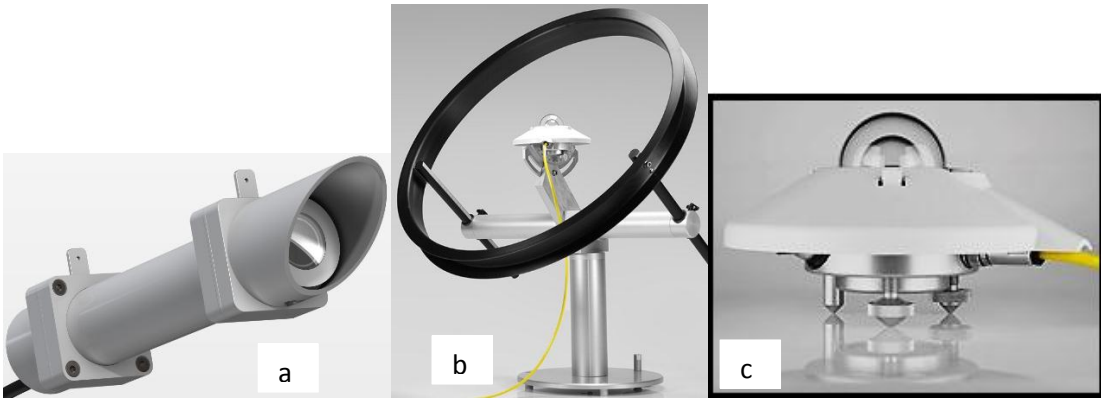

Figure 2.7 Examples of: a) Pyrheliometer b) shaded pyranometer c) Unshaded pyranometer: (source: Kipp Zonen)

Table 2.1: Classification of solar radiation measurement equipment

Basis of measurement	Type of instrument	Example of instrument	Comments/Difficulties in measurement
Calorimetric	Primary and secondary standard calibration	Abbot's Water pyrheliometer	1. Difficulty to use, requiring accurate measurement of flow rate and water temperature change 2. Used for calibration of other equipment
	Thermopiles	Type 'T' Cu-Constantan thermopiles	1. Series of interconnected pairs of thermo-junctions at collector and reference temperatures 2. Difficulty in packaging many pairs to give measurable collector to reference electric potential differences 3. Errors from collector to sky radiation exchange
	Resistance Temperature Detectors (RTDs)	Platinum Resistance Temperature Detectors (PRTDs)	1. Source of stable current – required for resistance measurement
	Thermistors		1. Implicit logarithmic function of resistance on collector temperature whose individual coefficient terms must be determined first 2. Source of stable current – required for resistance measurement
Photoelectric	Silicon photocell detectors		1. Limited spectral response (0.3-1.2 μm) due to a valence-conduction gap of 1.1 eV. 2. Small current from single cell – difficult to measure accurately 3. Dependence of cell current on temperature of cell junction

2.2.2.2 *Satellite data based estimation methods*

Ground based measurements, if done using first class, well maintained and calibrated instruments over a long time, are so far the most reliable practical source of irradiance data. They would have accuracies of within ±5% (Suri & Cebecauer, 2014). However, in addition to being expensive, they are point-specific and their readings may be of much less accuracy at areas farther away from their installation site. Zelenka et al., (1999:199-207) show that beyond 25 km from a measuring station, use of measured data may have uncertainties well in excess of 25% - calling for use of satellite derived data.

The basic principle used in satellite derived data is an application of the 1st law of Thermodynamics to extra-terrestrial and space bound short wave radiation from the earth and its atmosphere, processed and measured by radiometers in geostationary orbiting satellites. Figure 2.8 and equation 2.12 illustrate the principle.

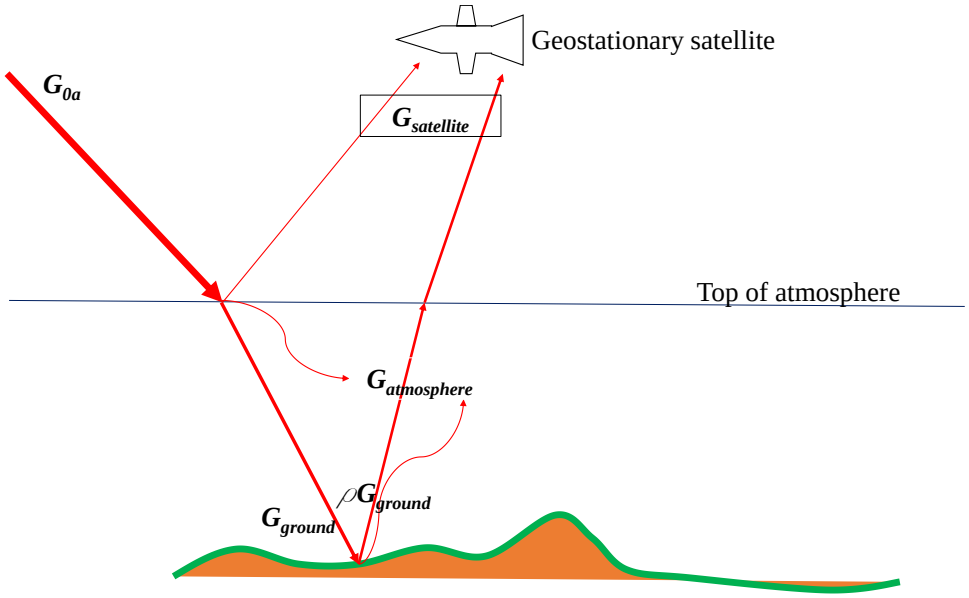

Figure 2.8 Illustrating 1st law application in satellite derived data: (Modified adoption from Zelenka, 2001:534)

$$G_{0a} = G_{satellite} + G_{atmosphere} + G_{ground}\left(1 - \rho_{ground}\right) \qquad (2.12)$$

In equation (2.12), G_{0a} and $G_{satellite}$ are known with near certainty. According to Suri and Cebecauer (2014), $G_{atmosphere}$ is derived by complex algorithms in the satellite from estimates of 3 or 6 hourly atmospheric ozone, aerosols and water vapour in areas of diameters varying between 22 and 125 km. The clouds are spectrally mapped in 5 - 12 bands every 15 or 30 minutes in spatial resolutions of 3 - 5 km. This inputs data to a clouds radiation attenuation program on board the satellite. The ground terrain is digitally mapped at resolutions of up to 90 m to enable obtain ρ_{ground}. Consequently, G_{ground} can then be solved for – and other important parameters like ***DNI***, G_d, can be computed. The data is then availed at a rate of either 2 or 4 per hour (depending on the clouds mapping frequency).

Advantages of satellite derived data include: coverage of entire Earth's surface – which is not possible by direct measurements; possible derivation of historical information from raw satellite data of those periods – which again is not possible with ground measurements. Setbacks of the methodology are many. In addition to the limitation on frequency of output data (not instantaneous), they include:

- Accuracy – Gueymard, (2011:1068-1084) estimated the Perez (2002 and 2004) SUNY models (on which satellite algorithms are based) to have up to 13% root mean square errors (RMSE) on DNI when compared with measurements from a rotating shadow ring pyranometer and up to 5.3% on G_{ground}. Myers gives 15% and 8% respectively (Myers, 2009).
- Absence of reliable ground equipment also means that it is not possible to tell the degree of accuracy of these data at those sites with unique physical and geographic features. The features include landscape, land use and vegetation transition regions.
- In tropical and equatorial areas – such as in much of SSA – the clouds can change faster than the 15 or 30 minute satellite imaging period. In rain forest areas, distinction between cloud cover and vegetation can be unclear to satellites, thus causing errors in the on board programs' inputs and outputs.
- Seasonal grass burning and fires in arid areas, sandy winds and ground reflections in desert areas and isolated concentrations of industrial activity in cities give unique challenges to aerosol/water vapour algorithms on board the satellite, sometimes leading to erroneous outputs.

In summary therefore, in spite of the near universal availability of this satellite data, there is still scepticism on its use. Many researchers seem to opt for empirical estimation methods in determining the available resource.

2.2.2.3 *Empirical estimation methods*

There are many different empirical methods available to estimate the components of irradiance on a horizontal surface. But reviews by Gueymard (2011) and Myers (2013: 15-42) give different levels of agreement in different test areas and conditions.

- *Methods based on hourly clearness index,* k_t – These relate the hourly diffuse radiation on a horizontal surface I_d to the measured total hourly irradiance I_h (kWh/m^2) and the hourly clearness index, k_t . They take the form of equation (2.13).

$$I_d = I_h f(k_t) \tag{2.13}$$

  Where the function f may take on different forms in different ranges of k_t.

Examples of these methods include the Orgill and Hollands, (1977:357-359); Erbs, *et al*., (1982:293-304), and Reindl, *et al*., (1990:9-17), Lam and Li, (1996:527-535). Skartveit, *et al*., (1998:173-183) considered effects of solar elevation α as well in similar functions so that the instantaneous diffuse irradiance G_d could be obtained from an equation of the form of (2.14) in different ranges of k_t, where G_h is the corresponding instantaneous total horizontal irradiance (kW/m^2).

$$G_d = G_h\left[1-\frac{(1-f(k_t))}{\sin\alpha}\right] \qquad (2.14)$$

- *Methods based on extra-terrestrial irradiance* G_0 *and* k_t – These methods primarily employ relations given by equations (2.15) Wong & Chow, (2001:191-224). They give different functions for parameters k_b, k_d, and k_D – defined as:

$$k_D = \frac{G_d}{G_0} \qquad k_b = \frac{G_{bh}}{G_0} \qquad k_d = \frac{G_d}{G_h} \qquad k_t = k_d + k_b \qquad (2.15)$$

The methods include the Liu and Jordan (1962:526-541) model relating the beam G_{bh} and diffuse G_d components on a horizontal plane to terrestrial irradiance G_0 and k_t. Louche, *et al*., (1991:261-266) related k_b to a single polynomial function of k_t only. But earlier, Spencer (1982:19-32) had added effects of latitude magnitude to empirical coefficients of k_t for values of k_t in the range 0.35 to 0.75. Maxwell (1987), had included polynomial and exponential functions of relative air mass m_a in expressions of k_b for different functions f of k_t that depended on whether k_t was less than 0.6 or not. Vignola and Mc Daniel (1986:409-418) worked out a variation of k_b with k_t as k_d varied with both k_t and season (i.e. day of year, n).

In Baghdad, Iraq, Al-Riahi, *et al*., (1998:1289-1294), did away with k_t altogether and worked with purely non meteorological data. They had k_b expressed as an exponential function of a function of day of year n and solar elevation α. Then, they related G_h to G_{bh} through another function of α and n. Their equations are given as:

$$k_b = \exp\left(-\frac{B}{(\sin\alpha)^{0.678}}\right) \qquad (2.16a)$$

$$B = 0.3917397 - 5.596X10^{-2}\sin A + 5.293X10^{-3}\cos A + 1.3594X10^{-2}\sin 2A + 4.0383X10^{-3}\cos 2A \qquad (2.16b)$$

$$A = \frac{4\pi n}{365} \qquad (2.16c)$$

$$G_h = G_{bh}(\sin\alpha + \zeta) \qquad (2.16d)$$

$$\zeta = 0.0936 + 0.041\sin\left(\pi\frac{n-104.5}{167}\right) + 0.004773\sin\left(\pi\frac{n+24.4}{83.5}\right) \qquad (2.16e)$$

- *Methods depending on parameterisation* – These methods look at the extra-terrestrial radiation and trace its path through the atmosphere, accounting for absorptions and scattering by various atmospheric species. They rely on estimated or better still, measured data of the atmospheric constituents to give an indication of beam and diffuse irradiance on a given terrestrial surface. They include: the Ångström (1924:121-126), Ångström-Prescott (Prescott,1940:114-125), Glover and Mc Culloch, (1958:56-60), Iqbal (1983), Rietveld (1978:243-252), Gopinathan,

(1988:581-583), Le Baron, *et al*., (1990:249-256), Perez, *et al*., (1990:111-114), Perez, *et al*., (1992:354-369), Skatveit, *et al*., (1998:173-187), and Battles, *et al*., (2000:81-93). More recent ones have included: Gueymard and Myers (2009), ASHRAE (2013) and Gueymard, (2014:74-82). These are only few of the approaches. From this list, the subject of estimation of both diffuse and beam radiation on a terrestrial surface can be expected to be complex. As a result, computer based approaches have been developed to model the estimation as though it were a network of neurons with various inputs and nonlinear outputs. This led to the artificial neural networking approach, described next.

2.2.2.4 *Artificial Neural Networking (ANN) based estimation methods*

In this method, actual statistical weather data measured over a long period for some stations is used to relate radiation as a complex function of well-known geographic and other weather data. Then, for the sites with unknown radiation data, information on the other variables is fed into the network to output a predicted radiation data. Basically, the method consists of measuring both radiation and other weather variables at the known stations. These are commonly called 'training' stations. The other variables are considered as signals emanating from neural input nodes to a set of 'hidden' or internal nodes – for processing. The strengths of the signals from each input node are adjustable during the 'training' period. From the internal nodes, signals are considered to be transmitted to the output node to produce a combined output message – in this case, solar radiation data corresponding to the network's input set of variables. Figure 2.9 illustrates the neural networking method.

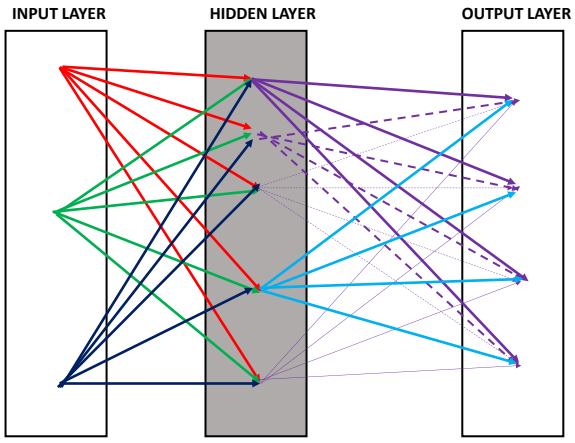

Figure 2.9: Artificial Neural Networking (ANN) method

2.2.3 *Examples of experimental work from within Africa*

Most of the work in SSA has been experimental validation of one or more of those discussed above.

Chendo and Maduekwe (1994:101-108) investigated diffuse radiation in Lagos, Nigeria and found it to depend on the hourly clearness index k_t, ambient temperature, T_{amb}, relative humidity

RH and solar elevation angle $\boldsymbol{\alpha}$. Ogolo (2010:121-131) divided Nigeria into 4 climatic zones running East to West and investigated 4 models for prediction of horizontal surface global irradiance. Two were based on the linear and quadratic forms of the Ångström-Prescott model. The other two considered were adaptations of the Hargreaves and Samani (1982:225-230) and Garcia (1994) models using the ambient temperature difference between maximum and minimum readings ($\boldsymbol{\Delta T_{amb}}$) during the day. Data used was of variable periods ranging from 3 years (1995-97) to 15 (1976-90). As a result, variations in predictive abilities were noticeable – and it was concluded that more work needed to be done to include other atmospheric variables. This work was followed up in 2014 (Ogolo, 2014:213-224) with an extension to 14 stations covering 31 years. Of these, 17 were for modelling and 14 for validating. The Ångström-Prescott equation was parameterised to take account of geographic variables (coordinates) and other meteorological data including temperature, rainfall or relative humidity and sunshine hours. There were still variations from measured data but the trend of results over the period was in agreement.

Agbo (2013:46-49) presented a correlation for average daily radiation for Nsukka, Nigeria as given by equation (2.17). In that equation, ***H*** and ***S*** stand for daily horizontal surface energy receipt and hours of sunshine respectively. The subscript *0* is for values at the "top of atmosphere". Its predictive power was compared with two previous ones of Awachie and Okeke (1990:143-156) and of Akpabio and Etuk (2003:161-167). Although the model was claimed to be more precise, the distinction between experimental data used to derive the model and that to test it against others was not clarified.

$$\frac{\overline{H}}{\overline{H}_0} = 0.1150 + 0.5666\frac{\overline{S}}{\overline{S}_0} \qquad (2.17)$$

Ibeh, *et al*. (2012:1213-1219) used 17 year meteorological data (1991-2007) to compare ANN and Ångström-Prescott modelling results for Uyo city, Nigeria (5.02˚N). It was found that the ANN modelling correlated better with coefficients of 97.4% and 74.7% respectively. Nwokoye and Okonkwo (2014:1058-1064) formulated and compared 4 variants of Ångström-Prescott models for monthly daily average global radiation on a horizontal surface in Bida, Nigeria (9.1˚N, 6.02˚E). Thirteen year data (2000-2012) was used to derive linear, quadratic, cubic and power forms of models. No differences in predictive potentials of the forms were reported – although as in Agbo's case above, the distinction between validation and test data was not clarified.

Many other Nigerian researchers have tried to determine the Ångström – Prescott coefficients in linear and polynomial forms for many cities in the country. They include: Chukwuemeka and Nnabuuchi, (2009:681-685) in Port Harcourt; Medugu and Yakubu (2011:414-421) in

Yola; Gana, *et al*. (2014:1636-1647) in Sokoto. Most recently, Innocent, *et al*. (2015: 27-32) made estimates for global horizontal surface monthly irradiance at Gusau (12.17˚N, 6.70˚E).

In the Ashanti region of Ghana, Quansah, *et al*. (2014) evaluated existing models based on daily sunshine hours and temperatures and found general agreement among themselves except for over estimates in the months of April and November.

In Cameroon, David and Ngwa, (2013:984-992) used 23 years data to compute linear Ångström coefficients and those for modified quadratic and cubic models in predicting horizontal surface total radiation for 5 cities. The coefficients were found to vary from city to city. Lealea and Tchinda (2013:370-381) formulated linear, quadratic, exponential and logarithmic models to estimate diffuse radiation in the north and far north of the country. In Malawi, Salima and Chavula, (2012:391-397) used 5 year data (1991-95) for 6 stations, distributed in the whole country, to approximate Ångström – Prescott coefficients as $\boldsymbol{a}$ = 0.29 and $\boldsymbol{b}$ = 0.38. The error on predicted monthly average daily global radiation was estimated at within ±10%.

In East Africa, Schillings, *et al*. (2004) present gridded DNI and GHI data derived from Met 7 and Met 5 satellites for Kenya. However, they report that the data was not verified against ground measurements because of absence of the latter. Mubiru (2011) compared prediction results from ANN with those from the quadratic version of Ångström-Prescott for 4 cities in Uganda. The former was found to be more representative of measured values. These findings were similar to what Tymvios, *et al*. had earlier found in Cyprus (Tymvios, *et al*., 2005). Muyimbwa (2016) presents a doctoral study on estimating aerosols and ultraviolet radiation correlation from satellite data for Kampala, Uganda, Dar es Salaam, Tanzania and Serrukunda in Gambia West Africa. He found overestimates by up to 28% under cloudy conditions and about 10% in clear skies. The aerosol index was low - but growing in the East African cities while the reverse was the case in Gambia.

2.2.4 *Estimation Methods used in this research*

For the estimation of solar radiation in this work, two methods were adopted. At the test site, direct measurement using a Campbell Scientific weather station was used. At other sites, reliance was on data in the TRNSYS software – most of which was originally derived from either measured historical weather data or from meteonorm empirical computations.

2.3 Applications – Using solar energy at the domestic home level

This section briefly reviews applications of solar energy at the domestic household level. It first gives a historical background. Then, it looks at classifications of the applications. It ends with a focus on the two areas addressed in this thesis: PV and water heating - thus, leading to the next one - on applications in the region.

2.3.1 *Historical background*

Solar energy utility on Earth predates humanity – as it is responsible for energising the evolution processes that led to the existence of life on the planet. Later - in harvesting solar energy - man discovered that sun-facing surfaces would yield more useful energy than those which faced otherwise (Bertarione & Magli, 2015). Thus, as far back as about 700 BC through to the first century AD, lenses and mirrors were used to focus the sun's beam radiation for purposes as diverse as burning ants, burning enemy ship fleets, lighting religious fires, etc. (United States Department of Energy - US DoE: n.d.). In later centuries, glass windows facing south were used by Romans to warm up bath rooms. By the eighteenth century - through manipulation of beam catchment area orientation - it was possible to concentrate solar power adequately enough to melt metals. Consequently, in 1772, Antonie Lavoisier achieved a high temperature of 1750°C in his furnace. (Behrman, 1979: 35-36; Kalogirou, 2004a: 231-295).

These early applications of solar energy were for harnessing the heating value of the radiation. Along with them was the mass transfer effort as in drying of foods and clothing. According to the US DoE (nd), from 1839 Becquerel's discovery of the photovoltaic effect, there was an increased effort toward the generation of electricity. The list of progress includes: Selenium photoconductivity by Willoughby Smith in 1873; Selenium solar cells by Charles Fritts in 1883; photoconductivity theory by Albert Einstein in1904; experimental photo electricity by Robert Millikan in 1916; Cadmium sulphide photoconductivity by Audobert and Stora in 1932. These developments led to commercial development and use of photo electricity. Space programmes were the earliest beneficiaries of the technology in the late 1950s partly because it was about the only choice but also because of the cost.

2.3.2 *Domestic applications of solar energy*

Solar energy applications at the household level cover the following areas:

- Electrification in form of PV applications (Green, 2001:291-355, Luque, 1991:177-227, Sayigh, 1991:5-15; Treble, 1991:78-96).
- Water heating in form of solar-siphons, pumped circulation and heat pump assisted systems (Morrison, 2001:223-289).
- Cooking by concentrated solar energy (Winston, 2001:357-436)
- Solar water purification/distillation (Norton, 2001:477-496)
- Solar crop drying (Norton, 2001: 477-496)
- Building space heating in the form of active and passive heating (Wang, *et al.*, 2015)
- Solar cooling and solar assisted refrigeration (Chien, *et al*., 2013)
- Wind energy applications (Milborrow, 2001:653-698)

This thesis focuses on solar energy harnessing using flat surfaces in electrification and to a small extent, in solar syphon water heating (SSWH). The review is therefore delimited to efforts in PV panels and SSWHs.

2.3.2.1 *Photovoltaic applications*

Tropical Africa's electric grid supply is miniscule even by the standard of the rest of the continent. Many researchers and energy practitioners have indicated that self-generation using PV panels is a possible approach to enable homesteads access electricity. Among others, these have included: Nieuwenhout et al., (2001:455-474); Chaury and Kandpal, (2010;3118-3129); Nkwetta et al. 2010; Oyodope, (2012); Bleeker, (2013); Sambo et al. (2014:22-38). But while the practice is taking root in some of the region's countries (e.g. see Gustavsson and Ellegård 2004:1059-1072; Rabah, 2005:33-42; Moner-Girona, 2009:2037-2041); Mulugetta, *et al*. (2009:1069-1080); Szabo, *et al*. (2011), there is limited in depth research based guidance on selection of equipment for the region.

2.3.2.2 *Water heating applications*

At domestic level, the basic technology of solar water heating involves the use of a flat plate collector deployed at a suitable slope. Figure 2.10 illustrates the concept. Circulation may be natural i.e. a solar-siphon or may be forced by a pump. The glazing may be non-existent or single or multiple sheets. In general, the bigger the number (up to 4) of sheets, the smaller the energy losses from the absorber plate, and hence, the more efficient is the collector (Morrison 2001:223-289, Duffie and Beckman, 2013:202-235).

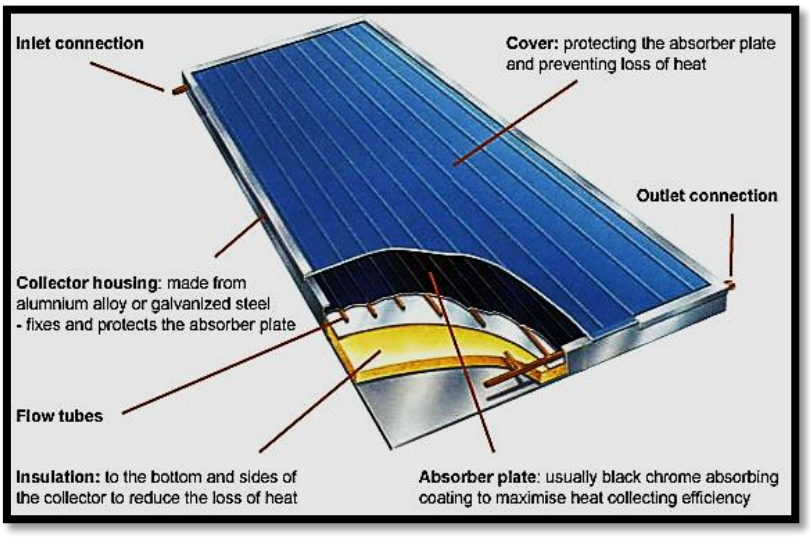

Figure 2.10: Elements of a flat plate collector (FPC) (source: Greenspec: http://www.greenspec.co.uk/building-design/solar-collectors/)

Kalogirou (2004a:231-295) gives a comprehensive review of Solar Thermal (ST) systems. Applications covered include water and air heating among others. From the review, one can

summarise the key performance parameters of the collectors as: Effectiveness (or useful heat gained), Efficiency and peak water temperature. These are influenced by the following variables.

Design Variables

- Glazing materials and numbers: Best materials are low iron content glasses with selective coatings to raise the transmittance to over 90%. The glazing material affects performance principally in two ways. First, through its refractive index, Duffie and Beckman, (2013) cite Fresnal's equation relating the reflectance at an interface of two transparent media to the refractive indices of the media. For air – glazing systems, the smaller the glazing's index, the smaller is the reflected loss. This makes some plastic materials like Poly fluorinated ethylene propylene of index 1.34 (cf. 1.526 of glass or 1.6 of polycarbonate) attractive (Biron, 2016:520). The second influence is due to the previously described Beer-Lambert-Bourger law on radiation absorption (Tagirov & Tagirov, 1997:664-669). Loss in the glazing is dependent on the thickness and composition which determines the Lambert extinction coefficient of equation 2.11. Glass, of low ferric oxide content is known to perform best.

  A bigger number of glazing covers reduces the net radiation transmitted to the absorber plate in line with Whillier's ray tracing analysis (Whillier, 1953). But it also reduces radiation and convection losses from within the collector to the outside. The latter effect more than compensates for the former, making multi glazing covers technically attractive.
- Absorber plate properties – The plate and the configuration of water flow tubes in/on it forms the most critical element of the collector (Tiwari, 2002). It is intended to receive and absorb as much radiation from the glazing as possible while emitting and transferring the minimum possible to the outside. As a result, it is normally made of highly thermal conductive material like copper, aluminium and steel. Juanicó and Dilalla (2014) have reported on the use of some plastics for low temperature applications. The material is coated with a high absorbing black layer. Such a surface has a very low reflectance for wavelengths below 3 μm. Kalogirou reported limited usage of other colours of coatings only to improve the aesthetics of the collector.

  The most important property of the selective surface is its absorptivity **α.** This, combined with the net transmittance of the glazing, τ forms a combination property of the collector, $(\alpha\tau)$ which is not simply a product of the two, but one just slightly bigger due to internal multiple reflections that accompany the initial absorption of the incident radiation (Duffie & Beckman, 2013; Kalogirou 2014; Tiwari, 2002). It relates the absorbed radiation in the plate to the received radiation on the glazing.

- Riser geometry and configuration in/on plate – the tubes or water pathways in or on the plate are called risers may be made of similar or of different material to the plate. The key parameters to consider are riser hydraulic diameters, spacing, and bonding to the plate. The bonding to the plate, which may be in form of brazing, conductive chemical bonding or direct contact pressing, forms a finned heat exchanging unit whose performance is governed by normal heat transfer equations (Çengel, 2006:609-661; Kumar, 2015:607-691, Wieder, 1982:181-207).
- Back and side insulation and casing – Insulation reduces the fraction of absorbed energy that is conducted as heat from the riser to the outside, thereby leaving more energy to be taken by the flowing fluid. Materials used include: high grade fibre glass, polyester fibre and slabs of foam insulation (Morrison, 2001).

  The combination of insulation and glazing arrangements yield an overall temperature dependent coefficient of heat transfer between the collector's surfaces and the environment $\boldsymbol{U_{plate\text{-}air}}$ used in the computation of key performance indicators.

Collector performance indicators

- Collector's efficiency factor $\boldsymbol{\eta_{cf}}$ – this is the ratio of heat transfer coefficient from circulating fluid to air to that from the plate to ambient air, represented by equation (2.18).

$$\eta_{cf} = \frac{U_{water-air}}{U_{plate-air}} \tag{2.18}$$

  This indicator varies as follows (Kalogirou, 2014)
  - Decreases with overall loss coefficient $\boldsymbol{U_{plate\text{-}air}}$
  - Decreases with riser centre to centre distance
  - Increases with plate conductivity and thickness
  - Increases with flow rate and riser hydraulic diameter
  - For a given collector and flow rate, remains approximately constant
- Collector heat removal factor $\boldsymbol{\eta_{Qrf}}$ – The effectiveness of the collector as a heat exchanger, defined as the ratio of actual energy taken by the fluid to the maximum possible if the whole absorber plate were at fluid inlet temperature. For a fluid flow rate $\dot{m}$, it is related to the efficiency factor through a flow factor $\boldsymbol{F_{flow}}$ and is given by equations (2.19):

$$\eta_{Qrf} = F_{flow}\eta_{cf} = \frac{\dot{m}c_p}{A_{collector}U_{plate-air}}\left[1-\exp\left(-\frac{\eta_{fc}A_{collector}U_{plate-air}}{\dot{m}c_p}\right)\right] \tag{2.19}$$

  This gives the rate of heat gain $\dot{Q}_{gain}$ as:

$$\dot{Q}_{gain} = \dot{m}c_p\left(T_{out}-T_{in}\right) = \eta_{Qrf}A_{collector}\left[G(\tau\alpha)-U_{plate-air}\left(T_{in}-T_{ambient}\right)\right] \tag{2.20}$$

  The collector heat removal factor thus varies as follows:

- Decreases with overall loss coefficient $\boldsymbol{U_{plate\text{-}air}}$
- Increases with mass flow rate
- Increases with collector efficiency factor

- The temperature gain is accordingly given by equation (2.21):

$$\Delta T_{gain} = \left(T_{out} - T_{in}\right) = \left[1 - \exp\left(-\frac{\eta_{fc} A_{collector} U_{plate-air}}{\dot{m} c_p}\right)\right]\left[\frac{G(\tau\alpha)}{U_{plate-air}} - \left(T_{in} - T_{ambient}\right)\right] \quad (2.21)$$

From which the gain reacts as follows:

- reduces with increase in mass flow rate and loss coefficient $\boldsymbol{U_{plate\text{-}air}}$
- reduces with increase of inlet temperature $\boldsymbol{T_{in}}$
- vanishes when $G(\tau\alpha) \leq U_{plate-air}\left(T_{in} - T_{ambient}\right)$

In summary, solar water heating at domestic level can be influenced by a choice of glazing, riser tube design and configuration, and weather conditions.

2.4 Sub-Sahara Africa's energy paradox: Rationale for the thesis

The energy paradox in Africa is well documented. A continent with 7.7, 7.6, 3.6, and 13 percentage points of the world's known oil, gas, coal and hydro electric energy reserves (British Petroleum, 2014) has 15.4% of the world population consuming 3.1% of the electric energy output (IEA, 2014b). The concerns in this thesis are not that levels of industrialization and electrified transport in the region are low (AfDB et al., 2014:123) but rather, the absence of convenient, safe, clean, reliable and sustainable forms of energy in the homes of most people amidst a plentiful unharnessed solar energy resource (European Commission and Heliochem-1, 2008).

2.4.1 *Some health problems in un-electrified homes*

In non-electrified tropical African homes, energy is mainly required for cooking food, boiling water, lighting and limited space heating at night. Excluding the latter, Williams (1994) estimated these activities to consume approximately 1 GJ per month per household in rural South Africa. As pointed out in chapter 1, in tropical Africa, this energy comes from incomplete combustion of bio fuels - mostly wood fuel and sometimes charcoal, in poorly ventilated kitchens and living spaces. In addition, daily chores like water sourcing, washing, animal tending, cultivation, crop harvesting and processing, etc. are handled manually. Many of these activities are left to women and children (United Nations, 2010:145).

Incomplete combustion of biofuels produces large quantities of particulates and poisonous gases which affect both the environment and the health of fire attendants. Klippel and Nussbaumer (2007:7-11) reported the presence of wood tar in soot and total particulate matter in concentrations of 5000 mg per m^3 in the flue products of poorly combusted wood. This is

two orders of magnitude as high as emissions from a well-run combustion unit. The World Health Organization (WHO) gives emissions guidelines on two particle aerodynamic size limits: the 10 μm (PM10) threshold particles, which can be filtered by the upper respiratory tract, and the 2.5μm (PM2.5) limit defining the observed smallest particle to exhibit a 95% chance of damaging lung and heart functions upon prolonged exposure. The annual mean limits are 20 and 10 $\mu g/m^3$ respectively while the daily values are 50 and 25 (WHO, 2006). Poor wood fuel combustion leads to exceeding these limits as reported by Ayazika (2002) in Uganda and by Klippel and Nussbaumer (2007) in Sweden.

Since most tropical African economies rely on productivity of women exposed to these off limit particulates, some governments' attention have been drawn to these problems. But resolution is still limited and slow.

2.4.2 *Some actions to alleviate the problems*

Efforts by governments to address the region's energy problems have so far included combustion improvements and rural electrification. Also, some individual researchers, institutions and even entrepreneurs have tried to work on the problem, with varying degrees of success.

2.4.2.1 *Actions on combustion*

Methods used to tackle the problems associated with the combustion of fuels include use of less polluting fuels and of improved stoves. Actions on fuels are however more expensive as some require capital expenditure in addition to running fuel costs. Thus, ethanol gels, plant oils, kerosene, natural and bio gas, - all require upfront investment in a suitable burner and/or a safe fuel storage system. More effort has been put in improving stoves partly due to a low investment cost (e.g. equivalent of US$ 2.00 in Ethiopia) but mainly because of the continuing use of the familiar wood/charcoal fuel. Thus, different stove designs capable of reducing fuel consumption and consequent emissions by up to 50% on 'typical' combustion modes have been introduced in Ethiopia, Kenya, Rwanda, Uganda, Nigeria and many other tropical African countries (Ayieko, 2011), Lyalabi. (2011); Uwamahoro (2013); Elusakin, *et al*. (2014:51-57). Both, the change of fuel and stove, however, do not remove the other less talked about risk: that of fires in grass thatched houses that many of Africa's rural populations reside in. For example in rural South African homes, where paraffin has been used to augment solid fuels, Lloyd (2014:2-5) reports of homes which have been burnt on annual basis.

2.4.2.2 *Rural electrification*

Many governments are trying to extend national electric grid systems to rural areas. For example, in 1989, Ghana started a series of 5 year rural electrification programs, intended to avail electricity to everyone by 2020 (Abavana, 2011). Starting at 28%, the access rate had

nearly doubled by 2005. Figure 2.11 below shows their current figure of electricity access at 75%. Nigeria set up a rural electrification agency in 2006 but had continuity problems. Up to 1946 electrification projects were put on hold until 2012, when they resumed. Zambia set up an authority in 2006, when rural electrification was at 3.1%. Because of challenges on tariffs, population distribution and low incomes, staffing and funding (Lyalabi, 2011), the country has struggled to maintain the rural access rate at 3%. Zimbabwe's agency focused on the electrification of rural income generating activities like Small to Medium scale Manufacturing Enterprises (SMMEs) (Mapako & Prasad, 2007).

Kenya's Rural Electrification Authority started work in 2008. Unlike Zimbabwe, they targeted public facilities and rural trading centres. By May 2013, 25873 schools, health and trading centres had been added to the grid. This brought the national household electrification rate to 26% (Ayieko, 2011). Between 2009 and 2012, Rwanda raised the generating and connections values from 69.5 MW and 110000 to 165 MW and 350000 respectively. Administration centres, health facilities and 50% of all primary and secondary schools were connected to the grid during this period (Uwamahoro, 2013).This raised the overall national access to electricity from 6 to 16%.

Notwithstanding these achievements, there are problems with centralized efforts to rural electrification. In addition to those identified in case of Zambia, Abeeku and Kemaausuor (2009:83-88) have included lack of energy marketing strategies for small systems as a hindrance to narrow the supply-demand gap. Mulugetta, *et al*. (2000) observed that more effort was being directed to a 'Technology push' than to a 'Market pull'. There is also a capacity problem. For example, Kanyarusoke (2013) estimates that tropical countries in the Nile basin alone will need to generate an additional 375 GW to attain present day South Africa's per capita energy consumption by 2050. This, is well beyond present day hydroelectric potential of the basin.

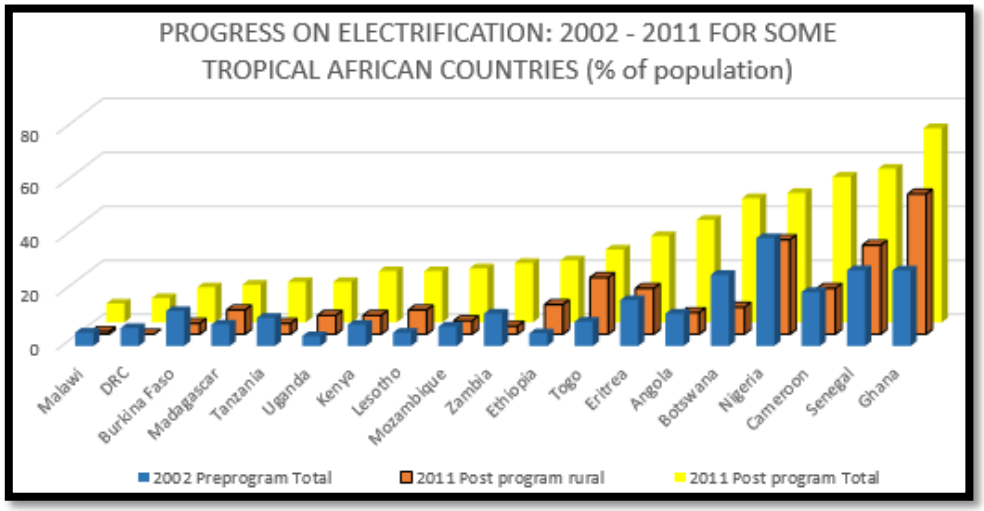

Figure 2.11: Changes in electrification for some countries between 2002 and 2011: Data compiled from National governments publications and IEA (2014).

2.4.2.3 *Actions by individual researchers and entrepreneurs*

Recent actions (i.e. post 2012) by individuals on domestic home applications are described under two subheadings of electrification and heating and refrigeration systems.

Electrification –

The first concern to individual researchers on electrification by PV systems seems to be economic and technical viability. Du Preez *et al*. (2014:2-11) investigated rollout of concentrated power PV systems in rural areas of Eastern Cape Province, South Africa. They found the system socially viable but economically unviable to private investors. A recommendation that government should take over the system as a supplement to normal grid supply was made. In the Western Cape, Votteler et al., (2014:70-80) analysed the solar service industry – and found that customer service was the key issue in the market. Musango and Brent (2015:2-15) mapped out a plan for South Africa to use solar thermal systems to generate electricity. But this was to be on a larger, non-domestic home scale, and found it viable only in the longer term. Mathews and Mathews (2016a:153-159) on the other hand, later reported economic viability for normal flat plate PV systems for medium and high income households in the North Western province. They even reported benefits to municipalities accruing from homes being able to store off peak excess electric energy for use during peak demand periods.

In Uganda East Africa, the issue of economic viability seems to be settled. Kimera, *et al*. (2014:33-43) used HOMER software to study a wind-solar PV mini grid system for a rural village in the eastern part of the country. The system was found to be theoretically viable. In the western part, not only does theory predict viability, but Hakiri, *et al*. (2016:74-81) report multi-dimensional successes in Kebisoni - Rukungiri district. Poverty was alleviated, indoor home air quality improved – and along with it, health; school going children were reading at night; and more importantly, women were reported to be doing business to raise household incomes.

Elsewhere in Africa, Nnadi et al. (2014:61-69) simulated a hybrid wind-solar PV system in South Eastern Nigeria and established theoretical viability. Akuru, Okoro and Maduko (2015:125-134) reported on the potential of using 'Nigeria's abundant solar energy' resources for export to Europe and listed benefits in agriculture, industrialisation and income diversification. In another paper, (Akuru, Okoro and Chikuni, 2015), they investigated the use of residential PV systems and reported a 5.883 Million tonne saving in CO_2 emissions. In very high irradiance areas such as Libya, North Africa, Almaktoof et al. (2016:29-37) conceived the idea of a battery-less PV Reverse Osmosis (RO) system for generating potable water.

In summary, it could be stated that in a number of countries, efforts of electrification using solar energy are being attempted – and for small scale such as at home level, and for water purification purposes, research seems to suggest viability. Okou et al. (2012:52-63) however were concerned about the costs of replacements of batteries and possible effects on the environment. They suggested an electromechanical battery in the form of a fly wheel – but that would be for a bigger system.

Heating and Refrigeration –

Bvumbe and Inambao (2013:16-112) designed and tested a solar powered absorption refrigeration system in Pretoria, South Africa. Alkelani and Kanyarusoke (2016:178-184) designed and tested an inverter-less PV - run refrigeration system for post-harvest cooling of fruit and vegetables for a small farmer harvesting up to 20 kg product a day. De Meyer et al. (2014:36-45) modelled design parameters for solar thermal water heaters but did not test their results. Elhabish and Gryzagoridis (2016:172-177) using several 1.5 m^2 area collectors showed that a square configuration produced a more efficient solar energy conversion unit. Mbadinga (2015) designed and tested an improved fixed water purification system, suitable for rural areas. But Mathews and Mathews (2016b:160-163) redesigned their earlier mobile rural system to achieve a temperature of 57°C by mid-afternoon – which they maintained well above 40°C by 8 pm, resulting in the elimination of most pathogens – including cholera causative agents.

In Nigeria, Okoroigwe, *et al*. (2015:38-51) redesigned a solar-biomass hybrid crop dryer to improve energy efficiencies. They were able to get between 3 and 11 percentage point improvement, depending on the crop being dried. Okonkwo et al. (2015:1058-1064) used reinforced fibre plastic to make a low cost parabolic heater that could produce a temperature range of 60 to 270°C and 33 to 80°C in clear and cloudy skies respectively. In Ethiopia, Tekle (2014:59-66) constructed and tested a pyra-box cooker. A water temperature of 94°C was obtained compared to 88°C from a larger conventional heater.

2.5 Conclusions

In this, chapter, a brief review of literature has been presented mainly as a background general knowledge for the work that follows in successive chapters.

The first sections covered theoretical foundations. It was presented that factors related to Astronomy and Atmospheric Science greatly influence the solar energy reaching the surface of the Earth. Resource estimation methods were reviewed – and the complexity of solar energy utilisation planning was made evident.

Recent examples of developments in resource utilisation in SSA were looked at. Earlier developments were not included at this stage on grounds that relevant ones are covered in subsequent chapters. These developments revealed the following gaps in the state of the art of harnessing solar energy at the domestic level in the region:

- Low level of not only modern energy utilisation but also, of modern ways of harnessing the abundant solar resource.
- Sparse and disjointed optimisation activity of harvesting solar energy. Gaps in application and optimisation on a wider, regional scale are evident.

The gaps - thus identified - form the rationale for this thesis. The aim is to have a set of optimised engineering/technological innovations and recommendations that could be adopted and used at the home level almost anywhere within the SSA region. Realising the infancy of the solar home systems market, the innovations and recommendations were delimited to tackling flat plate solar panel/collector surfaces only. This is because these form the easiest entry point for any home trying to emerge from energy poverty through the solar energy route.

References for chapters 1 and 2.

Abavana, C.G. 2011. Electricity access progress in Ghana. Noxie Consult, Ghana. Available on line at http://www.google.co.za/url?sa=t&rct=j&q=&esrc=s&source=web&cd=1&ved=0CBwQFjAA&url=http%3A%2F%2Fwww.unepdtu.org%2F~%2Fmedia%2FSites%2FUneprisoe%2FWorkshop%2520Presentations%2520(Powerpoints)%2FSE4%2520All%2520Presentations%2Fabavana%2520-%2520electricity%2520access%2520progress%2520in%2520ghana.ashx&ei=I_YzVPPSAYWxaYnsgtAJ&usg=AFQjCNFRyVgW58pefTozicDAnGxZdxsd8Q&sig2=XJtC2d31HuyoJDg3wBXs5A&bvm=bv.76943099,d.d2s [16 June 2014].

Abeeku, B-H., & Kemausuor, F. 2009. Energy for all in Africa — to be or not to be?! *Current Opinion in Environmental Sustainability*, 1(1):83–88, January.

Adeyola, Z.D. & Adedokun, J.A. 1991. Pyrheliometric determination of atmospheric turbidity in the harmattan season over Ile-Ife, Nigeria. *Journal of Renewable Energy*, 1(3-4):555-566.

AfDB: see African Development Bank.

African Development Bank. 2011. *The Middle of the Pyramid: Dynamics of the Middle Class in Africa*. Africa Development Bank. http://www.afdb.org/fileadmin/uploads/afdb/Documents/Publications/The%20Middle%20of%20the%20Pyramid_The%20Middle%20of%20the%20Pyramid.pdf [14th July 2011]

African Development Bank., Organisation for Economic Co-operation and Development. & United Nations Development Programme. 2014. Global Value Chains and Africa's Industrialisation. *African Economic Outlook 2014*, DOI: http://dx.doi.org/10.1787/aeo-2014-en [5 May 2015].

Agbo, S. 2013. Evaluation of the regression parameters of the Angstrom-Page model for predicting global solar radiation. *Journal of Energy in Southern Africa*, 24(2):46-49.

Akpabio, L.E. & Etuk, S.E. 2003. Relationship between global solar radiation and sunshine duration for Onne, Nigeria. *Turkish Journal of Physics*, 27:161-167.

Akuru, U. B., Okoro, O. I., & Chikuni, E. 2015. Impact of renewable energy deployment on climate change in Nigeria. *Journal of Energy in Southern Africa*, 26(3):125-134.

Akuru, U. B., Okoro, O. I., & Maduko. 2015. Harnessing Nigeria's abundant solar energy potential using the DESERTEC model. *Journal of Energy in Southern Africa*, 26(3):105-110.

Alkelani, F. & Kanyarusoke, K.E. 2016. Inverter-less solar assisted farm level refrigeration system for fruits and vegetables. *2016 Proc. of 24th International Commercial Use of Energy Conference, Cape Town 15-17 August 2016*. Cape Town. Cape Peninsula University of Technology: 178-184.

Allen, B. 2015. Atmospheric aerosols: what are they, and why are they so important? NASA website: https://www.nasa.gov/centres/langley/news/factsheets/Aerosols.html [30 May 2016].

Almakatoof, A. M., Raji, A. K., Kahn M. T. E. & Ekhalat, M. A. 2015. Batteryless PV desalination system for rural areas: a case study. *Journal of Energy in Southern Africa*, 26(4):29-37.

Al Riahi, M., Al-Jumaily, K. J. & Ali, H. Z. 1998. Modelling clear weather day solar irradiancy in Baghdad, Iraq. *Energy Conversion and Management*, 39(12):1289-1294.

American Society of Heating, Refrigeration and Air-conditioning Engineers. 2013. Climatic Design Information. *2013 ASHRAE Handbook – Fundamentals* (SI Edition). Chapter 14. http://app.knovel.com/hotlink/toc/id:kpASHRAEB2/ashrae-handbook-fundamentals [5 May 2015].

Ångström, A. 1924: Solar and terrestrial radiation. *Quarterly Journal of Royal Meteorological Society*, 50:121-126.

Arveson, P. 2012. Integrated solar cooking: an underutilised solution. *Perspectives on Science and Christian faith*, 64(1):62-69, March. www.asa3.org/ASA/PSCF/2012/PSCF3-12Arveson.pdf [27 March 2016].

ASHRAE - see American Society of Heating, Refrigeration and Air-conditioning Engineers.

Awachie, I.R.N and Okeke, C.E. 1990. New empirical solar model and its use in predicting global solar irradiation. *Nigerian Journal of Solar Energy*, 9:143-156.

Ayazika, W. 2002. Health related effects of traditional biomass fuels: the Ugandan case study. NEMA DfID KaR Project R8019. Kampala Uganda.

Ayieko, O.Z. 2011. Rural electrification programme in Kenya. Presentation at AEI Practitioner workshop in Dakar, Senegal, Nov 2011.

Battles, J. F., Olmo, F. J., Tovar, J., & Alados-Arboledas, L. 2000. Comparison of cloudless sky parameterisation of solar irradiance at various Spanish mid-latitude locations. *Journal of Theoretical and Applied Climatology*, 66:81–93.

Behrman, D. 1979. *Solar Energy: The awakening Science*. London: Routledge & Kegan Paul Ltd.

Bertarione, S., & Magli, G. 2015. Augustus' power from the stars and the foundation of Augusta Praetoria Salassoorum. *Cambridge Archaeological Journal*, 25(1):1-15.

Bird, R.E. & Hulstrom, R.L. 1981. Review, evaluation, and improvement of direct irradiance models. *Trans. ASME, J. Sol. Energy Engineering*, 103:182–192.

Biron, M. 2016. *Material selection for thermoplastic parts: Practical and advanced information for Plastics Engineers*, Amsterdam: Elservier.

Blank, L.P.E. & Tarquin, A.P.E. 2012. *Engineering Economy* 7th ed. Singapore: Mc Graw Hill.

Bleeker AEM. 2013. Diffusion of solar PV from a TIS perspective and its transnational factors: A case study of Tanzania. Institute of Environmental studies, VU University Amsterdam, 2013. http://english.rvo.nl/sites/default/files/2014/01/Diffusion%20of%20solar%20PV%20-%20A%20case%20study%20of%20Tanzania.pdf [5th May 2015].

BP. See British Petroleum.

British Petroleum. 2014. BP Statistical Review of World Energy June 2014. http://www.bp.com/content/dam/bp/pdf/Energy-economics/statistical-review-2014/BP-statistical-review-of-world-energy-2014-full-report.pdf [6 Oct 2014]

Brooks, M. J., du Clou, S., van Niekerk W. L., Gauché, P., Leonard, C., Mouzouris, M. J., Meyer, R., van der Westhuizen, N., van Dyk, E. E., & Vorster, F. J. 2015. SAURAN: A new resource for solar radiometric data in Southern Africa, *Journal of Energy in Southern Africa*, 26(1):2-10.

Bvumbe, T.J. & Inambao, F.L. 2015. Performance of an autonomous solar powered absorption air conditioning system, *Journal of Energy in Southern Africa*, 26(1):106-112.

Castellano, A., Kendall, A., Nikomarov, M., & Swemmer, T. 2015. Electric Power & Natural Gas Brighter Africa The growth potential of the sub-Saharan electricity sector. Mc Kinsey & Company Report, February 2015:3.

Çengel, Y. A. 2006. *Heat and Mass Transfer: a practical approach* 3rd ed., New York, NY: Mc Graw Hill.

Chaury, A. & Kandpal, T.C. 2010. A techno-economic comparison of rural electrification based on solar home systems and PV microgrids. *Energy Policy*, 38:3118–3129.

Chendo, M.A.C. & Maduekwe, A.A.L. 1994. Hourly distributions of global and diffuse solar radiation in Lagos, Nigeria, *Renewable Energy*, 4(1):101-108.

Chien, Z-J., Cho, H-P., Jwo, C-S., Chao, C-C, Chen, S-L & Chen, Y-L. 2013. Eperimental investigation on an absorption Refrigerator driven by solar cells. International Journal of Photoenergy, 2013. http://dx.doi.org/10.1155/2013/490124 [10 June 2016].

Chukwuemeka, A. & Nnabuchi, M.N. 2009. Solar Radiation in Port Harcourt: Correlation with Sunshine Duration. *The Pacific Journal of Science and Technology*, 10(1):681-685.

Corona Technologies. (n.d.). Overview of solar technologies. http://www.coronatech.net/ [14th July 2011]

David, A. and Ngwa, N.R. 2013. Global solar radiation of some regions of Cameroon using the linear Angstrom and non-linear polynomial relations (Part I) Model development. *International journal of Renewable Energy Research*, 3(4):984-992.

De Meyer, O., Okou, R., Sebitosi, A. B. & Pillay, P. 2014. Practical considerations for low pressure solar water heaters in South Africa. *Journal of Energy in Southern Africa*, 25(3):36-45.

Diabaté, L., Blanc, Ph., & Wald, L. 2004. Solar radiation climate in Africa. *Solar Energy*, 76: 733-744.

Du, J., Huang, L., Min, Q., & Zhu, L. 2013. The influence of water absorption in the 290-50 nm region on solar radiance: Laboratory studies and model simulation. *Geophysical Research Letters*, 40:4788-4792.

Duffie, J.A. & Beckman, W.A. 2006. *Solar Engineering of Thermal Processes.* 3rd ed. Hoboken, NJ: John Wiley & Sons.

Duffie, J.A. & Beckman, W.A. 2013. *Solar Engineering of Thermal Processes.* 4th ed. Hoboken, NJ: John Wiley & Sons.

Dugaria, S., Padovan, A., Sabatelli, V., & Del Col, D. (2015). Assessment methods of DNI resource in solar concentrating systems. *Solar Energy*, 121 (2015) 103-115.

Du Preez, M., Beukes, J. & van Dyke, E. 2014. A cost analysis of concentrator PV technology in South Africa: a case study. *Journal of Energy in Southern Africa*, 24(4):2-11.

Ehleringer, J.R & Hammond, S.D. 1987. Solar tracking and photosynthesis in cotton leaves. *Agricultural and Forest Meteorology*, 39: 25-35.

Elhabish, A. & Gryzagoridis, J. 2016. Optimising flat plate solar collector geometry for a solar water heating system. *2016 Proceedings of the 24th Domestic Use of Energy Conference, Cape Town 30th-31st March 2016.* Cape Town: Cape Peninsula University of Technology: 172-177.

Elshazly, S.M. 1996. A study of Linke turbidity factor over Qena, Egypt. *Advances in Atmospheric Sciences*, 13(4):519-532.

Elusakin, J.E., Ajide, O.O., & Diji, J.C. 2014. Challenges of sustaining off-grid power generation in Nigeria rural communities. *African Journal of Engineering Research* 2(2):51-57.

Encrenaz, T., Bibring, J.P., Blanc,M., Barucci, M.A., Roques, F.& Zarka, P.H. 2004. *The Solar System.* 3rd ed. Berlin: Springer.

Erbs, D.G., Klein, S.A. & Duffie, J.A. 1982. Estimation of the diffuse radiation fraction hourly, daily, and monthly-average global radiation. *Solar Energy*, 28(4):293-304.

European Commission and Heliochem-1, 2008. Africa - Photovoltaic Solar Electricity Potential. http://www.soda-is.com/eng/map/maps_for_free.html [6 Oct 2014]

Gana, N.N., Rai, J.K. & Momoh, M. 2014. Angstrom Constants for Estimating Solar Radiation in Sokoto, North-Western, Nigeria. *International Journal of Scientific & Engineering Research*, 5(1):1636-1647.

Garcia, J.V. 1994. *Principios F'iscos de la Climatolog'ia*. Ediciones UNALM Lima, Peru: Universidad Nacional Agraria La Molina.

Glover, J. & Mc Culloch, J. S. G. 1958. The empirical relation between solar radiation and hours of bright sunshine in the high-altitude tropics. *Quarterly Journal of the Royal Meteorological Society* 84(359):56–60.

Goel, N. 2007. Solar Radiation Data. In Kreith, F. & Goswami, D.Y. (eds). Handbook of Energy Efficiency and Renewable Energy. Boca Raton, FL: Taylor & Francis Group: A2-1 to A2-21.

Gopinathan, K.K. 1988. A simple method for predicting global solar radiation on a horizontal surface. *Solar & Wind Technology*, 5(5):581-583.

Green, M.A. 2001. Photovoltaic Physics and devices. In Gordon J (Ed.). *Solar Energy The state of the Art. ISES position papers*. London, UK: James & James, 291-355.

Greenspec. 2016. Solar hot water collectors. http://www.greenspec.co.uk/building-design/solar-collectors/ [10 June 2016].

Gueymard, C.A. 1995. SMARTS2: A simple model of the atmospheric radiative transfer of sunshine: algorithms and performance assessment. Florida Solar Energy Center/University of Central Florida. http://instesre.org/GCCE/SMARTS2.pdf [15th April 2016]

Gueymard, C.A. 2003. Direct solar transmittance and irradiance predictions with broadband models. Part I: detailed theoretical performance assessment. *Solar Energy*, 74:355–379.

Gueymard, C.A. 2014. Impact of onsite atmospheric water vapour estimation methods on the accuracyof local solar irradiance predictions. *Solar Energy*, 101:74-82.

Gueymard, C.A. & Myers, D.R. 2009. Evaluation of conventional and high-performance routine solar radiation measurements for improved solar resource, climatological trends, and radiative modelling. *Solar Energy*, 83:171–185.

Gueymard, C.A. & Wilcox, S.M. 2011. Assessment of spatial and temporal variability in the US solar resource from radiometric measurements and predictions from models using ground-based or satellite data. *Solar Energy*, 85:1068–1084.

Gustavsson, M. & Ellegard, A. 2004. The impact of solar home systems on rural livelihoods: experiences from the Nyimba Energy Service Company in Zambia. *Review, Energy*, 29:1059-1072.

Hakiri, J., Moyo, A., & Prasaad, G. 2016. Assessing the role of solar home systems in poverty alleviation: Case study of Rukungiri district in Western Uganda (November, 2015). *2016 Proceedings of the 24th Domestic Use of Energy Conference, Cape Town 30th-31st March 2016.* Cape Town: Cape Peninsula University of Technology: 74-81.

Hargreaves, G. & Samani, Z. 1982. Estimating potential evapotranspiration. *Journal of Irrigation drainage Engineering, (USA)*, 108:225-230.

Hermann, W. 2006. Quantifying global exergy resources. *Energy*, 31(12): 1349, 2006.

Ibeh, G.F, Agbo, G. A., Agbo., P.E & Ona. 2012. Comparison of Artificial Neural Network (ANN) and Angstrom-Prescott models in correlation between sunshine hours and global solar radiation of Uyo city, Nigeria. *Archives of Applied Science Research*, 4(3):1213-1219.

IEA *see* International Energy Agency.

Index Mundi. 2015. Country Comparison: Electricity consumption per capita. www.indexmundi.com/g/r.aspx?v=81000 [29 June 2016].

International Energy Agency. 2011. Renewables and Waste in Africa in 2008. http://www.iea.org/stats/renewdata.asp?COUNTRY_CODE=11 [30 June 2011].

International Energy Agency. 2013. *World Energy Outlook* (2013). http://www.worldenergyoutlook.org/resources/energydevelopment/energyaccessdatabase/ [6 October 2014].

International Energy Agency. 2014a. *Africa Energy Outlook. A Focus on prospects in sub-Saharan Africa. World Energy Outlook special Report, 2014.* Paris: OECD/IEA.

International Energy Agency. 2014b. *Key World Energy Statistics*. http://www.iea.org/publications/freepublications/publication/KeyWorld2014.pdf [6 Oct 2014].

Innocent, A. J., Jacob, O.E., Chibuzo, G.C., James, I. & Odeh, D.O. 2015. Estimation of global solar radiation in Gusau, Nigeria. *IMPACT: International Journal of Research in Engineering & Technology (IMPACT: IJRET)*, 3(2):27-32, February.

Iqbal, M. 1983. *An Introduction to Solar Radiation*. Toronto: Academic Press.

Johansson, T.B., Kelly, H., Reddy, A.K.N. & Williams, R.H. 1993. *Renewable Energy Sources for Fuels and Elecxtricity*. Washington D.C.: Island Press.

Juanicó, L. & Dilalla, N. 2014. Optimization of the hose-based low - cost solar collector. *International Journal of Renewable Energy & Biofuels*, 2014 (2014), Article ID 344621, DOI: 10.5171/2014.344621. http://ibima.net/articles/IJREB/2013/344621/344621.pdf [29 June 2016].

Jurik, T.W. &. Akey, W.C. 1994. Solar-tracking leaf movements in velvetleaf (Abutilon Thephrasti). *Vegatatio*, 112: 93-99.

Kalogirou, S.A. 2004a. Solar thermal collectors and applications. *Progress in Energy and Combustion Science*, 30:231–295.

Kalogirou, S. A. 2004b. Environmental benefits of domestic solar energy systems, *Energy Conversion and Management*, Vol. 45(18-19):3075-3092.

Kalogirou S. A. (2014). *Solar Energy Engineering Processes and Systems* 2nd ed. New York (NY), Elsevier.

Kane, A., & Leedy, T. H. (2013). *African migrations: Patterns and Perspectives*. Indiana Bloomington (IN), University Press.

Kanyarusoke, K. 2013. Water and energy needs in a developing Nile Basin. *The New Vision*, Kampala Uganda. Jul 22, 2013. www.newvision.co.ug/new_vision/news/1326864/water-energy-developing-nile-basin [5 May 2015].

Kanyarusoke, K. E., Gryzagoridis, J. & Oliver, G. 2012. Predicting photovoltaic panel yields in sub-Sahara Africa. *Proceedings of International Conference on Engineering and Applied Science 2012, Beijing, China, 24-27 July 2012*. Beijing: ICEAS: 223-255.

Karekezi, S. & Kithyoma, W. 2003: Renewable energy development - Renewable Energy in Africa: Prospects and Limits**.** *Proceedings of the workshop for African Energy Experts on Operationalizing the NEPAD Energy Initiative, 2- 4 June, 2003*. Dakar, Senegal: 1-27.

Kerker, M. 1982. Lorenz-Mie scattering by spheres: some newly recognised phenomena. *Aerosol Science and Technology*, 1(3):275-291.

Kimera, R., Okou, R., Sebitosi, A., B., Kehinde A. 2014. Considerations for a sustainable hybrid mini-grid system: a case for Wanale village, Uganda. *Journal of Energy in Southern Africa*, 25(1):33-43.

Klippel, N. & Nussbaumer, T. 2007. Health relevance of particles from wood combustion in comparison to Diesel soot, *Proceedings of 15th European Biomass Conference, International Conference Berlin, 7-11 May 2007*. Berlin: 7–11. www.verenum.ch/Publikationen/W1612Berlin2007.pdf [6 October 2014].

Kumar, D.S. 2015. *Heat and Mass Transfer* 9th ed. Luthiana Punjab, India: S.K. Kataria & Sons.

Lam, J. C. & Li, D.H.W. 1996. Correlation between global solar radiation and its direct and diffuse components. *Building and Environment*, 31(6):527-535.

Lealea, T. & Tchinda, R. 2013. Estimation of diffuse solar radiation in the north and far north of Cameroon. *European Scientific journal*, 9(18):370-381.

Le Baron, B.A., Michalsky, J.J. & Perez, R.R. 1990. A simple procedure for correcting shadow band data for all sky conditions. *Solar Energy*, 44:249-256.

Linke, F. 1922. Transmissions-Koeffizient und Tru¨bungsfaktor. *Beitr. Phys. fr. Atmos*. 10:91–103.

Liou, K.N. 2002. *An introduction to atmospheric radiation* 2 ed. San Diego, CA: Elservier Science (USA).

Liu, B.Y.H., & Jordan, R.C. 1962. Daily insolation on surfaces tilted towards the equator. *Transactions* of the ASHRAE, 67:526–541.

Lloyd, P. 2014. Challenges in household energisation and the poor. *Journal of Energy in Southern Africa*, 25(2):2-8.

Louche, A., Notton, G., Poggi, P. & Simonnot, G. 1991. Correlations for direct normal and global horizontal irradiations on a French Mediterranean site. *Solar Energy*, 46(4):261-266.

Lorenz, L. 1890. Lysbevægelsen I og uden for en af plane Lysbølger belyst Kugle. *Vindenstabernes Selskabs Skrifter* 6:2-62.

Luque, A. 1991. Photovoltaic concentration. In Treble F. C. (Ed.). *Generating electricity from the sun*. Oxford, England: Pergamon, 177-227.

Lyalabi, S. 2011. REA's experience in implementing rural electrification projects. Presentation at AEI Practitioner workshop in Dakar, Senegal, Nov. 2011. http://siteresources.worldbank.org/EXTAFRREGTOPENERGY/Resources/717305-1327690230600/8397692-1327691245128/Implementing_REAs_ZAMBIA.pdf [6 Oct 2014]

Madkour, M. A., El-Metwally M. & Hamed A.B. 2006. Comparative study on different models for estimation of direct normal irradiance (DNI) over Egypt atmosphere. *Renewable Energy* 31:361–382

Mapako M., & Prasad, G. 2007. Rural electrification in Zimbabwe reduces poverty by targeting income generating activities. CSIR, ECR, University of Cape Town. http://hdl.handle.net/10204/871 [6 October 2014].

Mathews, G. E. and Mathews E. H. (2016a). Household photovoltaics – A worthwhile investment? *2016 Proceedings of the 24th Domestic Use of Energy Conference, Cape Town 30th-31st March 2016.* Cape Town: Cape Peninsula University of Technology: 153-159.

Mathews, G. E. and Mathews E. H. (2016b). A redesign of a mobile solar water heater for rural housing in Southern Africa. *2016 Proceedings of the 24th Domestic Use of Energy Conference, Cape Town 30th-31st March 2016.* Cape Town: Cape Peninsula University of Technology: 160-163.

Maxwell, E.L. 1987. A quasi-physical model for converting hourly global to direct normal insulation. SERI/TR-215-3087. SolarEnergy Research Institute Golden, Co.

Mbadinga, P. K. J. 2015. A solar water purification system for rural areas. Unpublishrd MTech. Dissertation. Cape Peninsula University of Technology, Cape Town.

Medugu, D.W. & Yakubu, D. 2011. Estimation of mean monthly global solar radiation in Yola – Nigeria using angstrom model, *Advances in Applied Science Research*, 2 (2): 414-421.

Mie, G. 1908. Beiträge zur Optik trüber Medien, speziell kolloidaler Metallösungen. *Annalen der physic*, 25:377-445.

Milborrow, D. 2001. Wind energy review. In Gordon J (ed). *Solar Energy The state of the Art. ISES position papers*. London, UK: James & James: 653-698.

Moner-Girona, M. 2009. A new tailored scheme for the support of renewable energies in developing countries. *Energy Policy*, 37:2037-2041

Morrison, G. L. 2001. Solar Water heating. In Gordon J (ed). *Solar Energy The state of the Art. ISES position papers*. London, UK: James & James: 223-289.

Mubiru, J. 2011. Using Artificial Neural Networks to Predict Direct Solar Irradiation. *Advances in Artificial Neural Systems*, 2011, doi:10.1155/2011/142054. www.hindawi.com/journals/aans/2011/142054/ [20 May 2016].

Mugarza, A., Shimiu, T. K., Ogletree, D. F., and Salmeron M. 2009. Chemical reactions of water molecules on Ru(0 0 0 1) induced by selective excitation of vibrational modes. *Surface Science*, 603(13):2030-2036.

Mulugetta, Y., Nhete, T. & Jackson, T. 2000. Photovoltaics in Zimbabwe: Lessons from the GEF Solar Project. *Energy Policy*, 28:1069-1080.

Musango, J.K. & Brent, A.C. 2015. A road map framework for solar aided power generation in South Africa. *Journal of Energy in Southern Africa*, Vol. 26 (4):2-15.

Muyimbwa, D. 2016. Ground based and satellite remote sensing of atmospheric aerosols and ultraviolet solar radiation. Unpublished PhD Thesis. The University of Bergen.

Myers, D.R. 2009. Comparison of historical satellite-based estimates of solar radiation resources with recent rotating shadow band radiometer measurements. Conference Paper NREL/CP-550-45375 March 2009. http://www.osti.gov/bridge

Myers D.R. 2013. *Solar Radiation Practical Modelling for Renewable Energy Applications*. Florida: Boca Raton: Taylor and Francis.

NASA *see* National Aeronautics and Space Administration.

National Aeronautics and Space Administration. 2001. *Aphelion Away! On the 4th of July Earth will be at its greatest distance from the Sun -- an annual event called "aphelion."* **http://science.nasa.gov/science-news/science-at-nasa/2001/ast04jan_1/** [4th July 2011]

NASA National Administration of Space Agency https://www.nasa.gov/centres/langley/news/factsheets/Aerosols.html

Nieuwenhout, F.D.J., van Gijk, A., Lasschuit, P.E., van Rockel, G., van Dijk, V.A.P., Hirsch, D., Arriaza H, Hankins M, Sharma, B.D., Wade, H., 2001. Experience with Solar Home Systems in Developing Countries: A Review. *Progress in Photovoltaics: Research and Applications*, 9(9):455-474.

Nkwetta, D.N., Smyth, M., Thong, V.V., Driesen, J., & Belmans, R. 2010. Electricity supply, irregularities, and the prospect for solar energy and energy sustainability in sub-Saharan Africa, *J. Renewable & Sustainable Energy* 2, 023102(2010); doi: 10.1063/1.3289733. http://dx.doi.org/10.1063/1.3289733 [6 October 2014].

Nnadi, D.B.N., Odeh, C. I., & Omeje, C. 2014. Use of hybrid solar-wind energy generation for remote area electrification in South Eastern Nigeria. *Journal of Energy in Southern Africa*, 25(2):61-69.

Norton, 2001. Solar process heat: distillation, drying, agricultural and industrial uses. In Gordon J (ed). *Solar Energy The state of the Art*. *ISES position papers*. London, UK: James & James, 477-496.

Nwokoye, A.O.C. & Okonkwo, G.N. 2014. Testing the Predictive Efficiencies of Four Angstrom-Type Models for estimating Solar Radiation in Bida Nigeria, IOSR *Journal of Applied Physic*s (IOSR-JAP), 6(3):15-17.

Obiang, C. 2016. Integrated solar photovoltaic and thermal system for enhanced energy efficiency. Unpublished MTech. Dissertation, Cape Peninsula University of Technology, Cape Town.

Ogolo, E. 2010. Evaluating the performance of some predictive models for estimating global solar radiation across varying climatic conditions in Nigeria. *Indian journal of radio and space Physics*, 39:121-131, June.

Ogolo, E. 2014. Estimation of global solar radiationin Nigeria using a modified Angstrom model and the trend analysis of the allied meteorological components. *Indian journal of radio and space Physics*, 43:213-224, June.

Okonkwo, W.I., Echiegu, E.A., Ogbuisi, N.J. & Liberty, J.T. 2015. Characterisation of a fibre reinforced plastic concentrating solar cooker. *International Journal of Innovation and Applied Studies*, 10(4):1058-1064.

Okoroigwe, E. C., Ndu, E.C. & Okoroigwe, F.C. (2015). Comparative evaluation of the performance of an improved solar-biomass hybrid dryer. *Journal of Energy in Southern Africa*, 26(4):38-51.

Okou, R., Sebitosi, A.B. & and Pillay, P. (2012). A specification of a flywheel battery for a rural South African village. *Journal of Energy in Southern Africa*, 23(3):52-63.

Okundamiya, M.S., Emagbetere, J.O, & Ogujor, E.A. 2015. Evaluation of Various Global Solar Radiation Models for Nigeria, *International Journal of Green Energy*, DOI: 10.1080/15435075.2014.968921 http://dx.doi.org/10.1080/15435075.2014.968921 [29 June 2016].

Orgill, J.F., & Hollands. K.G. 1977. Correlation equation for hourly diffuse radiation on a horizontal surface. *Solar Energy* 19(4):357–359.

Oyedope, S.O. 2012. Energy and Sustainable development in Nigeria: The way forward. *Energy, Sustainability and Society*, 2:15. http://www.energsustainsoc.com/content/2/1/ [29 June 2016].

Pai, A.D., Escobedo, J.F., Martins, D., & Teramoto, E.T. 2014. Analysis of hourly global, direct and diffuse solar radiations attenuation as a function of optical air mass. *Energy Procedia* 57: 1060-1069.

Perez, R., Ineichen, P., Seals, R. & Zelenka, A. 1990. Making full use of the clearness index for parameterizing hourly insolation conditions. *Solar Energy*, 45:111–114.

Perez, R., Ineichen, P., Maxwell, E., Seals, R., and Zelenka, A. 1992. Dynamic global –to-Direct Irradiance Conversion Models. *ASHRAE Transactions Research Series*: 354-369.

Perez, R., Ineichen, P., Moore, K., Kmieccik, M., Chain, C., George, R. and Vignola, F. 2002. A new operational model for satellite-derived irradiances: description and validation. *Solar Energy* 73(5):307–317.

Perez, R., Ineichen, P., Kmiecik, M., Moore, K., Renne, D., & George, R. 2004. Producing satellite-derived irradiances in complex arid terrain. *Solar Energy*, 77:367–371.

Pope, R.M. & Fry, E.S. 1997. Absorption spectrum (380 – 700 nm) of pure water. II Integrating cavity measurements. *Journal of Applied Optics*, 36:8710-8723.

Population Reference Bureau. 2015. World Population Data sheet. USAID, www.prb.org/pdf15/2015-worlld-population-data-sheet_eng.pdf [29 June 2016].

Prescott, J. A. 1940. Evaporation from a water surface in relation to solar radiation. *Transactions of the Royal Society of South Australia*, 64:114-125.

Quansa, E., Amekudzi, L.K., Preko, K., Aryee, J., Boakye, O. R., Boli, D. & Salif, M. 2014. Empirical models for estimating global radiation over Ashanti region of Ghana. *Journal of Solar Energy*, 2014, doi. 10.1155/2014/897970, http://dx.doi.org/10.1155/2014/897970 [21 May 2016].

Rabah, K.V.O. 2005. Integrated solar energy systems for rural electrification in Kenya. *Renewable Energy*, 30(23-42).

Rayleigh, (Strutt J). 1871. On the scattering of light by small particles. *Philosophical Magazine*, 41(4):447-454.

Reindl, D.T., W.A. Beckman, & J.A. Duffie. 1990. Evaluation of hourly tilted surface radiation models. *Solar Energy*, 45:9–17.

Renné, D.S., Wilcox, S., Marion, W., Maxwell, G.L., Rymes, M. & Phillips, J. 2007. Solar Energy. In Kreith, F. & Goswami, D.Y. (eds.). *Handbook of Energy Efficiency and Renewable Energy*. Boca Raton, FL: Taylor & Francis Group: 19.3.

Rietveld, M.R. 1978. A new method for estimating the regression coefficients in the formula relating solar radiation to sunshine. *Agricultural Meteorology*, 19(2-3):243-252.

Salima, G. & Chavula, G.M.S. 2012. Determining Angstrom constants for estimating solar radiation in Malawi. *International Journal of Geosciences*, 3:391-397.

Sambo, A.S., Zarma, I.H., Uguoke, P.E., Dioha, I. J. & Ganda, Y.M. 2014. Implementation of standard solar PV projects in Nigeria. *Journal of Energy Technologies and Policy*, 4(9):22-28.

Sayigh, A.A.M. 1991. Photovoltaic and Solar radiation. In Treble, F.C. (Ed.). *Generating electricity from the sun*. Oxford, England: Pergamon, 5-15.

Schillings, C., Meyer R. & Trieb, F. 2004. Solar and wind energy resource assessment (SWERA). High resolution solar radiation assessment for Kenya. Final country report, UNEP / GEF October 2004.

Schwadron, N.A., Mc Comas, D.J., Elliott, H.A., Gloeckler, G., Geiss, J. & von Steiger, R. 2005. Solar wind from the coronal hole boundaries. *J. Geophys. Res*., 110, A04104, doi:10.1029/2004JA010896

Shafey, H.M. & Ismail, I.M. 1990. Thermodynamics of the conversion of solar radiation. *Journal of Solar Energy Engineering*, 112: 140, 1990.

Skartveit, A., Olseth, J.A. & Tuft, M. E. 1998. An hourly diffuse fraction model with correction for variability and surface albedo. *Solar Energy*, 63:173-183.

Sözen, A., Arcaklıoğlu, E., Özalp, M., & Çağlar, N. 2004. Forecasting based on neural network approach of solar potential in Turkey. *Renewable Energy 30*:1075–1090.

Spencer, J.W. 1982. A comparison of methods for estimating hourly diffuse solar radiation from global solar radiation. *Solar Energy*, 29(1):19-32.

Suri, M. & Cebecauer, T. 2014. Satellite-based solar resource data: model validation statistics versus user's uncertainty. Paper Presented at ASES SOLAR 2014 Conference, San Francisco, 7-9 July 2014.

Szabó, S., Bódis, K., Huld, T., Moner-Girona, M. 2011. Energy solutions in rural Africa: mapping electrification costs of distributed solar and diesel generation versus grid extension. *Environmental Research Letters*, 6 (2011) 034002. doi:10.1088/1748-9326/6/3/034002 http://iopscience.iop.org/article/10.1088/1748-9326/6/3/034002/pdf [29 June 2016].

Tagirov, R.V. & Tagirov, L.P. 1997. Lambert formula – Bouguer absorption law? *Russian Physics Journal*, 40(7):664-669.

Tekle, A. 2014. Experimental assessment on thermal performance and efficiency of pyra-box solar cooker. *Journal of Energy Technologies and Policy*, 4(7):59-66.

Tiwari, G.N. 2002. *Solar Energy Fundamentals, Design, Modelling and Applications*. New Delhi, India: Narosa.

Treble, F.C. 1991. Photovoltaic systems. In Treble F.C. (Ed.). Generating electricity from the sun. Oxford, England: Pergamon, 78-96.

Tsoutsos, T., Franteskaki, N., & Gekas, V. 2005. Environmental impact from the solar energy technologies, *Energy Policy*, 33:289-296.

Tymvios, F.S., Jacovides, C.P., Michaelides, S.C. & Scouteli, C. 2005. Comparative study of Ångström's and artificial neural networks' methodologies in estimating global solar radiation, *Solar Energy*, 78 (2005) 752–762.

UN 2010. The World's women 2010. http://unstats.un.org/unsd/demographic/products/Worldswomen/WW2010%20Report_by%20chapter(pdf)/Environment.pdf [6 Oct 2014].

United States Department of Energy, (n.d.). Energy Efficiency and renewable Energy: History of Solar. **http://www1.eere.energy.gov/solar/pdfs/solar_timeline.pdf** [30th June 2011]

Uwamahoro, Y. 2013. Rural electrification in Rwanda. PACEAA Available on line at: http://www.paceaa.org/workshops/Rwanda%20Training%20Workshop/02.%20Overview%20Of%20The%20Rural%20Electrification%20Strategy%20In%20The%20Country%20%20.pdf [6 Oct 2014].

Vignola, F. & McDaniels, D.K. 1986. Beam-global correlations in the Northwest Pacific. *Solar Energy*, 36(5):409-418.

Votteler, R., Hough, J. & Venter, C. 2014. An analysis of the solar service provider industry in the Western Cape, South Africa. *Journal of Energy in Southern Africa*, 25(2):70-80.

Wang, D. Liu, Y., Wang, Y., & Liu, J. 2015. Design performance of demonstration house with active solar heating in the Qinghai – Tibet plateau region. *Journal of Building Physics*, 40(1):55-76.

Warren, S.G., Brandt, R.E. & Grenfell, T.C. 2006. Visible and near-ultraviolet absorption of ice from transmission of solar radiation into snow. *Journal of Applied Optics*, 45(21):5320-5334, July.

Weiss, W. (nd). Solar Radiation, AEE INTEC, Austria. http://www.crses.sun.ac.za/files/services/events/workshops/02_Solar_Radiation%20and%20Measuring.pdf. [30 May 2016]..

Weissler, G.I., Lee P., & Mohr, E.I. 1952. Absolute absorption coefficients of Nitrogen in the vacuum ultraviolet, *Journal of the optical society of America*, 42(2):84-92.

Whillier A. 1953. Solar energy collection and its utilisation for house heating. ScD Thesis, MIT, Cambridge, MA.

WHO: see World Health Organisation.

Wieder S. 1982. *An introduction to solar energy for Scientists and Engineers*. John Wiley & sons New York, USA.

Williams. 1994. Energy supply options for low income urban households. Paper No. 11, University of Cape Town.

Winston, R. 2001. Solar concentrators. In Gordon J (ed). *Solar Energy The state of the Art*. *ISES position papers*. London, UK: James & James, 357-436.

Wong, L.T. & Chow, W.K. 2001. Solar radiation model. Applied Energy, 69:191-224.

World Bank. 2015. Fact sheet: The World Bank and Energy in Africa, http://ideas4development.org/medias/2015/07/M3640N-3-39n@ilo-org_20150714_121049.pdf [29 June 2016].

World Health Organization (WHO): Air quality Guidelines for particulate matter, ozone, nitrogen, dioxide and sulphur dioxide, Global Update 2005, 2006.

Yu, J-Y. nd. Composition and structure of the atmosphere. www.ess.uci.edu/~yu/class/ess5/chapter.1.composition.all.pdf [21 May 2016]

Zelenka, A., Perez, R., Seals, R. & Renne,´ D. 1999. Effective accuracy of satellite-derived irradiance. *Theoretical and. Applied Climatology*, 62:199–207.

Zelenka, A. 2001. Satellite models. In Gordon J (ed.) *Solar Energy: The state of the Art ISES position papers*. James & James, London: 534.

Zell, H. 2015. Earth's atmospheric layers. NASA, www.nasa.gov/mission_papers/sunearth/Science/atmosphere-layers2.html [21 May 2016].

Zhang, M., Dai, S. & Song, Y. 2015. Decomposition analysis of energy-related CO_2 emissions in South Africa, *Journal of Energy in Southern Africa*, 26(1):67-73.

CHAPTER THREE:

FIRST ARTICLE:

"VALIDATION OF TRNSYS MODELLING FOR A FIXED SLOPE PHOTOVOLTAIC PANEL"

Kant KANYARUSOKE; Jasson GRYZAGORIDIS, Graeme OLIVER

Turkish Journal of Electrical Engineering & Computer Sciences: September 2015 - online document doi: 10.3906/elk-1502-38:
Turk J Elec Eng & Comp Sci (2016) 24: 4763 – 4772 © TÜBİTAK

3.0 Introducing the paper

The literature survey presented in chapter 2 revealed wide gaps in sub-Sahara Africa's electrification and use of modern energy forms at the home level. It also revealed that although there is general agreement that annual insolation in the region is higher than the one in the temperate lands, reliable measurements on the continent are scarce and sparse.

The first issue for Research and Development (R&D) targeting the entire region was to have a good estimating tool for the levels of solar energy. From the several that are available, a transient system simulation software (TRNSYS) was selected because of its fairly extensive weather data - based on long period (40 years + for some places), and its versatility in handling electrical, mechanical and Thermo-fluids systems. Moreover, its libraries were extendable to include new devices that a designer/innovator may come up with. The software needed to be validated to build the confidence necessary to use it on a wide scale. Hence, this chapter describes the procedure which was used to validate a TRNSYS model for estimating the yield of electricity from a fixed slope photovoltaic (PV) panel. The issue on hand was: Would the modelling give a reliable prediction of energy yield for places near the software's listed stations? If so, then one could proceed to apply it in the region.

3.1 The paper

Turkish Journal of Electrical Engineering & Computer Sciences
http://journals.tubitak.gov.tr/elektrik/
Research Article

Turk J Elec Eng & Comp Sci
(2016) 24: 4763 – 4772
© TÜBİTAK
doi:10.3906/elk-1502-38

Validation of TRNSYS modelling for a fixed slope photovoltaic panel

Kant KANYARUSOKE*, Jasson GRYZAGORIDIS, Graeme OLIVER
Mechanical Engineering Department, Cape Peninsula University of Technology, Cape Town, South Africa

Received: 07.02.2015 • **Accepted/Published Online:** 09.09.2015 • **Final Version:** 06.12.2016

Abstract

TRNSYS stands for "transient system simulation" software. This paper describes a procedure which was used to validate a TRNSYS model for estimating electricity yields from a fixed slope Photovoltaic (PV) panel. The objective was to find how close to reality predicted energy yield for a specified panel can be - at a location near one of the weather stations listed in the software's data base. The software was used to predict daily total incident radiation on a horizontal plane and electrical energy yields from a 90 Wp panel when sloped at 34° facing North at a test site in Cape Town, South Africa. The panel and other system components were then installed and tested to give actual electrical energy yields. The site was 5 km from a TRNSYS listed weather station. A local weather station logging 10 minute data of actual total incident radiation on a horizontal plane enabled comparison with the model's estimate. Analysis of electrical energy yield gave statistical kappa values of 0.722 and 0.944 at actual to model acceptance ratio levels of 90% and 80%, respectively. Regression analysis of measured and model incident horizontal plane energy gave a coefficient of 0.782 across the year. It was thus concluded that within limits of meteorological phenomena behaviour, TRNSYS modelling reliably predicted energy yields from the PV panel installed in the neighbourhood of one of the software's listed stations.

Key words: TRNSYS, PV panel, solar radiation, horizontal surface radiation, electricity yield

3.1.1 *Introduction*

Many people in least developed countries do not have access to electricity. In tropical Africa for example, out of a mid-2013 population of about 880 million people [1], 591 million had no access to electricity [2]. Attempts at electrifying the region through national grids have made little impact. In some cases, hopes for a quick solution have faded. In Tanzania for example, Bleeker reports that 90% of the population rely on paraffin for lighting [3]. He adds that connecting to the grid in future is doubtful because of high grid extension costs. In Nigeria, there is 60%-70% inaccessibility. Moreover, the crisis is expected to continue until renewable energy and energy efficiency are aggressively pursued [4]. Sambo et al. [5] list issues - such as the use of substandard parts - to be addressed in getting quality PV installations in the country.

PV panels are assemblies of current generating cells. The total current generated is primarily a function of the amount of solar radiation incident on the panel and the number of cells arranged in parallel. The panel voltage depends mainly on the number of cells connected in series and mildly on incident radiation. A MATLAB based method to estimate actual energy output of a panel at a given location is described in [6]. A simpler model is given in [7]. Furthermore, there is industry specific software to assist in different design and selection circumstances. It includes PVsyst, RETScreen, PVWatts, HOMER, and WATSUN-PV among others [8-13].

Many of these are better suited for large systems. Mottillo et al. [13] for example modelled a 56-m^2 array in WATSUN-PV. When they modelled the same system in TRNSYS on 4 different days, results were reported to agree with experimental data on sunny days but to underestimate yields on cold and on cloudy days. A smaller 9.29-m^2 panel area is reported by Mao et al. [14] in a TRNSYS - PVF-CHART simulation comparison. Although close agreement between the two is reported, no experimental data to validate the models are given.

In Malaysia, Al Riza et al. [15] simulated 4 parallel connected 100 Wp multi-crystalline silicon PV panels in TRNSYS. They validated the model over a period of 10 days and concluded that for a 1.2 kWh daily lighting load the model adequately predicted the yield.

The work being reported now considered an even smaller standalone system, such as one suitable for a homestead attempting to emerge from energy poverty. Would TRNSYS modelling give a reliable energy yield prediction for this home across a period longer than indicated in the above citations? In answer to this question, the rest of the paper is organized as follows: Section 3.1.2 describes a sample PV system layout to serve the home; Section 3.1.3 introduces the TRNSYS PV model. Experimental work to validate it at a location in the neighbourhood of one of the software's listed weather stations is described in Section 3.1.4. Results are analysed and conclusions drawn in sections 3.1.5 and 3.1.6, respectively.

3.1.2. *PV system for an energy poor home*

For purposes of this work, we define an energy poor home as that in which electricity is not being used. Apart from muscle power, the other sources of energy are mainly biomass, used for cooking and lighting. Some energy poor homes also use kerosene for lighting. When sufficient funds become available to support self-generation, it is supposed that lighting receives first priority. Consequently, a standalone PV panel system is more likely to be the first step in overcoming energy poverty for those with no hope of accessing the grid.

3.1.2.1 *Domestic lighting system layout*

The essential components required to upgrade a home from energy poverty are shown in Figure 3.1. Their brief descriptions are:

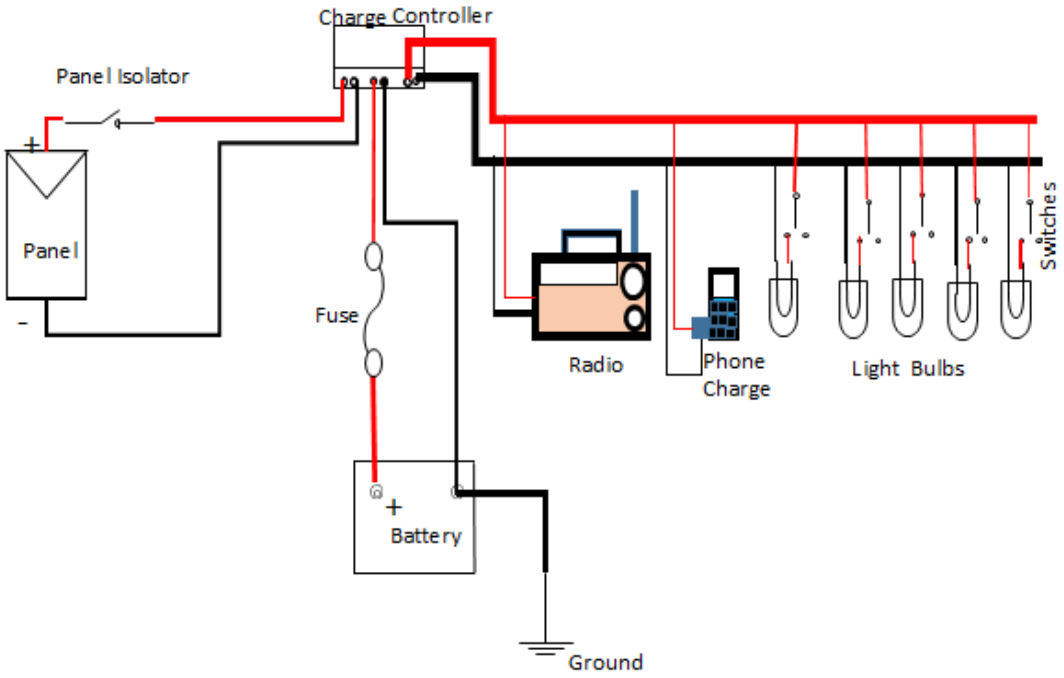

Figure 3.1. Suggested start-up PV system for an energy poor home.

- The panel – could be mono, or polycrystalline or amorphous silicon based. Operating voltage (V) and peak power rating (Wp) are the key specifications looked for by a user.
- The battery – stores electrical energy produced by the panel for later use. The main specifications the consumer is interested in are the voltage and the capacity in ampere hours (Ah).
- The charge controller – limits the battery charging voltage to a safe rated level. The user is principally interested in the voltage and peak current that can be handled by the controller.
- DC – Light bulbs. Suitable types include incandescent and light emission diodes.
- Connecting wires and switches.

3.1.3. *PV energy TRNSYS modelling for Cape Town, South Africa*

TRNSYS was developed at the solar laboratory of Wisconsin University [16], and has been in use for almost 40 years. It is normally used to analyse thermal-fluid systems but it has an extensive library of components that enable users to apply it in other areas. In the present case, the PV part of the electrical library was used to formulate a model for the university site located at 33.9° S, 18° E, and 68.5 m above sea level. The nearest TRNSYS listed weather station is: ZA - Cape Town – 688160, about 5 km away. Daily PV energy yield and total horizontal surface incident radiation results were extracted for comparison with experimental data.

3.1.3.1 *The PV energy yield model and its elements*

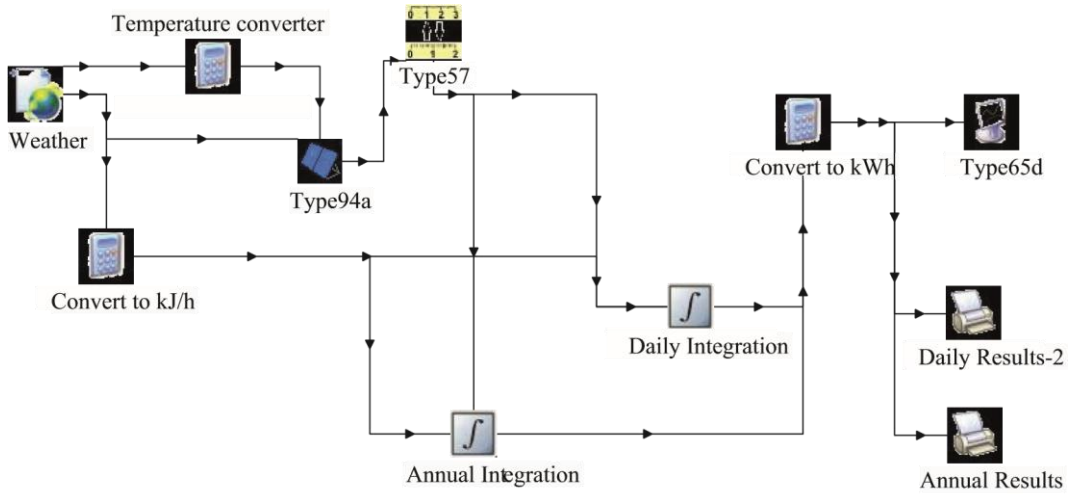

Figure 3.2. TRNSYS model used in deriving Cape Town's PV energy yield.

A basic PV TRNSYS model, shown in Figure 3.2, consists of the following elements:

- Weather – data for the site were approximated to those observed at the nearest weather station from a weather meteonorm file accompanying the software. The modeller specifies the slope of the surface and the diffuse radiation model to be used in the computations.
- Temperature converter – to absolute Kelvin scale because the PV panel performance equations use this scale.
- Converters of units – Two change panel total incident radiation and maximum power output from W to kJ/h. Two others change daily and annual energies to kWh while also computing 1st law panel efficiencies.
- Type 94a – The PV panel: In this case, a 90 Wp panel from one South African manufacturer was used.
- Integration elements – determine total daily and annual energy incident on panel and that yielded by the panel in kJ.
- Type 65d – plots and displays a graph of daily results for the whole year.
- Daily and annual results – record respective total incident solar, output electric energy, and 1st law efficiency for filing.

3.1.3.2 *The total incident horizontal surface energy yield*

The slope surface parameter in the weather element of Figure 3.2 was set to 0˚ so that element Type 94a could be horizontal. Then the daily integration results of the 'convert to kJ/h' element yielded the daily incident energy at element 'Daily Results - 2'. This was read off in the output file after the simulation for each day.

3.1.4. *Experimental work*

3.1.4.1 *Aim and objectives*

The aim was to establish a level of confidence in using TRNSYS software, to predict PV panel electrical energy yield before attempting its use in guidance for small system components selection for use in different places. The specific objective in this experiment was to answer the question: Do TRNSYS's energy yield results of a typical South African assembled 90 W(p) mono crystalline silicon panel, using Cape Town airport weather data, agree with actuals at a site a few kilometres away from the airport?

3.1.4.2 *Theoretical basis – a summary*

Many researchers have described factors influencing the electrical energy yield of a PV panel [17, 18]. In summary, they can be grouped into 3 categories: astronomy and geography based, panel design and manufacture, and lastly panel installation, usage, and maintenance. The first group is mainly controlled by nature, i.e. sun–earth–moon system dynamics and local physical and geographic climate. These contribute directly to incident beam radiation on a horizontal surface and to general diffuse radiation at the site as functions of time. In the experimental work, these have been directly measured every 10 min at the site since May 2013.

The second group is influenced by the scientific and technical expertise that is used in making the PV panel. A mono crystalline panel such as used in these experiments has an output current–voltage (I − V) characteristic modelled by TRNSYS type 94a to approximate Eq. (1) [16].

$$I = I_L - I_D\left[\exp\left(\frac{V+IR}{a}\right)-1\right] \quad (1)$$

The panel's output current $\boldsymbol{I}$ is thus modelled to depend on 4 parameters: generated current $\boldsymbol{I_L}$, p-n junction diode current $\boldsymbol{I_D}$, panel internal resistance $\boldsymbol{R}$, and the indicative quality of manufacture—junction temperature dependent—parameter $\boldsymbol{a}$.

Some authors and researchers, e.g., [19-21], use a 5-parameter model that includes a shunt resistor $\boldsymbol{R_2}$, thereby giving the output current as in Eq. (2).

$$I = I_L - I_D\left[\exp\left(\frac{V+IR_1}{a}\right)-1\right] - \frac{V+IR_2}{R_2} \quad (2)$$

TRNSYS, however, recommends the latter equation as best suited for amorphous silicon modules in the form of a type 94b component. This experiment used a mono crystalline silicon panel. The peak power, $\boldsymbol{V_{mp}I_{mp}}$, directly computed from measured current $\boldsymbol{I_{mp}}$ and corresponding voltage $\boldsymbol{V_{mp}}$ at terminals of a maximum power point tracking (MPPT) battery charge controller, was thus compared with the simulation results of Equation (1).

The third group of factors interact with the above two to yield a specific energy quantity for a particular installation and maintenance at the user's premises. The present work refers to the installation of a South African manufactured 90 Wp mono crystalline panel, atop a flat roof of a 2-storey building at a fixed 34° slope facing north. Apart from the grey painted roof, there were no nearby surfaces (where 'near' means up to 200 m) that could cast a shadow or reflect light onto the panel.

3.1.4.3 *Tools and equipment*

- 1 – Mono crystalline silicon solar panel 90 W(p); $\boldsymbol{V_{oc}}$ = 22.4 V; $\boldsymbol{I_{sc}}$ = 5.50 A; $\boldsymbol{V_{mp}}$ = 18.4 V; $\boldsymbol{I_{mp}}$ = 4.90 A; Manufacturer: SetSolar, Cape Town.
- 1 – MPPT charge controller 10 A;
- 1 – Battery: Deep cycle lead-acid; 12 V; 105 Ah.
- 1 – bulb: MR - 16 Dichroic halogen lamp; 50 W, 3000 h
- 2- Multi-meters: The UNI-T UT53 Multi-meter and the UNI-T UT203 clamp meter
- Interconnecting wiring
  - Weather station – Campbell Scientific. The relevant parts of the station used in the experiment were: 1 Kipp Zonen CMP06 Pyranometer, ISO First class; 2 SP LITE silicon pyranometers

with integrated fixture; an 8-channel Campbell Scientific measurement and control data logger.

- Ground-mounted support stand consisting of: a welded and painted rectangular steel frame of 25 mm × 25 mm angle sections; 20 mm diameter mild steel shaft mounted in three lockable plain bearings welded to the frame, coaxial with two central holes on the rectangular frame and inclined at a 34° to the horizontal.
- Two weather-proof enclosures: one for the battery and charge controller, the other for the electric bulb. The bulb's enclosure allowed free air circulation for cooling and visual check indicating the state of the circuit.

3.1.4.4 *Set up and procedure (Figure 3.3)*

Figure 3.3 shows the experimental setup. The detailed procedure followed was:

- The 90 Wp solar panel was bolted onto the rectangular frame of the stand facing true north.
- The battery, charge controller, and bulb were wired up in line with Figure 3.1.
- Half hourly readings of panel current and voltage at the charge controller terminals were made and recorded every day from 05:00 to 20:00 hours using the UT203 multi-meter. The voltage reading was crosschecked using the UT53 meter, just in case there was disagreement exceeding 0.1 V.

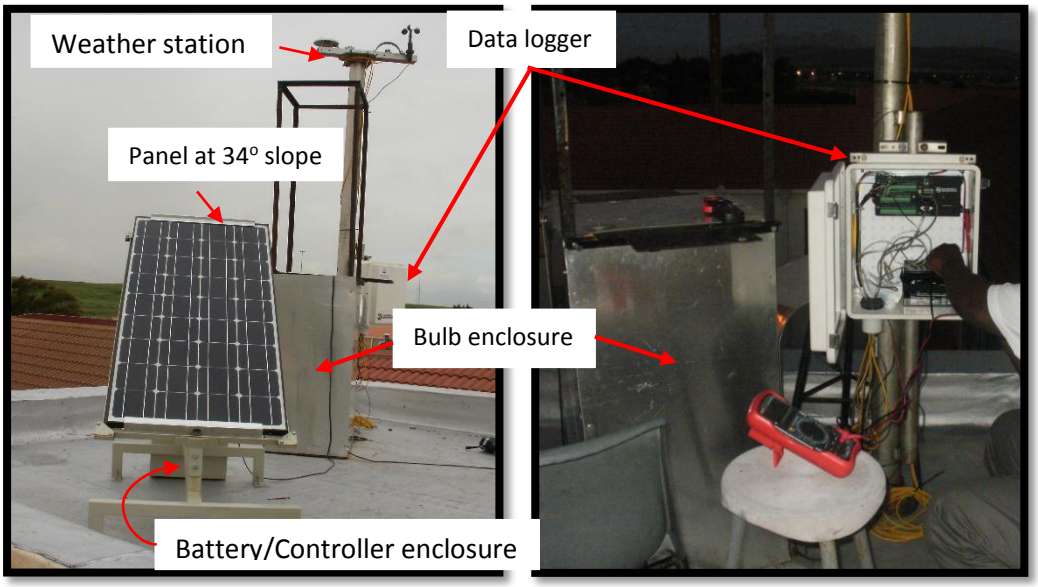

Figure 3.3. Experimental setup.

Out of a possible total of 558 data sets during the period, 533 or 95.5% were obtained. At the end of each day, the data were entered in an Excel spreadsheet to compute instantaneous half hourly power and the day's photoelectric energy yield by numerical integration using the ordinary trapezium rule.

The weather station is a long established, calibrated unit (installed in May 2013), recording weather data every 10 min. During the experiments, the main concern was routine maintenance work, i.e. checking that the station battery voltage was acceptable (≥12.0 V) and that the pyranometer surfaces were clean. The data recorded with the logger were: total radiation on a horizontal plane, G_h – read from the Kipp Zonen

pyranometer and reconciled with the reading of the unshaded SP LITE silicon pyranometer.

After the experiments, the TRNSYS model results were compared with the experimental ones in a statistical analysis.

3.1.5. *Results and analysis*

Table 3.1 shows a typical day's results and energy yield computation. Figure 3.4 shows the TRNSYS modelling results for the 18 days. Figure 3.5 compares the experimental and model results.

In Figure 3.5, two things are noted: that the airport weather station data used in the TRNSYS software could be used to predict total energy yield in nearby locations, and that daily energy yield variations from the TRNSYS model seem to be 'gentler' than those of an actual PV installation.

From a statistical viewpoint, however, these results are too few to warrant a parametric analysis. Therefore, they had to be transformed into a categorical form for nonparametric analysis. According to [22], this is the recommended treatment for small samples.

For the transformation, four possible model acceptance levels were analysed: actual yields to model ratios of 80%, 85%, 90%, and 95%. In practical terms this meant that if a day's actual yield was below the acceptance level, the model was unsuitable and therefore its result unacceptable for planning purposes. The reason for an 80% cut-off level stems from a separate consideration of the battery storage system. At this level, users choosing recommended deep cycle batteries can hope to have 4.5 consecutive days of overestimation by the model without discharging the batteries to a target 30% limit: ($0.8^{4.5} = 0.366$). Those using ordinary car batteries, however, would need to take the 90% level in order not to discharge the batteries below a target of 60% limit in the same overestimation period. Table 3.2 gives the κ test measures of agreement between the model and experimental results for the 4 scenarios. Peat [23], suggests that κ values of 50%, 70%, and 80% respectively indicate thresholds of "Quite good", "Good", and "Very good" measures of agreement between two data sets. The results therefore show that TRNSYS's model prediction was a reasonable approximation to actual panel performance.

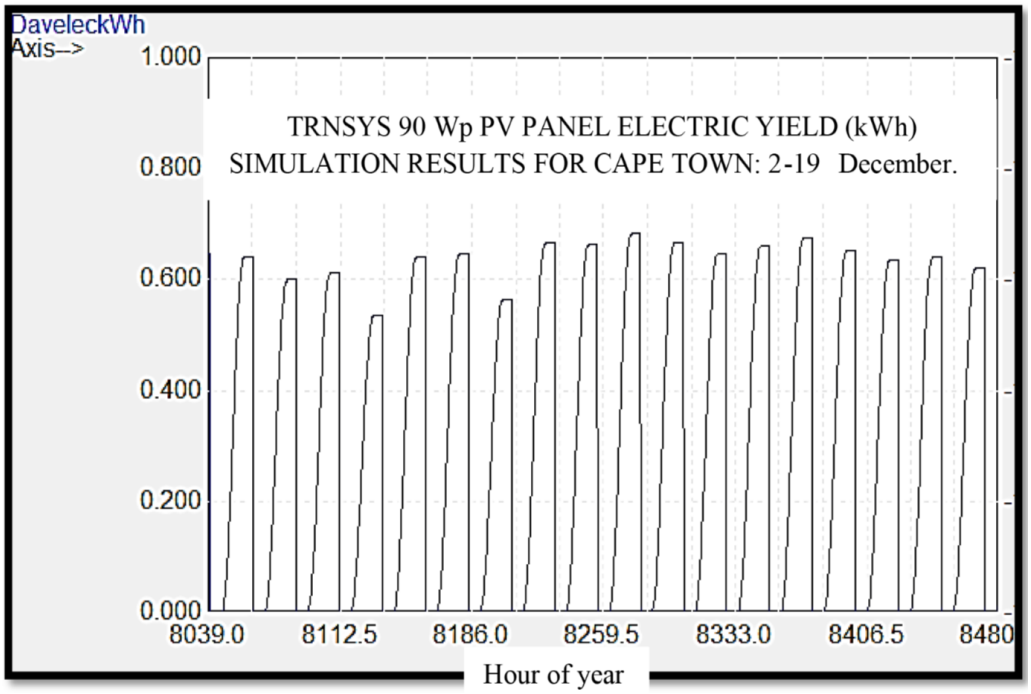

Figure 3.4. Screen shot of TRNSYS model results.

Table 3.1. Typical day's results: 12 December 2013.

Local Time	Voltage (V)	Current (A)	Power (W)	Cum. energy (kWh)	Local Time	Voltage (V)	Current (A)	Power (W)	Cum. energy (kWh)
0500	14.12	0.05	0.7	-					
0530	14.15	0.08	1.1	0	1300	14.51	6.75	97.9	0.317
0600	13.99	0.10	1.4	0.001	1330	15.06	6.59	99.2	0.367
0630	14.21	0.12	1.7	0.002	1400	15.82	6.23	98.6	0.416
0700	14.35	0.16	2.3	0.003	1430	15.73	6.21	97.7	0.465
0730	14.38	0.15	2.2	0.004	1500	14.44	6.06	82.5	0.511
0800	14.41	0.72	10.4	0.007	1530	14.49	5.58	80.9	0.554
0830	14.29	0.38	5.4	0.011	1600	14.50	5.39	78.2	0.598
0900	14.48	1.01	14.6	0.016	1630	14.48	4.54	65.7	0.629
0930	14.48	4.33	59.8	0.035	1700	15.94	3.89	62.0	0.661
1000	14.47	4.08	59.0	0.064	1730	14.48	3.46	50.1	0.689
1030	15.03	5.99	90.0	0.102	1800	14.45	2.48	35.8	0.711
1100	14.49	5.03	72.9	0.142	1830	14.35	1.38	19.8	0.725
1130	14.53	5.59	81.2	0.181	1900	14.30	0.59	8.4	0.732
1200	14.52	5.76	85.9	0.223	1930	14.41	0.03	0.4	0.734
1230	14.65	6.65	97.4	0.269	2000		Day's total energy:	0	0.734

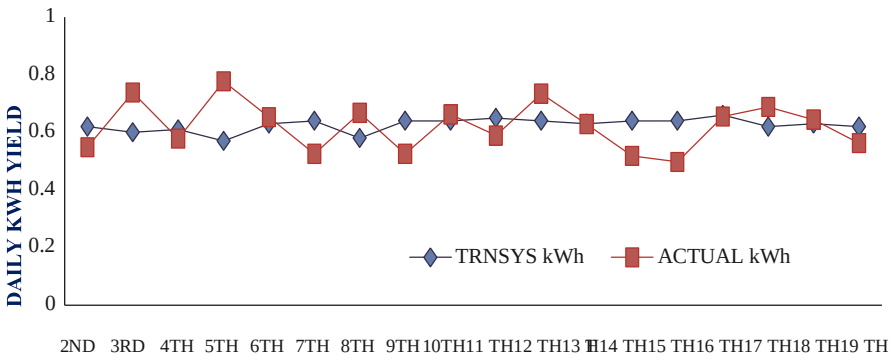

Figure 3.5. Model and experimental results compared

Table 3.2. Kappa (κ) analysis of transformed model and experimental results for different acceptance scenarios.

Cut-off model acceptance level	κ	Agreement level
Actual: Model = 80%	0.944	Very good
Actual: Model = 85%	0.778	Good
Actual: Model = 90%	0.722	Good
Actual: Model = 95%	0.556	Quite good

The second experiment used site weather data for the months August 2013 to July 2014 from the data logger and compared them with the software's airport data. The two correlated as evidenced in Figure 3.6 and in the regression analysis of Table 3.3. There were 342 valid points out of a possible 365 (93.7%). For the 342 days, the mean daily energy yield was 5.048 and 5.244 kWh/m^2 for measured and model, respectively. Regression analysis yielded a regression coefficient R of 0.782. According to Cohen [24], a strong relationship is implied if R $\geq$ 0.5. It is, however, noted that in many closely controlled experiments in science and engineering, researchers report coefficients in the range 0.9 to 0.99 as indicators of very close relationships [25]. For less controlled variables as in Cohen's human behaviour cases and in meteorological data in this paper's experiments, Taylor [26] and Frost of Minitab statistical software indicate that lower values can still predict a strong relationship. Hence, the result further confirmed the closeness between TRNSYS model results and actuals for this site.

Table 3.3. Regression analysis between experimental data and TRNSYS total incident radiation on a horizontal plane at CPUT Bellville campus.

Multiple R	0.782
R Square	0.611
Adjusted R Square	0.610
Standard Error	1.557
Observations	342

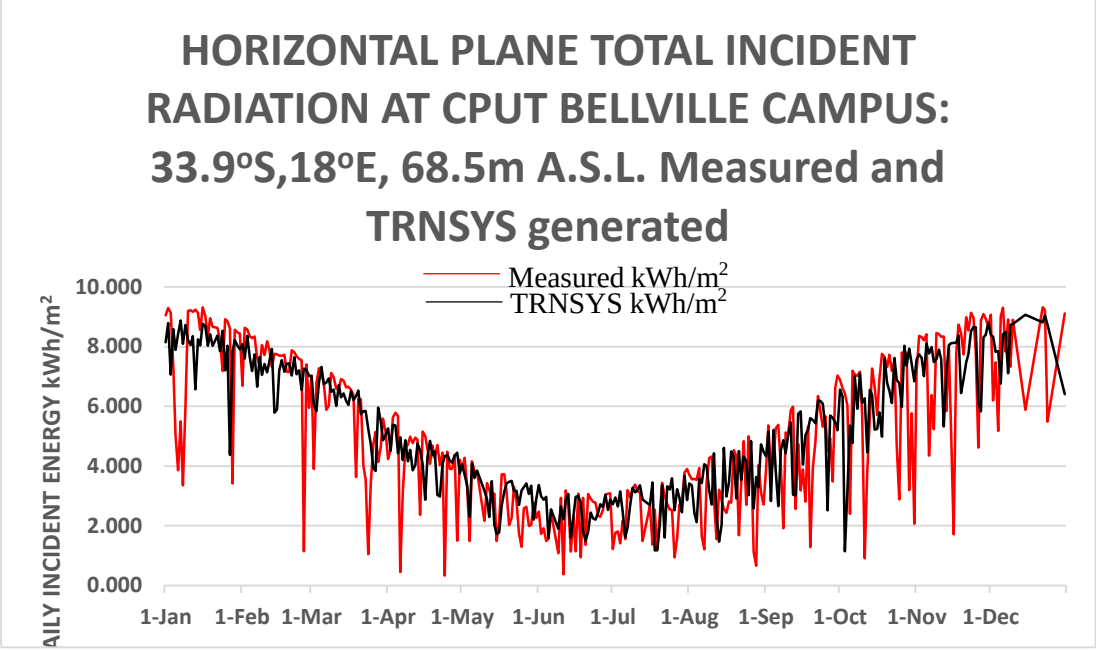

Figure 3.6. Aug 2013 to July 2014 CPUT horizontal plane total radiation flux comparison.

3.1.6. *Conclusions*

TRNSYS modelling for predicting electrical energy yield from a 90 Wp panel was validated for a site in Cape Town. Model reliability was tested at two levels: first, a limited period experiment was done on site in December 2013. Results were found to agree closely with the predicted yields. In a second and longer test, measured data on daily total incident radiation on a horizontal plane over a period of 1 year were compared with the software's prediction. The two correlated with a regression coefficient of 0.782 and hence a shared variance of 0.681. Given that the two sets of data were of uncontrollable weather parameters, it can be said that the results showed a strong relationship. Hence, it was concluded that TRNSYS could - within limitations of natural weather phenomena - be used to predict energy yields from the said PV panel at a place in the neighbourhood of the software's listed weather station. Supposing that tests at other sites and with other panel sizes, could yield similar results, this would open opportunities to apply the modelling to guidance on selecting fixed panel slopes, panel sizes, and battery types and numbers for homes nearby software listed stations.

Acknowledgements

We would like to thank CPUT University Research Fund committee and the entire Research Directorate staff for the funding and support during the entire 3-year period of this and other related work.

References

[1] OECD/AfDB/UNDP. African economic outlook 2014: Global value chains and Africa's industrialisation. Paris, France: OECD Publishing, 2014.

[2] International Energy Agency. 2014 Key world energy statistics. Paris, France: OECD/IEA, 2014.

[3] Bleeker AEM. Diffusion of solar PV from a TIS perspective and its transnational factors: A case study of Tanzania. 468017 ERM Research Project, Institute of Environmental studies, VU University Amsterdam, 2013.

[4] Oyedope SO. Energy and sustainable development in Nigeria: the way forward. Energy, Sustainability and Society 2012; 2: 15.
[5] Sambo AS, Zarma IH, Uguoke PE, Dioha IJ, Ganda YM. Implementation of standard solar PV projects in Nigeria. J Energy Tech & Policy 2014; 4: 22-28.
[6] Kanyarusoke KE, Gryzagoridis J, Oliver G. Predicting photovoltaic panel yields in sub-Sahara Africa. In ICEAS 2012 International Conference on Engineering and Applied Science; 24-27 July 2012; Beijing, China: ICEAS. pp. 223-255.
[7] Aste N, Pero CD, Leonforte F, Manfren M. A simplified model for the estimation of energy production of PV Systems. Energy 2013; 59: 503-512.
[8] Lalwani M, Kothari DP, Singh M. Investigation of solar photovoltaic simulation softwares. Int. J Appl Eng Res 2010; 1: 585-601.
[9] Ames DP, Pinthong K, Scott M, Khattar R, Solan D, Lee R. Open source map based software for photovoltaic System layout design. In iEMSs 2014 Conference 15-19 June 2014; San Diego, CA, USA.
[10] Siddique MN, Ahmad A, Nawaz MK, Bukhari SBA. Optimal integration of hybrid (wind-solar) system with diesel power plant using HOMER. Turk J Elec Eng & Comp Sci 2014; 23: 1547-1557.
[11] Mermoud A, Wittmer B. PVSYST User's Manual PVSyst 6. Satigny - Switzerland, PVSYST SA, 2014.
[12] Lee GR, Frearson L, Rodden P. An assessment of photovoltaic modelling software using real world performance data. In: 26th European Photovoltaic Solar Energy Conference and Exhibition, Hamburg, Germany, 2011.
[13] Mottillo M, Beausoleil-Morrison I, Couture L, Poissant Y. A comparison of two photovoltaic models. In: Canadian Solar Building Conference, Montreal, Canada, 2006.
[14] Mao C, Baltazar JC, Haberl J. Comparisons between TRNSYS software simulation and PV-CHART program on Photovoltaic system. Texas Engineering Experiment System, Texas A&M University, 2012.
[15] Al Riza DF, Gilani SI, Aris MS. Measurement and simulation of a standalone photovoltaic system for residential lighting in Malaysia. J Hydrocarb Mines Environ Res 2011; 2.
[16] Klein SA, Duffie JA, Mitchell JC, Kummer JP, Thornton JW, Bradley DE, Arias DA, Beckman WA, Duffie NA, Braun JE et al. TRNSYS 17: A transient system simulation program. Madison, WI, USA: Solar Energy Laboratory, University of Wisconsin, 2012.
[17] King DL, Boyson WE, Kratochvil JA. Photovoltaic Array Performance Model.
Albuquerque, New Mexico, USA: Sandia National Laboratories, 2004.
[18] Mani M, Pillai R. Impact of dust on solar photovoltaic (PV) performance: research status, challenges and recommendations. Renew Sust Energ Rev 2010; 14: 3124-3131.
[19] Duffie JA, Beckman WA. Solar Engineering of Thermal Processes. 4th ed. Solar Energy Laboratory, University of Wisconsin-Madison, WI, USA: Wiley, 2013.
[20] Marnoto T, Soplan K, Daud WRW, Algoul M, Zaharim A. Mathematical model for determining the performance characteristics of Multi crystalline photovoltaic modules. In: Proc. 9th WSEAS Int. Conf. on

Mathematical and Computational Methods in Science and Engineering, 5-7 Nov 2007, Trinidad and Tobago: WSEAS 2007. pp. 79-84.
[21] Pandiarajan N, Muthu R. Mathematical modelling of photovoltaic module with Simulink. In: ICEES 2011 International Conference on Electrical Energy Systems; 3{5 Jan 2011, Newport Beach, CA, USA: ICEES 2011. pp.314-319.
[22] Pallant J. A Step by Step Guide to Data Analysis using IBM SPSS: SPSS Survival Manual. 5th ed. Maidenhead, Berkshire, UK: McGraw-Hill, 2013.
[23] Peat J. Health Science Research: A Handbook of Quantitative Methods. Sydney, Australia: Allen & Unwin, 2001.
[24] Cohen JW. Statistical Power Analysis for the Behavioural Sciences. 2nd ed. Hillsdale, NJ, USA: Lawrence Erlbaum Associates, 1988.
[25] Mason RL, Gunst RF, Hess JL. Statistical Design and Analysis of Experiments With Applications to Engineering and Science. 2nd ed. Hoboken, NJ, USA: Wiley, 2003.
[26] Taylor R. Interpretation of the correlation coefficient: a basic review. JDMS 1990; 1: 35-39.

3.2 Concluding the chapter

The two sets of experiments showed that TRNSYS modelling could be relied upon – at least in Cape Town. As one was for a PV panel, and the other, for incident solar energy on a horizontal surface, it was considered reasonable to extend the modelling to the rest of the region - where there were software-listed weather stations. For purposes of developing region wide innovations in this work, the modelling will therefore be used as a tool for estimating both solar irradiance at different places and potential electric energy yields from PV panels appropriately oriented and tilted to the sun. The findings of this chapter therefore form a foundation on which the next two chapters build.

CHAPTER FOUR:

"FIXED PV PANEL SLOPES IN TROPICAL AFRICA: WHERE IS THE SUN?"

Kant E Kanyarusoke; Jasson Gryzagoridis; Graeme Oliver

Mechanical Engineering Department, Cape Peninsula University of Technology, P.O. Box 1906 Bellville (7535), Cape Town – South Africa.

Paper presented at the International Conference on Clean Energy for Sustainable Growth in Developing Countries

Palapye, Botswana, September 2015.

AND

SECOND ARTICLE:

"RE MAPPING SUB SAHARA AFRICA FOR EQUIPMENT SELECTION TO PHOTOELECTRIFY ENERGY POOR HOMES"

Kant E KANYARUSOKE; Jasson GRYZAGORIDIS, Graeme OLIVER

Journal of Applied Energy 175(2016) 240-250

4.0 Introduction

This chapter consists of two parts: a conference paper, and a journal paper. The former describes a model some of whose solutions were used in the journal paper. It focuses on the basic question of orienting a fixed flat solar energy collecting surface with respect to the sun's rays. The journal paper discusses the more important questions of a start-up home's basic electricity needs and PV equipment to meet those needs.

Answers provided by the content in both the conference and the journal papers form the first set of innovative material in this thesis. They respond to the presumed needs of most sub-Sahara Africans trying to start using fixed and/or semi fixed installations. The material can be grouped into 2 categories: the purely technical - which maximises energy yield from the installation; and the sociological ones – which simplify the communication of the technical solutions to someone making a start. In this way, it is hoped this innovative material will find more acceptance, and hence, might diffuse faster in the region.

4.1 Introducing the conference paper

With the knowledge that fairly accurate estimates of the solar resource can be obtained for any place in the SSA region using validated TRNSYS software as described in chapter 3, work in this project progressed in attempting to determine how a solar energy collection surface should be oriented to the sun's rays to maximise the harvesting of energy. Ideally, this orientation should always be direct – so that the beam radiation incidence angle is always zero. This ideal is hardly practical for reasons which will become apparent in chapter 5. Homes using solar

panels/collectors for the first time therefore almost universally do so at fixed orientations and tilts. But: which are the optimal orientations and tilts in sub -Sahara Africa? This study used TRNSYS to answer this question at an international conference on '*Clean Energy for Sustainable Growth in Developing Countries*' in Botswana.

4.2 The conference paper

FIXED PV PANEL SLOPES IN TROPICAL AFRICA: WHERE IS THE SUN?

Kant E Kanyarusoke; Jasson Gryzagoridis; Graeme Oliver

Mechanical Engineering Department, Cape Peninsula University of Technology, P.O. Box 1906 Bellville (7535), Cape Town – South Africa.

kanyarusokek@cput.ac.za; Gryzagoridisj@cput.ac.za; OliverG@cput.ac.za

ABSTRACT

This paper addresses fixed PV panel orientation and tilt to the sun in tropical Africa. It critically examines the panel azimuth and uses previously validated TRNSYS modelling to give simplified recommendations on fixed panel slopes for the region. Literature on conventional practices in form of azimuthal and tilt angles is reviewed. Seasonal Sun-Earth relative motion analysis reveals that these practices err on azimuthal angles in tropical areas - from a maximum annual electric energy yield point of view. It is suggested that whenever possible, 'free standing' fixed slope panels be installed to have two azimuthal angles annually: 0° and 180°, with changeover occurring when the sun is directly overhead the latitude in question. Using MATLAB®, we map the region for dates when the changeovers should occur. It is also noted that many installations are not 'free standing'. For these, we use TRNSYS software to determine best panel slopes; extend the work to include South Africa and map recommended slopes for the part of sub-Sahara Africa with software-listed weather data. We conclude that while optimal slopes can vary widely from normally assumed latitude values, variations within ±5° from optimality do not significantly affect annual energy yields in the region.

KEY WORDS

Tropical Africa; PV panel; Electric energy yield; Azimuthal angle; Panel slope.

4.2.1 *Introduction*

Photovoltaic (PV) panels generate different amounts of electricity depending on a myriad of factors including type of cells, local geography at installation site, date, time, weather and orientation with respect to beam radiation [1-3]. Of these factors for a given panel and place, it is only the orientation which can be manipulated to maximise electric energy yield. But this is not always straightforward because, off the planet's poles, the relative motion between the sun and any flat surface on the planet has 2 degrees of freedom. Hence, to orient the panel for maximum yield would generally require it to be double axis tracking. Perhaps because of cost, complexity and low availability of trackers [4], most panels in tropical Africa are installed as fixed non tracking units. Figure 4.1 shows examples of small scale installations in the region.

Figure 4.1: Some PV panel installations in sub-Sahara Africa: a) Mounting on a 29° roof at the equator in Uganda; b) Mounting at 50° in Cape Town, South Africa; c) Starter panel unit near the equator in Kenya.

Even with fixed installations, the possibility to increase yield by careful choice of panel surface orientation exists. In this case however, one needs to define the time period for which the increase is

required. Because the earth-sun relative motion has a period of approximately one year, and also considering the longevity of panels to be in excess of 20 years [5-9], it is more common to consider one off installations for maximising annual energy yield. But there can be other possibilities as well. In the tropics, we explore these. Then for sub-Sahara Africa - which includes temperate South Africa - we look at the one off installation and use previously validated TRNSYS modelling [10] to recommend panel tilt angles that would maximise annual energy yield. In summary therefore, section 4.2.2 of the paper gives a brief overview of the geometry of beam radiation incidence onto the PV panel. Section 4.2.3 discusses in detail the azimuth angle and how it could be used to advantage in the tropics. Section 4.2.4 addresses the tilt angle in the region. Finally, section 4.2.5 wraps up the work on both tropical azimuths and regional panel tilts by looking at effects of combining the two sets of recommendations.

4.2.2 *The solar angles on an inclined PV panel*

The geometry of the sun – panel installation can be presented as in Figure 4.2. The light which helps generate power in the PV cells is a combination of both diffuse and beam radiation. The two are attenuated by the panel glazing differently before reaching the cells [2]. Generally, the most significant contribution in electricity generation is from the beam part. The angle of concern in regard to this part is that of incidence, ***i***. It is a function of date, time of day, panel tilt β and azimuth ψ shown in the figure. Since date and time are beyond anyone's control, it is the angles at which the fixed non tracking panel is initially installed that will determine its effectiveness as a power generator. The two affect the angle ***i*** through equation (1) [2]:

$$i = \cos^{-1}\left[\cos z \cos\beta + \sin z \sin\beta \cos(\psi_s - \psi)\right] \quad (1)$$

Where it is understood that both the zenith angle ***z*** and the sun azimuth ψ_s are functions of date and time. Date affects them through the sun's relative position with respect to the earth in the latter's orbit. This defines the declination angle, δ. The latter, derivable from local noon sun elevation and installation latitude is perhaps best described as the latitude of a place on earth (not necessarily that of installation) where the sun is directly overhead at the instant in question. Looked at from another perspective, it is the answer to the question: *Where is the sun?* It is given either by the approximate Cooper equation suitable for hand calculations or by the more exact, truncated Fourier series equation of Spencer as cited by Duffie and Beckman [2]. Computations by computer in this paper used the latter as in equation (2).

$$\delta = \frac{180}{\pi}\begin{bmatrix} 0.006918 - 0.399912\cos B + \\ 0.070257\sin B - 0.006758\cos 2B \\ + 0.000907\sin 2B \\ - 0.002697\cos 3B \\ + 0.00148\sin 3B \end{bmatrix} \quad (2)$$

With ***n*** as day of year (1st Jan = 1; 31st Dec = 365), *B* is the date function:

$$B = \frac{360}{365}(n-1) \quad (3)$$

Figure 4.3 is a graphical representation of equation (2).

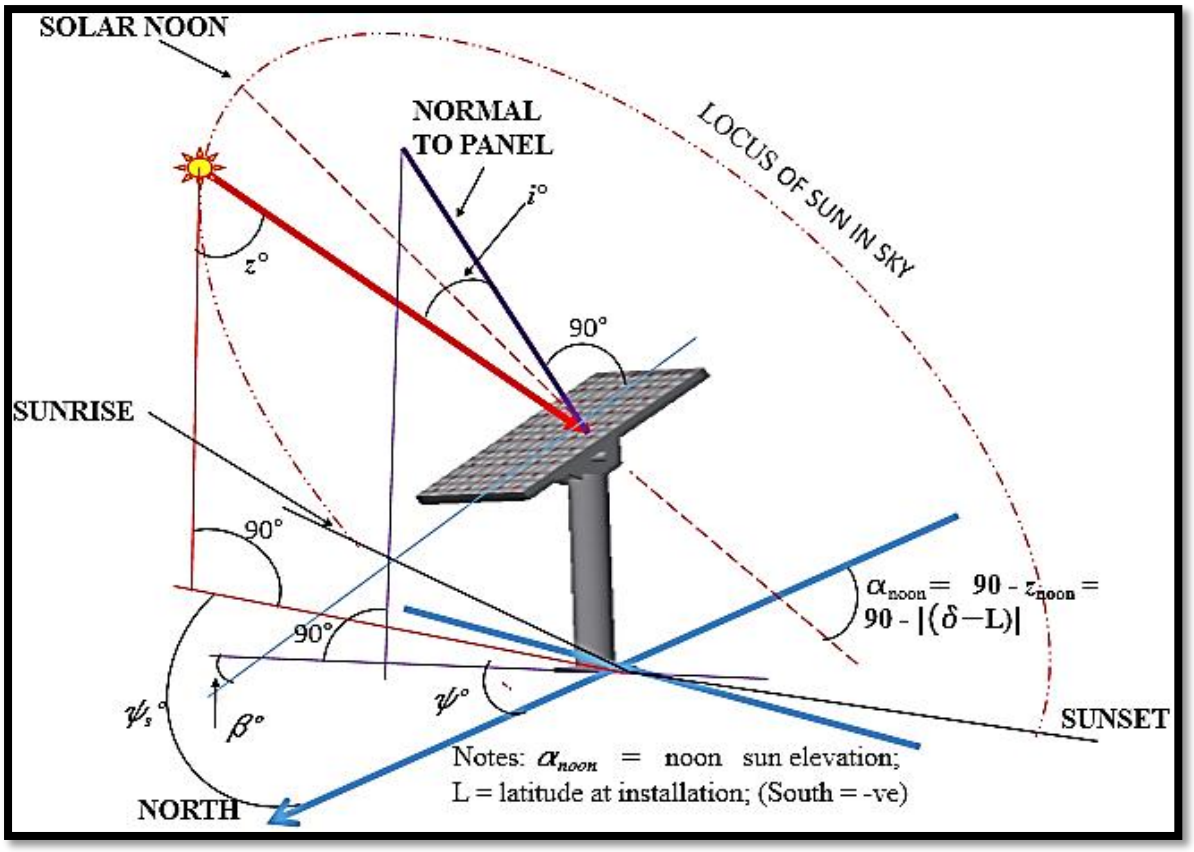

Figure 4.2: The geometry of beam radiation incidence on a solar panel

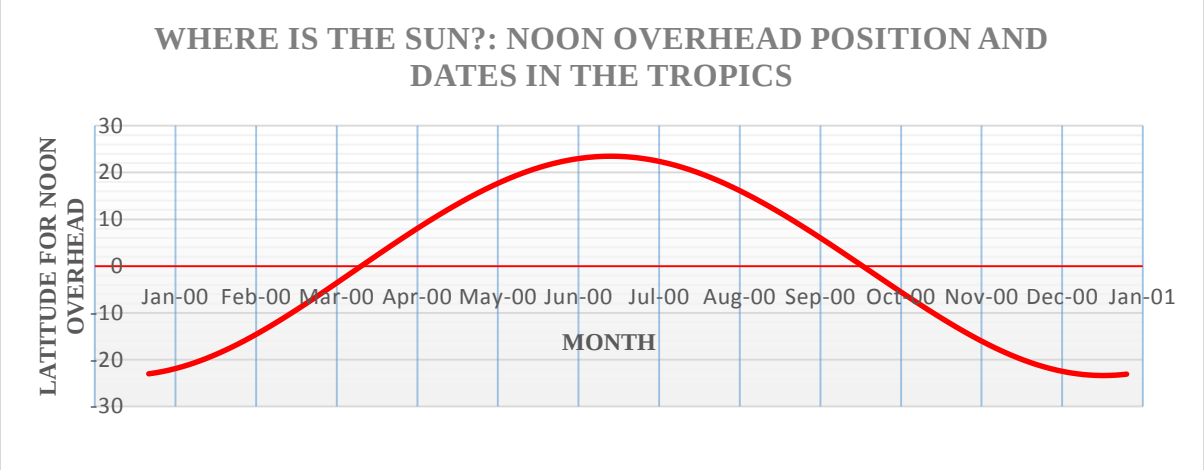

Figure 4.3: The sun's declination as computed from Spencer's equation

4.2.3 The panel azimuth angle ψ

In Figure 4.2, the panel azimuth angle is that between two vertical planes through the surface, one of which is normal to it while the other is a north-south (or meridian) plane. On any given day, the sun's relative path is symmetrical about the meridian plane, with solar noon being the instant when beam radiation reaches the panel in meridian planes. The issue about ψ for a non-tracking panel is that when neither 0° nor 180°, it defines an unsymmetrical relative path of the sun with respect to the panel. Thus, if the panel is installed with an eastern bias say, the afternoon incidence angles will increase and more of the evening beam radiation will be lost (i > 90°). The converse is true for west bias.

In the literature, there are reports of desirable biases depending on the climate of the area. Matshoge and Sebitosi [11] used *Meteonom* weather files and simulated electricity yields from panels using PV Design Pro-S software for the whole of South Africa. They reported optimal azimuth angles varying between 26.3° and 57.6° as one moves west to east of the country. There was however no experimental data to check some of these results. In a one short time experiment in Baghdad, Iraq, Ali reported an optimal result of -36° [12]. But many other researchers tend to use 0° e.g. [13-19]. In the present work, after validating TRNSYS at 0° in Cape Town [10], simulations for annual energy yield for all TRNSYS reported stations in sub-Sahara Africa seemed to indicate 0° as the optimal value. Figure 4.4 shows examples of 'normalised' results for equatorial, mid and outer tropical stations. Although these results seem to confirm the general convention, effects of local climate in some cases may not be negligible. For example if mornings are generally of clearer skies than afternoons - as is typical of areas which receive convectional rainfall, it might be better to bias the panels eastward (and consequently gain on morning yields) since there is little to lose in the afternoons.

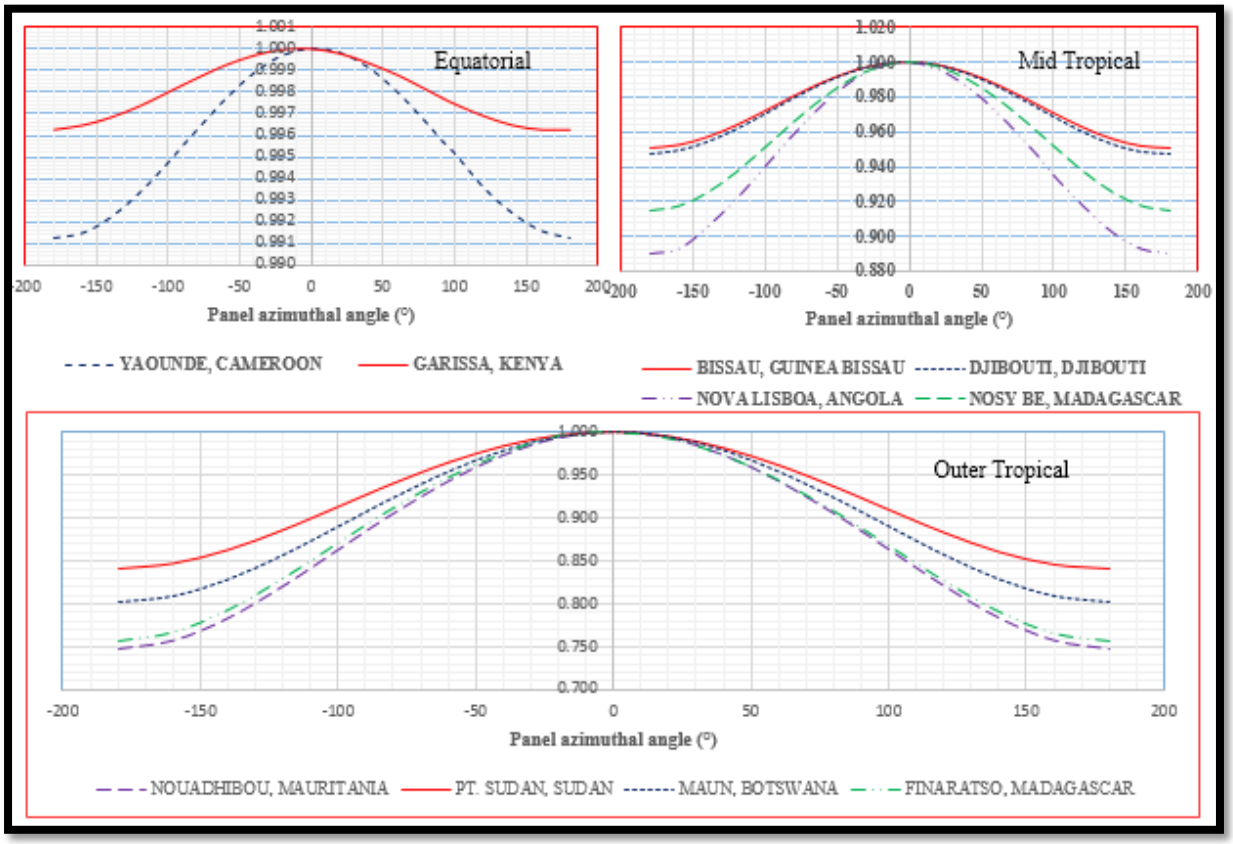

Figure 4.4: Yield variations with azimuth for different tropical Africa areas – (as fractions of those at 0°)

4.2.3.1 *The case for two azimuths in the tropics*

As implied by the sun-earth path symmetry explained above, an azimuth of zero would mean that in clear weather all day long, the incident beam radiation on the panel in the morning and afternoon would very nearly be equal – which could possibly maximise the day's yield. This alone however may not maximise annual energy yield for tropical areas. This is because there will be periods in the year when a zero azimuth means a big increase in beam radiation incidence angle from noon onwards. Moreover, these periods coincide with the time when the days are much longer than nights. Even when the sun declination coincides with the latitude of the location. This is illustrated in Figure 4.5 for a southern tropical location.

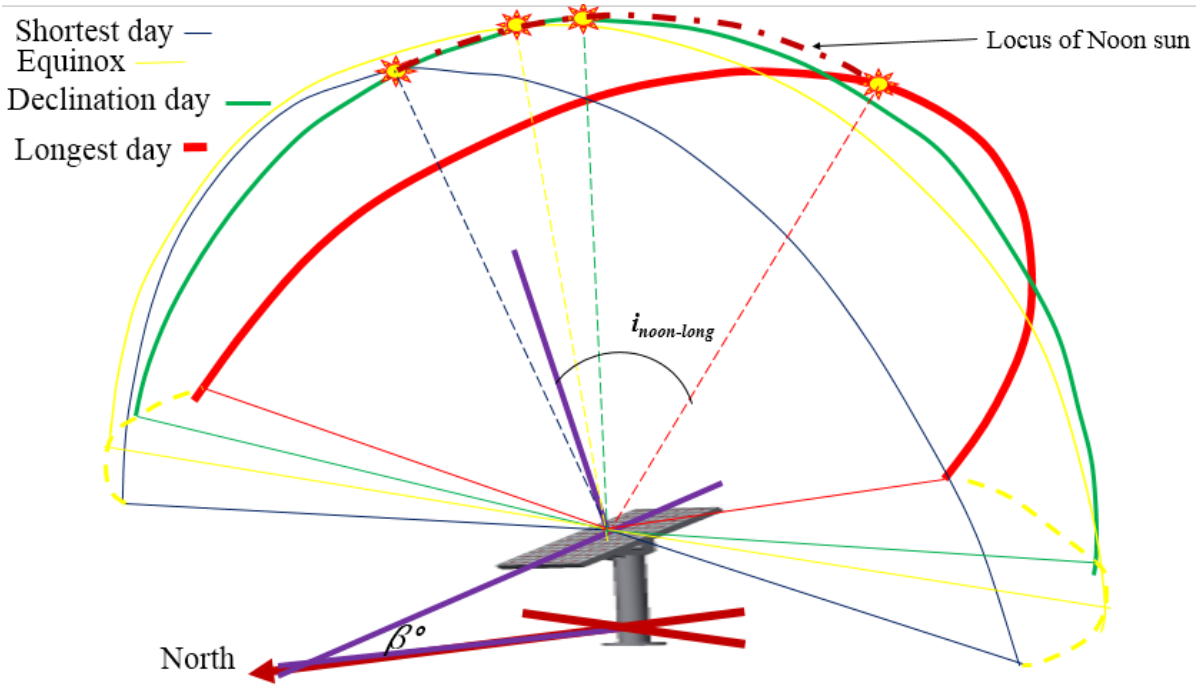

Figure 4.5: The vacillating tropical noon sun problem and its effect on beam radiation incidence angle at zero panel azimuth

This phenomenon is not well addressed in the literature. Nor is it commonly addressed in practical fixed non-tracking panels. We therefore propose *2-azimuth* free standing 'fixed' panel slope installations for the tropics. These would have their azimuths changed to 180° (i.e. face away from the equator) approximately after the sun has 'passed' the place on its apparent journey to the extreme of the hemisphere (i.e. North or South) in which the installation is located. The 'fixed' installation would have to be flipped back during the sun's 'return' journey.

One simple way of achieving the flipping is by a 180° rotation about a vertical axis – running along a panel support pillar. A second method is by rotation about a horizontal axis through an angle of 2β. Here, the panel could be installed atop a pillar as in Figure 4.2 and its support allowed to rotate to cause a flip over when required. Figure 4.6 shows the two possibilities.

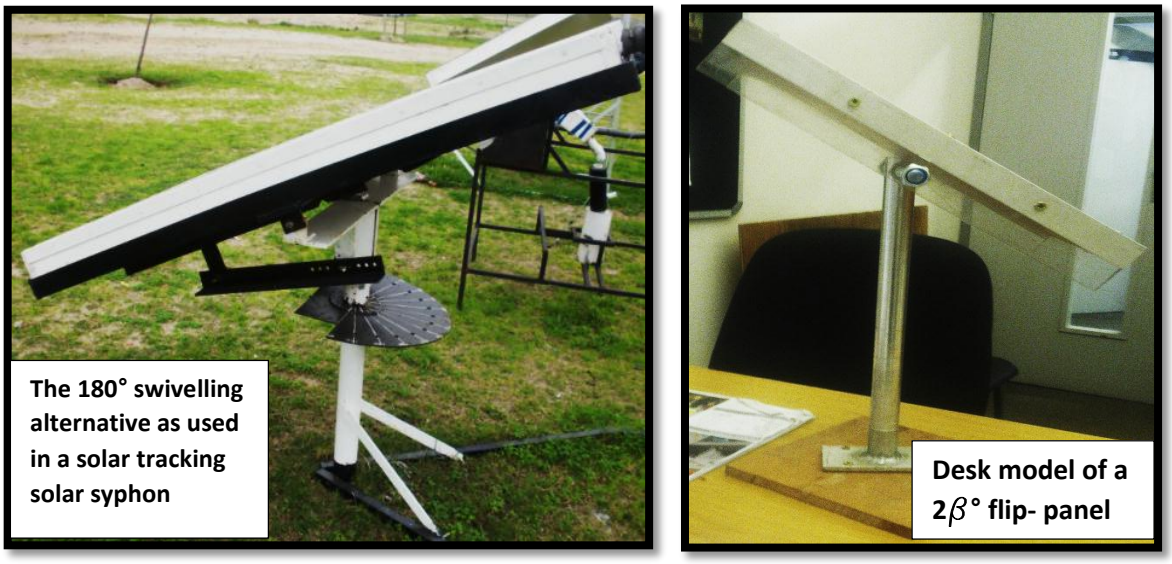

Figure 4.6: Possible alternatives to help achieve 0° and 180° azimuths with same installation: (Designs and photos by Kanyarusoke)

4.2.3.2 *The Declination day*

The next issue is: when does one actually flip over and back? Equation (2) as graphed in Figure 4.3 provides a solution. For greater clarity, dates are plotted against latitude as the independent variable in Figure 4.7. Therefore if one knows the local latitude, the flip dates can be read off. It is however born in mind that many installers in tropical Africa may not even have a clue about latitude – in spite of availability of Global Positioning Systems (GPS) on some cell phones.

Considering that the relative North-South angular 'speed' of the sun is low, averaging just below 0.26° per day (though appreciably 'faster' towards the fringes of the region), the changeover dates have been simplified by referring to the months in which they occur, and then mapped using MATLAB®'s mapping toolbox for easy interpretation. It is supposed that most installers would be able to locate their installation on one of the 5 bands of the regional maps. The two maps are given in Figure 4.8.

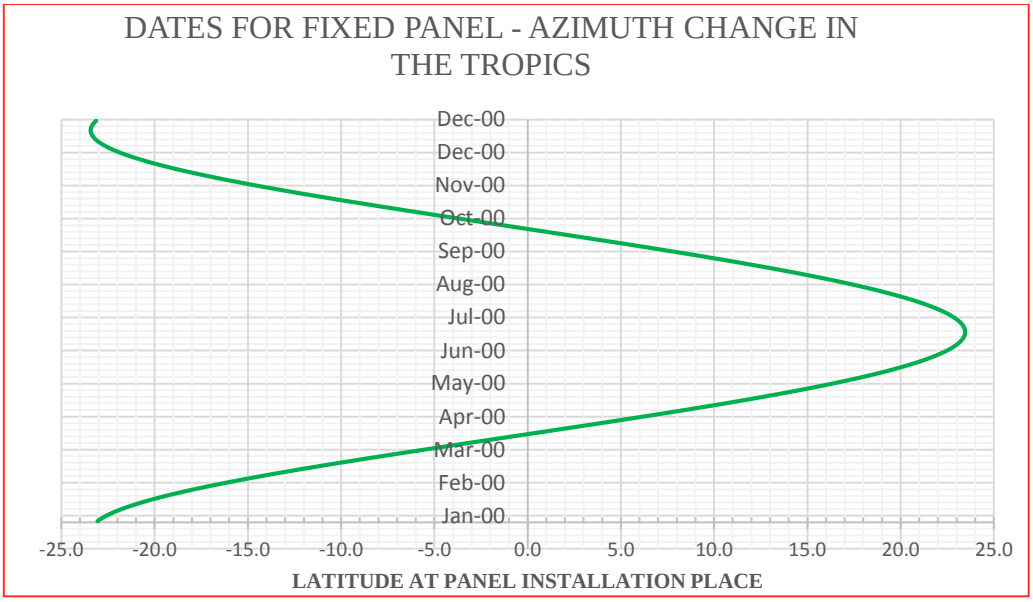

Figure 4.7: Dates of 'fixed' slope panel flip over in the tropics

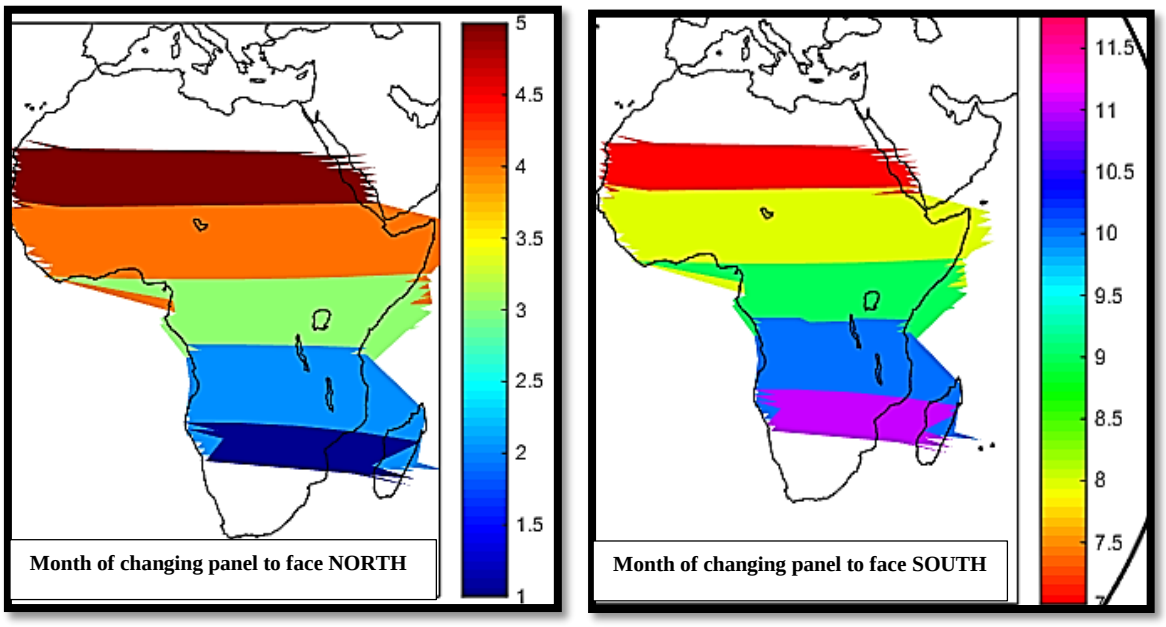

Figure 4.8: MATLAB® generated maps on flip over months recommendations

4.2.4 *The panel slope angle β*

A functional PV panel produces current as long as some light can reach its cells. The only issue is how much – and at what voltage (hence, quantity of power generated). Many researchers e.g. [13-19] have tried to determine so called best slopes and azimuthal angles for specific places. On slope or tilt, consensus seems to gravitate around monthly – or at least seasonal adjustments. Skeiker [17] for example reported a 30% annual energy gain over horizontal panel yields when monthly adjustments were done in Syria. But this might not be practical for many installations – such as those on rooftops. Hereunder, TRNSYS modelling in [10] is developed further to determine 'best' single fixed slope for places near the software's listed stations. In release 17 of the software [20], there are 140 such stations in tropical Africa and 12 others in temperate South Africa. This makes a total of 152 in sub-Sahara Africa – distributed as in Figure 4.9.

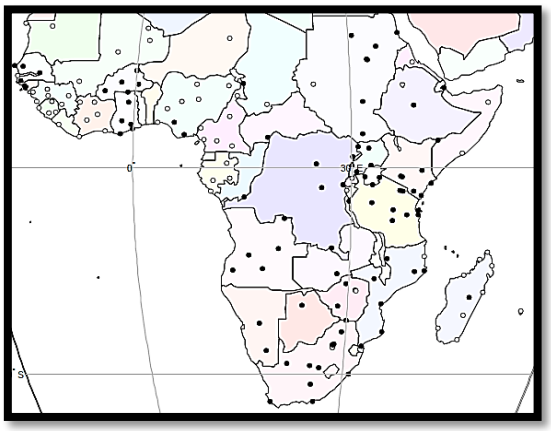

Figure 4.9: The 152 TRNSYS listed weather stations in sub-Sahara Africa [20]

4.2.4.1 *Best fixed panel slopes in sub-Sahara Africa*

There can be different ways of defining the 'best' fixed slope. The simplest is: "that which maximises annual energy yield". Another could be: "that which maximises energy yield at time of most need". Yet a third could be: "that which minimises total system costs to meet a given load". In the first and second cases, the slope parameter of the weather element in the model is varied and the simulation run in turn to determine the magnitude of the decision criterion. A plot of the criterion magnitude against slope determines the best slope. Figure 4.10 illustrates this for 'annual energy yield' criterion for Mbarara, Uganda and Cape Town, South Africa.

The simulations were effected for each of the region's 152 stations. Results of 'best slope' were corrected to the nearest 5° to achieve easy to remember and to install values. This latter simplification step was considered necessary for two main reasons. First, the numbers of technically skilled persons in the region are low [21], thus necessitating an easy to measure angle during installation. Secondly, a coarser slope variation yields a geo-raster map with better colour contrast - thus minimising map reading errors for those who might prefer using the maps presented in this work during installations. The simplification would have been inappropriate if it were not for the observation that small slope variations about the 'best' value do not lead to significant energy loss. For example for the Mbarara case in Figure 4.10, the annual loss is 0.02 kWh or less than 0.01% for the 1° slope difference. Among the 152 stations in the whole region, the peak %age loss was less than 0.1.

The corrected slopes were then exported to MATLAB® software where the mapping toolbox was used to produce a recommended slope raster geo-map for the region. This is shown in Figure 4.11.

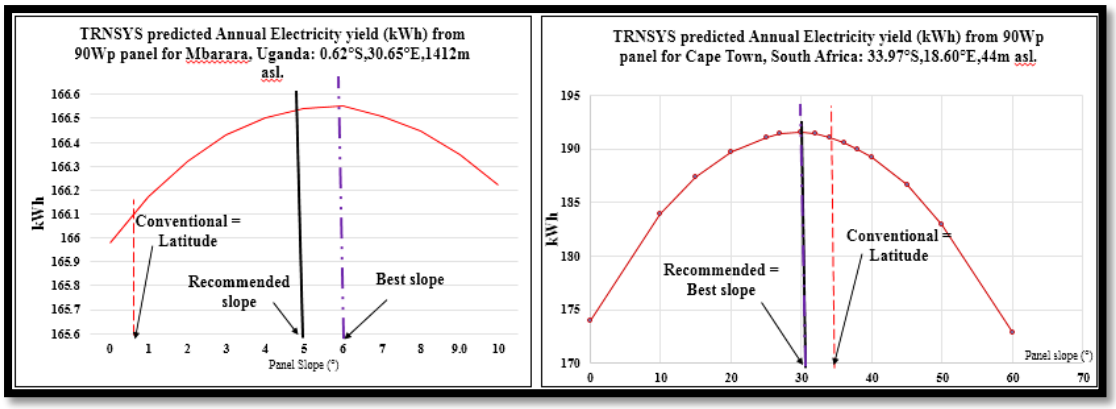

Figure 4.10: Determining 'Best slope' based on annual electric energy yield

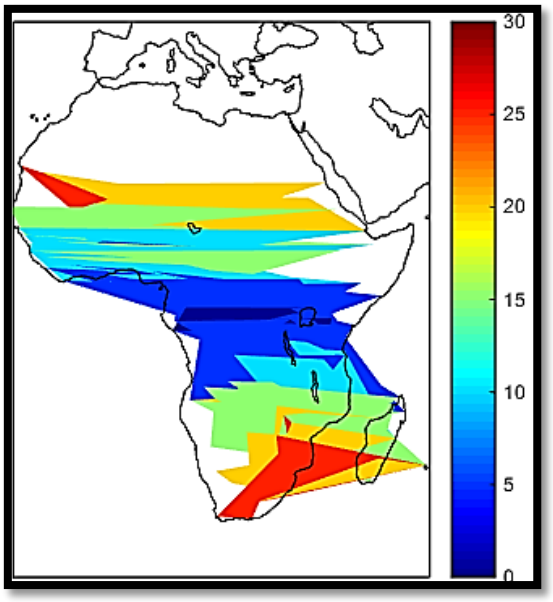

Figure 4.11: MATLAB® generated map for recommended panel slopes

4.2.5 *Combining the recommendations on ψ and β in Tropical Africa*

When a two azimuth installation is adopted, it is possible that the slope recommended for a single azimuth unit as in section 4.2.4, - though giving more yield - may not be the optimal one in the changed scenario. However, considering the low rates of energy yield deviations with respect to both β and ψ i.e. $(\partial E/\partial\beta$ and $\partial E/\partial\psi)$, in this work, we checked the potential gains from a flip over panel at the recommended non flip slope of section 4.2.4 when flips occur at beginning of months indicated in the maps of section 3. TRNSYS simulation was run for the two periods (i.e. when $\psi = 0°$ and $\psi = 180°$) and the results compared with those of the non-flip unit running throughout the year. Figure 4.12 gives indicative seasonal and annual percentage energy gains due to the flip for 2 equatorial, 4 mid and 4 outer tropical stations when running a 200 Wp panel.

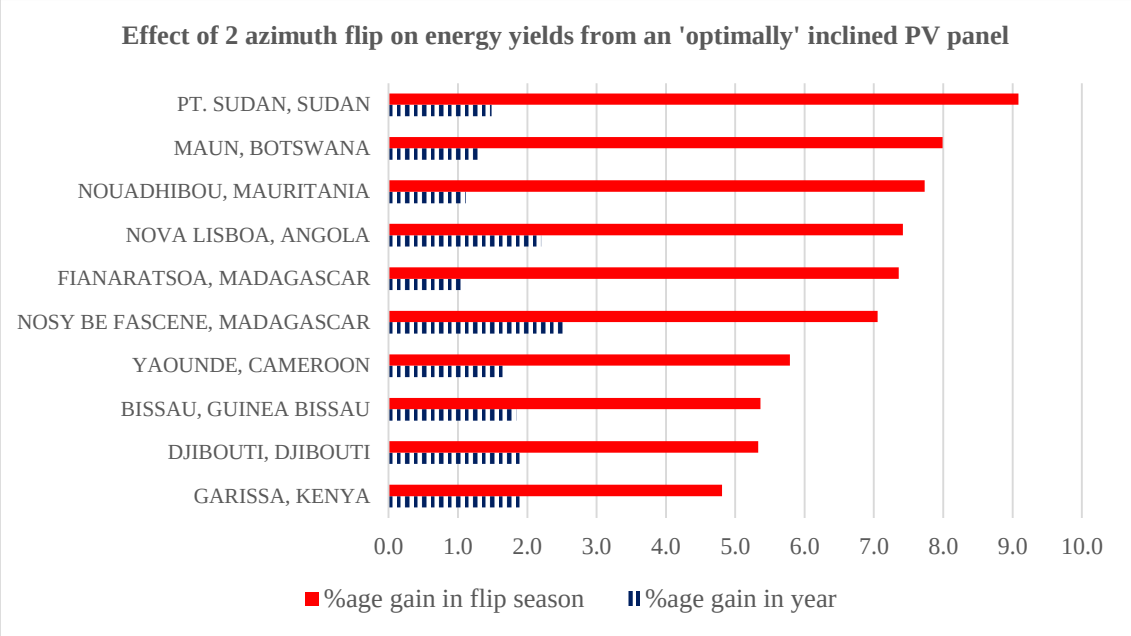

Figure 4.12: Some potential electric energy gains from 2-azimuth fixed slope non tracking PV panels

4.2.6 *Conclusions*

The main aim in this paper was to make informed recommendations on installation of fixed slope non tracking PV panels in tropical Africa. The geometry of beam radiation incidence was reviewed and angles which an installer can directly influence were pointed out to be the panel azimuth and tilt. Research and current practices on these angles were highlighted. On azimuth, it was found that although there are efforts to investigate climatic effects on optimality, current practice consensus seems to be on 0° - i.e. always facing the equator. On slope or tilt, researchers talk of equating it to latitude but also suggest seasonal - or at most - monthly adjustment. Practice seems to vary widely from roof – dictated mounting to discretionary operator-manipulated units.

Using previously validated TRNSYS modelling, effects of azimuth were investigated across tropical Africa. It was found that there was need to adopt two values for the region: 0 and 180°. The first would be during periods when the sun is actually on the equator side relative to the installation while the second would be when the installation is now on the equator side relative to a noon sun. Times for these changeovers were worked out and presented in different forms, including mapping. Also, 2 suggestions on how to effect the changeovers were made. Tilts (or slopes) were similarly investigated - and this time - across the whole of sub-Sahara Africa. It was found that optimal values deviated from previous research suggestions of equalling latitude, in some cases by as much as 10°. However, the rate of deviation of energy yield with respect to the angle around optimality was very small – indicating that one needn't be very exact in making recommendations. Therefore, all recommendations were made as multiples of 5 for ease in measurement during installations. As a summary, these were presented in map form.

After the separate recommendations on tilt and slope, potential energy yield gains when both are effected together across tropical Africa were estimated. It was found that the biggest benefit would be in increasing yield at times energy was most needed, i.e. during the time panels were flipped over to have a 180° azimuth. For regions towards the fringes of the tropics, this could be as high as 10%. Annual energy gains were most pronounced in the equatorial to mid tropical areas because of the longer periods the 'correction' on conventional practices these regions would encounter.

In conclusion therefore, it can be said that:

- From an energy yield perspective, as much as possible, two azimuth flip PV panel installations should be adopted for tropical Africa's free standing non tracking units.

- Panel slopes for the region may be taken as multiples of 5° in line with the mapping in this paper without significant loss of potential energy yield.

With these suggestions, it is hoped that more energy related benefits can accrue from a given PV installation. For example, the long term effects on storage battery requirements and on unit energy costs may be substantial. These are areas for further investigation.

References:

[1] M. Boxwell, *Solar Electricity Handbook 2012 Ed. A simple, practical guide to solar energy – designing and installing photovoltaic solar electric systems*. (Warwickshire, UK: Green**stream** Publishing, 2012).

[2].A. Duffie, & W.A.Beckman, *Solar Engineering of Thermal Processes* 4th ed. (Solar Energy Laboratory, University of Wisconsin-Madison, Wiley, 2013).

[3] T. Markvart, (Ed.) *Solar Electricity*, 2nd ed. (Chichester, UK: John Wiley & Sons, 2000).

[4] K.E. Kanyarusoke, J. Gryzagoridis & G. Oliver, Are solar tracking technologies feasible for domestic applications in rural tropical Africa? *Journal of Energy in Southern Africa*, 26(1), 2015, 86-95.

[5] D.C. Jordan, & S.R. Kurtz, Photovoltaic degradation – An analytical Review, National Renewable Energy Laboratory, Photovoltaics: Research and Applications, 2012. www.nrel.gov/docs/fy12osti/51664pdf [20 June 2015].

[6] A. Skoczek, T. Sample, & E.D. Dunlop, The results of performance measurements of field-aged crystalline Silicon PV modules, *Progress in Photovoltaics Research and Applications, 17*(4), 2009, 227-240.

[7] E. Dunlop, & D. Halt, The performance of crystalline Silicon Photovoltaic Solar modules after 22 years of continuous outdoor exposure, *Progress in Photovoltaics Research and Applications*, DOI: 10.1002/pip.627.

[8] M. Reese, Life expectancy of Solar Photovoltaic panels, *Power-Gen Africa*®, 04 July 2010. Available on line at: www.ezinearticles.com/?Life-Expecrancy-of-Solar-Photovoltaic-Panels&id=4603510 [20 June 2015]

[9] E.D. Dunlop, D. Halton,& H.A. Ossenbrink, 20 years of life and more: Where is the end of life of a PV module? *Proc. 31st IEEE Photovoltaics Specialists conference*, Lake Buena Vista, Florida, USA, 2005, 1593-1596.

[10]] K.E. Kanyarusoke, J. Gryzagoridis & G. Oliver, Validation of TRNSYS modelling for a fixed slope photovoltaic panel, *Forthcoming -. Turkish journal of Electrical Engineering and Computer Science.*

[11] T. Mashoge, and A. B. Sebitosi, The mapping of maximum annual energy yield azimuth and tilt angles for photovoltaic installations at all locations in South Africa, *Journal of Energy in Southern Africa*, 21(4), 2010, 2-6.

[12] F.H. Ali, The effect of tilt angle, surface azimuth and mirror in solar cell panel output in Baghdad, *Baghdad Science Journal*, 8(2), 2011, ---

[13] M. Kacira, M. Simsek, Y. Babur, & S. Dermikol, Determining optimum tilt angles and orientations of photovoltaic panels in Sanlirfa, Turkey, *Renewable Energy* 29(8), 2004, 1265-1275.

[14] E.D. Mehleri, P.L. Zervas, H. Sarimveis, J.A. Palyvos, & N.S. Markatos, Determination of the optimal tilt angle and orientation for solar photovoltaic arrays, *Renewable Energy*, *35*, 2010, 2468-2475.

[15] H. Gunerhan, & A. Hepbasil, Determination of the optimal tilt angle of solar collectors for building applications, *Building and Environment*, 42, 2007, 779-783.

[16] H.K. Elminir, A.E. Ghitas, F. ElHussainy, R. Hamid, M.M. Beheary, & K.M. Abdel-Moneim, Optimum solar flat plate collector slope: case study for Helwan, Egypt, *Energy Conversion and Management, 47*(5), 2006, 624-637.

[17] K. Skeiker, Optimum tilt angle and orientation for solar collectors in Syria, *Energy Conversion and Management, 50*(9), 2009, 2439-2448.

Acknowledgements:

We would like to thank CPUT Research Fund committee and the entire research directorate staff for the funding and support during the entire three year period of this and other work.

[18] D. Lubitz, Effect of manual tilt adjustments on incident irradiance on fixed and tracking solar panels, *Applied Energy* 98, 2011, 1710-1719.

[19] P. Shunmugakani, M. Visalakshi, P. Gomes, & N. Ayishwariya, Energy improvement in solar PV tracking systems, *Journal of Chemical and Pharmaceutical Sciences* 8(2), 2015, 459-462.

[20] Klein SA, Duffie JA, Mitchell JC, Kummer JP, Thornton JW, Bradley DE, Arias DA, Beckman WA, Duffie NA, Braun JE et al. TRNSYS 17: A transient system simulation program. Madison, WI, USA: Solar Energy Laboratory, University of Wisconsin, 2012.

4.3 Introducing the journal paper

Knowing how to place their solar panels in optimum orientation and tilt, what loads should be considered for start-up middle class homes and what devices would be suitable? The journal paper attempts to answer these questions. Like for the conference paper, it presents key results for the whole region in map forms.

4.4 The journal paper

Contents lists available at ScienceDirect

Applied Energy

journal homepage: www.elsevier.com/locate/apenergy

Re-mapping sub-Sahara Africa for equipment selection to photo electrify energy poor homes

Kant E. Kanyarusoke *, Jasson Gryzagoridis, Graeme Oliver

Mechanical Engineering Department, Cape Peninsula University of Technology, P.O. Box 1906, Bellville, 7535 Cape Town, South Africa

HIGHLIGHTS

- We estimate daily electrical energy requirements for start-up rural homes at 500 W h.
- We model PV panel and BOS components selection for optimisation to meet the load.
- We solve the model at 152 stations in sub-Sahara Africa and map the solutions.
- Optimal panel selections range between 160 and 275 Wp.
- Battery capacities range between 70 and 360 A h while 15 A charge controllers dominate.

GRAPHICAL ABSTRACT

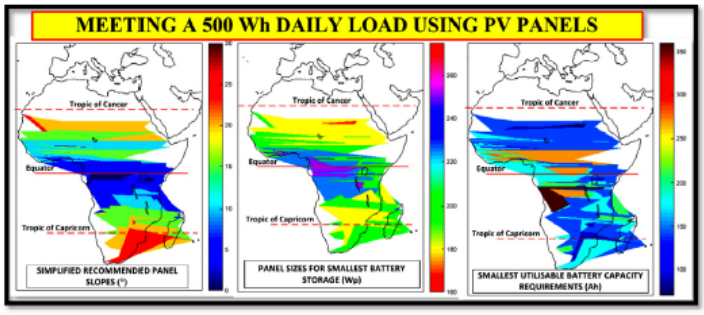

ABSTRACT

This paper provides a missing integrated guide to budding middle class rural sub-Saharan Africa (SSA) homesteads trying to photo-electrify. It first estimates bare minimum requirements for these homes to start emerging from energy poverty. Guidance is given on optimal selection of the most important device for such homes: the light bulb. Along with other essential devices, this gives a daily electrical load of 500 Wh, 42 Ah at 12 V DC. Building on earlier experimental work on validating TRNSYS in Cape Town, it extends usage of the software to the rest of SSA, aiming to recommend panel and balance of system component sizes to meet the above load all year round. Use is made of panel slopes derived in a related piece of work to formulate an optimisation model for selecting panel-battery-charge controller combinations. A survey of South Africa-made panels and components is done. Then, a method of solving the model is demonstrated by an example in Uganda which selects from the surveyed components to satisfy two alternative technical objectives of 'least battery storage' and 'smallest panel size'. At each of the other 151 stations in SSA, the model is solved only for the first objective. The overall results are then mapped using MATLAB®. It is concluded that from a 'smallest battery storage' perspective, usable battery storage capacities in the region range between 70 and 360 Ah, with the biggest being in equatorial/tropical rain forest areas of Congo basin and along the mid-western coastal areas. Panel sizes range between 160 and 275 Wp. The dominant recommendation on charge controllers is 15 A.

KEY WORDS

Mapping sub-Sahara Africa; PV panel; Battery selection; Charge controller; Energy poor; Rural electrification.

4.4.1 *Introduction*

Tropical Africa's electric grid supply is miniscule not only by world standards but by those of the rest of the continent as well. For

example, the 2014 International Energy Agency (IEA) report says that 620 Million tropical Africans have no access to electricity. This makes about half of the world's energy poor population [1] and is about 71% of the region's population [2]. Yet percentages for temperate Northern and Southern Africa are 1 and 14 respectively [1, 3]. Many researchers and energy practitioners have pointed to self-generation using photovoltaic (PV) panels as a possible approach to enable homesteads access electricity [4 – 9]. The authors have also argued for this approach in the past on grounds of costs, health and safety, ease and speed of rollout among others [10 – 11]. Whereas these - and many more - works recommend photo electrification, and while the practice is taking root in some of the region's countries [12 – 15], there is as yet, limited recorded in depth research - based guidance on selection of equipment for the region. The paper therefore begins with a brief review of recent literature on work that comes closest to guiding these selections.

4.4.1.1 *Economic viability*

From within Africa, literature on photo-electrification in general is quite limited. That on system optimisation is even scarcer. In 2006 for example, Moner-Girona *et al*. [16] reported that not much was "very well-known" about the status of solar home systems (SHS) in sub-Sahara Africa. They did a review and found a necessity for local manufacture of the systems in the region. But in 2007, Wamukonya [17] reviewed the effectiveness of the systems as an option in helping develop Africa. She concluded that the option was unviable on account of costs. Ondraczek [18] pointed to the fact that most governments in Africa still regarded PV electricity as expensive. They reserved its usage for isolated rural installations. This was partly responsible for slow take up of SHS. But in another article, he cited the exception of Kenya [19] where a SHS market had developed fast and PV energy prices were beginning to be competitive by 2011. In that year, the grid supply cost reached US$ 0.21 per kWh. A year later, Rose, *et al*. [20] confirmed that the economic value of PV electricity was higher than the total cost of acquisition and operation in the same country.

In 2009, Breyer *et al*. [21] did an economic analysis of small off grid PV systems in Ethiopia. The systems had been aligned to the basic needs of lighting, communication and entertainment. Even without a rigorous optimisation procedure, they determined a payback period of between 2 and 4 years for homesteads, depending on the energy demand by the homes (the larger the demand, the shorter the payback period). A few years later, Bazillan, *et al*. [22] discussed the economics of PV electricity with intention of demystifying the costs to policy makers, investors and financiers. For example, they cited a 2012 US$ 0.85 per Wp rating for poly crystalline silicon panels from China as an example of how the prices were falling. Clearly, these and other works go to show that the economic viability of SHS in the region is now less debatable. What may not be quite clear however, are the technical details. Their literature is briefly surveyed next.

4.4.1.2 *Technical gaps in optimisation for the region*

Udoakah and Umoren [23] investigated monthly optimal tilts of PV panels at two cities in Southern Nigeria at latitudes 4.95°N and 5.64°N. They found that for 6 summer months, a zero slope was preferred. Adjustments were necessary each winter month. In the bigger system optimisation picture, these findings tackled only one part of the problem: how to maximise semi fixed panel energy yields at these locations. Excluded were issues of load optimisation, equipment selection and installation, and how the rest of the country and continent could make easy use of the findings. For

example, despite the fact that many PV panels for households emerging from energy poverty are installed on roofs (e.g. see Figure 4.13 in section 4.4.2), the feasibility of monthly adjustments was not discussed.

Wansah *et al*. [24] addressed the load issue in remote places by studying performance of a stand-alone system in Eastern Nigeria. The system provided 3.3 kWh daily to a remote household. The load included a 21" plasma TV, a satellite dish, and a refrigerator among other items. Itodo and Aju [25] studied a commercial application in which a 750 W rice thresher was powered by a PV system for 2 hours a day. This required a string of 3 modules of 260 Wp, 4 series-connected 100 Ah-12 V batteries, a 15 A charge controller and an inverter. From the loads handled by these two studies, it is clear that it was not the energy-poor's needs which were being addressed. And whereas, the studies demonstrated performance of the selected system components, they did not tell us whether the selections were optimised – and if so, how. Thus, the question of optimisation modelling for the poor still persists. And unfortunately, energy research work involving optimisation in less energy poor societies seems to be preoccupied with other issues now. We illustrate these with a few examples.

4.4.1.3 *More electricity - different problems*

At 85.4%, South Africa has the highest population access rate to electricity in SSA [26]. The focus now seems to be more on optimising energy resources usage for income generating activities and on carbon footprint reduction. Azimoh, *et al*. [27] describe a mini grid approach to provide 300 remote households with an average 2.4 kWh per day each. They find that SHS as served by PV panels cannot optimally supply this load. Hence, they conclude that the system would work better where there is local small hydroelectric potential. In urban South Africa, the issue of consumer willingness to pay for green energy arises. Chan, *et al*. [28] investigated it and found that willingness to pay depended on geography. It could not be generalised. In none of these two studies are the needs of the 14.6% energy poor South Africans addressed.

Outside SSA, documented work still focuses on the not so energy poor households. Not least, the reason being that there are very few energy poor people in most of the countries. Emphasis - like in South Africa - is on reducing the carbon footprint. In Argentina with 99.8% electrification, Reinoso, *et al*. [29] evaluated energy costs of a 10 MWp PV power plant at the foothills of the Andes. In Mexico, with 99.1% electrification, Vidal-Amaro, *et al*. [30] gave an optimisation model for a renewable energy-fossil fuel energy mix for the country. In Hong Kong, Ma, *et al*. [31] optimised a solar PV-wind-water turbine/pump hybrid micro grid system to improve energy source reliability for remote communities. Their work addressed the problem of maintaining electricity supply reliability at close to 100%. On the other hand, the problem in most of SSA is to have this reliability take off from 0%.

In the UK, Rogers *et al*. [32] investigated, and demonstrated the feasibility of reducing home carbon emissions to 20% of a 1990 "typical house". That UK "typical house" is totally different from SSA's. The energy needs are different. In SSA, lighting needs dominate - as space heating in most of tropical Africa is not an issue. Perhaps the work elsewhere closer to what is addressed in this paper is that by Olcan [33] in Turkey. He optimised sizing of a PV powered water pumping system for irrigation. But even then, it is seen that it is not the energy poor's selection problems that are addressed.

In summary therefore, as of now, there is only limited documented guidance on optimal selection of load elements, power supply and control elements for any homestead in SSA

trying to emerge from energy poverty. It is therefore not surprising that current practice mainly relies either on panel suppliers' recommendations or on books such as [34] and [35] or simply on the installer's experience. While these provide general 'rule of thumb' guidelines, they do not necessarily reflect optimality. Moreover, they assume the consumer has already made a good choice on the load elements. In an assessment of "decentralised rural electrification", Chaurey and Kandpal [36] show that it is critical to optimise equipment selection as standardised integrated systems when rural-electrifying. This paper's originality and innovation therefore is in its integration of basic needs, required supplies, *and* optimised installation guides. Moreover, for the region in question, the paper considers the ease in interpreting pictorial messages relative to alpha-numeric ones and presents recommendations on simplified maps for the part of SSA with TRNSYS listed weather data. Consequently, the remainder of the paper is organised as follows: Section 4.4.2 models bare minimum needs for a middle class rural home attempting to emerge from energy poverty – and then recommends suitable key load devices for it. That forms the first set of results of this work. Then, given the loads, and noting the dynamic interaction between balance of system (BOS) components and the panel, section 4.4.3 makes informed recommendations on selection of panel and BOS components to meet them all year round. This is done by way of optimisation modelling. We illustrate how to solve the model for two mutually exclusive objective functions by reference to one particular place. The methodology and illustration of a *particular* solution form a second results-set of this work. Section 4.4.4 presents the solutions corresponding to one of the objective functions for the entire region in form of MATLAB® generated maps and discusses them. The maps constitute the major results-set of this work and accord the paper its title. We also give an abridged table of results for representative places in the region. We conclude the work in section 4.4.5 with a summary and a comment about its further enhancements.

4.4.2 *PV- lighting a typical rural African household*

The most pressing problem arising out of lack of electrification is darkness in the region at night. For a human being needing 8 hours of rest a day, we estimate that this darkness reduces available economic productive hours by a fraction between 25% and 50%. And if we were to factor in productivity enhancements by cool and quiet environments on some human activities, the actual loss of daily productivity due to darkness could well exceed 50%. This could be the reason why almost all literature on the subject reports that the first need for electricity in the region is lighting. We therefore begin with an analysis of this need.

4.4.2.1 *Lighting requirements in a household*

Because of PV module capacities and rural household financial limitations, it was supposed that people wanting to upgrade into electricity usage would want to use it principally for lighting of the main house. This is supported by almost all available literature and anecdotal evidence. At a sustainable development conference in South Africa in 2014 for example, participants were emphatic about a need for lighting in preference to heating [37]. In this work therefore, light bulbs in the living room and in four other rooms were assumed. Two of the rooms were for children living and reading purposes while the others were for adults. It was also supposed that there were outside light bulbs to cater for moderate compound lighting. In a majority of rural African homes for example, both the bath and toilet facilities are located outside the main house. A cell phone-charging outlet and a small radio were added since

these devices are now almost universal in homes that could afford the system [38, 39]. Figure 4.13 shows a photograph of a typical rural middle class house in Uganda and a schematic of the PV system for it.

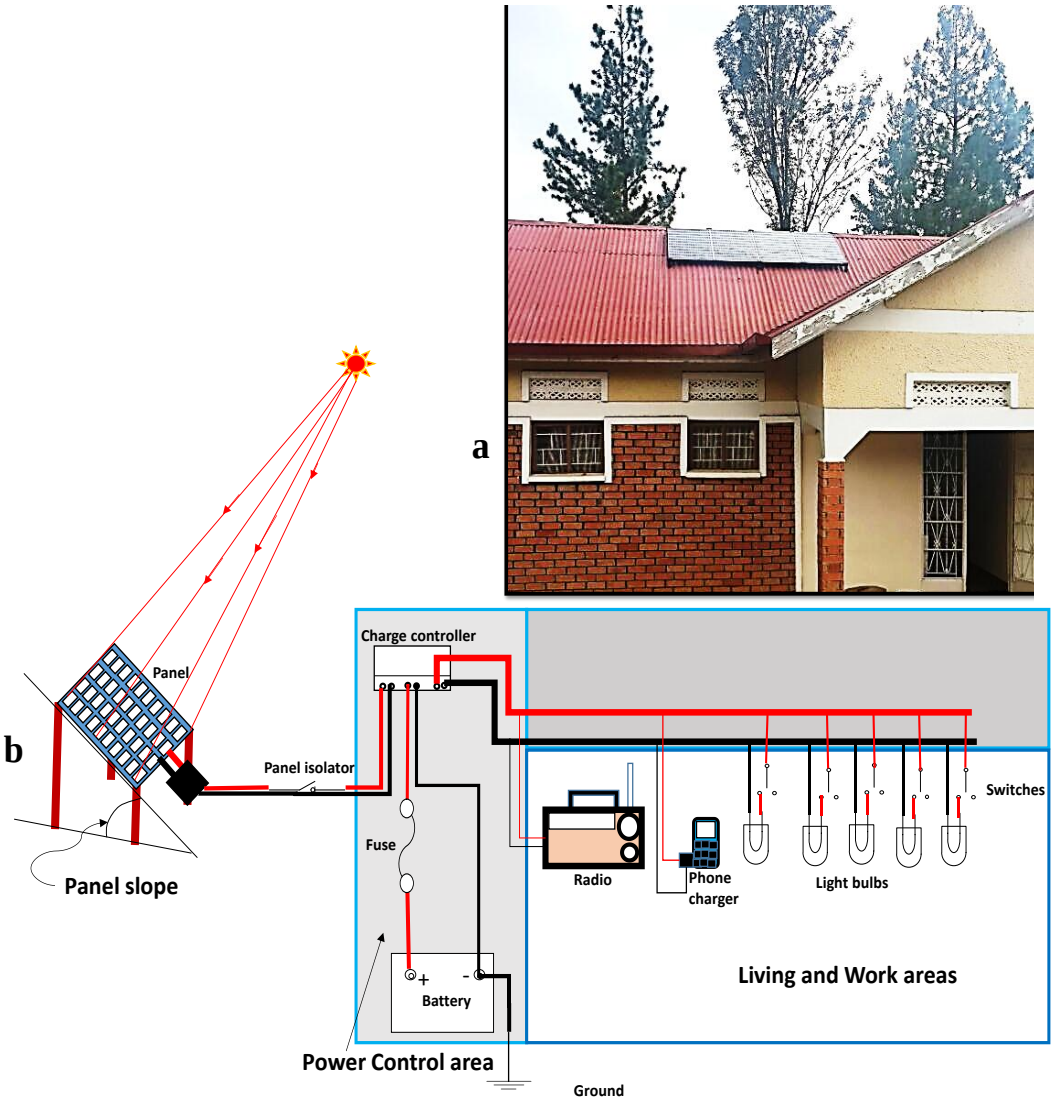

Figure 4.13: a) A typical sub-Saharan Africa rural middle class house emerging from energy poverty b) Schematic wiring for the house

Using the Rae method [40], the light flux required for in-house activities was computed. The number of bulbs and their power consumption were determined - as in Table 4.1. Focused LED array bulbs were chosen for the analysis because of their higher luminosity per Watt and longer life. For example, cool white bulbs give about 80 Lumen per Watt consumed against 13 from filament ones [41, 42]. They are reported to have a potential life of 25000 to 50000 hours against 1000 of the latter [43]. Table 4.2 gives the daily energy and charge requirements when these bulbs are used to meet the household's needs. It is seen that the load is 500 Wh. For a well wired 12 V battery system, the utilisable charge load is about 42 Ah.

Table 4.1: Light bulb requirements for a medium sized rural tropical African home

	Nos.	Eff. Work area (m^2)	Height above wk. surface (m)	Light intensity (Lux)	Area @ focused bulb (m^2)	Bulb Nos.	Lumen at wk. surface	Bulb Types Power consumption (W)		Required LED array rating (W)	Available LED array rating (W)	Tot. LED bulbs to install
								Filament	Focused LED			
Living Room	1	20	2	75	4.2	4	1500	115.4	18.8	5	11	**2**
Children rooms	2	3	1	510	1.0	2	1530	117.7	19.1	10	11	**4**
Other rooms	2	12	2	75	4.2	2	900	69.2	11.3	6	**8**	**4**
Total bulbs in house												**10**
Outside	2	10	15	50	24	4	500	38.5	6.25	2	**8**	**2**
Total No. of focused LED Array Bulbs required												**12**

Table 4.2: Estimated daily electrical load for a rural tropical African home emerging from 'energy poverty'.

	Power (W)	Current (A)	Hours @ day	Energy (Wh)	Charge (Ah)	Comments
Living Room	22	1.8	4	88	7.3	On, between 7 and 11 pm
Children rooms	44	3.7	5	220	18.3	On, between 8 and 11 pm; then between 5 and 7 am
Other rooms	32	2.7	1	32	2.7	On, half an hour before sleep and after wakeup.
Outside lights	16	1.3	2	32	2.7	On, when someone is going out
Phone charging	5	0.4	4	20	1.7	
Radio	10	0.8	6	60	5.0	
Subtotal				452	37.7	
Other Loads (10%)				45.2	3.8	
Total daily load				**497.2**	**41.4**	**Say, 500 Wh and 42 Ah respectively**

4.4.3 *Selection of PV Panels, Batteries and Charge controllers*

A small scale domestic PV system requires the panel and a storage system at the very least. Zahedi [44] gives the battery and a super capacitor as possible storage devices for domestic applications. Bianchi *et al*. [45] explore a battery and a battery-fuel cell hybrid system. In sub-Sahara Africa however, super capacitors and fuel cells are not readily available for mass market penetration. Batteries dominate [46]. This then calls for a means to control the charge rate and to protect the battery against excessive discharge. Hence, the charge controller. Reputable manufacturers and suppliers give guidelines on how to select their panels – and sometimes, other components. On a website of one South African manufacturer (name withheld because of ethical reasons) for example, there is a 3 sheet MS Excel work book guiding potential customers in South Africa on how to select the manufacturer's panels. Apart from being company and country-specific, it requires the user to be both 'Excel literate' and electrically skilled to interpret and use. The workbook is thus not easy to use across a region as diverse and as skill deficient as Tropical Africa. This section therefore presents a generalised

model that was used to make recommendations for the entire region. It considers suitable samples of available panels, batteries and charge controllers in South Africa as reported on PV panel manufacturers' websites. As of June 2015, there were a total of 5 such manufacturers profiled by ENF Solar (an Energy Focus global market research company) in the country [47].

4.4.3.1 *Samples of panels, batteries and charge controllers*

Preliminary MATLAB® analysis [10] and experimental work in Cape Town [48] seemed to indicate that for the annual load of 182.5 kWh - implied by consumption patterns of section 4.4.2, the panel sizes to consider would have to be rated at not less than 90 Wp and that the charge controllers would have to be able to give at least 10 A output for a 12 V system. These values therefore formed the lower limits of sampling on these items. For batteries, only deep cycle lead acid types of utilisable capacities in excess of 45 Ah were considered – since the daily load is 42. By utilisable capacity here, is meant the manufacturer – recommended peak depth of discharge (DOD), expressed in Ah. Another limitation considered on batteries was weight. Only those weighing not more than 30 kg were considered because of necessity for easy handling by installers and users in rural villages. Tables 4.3 to 4.5 give available units in line with these limitations. In these tables, prices are based on the minimum surveyed values (for the type and quality) exclusive of Value Added Tax (VAT). The exchange rate used was 1 US$ = 12 ZAR.

Table 4.3: Typical South African manufactured 12 V crystalline silicon PV panels

PANEL O/P (Wp)	Type[1]	Area (m^2)	Price (US$)	V_{mp} (V)	I_{mp} (A)	V_{oc} (V)	I_{sc} (A)	NOCT (°C)	[2]α_i (mA or %/K)	[2]β_v (mV or %/K)
90	1	0.5625	95	18.4	4.90	22.4	5.50	45	**1.55**	**-79.2**
100	2	0.718848	106	18.4	5.44	22.2	6.89	48	0.035%	-0.37%
125	2	0.876096	120	17.4	7.2	21.7	7.6	45	**4.50**	**-79.2**
135	2	0.876096	134	18.5	7.30	22.2	8.43	48	0.033%	-0.36%
150	2	0.876096	183	18.3	8.27	22.5	8.81	46	0.081%	-0.37%
160	2	0.97344	170	20.2	7.85	24.1	8.2	46	0.081%	-0.37%
180	1	1.125	171	35.7	5.00	43.2	5.40	45	**1.55**	**-158.40**
200	2	1.314144	212	27.4	7.40	33.4	7.80	45	**4.50**	**-115.30**
225	2	1.314144	199	28.5	7.90	34.6	8.40	45	**4.50**	**-115.30**
250	2	1.752192	220	34.1	7.33	40.9	8.06	45	**4.50**	**-152.64**
275	2	1.752192	267	34.9	7.88	41.8	8.67	45	**4.50**	**-152.64**

[1]Type: 1 = Mono crystalline silicon; 2 = Poly crystalline silicon; [2]Different manufacturers' specs.

Table 4.4: Typical South African sourced 12 V Deep cycle Lead-acid batteries

CAPACITY (Ah)	Price (US$)	DESIGN LIFE @25°C (Years)	ALLOW. DOD (%)	DERATED LIFE (Years)	MASS (kg)
70	180	10	100	7	23
85	149	7	80	5	21
90	268	10	100	7	28
100	149	12	40	6	30
105	179	5	50	3	27
115	186	7	80	5	27

Table 4.5: Typical South African manufactured 12 V charge controllers

Current (A)	Type	Price (US$)	$I_{out\text{-}max}$ (A)	$I_{panel\text{-}max}$ (A)	$V_{out\text{-}max}$ (V)	$V_{cut\text{-}out}$ (V)
10	PWM	36	10	10	13.7	11.1
10	MPPT	77	10	10	13.8	11.2
15	PWM with D/L	123	15	15	17.2	6.9
15	MPPT	127	15	15	13.8	11.1
20	PWM	88	20	20	13.7	11.1
20	PWM with D/L	159	20	20	17.2	6.9
20	MPPT	143	20	20	System dependent	System dependent

PWM = Pulse Width Modulated; MPPT = Maximum Power Point Tracking; D/L = Data Logger

4.4.3.2 *Panel-Batteries-charge controller combination*

Although manufacturers - such as the one referred to at beginning of section 4.4.3 - tend to recommend panel selection first and then BOS components, optimisation of the entire system requires that the combination be looked at as a unit because of dynamic interactions between the components. Moreover, whereas lab experimentation, TRNSYS and/or other modelling of panel performance enable estimation of energy delivery to the charge controller, in the longer term, not all this energy is available to the user because of battery capacity and loading pattern issues. Thus, for a predominantly lighting load as being discussed in this paper, the mismatch between generation and loading means that either the panel or the battery capacity (or both) would have to be bigger than when there is no mismatch. This leads to a feasibility space of panel-battery-controller capacities matrix, in which the same load can be served by multiple combinations of components. The issue therefore is to determine which combination in this space is optimal.

Model formulation

Variables - Let the following be denoted as:

- Panel size and characteristics: $\boldsymbol{W}$ (Wp);
- Battery type and characteristics: Standard battery size; $\boldsymbol{Q_s}$ (Ah); DOD $\boldsymbol{d}$ (%), Charge efficiency $\boldsymbol{\eta_c}$, (%), Energy efficiency $\boldsymbol{\eta_e}$ (%); Number of batteries in system: $\boldsymbol{z}$;
- Standard charge controller characteristics: Peak delivery current: $\boldsymbol{I_{cc}}$ (A); Energy efficiency η_{cc} (%).
- Day of year: $\boldsymbol{i}$;

- Instantaneous charging current from controller: $\boldsymbol{I_{charge}}$ (A)
- Daily night constant electric load: $\boldsymbol{Q}$ (Ah), $\boldsymbol{E}$ (Wh);
- Added charge to batteries on day $\boldsymbol{i}$: $\boldsymbol{Q_{i\text{-}add}}$ (Ah)
- End of day $\boldsymbol{i}$ total charge in system: $\boldsymbol{Q_i}$ (Ah)
- Peak instantaneous power generated on day $\boldsymbol{i}$: $\boldsymbol{W_{i\text{-}max}}$ (W)
- Tracking to fixed slope output ratio: $\boldsymbol{R_{track}}$
- Annual energy delivered by panel to charge controller at rated panel capacity: $\boldsymbol{E_{annual}}$ (Wh).
- Minimum guaranteed output as fraction of rated panel capacity: $\boldsymbol{f_g}$.

Problem and constraints - The problem is to select five variables: $\boldsymbol{W}$, ($\boldsymbol{d}$, $\boldsymbol{\eta_c}$, $\boldsymbol{\eta_e}$), $\boldsymbol{Q_s}$, $\boldsymbol{z}$ and $\boldsymbol{I_{cc}}$ so that a specific objective function is satisfied by a fixed slope panel subject to the constraints:

Annual energy delivery to controller satisfies the load: $E_{annual} \geq \frac{365E}{f_g \eta_{cc} \eta_e}$ (1a)

No use of tracking to meet annual load:

$$E_{annual} \leq \frac{365ER_{track}}{f_g \eta_{cc} \eta_e} \qquad (1b)$$

These two give the relationship:

$$1 \leq \frac{f_g \eta_{cc} \eta_e E_{annual}}{365E} \leq R_{track} \qquad (1c)$$

Batteries minimum charge constraint:

$$Q_i \geq \frac{100-d}{100} zQ_s \qquad (2)$$

Batteries capacity constraint:

$$Q_i \leq zQ_s \qquad (3)$$

Batteries total charge at end of day $\boldsymbol{i}$:

$$Q_i = Q_{i-1} + Q_{i-add} - \frac{Q}{\eta_c} \qquad (4)$$

Charge Controller capacity:

$$I_{ch-\max} = \frac{W_{i-\max}}{V_{battery}} \leq I_{cc} \qquad (5)$$

Availability constraints:

W = {Available panel sizes} (6)

Q_s = {Available battery sizes} (7)

I_{cc} = {Available Charge controller sizes} (8)

Natural Number constraints:

z = {Natural number} (9)

i = {1, 2, 3, ----------, 365} (10)

Objective function - This may take different forms depending on what is considered most important to the system owner. Here, we consider only the technical issues of power generation (smallest panel size in the feasibility space) and energy storage (smallest usable battery storage in the space).

- Smallest panel size to meet load:
  Minimise $\boldsymbol{W}$ (11a)
- Least battery utilisable storage capacity:
  Minimise $Q_{storage} = \frac{dzQ_s}{100}$ (11b)

Model solution flow chart

Equations (1) to (11) define the optimisation model. Figure 4.14 shows the flow chart which can be used to deduce the feasibility space of panel-batteries-charge controller matrices from equations 1 to 10. Combinations in the feasibility space can then be evaluated for any of objective functions (11a) and (11b). For the case of Mbarara, Uganda, Figure 4.15, illustrates how the recommended slope (for use in Figures 4.13 and 4.14) was obtained. Table 4.6 gives the corresponding feasibility space (arising from Figure 4.14) and evaluations of the 2 objective functions. By effecting a minimisation test on the

evaluations, the respective optimisation solutions were obtained.

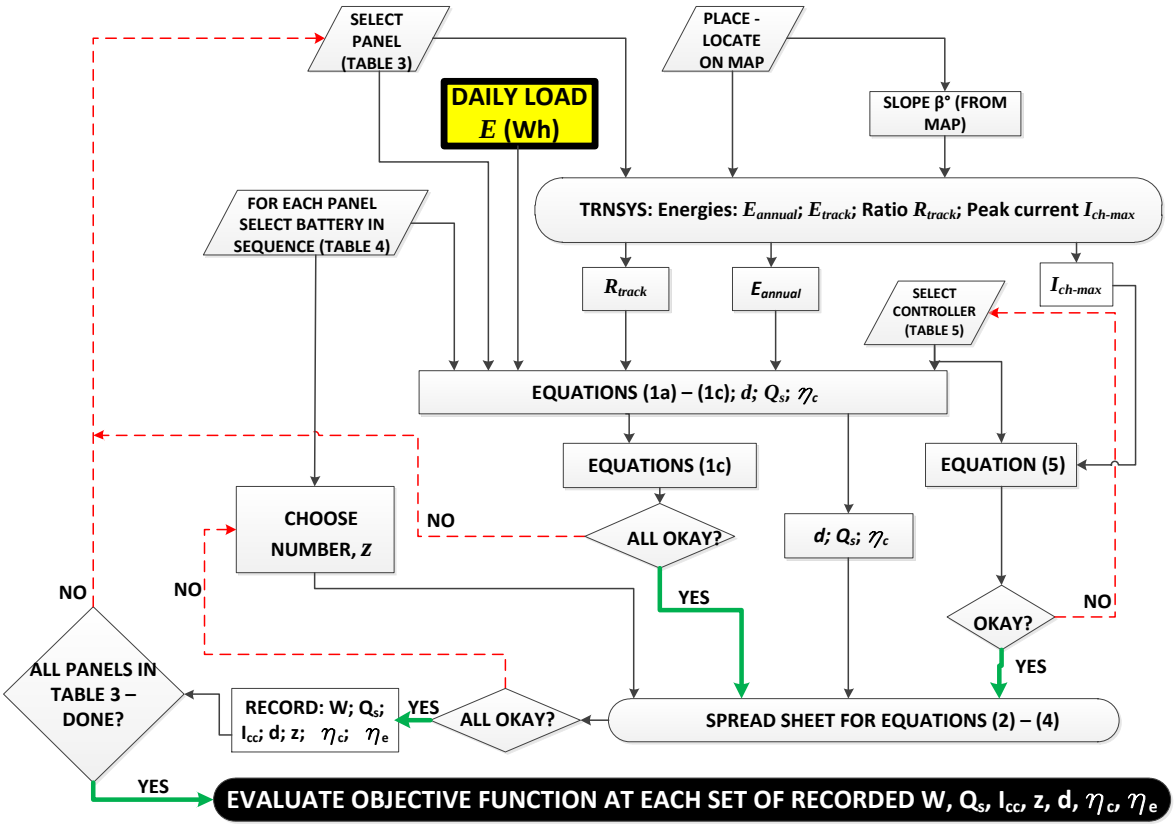

Figure 4.14: Optimisation model solution flow chart

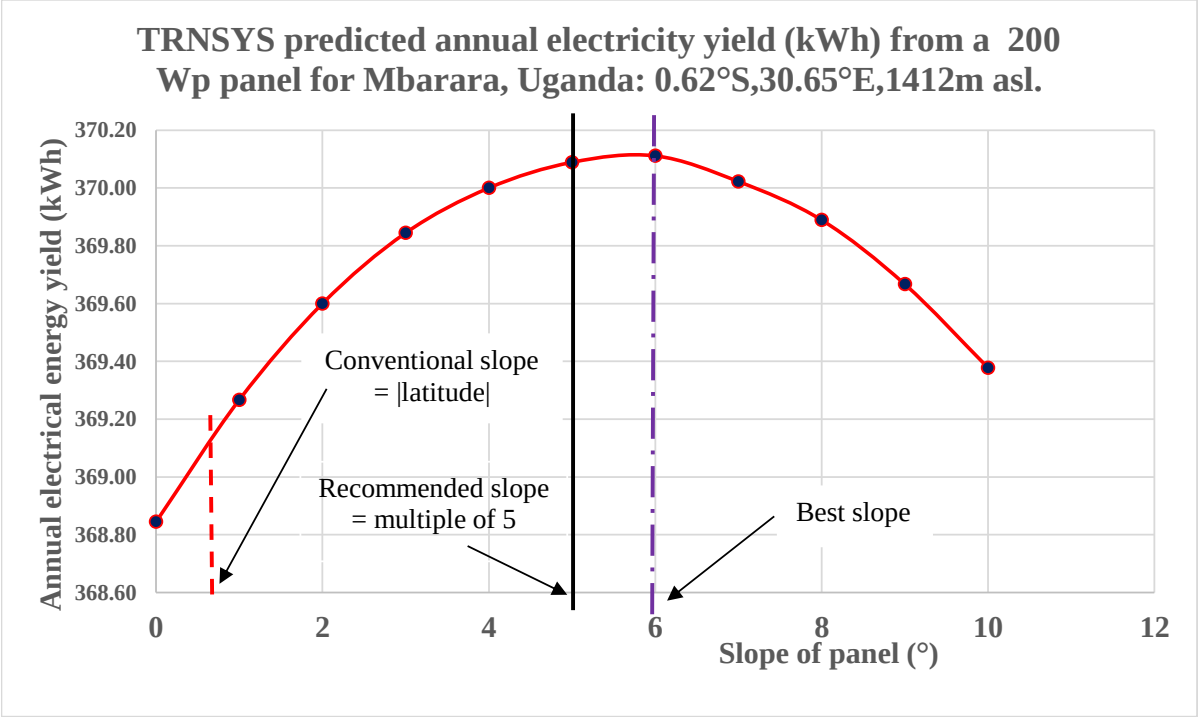

Figure 4.15: Illustration of how to determine 'recommended' slope

Table 4.6: Mbarara, Uganda: Feasibility space (Part) and optimal solutions identification

PANEL SIZE, W (Wp)	BATTERIES			CHARGE CONTROLLER (A)	OBJECTIVE FUNCTIONS		
	Q_s (Ah)	d (%)	z		W (Wp)	$dzQ_s/100$	
180	70	100	3	10	180	210	
180	85	80	3	10	180	204	
180	90	100	3	10	180	270	
180	100	40	5	10	180	200	
180	105	50	4	10	180	210	
180	115	80	2	10	180	184	Smallest panel solution
200	70	100	2	15	200	140	Smallest battery storage solution
200	85	80	3	15	200	204	
200	90	100	2	15	200	180	
200	100	40	4	15	200	160	
200	105	50	3	15	200	157.5	
200	115	80	2	15	200	184	
225	70	100	2	15	225	140	
225	85	80	3	15	225	204	
225	90	100	2	15	225	180	
225	100	40	4	15	225	160	
225	105	50	3	15	225	157.5	
225	115	80	2	15	225	184	
etc.	etc.	etc.	etc.	etc.	etc.	etc.	
				MINIMISE	180	140	

In deriving the possibility space, the key point is to make sure that on no single day, does the closing usable charge in Ah drop to zero. This is what the penultimate decision step in Figure 4.14 (i.e. immediately after 'spread sheet for equations 2 – 4') does. Figures 4.16 and 4.17 show the resulting system performances for the two alternative optimal solutions. In both figures, the system is put to use for the first time on 1st January. In that case, it is seen that the most critical day of the year is 5th May - when the closing usable charges are 28.0 and 5.1 Ah respectively. But what happens if the system starts on any other day – as is more likely to be the case in practice? That day's potential energy production is missed in the first year of service (just like the one of 1st January in the present scenario). Because the batteries are assumed to always start the life service in a fully charged condition, it does not matter which day of the year the system starts. Hence, the selections shown are valid for any continuous 365 day period.

Might we have problems on the 366th day of service? For the case of Mbarara, certainly 'No' - because the closing balance charges on 31st December and the 1st January productions ensure full battery statuses on the 366th day. Hence, the performance is cyclic with a period of 365 days. For other places – especially those outside the tropics (South Africa in this paper), a small possibility of inadequate supply on the 366th day exists only if that day is deep in rainy winter and the particular solution happens to leave marginal closing balances on the 365th day. To overcome this problem, the optimisation for such places is done over a 366 day

period irrespective of day of system installation. The long term period for solutions from such cases will however still be 365 days.

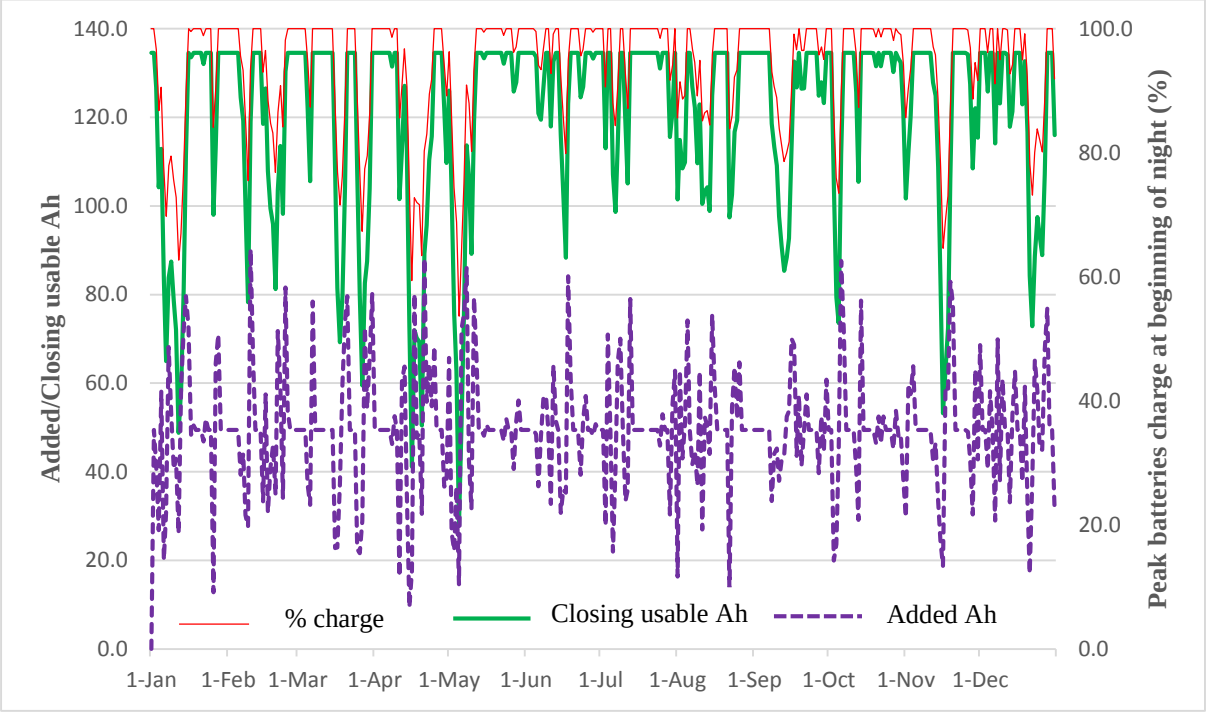

Figure 4.16: Mbarara – Uganda: Year performance for the 'Smallest' panel solution: ***W*** = 180 Wp; Deep cycle 115 Ah Lead acid batteries with ***d*** = 80%; ***z*** = 2; *L* = 5 years; MPPT controller I_{cc} = 10 A.

Figure 4.17: Mbarara – Uganda: Year performance for the 'Smallest' battery storage solution:

W = 200 Wp; Deep cycle with peak usable 140 (2X70) Ah Lead acid batteries and ***L*** = 7 years; MPPT controller I_{cc} = 15 A.

4.4.4 *Results: Sub-Sahara Africa's optimal selections for minimum charge storage*

In the rest of the region, it was decided to evaluate the feasibility spaces only for objective function (11b), i.e. minimum storage. This was because batteries are the most perishable component in the model, and therefore, would most likely be the long term drivers of energy costs. Table 4.7 gives a sample of 20 out of 152 result sets for the region.

4.4.4.1 *Mapping optimal solutions using MATLAB®*

For each of the 152 stations, an optimal combination was obtained. Ordered matrices of latitude [L], longitude [Lo], minimum Battery storage [B], panel size [P] and charge controllers [C] were then constructed.

The geo matrices **B**, **P** and **C** were each plotted using the program – illustrated for panels - below:

```
      axesm Mercator  gridm
off   framem on
      Panel=surfm(L,Lo,P);
      load coast
      plotm(lat,long,'black')
      setm(gca,'mapProjection
',
      'polycon','Origin',[0,1
5,0])
```

The results are given in Figure 4.18. This figure includes a map of recommended slopes extracted from the related work [49]. It is these slopes that are used in the solution flow chart of Figure 4.14.

Table 4.7: Sample of results for the objective of 'least battery storage'

SUB REGION	COUNTRY	STATION	LATITUDE (º)	LONGITUDE (º)	ALTITUDE (m)	REC. SLOPE (º)	PANEL SIZE (Wp)	USABLE BAT. CAPACITY (Ah)	CONTROLLER (A)	TRACKING GAIN (%)
NORTH SSA	MAURITANIA	ATAR 614210	20.48	-13.05	225	**20**	180	140	15	27
	SUDAN	PORT SUDAN 626410	19.58	37.22	3	**20**	180	140	10	26.5
	MALI	KIDAL 612140	18.3	1.35	459	**20**	180	90	15	27.3
	ERITREA	ASMARA 630210	15.28	38.92	2325	**15**	180	140	15	29
WEST SSA	SENEGAL	DIOURBEL 616660	14.65	-16.23	9	**15**	180	180	15	25.6
	GAMBIA	BANJUL AIRPORT 617010	13.35	-16.8	36	**15**	200	140	15	23.3
	GUINEA BISSAU	BOLAMA 617690	11.58	-15.48	20	**10**	200	140	15	21.9
	GHANA	NAVRONGO 654010	10.88	-1.08	198	**5**	200	90	15	22.3
CENTRAL SSA	CENTRAL AFR REP	BANGUI 646500	4.4	18.52	367	**5**	225	180	15	20.9
	CAMEROON	LOMIE 649610	3.15	13.62	624	**5**	225	270	15	20.6
	DRC	KISANGANI 640400	0.52	25.18	415	**5**	225	180	20	20
	GABON	MOUILA 645560	-1.87	11.02	89	**5**	250	210	20	17.9
EAST SSA	UGANDA	KAMPALA 636800	0.32	32.62	1144	**5**	225	180	20	22.9
	KENYA	NAIROBI DAGORETTI 637410	-1.3	36.25	1798	**0**	200	180	15	25.8
	BURUNDI	BUJUMBURA 643900	-3.32	29.32	782	**5**	225	180	15	19.2
	TANZANIA	ARUSHA 637890	-3.33	36.62	1387	**5**	180	210	15	26.2
SOUTH SSA	MOZAMBIQUE	LICHINGA 672170	-13.28	35.25	1365	**15**	200	210	15	26.3
	ANGOLA	SADA BANDEIRA	-14.9	13.48	1761	**15**	180	140	15	28.5
	MADAGASCAR	MAJAHANG 670270	-15.67	46.35	18	**15**	180	140	15	26.8
	South Africa	ZA-Cape-Town-688160.tm2	-33.97	18.6	44	**30**	180	210	15	29.8

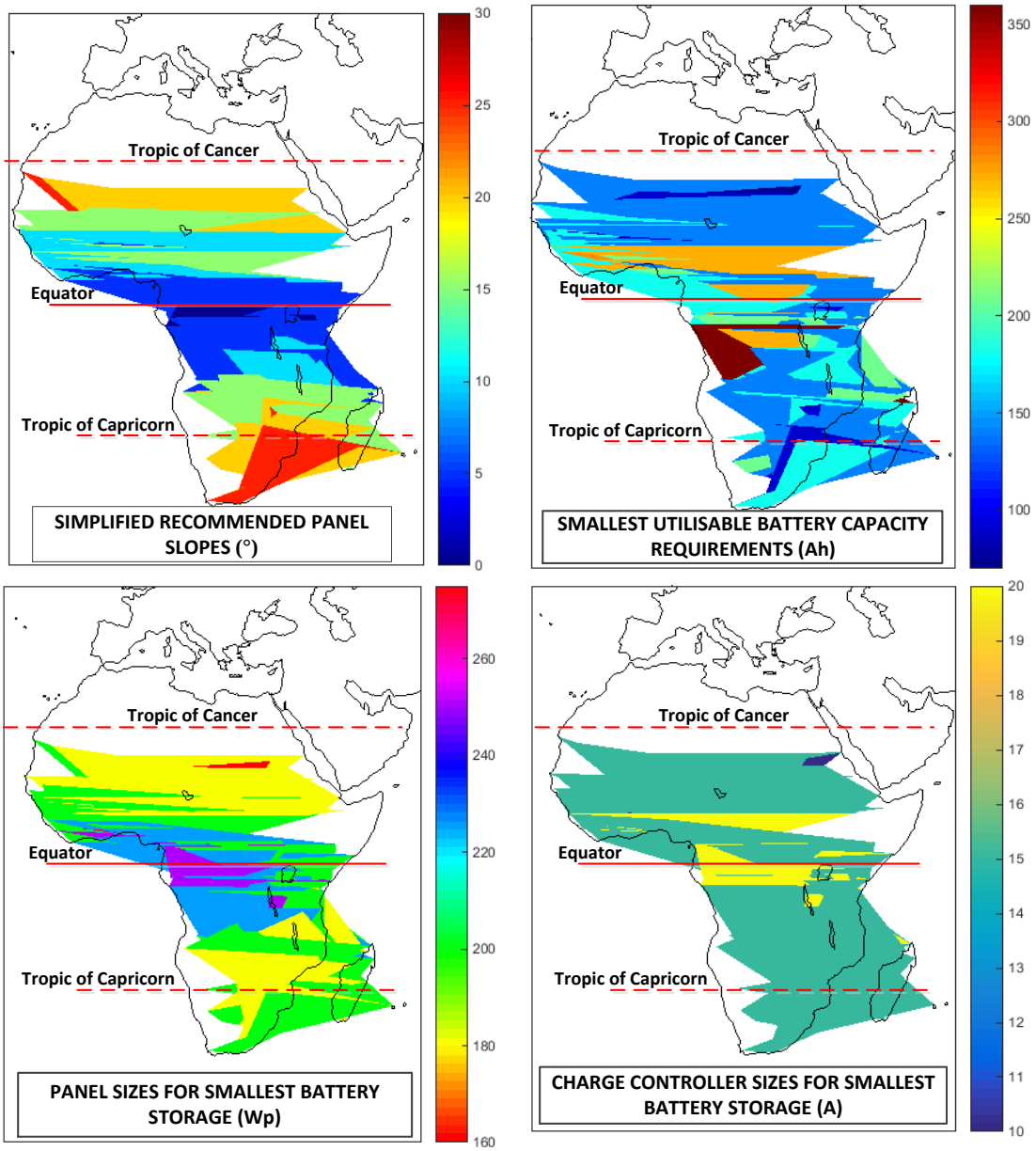

Figure 4.18: Mapping sub-Sahara Africa for component selections to minimise battery storage capacity

4.4.4.2 *Discussion*

Recommended slopes and the reasons for choosing only multiples of 5° are discussed in [49]. Suffice to mention here, that "ease and simplicity in installation" for a technical skills–deficient region was a major consideration. Here, we focus on the components. Referring to Figure 4.18, in general the distribution of sizes of optimal panels and batteries seems to have an underlying reliance on the latitude magnitude of the installation – with a marked symmetry about the equatorial belt. However, local distortions are introduced by geography. Thus, the rain forests of the Congo basin and the high tropical rainfall regions of coastal West Africa show a need for bigger panels and batteries than corresponding latitude areas on the Eastern plateau and highlands. The influence of the

Kalahari and Namib deserts in the south western part vis-à-vis the cloudier eastern mainland and Indian Ocean islands is well pronounced in the smaller sizes of components required in Namibia and Botswana.

Whereas this optimisation was for a fixed and largely night load, one could ask: what happens when consumers decide to use some of the electricity during the day? First, this would help improve the panel capacity utilisation ratio (defined as ratio of total consumed annual energy to maximum annual production possible) because production losses due to battery storage limitations would be reduced. To illustrate, for the Mbarara case of Figure 4.17, the ratio is computed as 73.1% for the night loading (i.e. 182.5 kWh / {364.91 kWh*0.95*0.72}) where 0.95 and 0.72 are the charge controller and battery energy efficiencies corresponding to the selections. This means, there is some capacity to take on some load during the day. However, it would generally be erroneous to expect a nil blackout on some days of the year, unless the actual night demand is deliberately reduced.

Would optimising for 'smallest panel' improve ability to handle day loads? In Figures 4.16 and 4.17 we see that optimisation based on 'smallest panel size' would give a bit more reserve capacity in the batteries than that based on minimising battery storage (Minimum closing usable charge of 28.0 Ah against 5.1 Ah on 5th May). However, the present design load of 500 Wh now consumes about 81.2 % of the panel capacity, leaving a smaller quantity for day loads. Thus, although there is more storage capacity, there is less energy to fill that storage – leading to inefficient use of the battery system. Therefore, the answer for handling substantial day loads without offsetting the primary objective of this paper – of not having darkness at night – is in a different optimisation scheme which would have to use the day load profile as one of its inputs. The procedure to follow in that case is to change the time series computations to hourly instead of daily basis. The solution procedure remains the same. The only issue in such a formulation is that the hourly weather data for long term planning would exhibit greater variability, and hence, would increase the unreliability of the model. The decrease of reliability (i.e. increase of probability of failure) arises from statistics and probability theory. For it can be shown that a data set $\boldsymbol{S}$ consisting of independent subsets $\boldsymbol{S_1, S_2, ----, S_i, S_{i+1}, ----, S_n,}$ has a normalised standard deviation σ/μ, which is always less than or equal to the mean of normalised values for its subsets - as in equation (12). Hence, long term planning based on statistical daily weather data exhibits relatively 'greater' accuracy than that based on the constituent hours.

$$\frac{\sigma}{\mu} \leq \frac{1}{n}\sum_{i=1}^{n}\frac{\sigma_i}{\mu_i} \qquad (12)$$

Related to the question of using some of the electricity during the day is that of a wish by the consumer to expand the demand either for domestic or for commercial purposes. In each case, the model could be reformulated to cater for the additional load (and its timing), taking the consumer's current equipment into consideration. However, such a consumer would perhaps no longer be an "energy poor" person and would therefore lie outside the scope of this paper. Kabir, *et al*. [50], Balcombe, *et al*. [51], Merei, *et al*. [52], and Cole, *et al*. [53] have recently addressed different aspects of optimising for such consumers.

4.4.5 *Summary and Conclusions*

The primary objective of this paper was to present better informed recommendations on selection of PV system components to serve a 'medium sized' homestead attempting to emerge from energy poverty in sub-Sahara Africa. This arose from observations in the literature that there are hardly easy to follow and implement guidelines for optimised integrated work suitable for an extremely energy-poor region. The first task was to estimate basic needs of a mid-class homestead starting its journey out of energy poverty. The load – when using the more efficient LED bulbs - was about 500 Wh or 42 Ah a day on a 12 V DC system.

Recommendations by PV panel manufacturers and by other practitioners on component selections were critically examined. It was noted that these tended to be both localised and quite specific. To be more general, we built on earlier TRNSYS experimental validation work, and on that in a related study of panel slopes; we surveyed available components in South Africa, and presented a mathematical optimisation model to help select surveyed components that meet the above load at any area in neighbourhood of sub-Sahara Africa's 152 TRNSYS listed weather stations. Finally, for the objective of minimising energy storage requirement, we presented our findings on panels, batteries and controllers in easy-to-read regional maps. From these findings we can conclude:

- 15 Amp charge controllers are the most dominant recommendation in the region. A few isolated areas around the equator require 20 A while still fewer in north of Sudan require 10 A. The latter controllers seemed unsuitable in most of the region.
- Panel sizes that meet the load at minimum storage requirement vary between 160 Wp in dry, clear sky areas and 275 Wp, in heavy rainfall areas of the continent.
- Minimum usable battery charge capacities vary between 70 and 360 Ah.

Finally, we comment that the distribution of TRNSYS listed weather stations in the region is both sparse and uneven. The maps presented can therefore be improved as data for other areas becomes available. That notwithstanding, it is hoped that the rather complicated selection problem has been simplified, and presumably, the paper's objective achieved.

Acknowledgements:

We would like to thank CPUT Research Fund committee and the entire research directorate staff for the funding and support during the entire three year period of this and other work.

References:

[1] International Energy Agency. *Africa Energy Outlook. A Focus on prospects in sub-Saharan Africa. World Energy Outlook special Report, 2014*. OECD/IEA, Paris: 30-33.

[2] Population Reference Bureau. 2014 World Population Data sheet. USAID, www.prb.org/pdf14/2014-worlld-population-data-sheet_eng.pdf

[3] Pode R, Diouf B. *Solar lighting.* London, UK: Springer-Verlag, 2011.

[4] Oyedope SO. Energy and Sustainable development in Nigeria: The way forward. Energy, Sustainability and Society 2012;2:15. http://www.energsustainsoc.com/content/2/1/

[5] Bleeker AEM. Diffusion of solar PV from a TIS perspective and its transnational factors: A case study of Tanzania. Institute of Environmental studies, VU University Amsterdam, 2013. http://english.rvo.nl/sites/default/files/2014/01/Diffusion%20of%20solar%20PV%20-%20A%20case%20study%20of%20Tanzania.pdf

[6] Sambo AS, Zarma IH, Uguoke PE, Dioha IJ, Ganda YM. Implementation of standard solar PV projects in Nigeria. Journal of Energy Technologies and Policy 2014;4(9):22-28.

[7] Chaury A, Kandpal TC. A techno-economic comparison of rural electrification based on solar home systems and PV microgrids. Energy Policy 2010;38:3118–29.

[8] Nieuwenhout FDJ, van Gijk A, Lasschuit PE, van Rockel G, van Dijk VAP, Hirsch D, Arriaza H, Hankins M, Sharma BD, Wade H. Experience with Solar Home Systems in Developing Countries: A Review. Progress in Photovoltaics: Research and Applications 9, 2001;9:455-74.

[9] Nkwetta DN, Smyth M, Thong VV, Driesen J, and R. Belmans R. Electricity supply, irregularities, and the prospect for solar energy and energy sustainability in sub-Saharan Africa, J. Renewable & Sustainable Energy 2, 023102(2010); doi: 10.1063/1.3289733. http://dx.doi.org/10.1063/1.3289733

[10] Kanyarusoke KE, Gryzagoridis J, Oliver G. Predicting photovoltaic panel yields in sub-Sahara Africa from manufacturers' specifications. *Proc. International Conference on Engineering and Applied Science* Beijing, July 2012:223-55.

[11] Kanyarusoke KE, Gryzagoridis J, Oliver G. Solar lighting and Water preheating in tropical African homes: What sustainable possibilities? Paper presented at *OIDA conf. on sustainable development* Richards Bay, Dec 2014.

[12] Mulugetta Y, Nhete T, Jackson T. Photovoltaics in Zimbabwe: lessons from GEF Solar project. Energy Policy 2009;28(4):1069-80.

[13] Szabó S, Bódis K, Huld T, Moner-Girona M. Energy solutions in rural Africa: mapping electrification costs of distributed solar and diesel generation versus grid extension. Environ. Res. Lett. 6 (2011) 034002. doi:10.1088/1748-9326/6/3/034002 http://iopscience.iop.org/article/10.1088/1748-9326/6/3/034002/pdf

[14] Gustavsson M, Ellegård A. The impact of solar home systems on rural livelihoods. Experiences from the Nyomba Energy Service Company in Zambia. Renewable Energy 2004;29(7):1059-72.

[15] Rabah KVO. Integrated solar energy systems for rural electrification in Kenya. Renewable Energy 2005;30(1):23-42.

[16] Moner-Girona M, Ghanadan R, Jacobson A. Decreasing PV costs in Africa: Opportunities for rural electrification using solar PV in sub-Saharan Africa. *Refocus*, Jan/Feb 2006, 40-45.

[17] Wamukonya N. Solar home system electrification as a viable technology option for Africa's development. Energy Policy 2007;35:6-14.

[18] Ondraczek J. Are we there yet? Improving solar PV economics and power planning in developing countries: The case of Kenya. Renewable and Sustainable Energy Reviews 2014;30:604-615.

[19] Ondraczek J. The sun rises in the east (of Africa): A comparison of the development and status of solar energy markets in Kenya and Tanzania. Energy Policy, 2013;56:407-17.

[20] Rose A, Stoner R, Pérez-Arriaga I. Prospects for grid-connected solar PV in Kenya: A systems approach. Applied Energy 2016:161:583–90.

[21] Breyer, Ch, Gerlach A, Hlusiak M, Peters C, Adelmann P, Schützeichel H, Tsegaye S, Gashie W. Electrifying the poor: Highly economic off-grid PV systems in Ethiopia – a basis for sustainable rural development. In *Proc. European PV Solar Energy Conf*. Hamburg, Germany, Sept 2009, 3852-3860.

[22] Bazilian M, Onyeji I, Liebreich M, MacGill I, Chase J, Shah J, Gielen D, Arent D, Landfear D, Zhengrong S. Re-considering the economics of photovoltaic power. Renewable Energy 2013:53:329–38.

[23] Udoukah YN, Umoren M. Analysis of Solar potential and Energy production of photovoltaic modules at optimal tilt angles in Nigeria. Nigerian Journal of Solar Energy 2015;26:92-99.

[24] Wansah JF, Udounwa AE, Ezike SC, Akpan MS. Standalone Solar photovoltaic system for remote residential house in Ikot, Obio, Nsu, Nigeria. Nigerian Journal of Solar Energy, 2015:26:100-108.

[25] Itodo I, Aju ASE. Design of a Solar Photovoltaic System to Power a Rice Threshing Machine. Nigerian Journal of Solar Energy 2015;26:109-16.

[26] The World Bank, Access to electricity (% of population). http://data.worldbank.org/indicator/EG.ELC.ACCS.ZS (visited 22.06.15).

[27] Azimoh CL, Klintenberg P, Wallin F, Karlsson B, Mbohwa C. Electricity for development: Mini-grid solution for rural electrification in South Africa. Energy Conversion and Management 2016;110:268-77.

[28] Chan K-Y, Oerlemans LAG, Volschenk J. On the construct validity of measures of willingness to pay for green electricity: Evidence from a South African case. Applied Energy 2015;160:321–28.

[29] Reinoso CRS, De Paula M, Buitrago RH. Cost benefit analysis of a photovoltaic power plant. International Journal of Hydrogen Energy 2014:39:8708-11.

[30] Vidal-Amaro JJ, Østergaard PA, Sheinbaum-Pardo C. Optimal energy mix for transitioning from fossil fuels to renewable energy sources – The case of the Mexican electricity system. Applied Energy 2015;150:80–96.

[31] Tao Ma, Yang H, Lu L, Peng J. Optimal design of an autonomous solar–wind-pumped storage power supply system. Applied Energy 2015;728–36.

[32] Rogers JG, Cooper SJG, O'Grady A, McManus MC, Howard HR, Hammond GP,The 20% house – an integrated assessment of options for reducing net carbon emissions from existing UK houses. Applied Energy 2015;138:108-20.

[33] Olcan C. Multi-objective analytical model for optimal sizing of stand-alone photovoltaic water pumping systems. Energy Conversion and Management 2015;100:358–69.

[34] Boxwell B. *Solar Electricity Handbook 2012 Ed. A simple, practical guide to solar energy – designing and installing photovoltaic solar electric systems*. Warwickshire, UK: Green**stream** Publishing, 2012.

[35] Markvart T. (Ed.) Solar Electricity, 2nd ed. Chichester, UK: John Wiley & Sons, 2000.

[36] Chaurey A, Kandpal TC. Assessment and evaluation of PV based decentralised rural electrification: An overview. Renewable and Sustainable Energy Reviews 2010;14:2266-78.

[37] Kanyarusoke KE. KK answering qns. on his presentation 3 Dec 14. You tube video, https://www.youtube.com/watch?v=aT4%KSEmMKw (visited 25.02.16)

[38] Bohler-Muller N, van der Merwe C. The potential of social media to influence socio-political change on the African Continent, Policy brief. *Africa Institute of South Africa, Briefing No. 46*, March 2011.

[39] Wesolowski A, Eagle N, Noor AM, Snow RW, Buckee CO. Heterogeneous Mobile Phone Ownership and Usage Patterns in Kenya. PLoS ONE 7(4):e35319.doi:10.1371/journal.pone.0035319. http://journals.plos.org/plosone/article/journal.pone.0035319

[40] Williams. Foot-candles and Lux for Architectural Lighting (An introduction to illuminance). 1999. http://www.mts.net/~williams5/library/illum.htm (visited 08.07.14).

[41] Inan MN, Arik M. A multi-functional design approach and proposed figure of merits for solid state lighting systems. Journal of Solid state lighting 2014;1(8) doi: 10.1186/2196-1107-1-8.

http://journalofsolidstatelighting.springeropen.com/articles/10.1186/2196-1107-1-8

[42] Machala M. Kerosene Lamps vs. Solar lanterns. Stanford University. http//large.stanford.edu/courses/2011/ph240/Machala/1 (visited 08.07.14).

[43] OSRAM Opto Semicnductors. Life cycle Assessment of Illuminants: A comparison of light bulbs, Compact Fluorescent lamps and LED lamps. http://seeds4green.net/sites/default/files/OSRAM_LED_LCA_Summary_November_2009.pdf (visited 08.07.14).

[44] Zahedi A. Maximising solar PV energy penetration using energy storage technology. Renewable and Sustainable Energy Reviews 2011;15:866-870.

[45] Bianchi M, Branchini L, Ferrari C, Melino F. Optimal sizing of grid – independent hybrid photovoltaic-battery power systems for household sector. Applied Energy 2014; 136:805-816.

[46] Hansen UE, Pedersen MB, Nyagaard I. Review of solar PV market development in East Africa. UNEP Riso Centre working paper Series no. 12, Mar 2014 UNEP RISO Centre.

[47] ENFsolar. Solar panels Manufacturers from Africa. www.enfsolar.com/directory/panel/Africa (visited 25.06.15).

[48] Kanyarusoke KE, Gryzagoridis J, Oliver G. Validation of TRNSYS modelling for a fixed slope photovoltaic panel, Turkish journal of Electrical Engineering and Computer Science. In press. http://journals.tubitak.gov.tr/elektrik/accepted.htm DOI: 10.3906/elk-1502-38.

[49] Kanyarusoke KE, Gryzagoridis J, Oliver G. Fixed PV panel slopes in tropical Africa: Where is the sun? *Paper presented at. International Conference on Clean Energy for Sustainable Growth In Developing Countries*, Palapye, Botswana, September 2015.

[50] Kabir MN, Mishra Y, Ledwich G, Xu Z, Bansal RC. Improving voltage profile of residential distribution systems using rooftop PVs and battery energy storage systems. Applied Energy 2014; 134:290-300.

[51] Balcombe P, Rigby D, Azapagic A. Environmental impacts of microgeneration: Integrating solar PV, Stirling engine nd battery storage. Applied Energy 2015;139:245-59.

[52] Merei G, Moshovel J, Magnor D, Sauer DU. Optimisation of self-consumption and techno-economic analysis of PV-battery systems in commercial applications. Applied Energy 2016;168:171-78.

[53] Cole W, Lewis H, Sigrin B, Margolis R. Interaction of rooftop PV deployment with capacity expansion of the bulk power system. Applied Energy 2016:168:473-481.

4.5 Concluding the chapter

This chapter presented innovative material that concerned fixed panels of solar energy collectors. Optimised slopes for solar panel collectors were given, which could be used across most of the SSA region when installing PV equipment. In the tropical areas, two slope panel installations were suggested – and when and how to implement them. Because of the dearth of information on solar energy equipment selection and installation guides for the SSA region, the work focused on PV systems. It formulated requirements for 'modern energy' in start-up homes. A guide on what equipment to buy was provided where, with simple but distinctly colourful mapping, the requirements for slopes, panels, batteries and charge controllers for fixed PV installations could now all be 'optimally' selected by anyone who wishes to attempt use of the 'modern energy' home in SSA.

CHAPTER FIVE:

THIRD ARTICLE:

"ARE SOLAR TRACKING TECHNOLOGIES FEASIBLE FOR DOMESTIC APPLICATIONS IN RURAL TROPICAL AFRICA?"

Kant E KANYARUSOKE; Jasson GRYZAGORIDIS, Graeme OLIVER
Journal of Energy in Southern Africa • Vol 26 No 1 • February 2015, pp. 86-95

5.0 Introducing the Journal paper

The innovations in the last chapter were for fixed slope and fixed or semi fixed orientation flat solar energy collecting surfaces. These collectors are by far the most prevalent among all domestic users trying to harness the sun's energy for the production of electricity or for heating and crop drying purposes. In fact, for the latter two, it is virtually universal that when flat collector surfaces are used they are of the fixed type. Solar energy engineering experts accept that flat heating collectors do not track the sun ((Duffie and Beckman 2013; Kalogirou, 2014; Tiwari, 2000; etc.).

Regarding PV solar panels, as reported in section 4.2.5, innovations on azimuths improve yields by a small percentage, generally below 10%. The improvements are easy to implement and there is still plenty of room for further innovation. However, it would probably be easier to seek a tracking solution. Tracking solutions exist elsewhere and in non-domestic applications on the continent.

This chapter presents a journal paper that reviews small tracking systems that could possibly be used in SSA's homes. The paper examines the technical challenges that would have to be overcome before a practical tracker system is made available. The chapter ends by stating that presently the - would be beneficiaries - do not have practical information about tracking systems (let alone having the collectors on which to apply them).

5.1 The Journal paper

Are solar tracking technologies feasible for domestic applications in rural tropical Africa?

Kant E Kanyarusoke[a]

Jasson Gryzagoridis[b]

Graeme Oliver[a]

a. Department of Mechanical Engineering, Cape Peninsula University of Technology, Cape Town, South Africa
b. Department of Mechanical Engineering, University of Cape Town, South Africa

Received 28 July 2014; revised 26 December 2014 Journal of Energy in Southern Africa.

Abstract

That solar tracking improves energy yields from solar harvest systems is not debatable. Nor is the under powering of tropical Africa amidst plenty of energy resources – including solar. This paper presents a review of recent literature on tracking as applied to domestic solar harnessing devices. The purpose is to find basic requirements in design of a suitable solar tracker for the region's rural homes. It is concluded that Single axis passive trackers possibly will stand better chances of acceptability in the region.

Keywords: tropical Africa, solar tracking, solar energy, domestic application

5.1.1. *Introduction*

It is an established fact that tracking improves energy yields from solar harvest devices. But there are doubts about the efficacy and economics of this improvement for small systems and in high diffuse radiation areas. Mousazadeh et al. (2009) for example advise against use of tracking for small systems because of disproportionate energy consumption by the tracking mechanisms. Elmer (2006) reported lack of significant total energy gain from solar tracking in Great Britain because of excessive diffuse radiation. In Hanover, Germany, Beringer et al. (2011) reported that the tilt angle of fixed panels was nearly irrelevant as far as total annual yields were concerned. Does this mean tracking does not yield more energy? – Not necessarily. Kanyarusoke *et al* (2012a) showed that at latitude (L), a fixed slope (β) surface receives radiation at a best angle on the day when the sun declination (δ) satisfies the condition in equation (1). Hence all fixed surfaces do so at their appropriate times. Whether the total annual yield for one inclination is higher than that at another depends on additional factors like climatic conditions.

$$\left|\beta - \left|L - \delta\right|\right| = Minimum \qquad (1)$$

Tracking enables multiple repetition of this condition – and hence can in general be

expected to increase yield as reported by many researchers and inventers in different circumstances. Theoretical analysis on photovoltaic yields from a 180 Watt peak panel at 80 African weather stations by the above investigators (Kanyarusoke *et al*, 2012b) seemed to suggest there can be substantial gains using various modes of tracking except in rainy equatorial and sandy, windy Sahel regions. There, effects of diffuse radiation were as important as in Elmer's case above. Focusing on systems as small as the above panel – for home use - we will therefore review available literature on suitable tracking devices.

5.1.2. *Tropical Africa: Energy Issues and solar tracking needs*

Tropical Africa is that part of the continent lying between latitudes ±23.45°. This means the sun is directly overhead two times annually at most places in the region. It also means the sun's rays do come from the northern and southern directions at different times of the year. Hence, as pointed out by (Kanyarusoke *et al* (2012a) the use of fixed slope panels facing either direction poses problems of missing beam radiation at certain times of the year.

This region is described by the International Energy Agency (IEA) as underpowered because of inadequate grid power supply (IEA 2011). Hence, self-generation is a necessity in many situations. At village level, the easiest, safest and most convenient form of self-electric generation is to use photovoltaic (PV) systems. But PV systems thermodynamic efficiencies are in the 10 to 16% range (Kanyarusoke *et al*, 2012b). Ideally therefore, they should be installed to track the sun so as to maximise incident energy if costs of doing so are justified by additional yields.

There are other problems. Not least of which are: Capital costs – though rapidly coming down now; Skill shortages (Kanyarusoke *et al,* 2012b) and slow behavioural changes at the rural level (Murphy, 2001). Reports by the Africa Development Bank (ADB) on growth of the middle class (ADB, 2011) however, seem to suggest that some problems are slowly being overcome. In rural Kenya for example, Eveleens (2011) and Solar Buzz (2012) report that PV installations are now outpacing grid supply. Tracking has however not yet been adopted.

The only area where tracking is being used out of necessity is in concentrated solar power (CSP) systems. Nigeria leads in documented research outputs on this. Between Oyetunji's 1989 work on composite conical concentrators (Oyetunji et al. 1989) and Abdulrahim's 2008 PhD work on bi focal solar tracking (Abdulrahim et al. 2010) there were not less than seven significant contributions at honours and MSc degree research levels in the area.

The extensive energy poverty in tropical Africa amidst an abundant solar resource supply and a growing middle class means that a large potential for innovative solar energy harvesting devices exists. The progressive efforts by African governments to increase the solar resource component in their energy mixes (Karekezi, 2002; Bugaje, 2006; UN, 2007; Brew-Hammond and Kemausuor, 2009) and to rural-electrify (UNEC, 2006; Fluri, 2009; Brent and Rogers, 2010; Pegels, 2010; UN, 2014) create opportunities for a mass market of suitably designed solar tracking devices not just to cater for PV and CSP but also for Solar Thermal (ST) applications.

But constraints to penetrating this potential market abound. One fact is that the number of solar harvesting devices is as yet still low

(Fluri, 2009; Brent and Rogers, 2010; Pegels, 2010). But even if it increased, failure to critically examine existing tracker designs in relation to the region's market dynamics could still keep the designs out.

In summary therefore: first, there is a big potential for solar engineering development for tropical African homes. Secondly, some of these applications need to track the sun. But even where systems are being developed, tracking is limited only to where it is absolutely essential. Why is this so? Could it be that existing technologies do not adequately address issues at the rural African home? We now review the technologies to check this hypothesis.

5.1.3 *Solar tracking technologies*

Solar tracking is the act of making a solar collection surface change its orientation with apparent movement of the sun in the sky. There are two significant relative motions in the earth-sun system. The first is the diurnal movement due to the earth's rotation about its axis, causing day and night. This is responsible for the hourly variation of incident solar radiation on a surface. The second is the much slower movement due to the earth's elliptical voyage round the sun. Two factors in this motion combine to affect incident radiation. First, the actual sun-earth distance affects the extra-terrestrial radiation in accordance with an inverse square law. Secondly, the angle between the earth's equatorial plane and its orbit causes an apparent seasonal north-south range of travel of the sun in the upper celestial hemisphere. Figure 5.1 shows the relative motions.

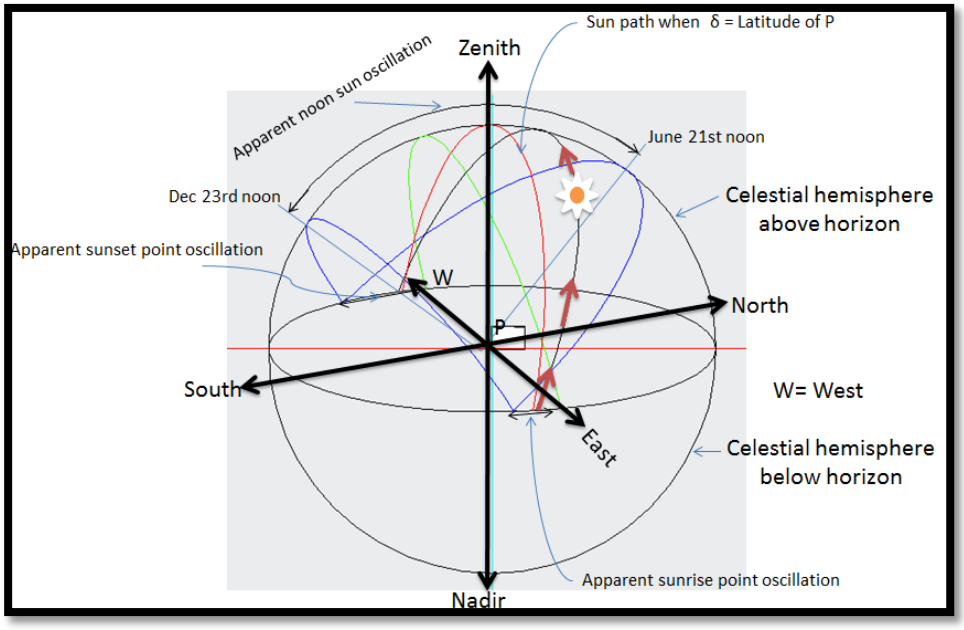

Figure 5.1: Apparent sun motion on the 'inside' surface of an inverted celestial hemisphere for a place 'P' within the tropics

Full control of solar harvest surface orientation is therefore a 2-degree of freedom problem. In practice, control is achieved by manipulating rotations about 2 of any 3 orthogonal axes. Commonly used axes are: West-East; North-South in the horizontal plane and the vertical Nadir-Zenith. Mousazadeh et al. (2009), Kelly and Gibson(2010), Barsoum and Vasant (2010), Seme et al. (2011), Tina and Gagliano,

(2011) - among others - report the following pairs to constrain the rotation as to keep the surface facing the sun all day long.

- W-E and S-N
- S-N and Nadir – Zenith
- Nadir – Zenith and W-E

Rotation about these axes affects the surface slope β and its azimuth ψ. Tracking manipulates these angles to vary with the sun angles: the elevation α and the solar azimuth ψ_s. These are dependent on the time and day of year. Hence from a tracking point of view, they are independent variables. Figure 5.2 shows the four angles.

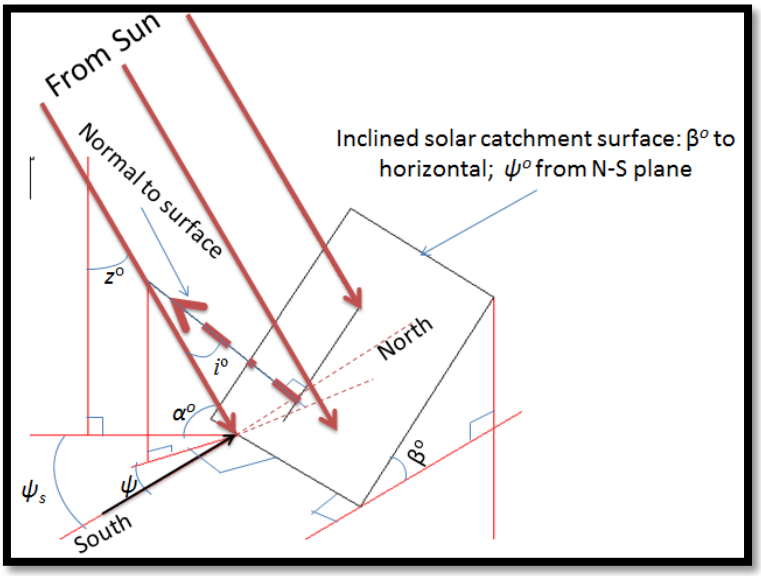

Figure 5.2: Important angles for a solar tracking surface: '*i*' is the incidence angle to be minimised

Broadly, the angles β and ψ track α and ψ_s using mechanisms classified according to two criteria (Helwa, et al. 2000; Markvart, 2000; Chong and Wong, 2009):

- Passive or Active tracking
- One axis or Two axes tracking

We now turn to examples in each subdivision.

5.1.3.1 *Passive Tracking*

When the radiation catchment plane or aperture is adjusted without use of electrical power, the tracking is said to be passive. When the radiation catchment plane or aperture is adjusted without use of electrical power, the tracking is said to be passive.

Passive single axis trackers -

Passive tracking on one axis is commonest in solar thermal systems employing tubular absorbers. These include (Winston, 2001; Kalogirou, 2007): compound parabolic collectors (CPCs), linear Fresnel reflectors (LFRs), parabolic trough collectors (PTCs) and cylindrical trough collectors (CTCs). However, in many tropical and mid latitude areas, solar voltaic systems can be similarly tracked. In doing so, the radiation catchment plane is directed to the sun usually in

incremental steps about either a horizontal S-N or one parallel to the earth rotational axis.

One example of a passive tracker is that by Zomeworks (Zomeworks, n.d.). This uses a refrigerant under suitable pressure in two cylinders running along the edges of the radiation catchment surface as shown in Figure 5.3. The cylinders are shaded and connected by a pipe/tube. When the incident radiation is not normal to the catchment plane, one of the cylinders is heated more than the other. Some of the refrigerant in the affected cylinder evaporates to create a new saturation pressure. The pressure rise forces some liquid into the cooler, shaded cylinder causing an extra torque to act on the structure's rotational axis. The shading is designed such that this torque turns the un-shaded cylinder into a shade. Damping helps stabilise the system quickly.

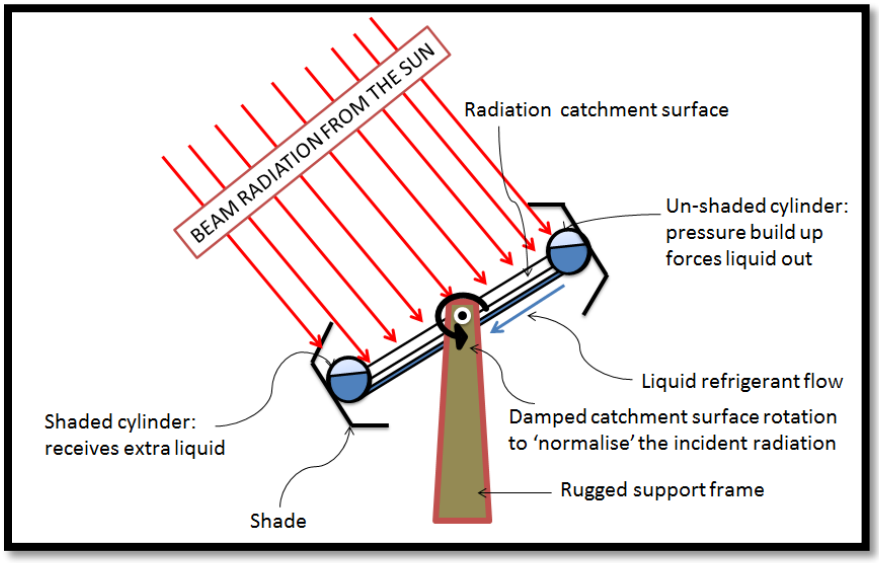

Figure 5.3: Zomeworks solar tracker – principle of operation

Although good and popular, the main problems with the Zomeworks tracker are: lack of an evening/night return mechanism; slow wakeup response in the mornings due to limitation on the surface inclination angle β. Poulek (1994) and Full (2010) have faulted use of refrigerants in the system on account of environmental and safety concerns. Use of safer refrigerants like R134a can help address this issue but cost and pressurisation would still be problematic.

Poulek developed a tracker using a shape memory alloy (SMA) to actuate the rotation. Two identical cylindrical actuators were symmetrically encased in a rotating cylinder with a lens at its opening as shown in Figure 5.4. Two of the ends were joined to a plane mirror attached to the rotating case while the other ends were fixed to the frame (stator) supporting the radiation catchment plane and casing. When the plane is properly oriented to the sun, the lens focuses the radiation onto the mirror which reflects it back preventing the SMAs from receiving it. On misalignment however, one of the SMAs receives the radiation, gets heated above its transformation temperature and then changes shape, rotating the mirror - and

hence the plane - until radiation is again incident on the mirror.

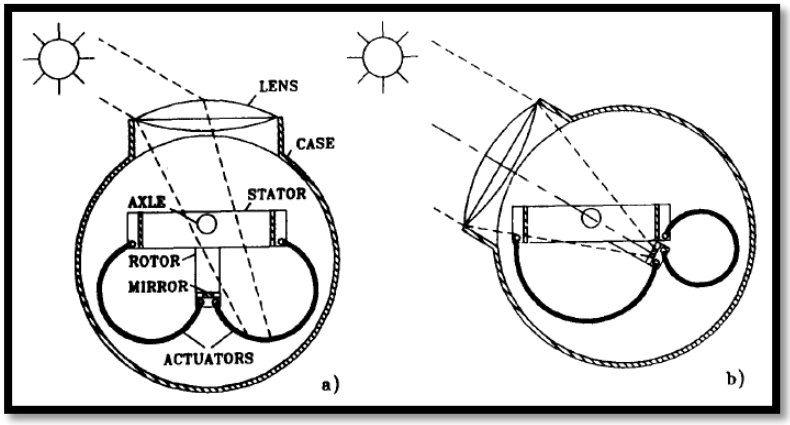

Figure 5.4: Poulek's single axis passive solar tracker: With permission from Elsevier: Solar Energy Materials and Solar cells: 33 (1994): 288 &289.

The tracker uses Cu-Zn-Al alloy because of the material's high damping characteristics. Thus, oscillations do not arise. It returns itself to morning conditions at night and might cost less than Zomework's (A 1994 US$ 150 versus March 2011 US$ 819 to 2820 for the latter). Its downside is the 140° swing limit – meaning some energy harvest in mornings and evenings is lost.

Clifford and Eastwood (2004) designed a tracker using the more common and robust aluminium/steel bimetallic strips. The strips are shaded and attached to the edges of the radiation catchment plane like the cylinders in the Zomeworks tracker. The more expansive aluminium is on the outside. Connected to the strips midpoints are masses which help amplify moments caused by the differential expansion on heating. The resulting net moment turns the radiation catchment plane to shade the hot strip. A mass-damper-thermally induced spring system was able to achieve a tracking range of 120° under lab conditions in the UK.

Although the design had equatorial regions in mind, it wasn't field tested in the target area. Full (2011) made a similar design in Kenya, East Africa. Using the strips and turning on a shaft from locally available bamboo plants, the tracker was reported to help increase photo-electricity generation by 38% and to cost between US$ 10 and 20 to produce (Hernandez, 2011; Anonymous, 2011). Still in equatorial and rural Kenya, Mwithiga and Kigo (2006) developed a manually operated coffee beans dryer. But after looking at the tracking labour cost, they concluded that the energy gains could not be justified for a low value crop like coffee.

Their design in Figure 5.5 however, has potential for development into a viable mechanically operated and improved system. For example, heat loss through the sides could be reduced by simple insulation; air flow through and over the carpet could be improved by providing an opening at the lower face and using a stack effect at exit; the system could be run using a mechanically stored energy device.

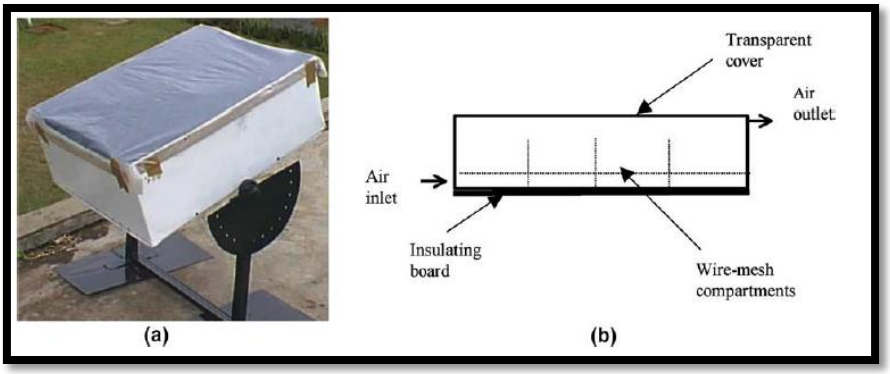

Figure 5.5: Mwithiga and Kigo's Coffee bean manual sun tracking dryer. With permission from Elsevier: Journal of Food Engineering 74 (2006):248.

In sub-Sahara Africa, manual tracking - particularly of solar thermal systems dominates. In his PhD thesis, Abdulrahim (2010) reviewed work that had been done in Nigeria especially on solar concentrators. Works by Oyetunji, et al. (1989) and by Suleiman, et al. (1989)] at Ahmed Belo University (ABU) were cited. Oyetunji's group was reported to have worked on conical concentrators while the latter group worked on cylindrical collectors. All tracking was manual. In the 1990s, works by Musa, et al. (1992), Ajiya (1995), and Mshelbwala (1996) were reported. Musa's work group designed, constructed and tested a Fresnel concentrator which they manually tracked every 20 minutes. In spite of the improved performance, the labour requirement was too much to let the project proceed. Ajiya designed and tested a manually steerable parabolic cooker. It performed satisfactorily – achieving 30% energy efficiency. Mshelbwala modified the cooker by supporting the cooking pot to directly receive the reflected radiation. He reports to have raised the efficiency to 46.6%.

This century has seen improvements on earlier designs and further developments at many research centres across Nigeria – eventually culminating in the mechanically tracked bifocal collector of Abdulrahim's doctoral thesis in 2008. Ahmed (2001) improved parabolic trough collection at ABU. Pelemo, et al. (2002a, b, 2003) worked on circular paraboloid concentrators - improving concentrating ability, developing innovative collecting pot materials and demonstrating applications in water distillation. Abdulrahim's mechanical tracker – the first recorded mechanical tracker in Nigeria - was powered by a dropping weight that operates a clock mechanism driving the collectors through a chain drive. Peak water temperatures achieved varied between 42 and 83°C depending on the time of year and flow rate.

Outside Africa, only a few additional passive devices have been developed because focus has been on active systems. We look at representative devices from a system primary energy point of view. Hitchcock (1976) patented a buoyancy powered unit for the US navy. An array of Fresnel reflectors was kept pointed to the sun using water. Buoyancy actuated movement whenever individual reflector elements were out of alignment. The issues with this tracker are that in morning hours, it takes about one hour to 'wake' up; it needs very precise manufacturing and assembly and uses a lot of water. It is big and not suitable for

domestic applications. However, its use of water and actuating gear mechanism points to suitable smaller designs.

Yi and Hwang (2009) patented a water driven tracker for Kun Shun University, China. A frame carries a pivoted radiation catchment surface. On either side of the pivot are spring supported water tanks with inlet and outlet valves. With the frame oriented in a W-E direction, one tank is filled with water at night while the other is emptied. This makes the surface face eastward. In the morning, the full tank is emptied in predetermined steps such that the frame incrementally tilts westward at an approximate uniform rate of 15° per hour. By solar noon, the tank is empty – and the frame takes on a horizontal position. When this happens, incremental filling of the western tank begins. Consequently, the catchment surface continues its westward rotation tracking the sun in the afternoon. The night operation of emptying the western tank and filling the other ends the cycle for the day.

The invention's merit is in its relative simplicity and automated filling and refilling of tanks as driven by a pre-programmed clock mechanism. It has no 'wake up' issues of its predecessors. The drawbacks might include: Turning angle limits – which are dependent on support springs. Second is the issue of water supply. A possibility is that water from one tank is preserved for use in the other. If this be the case, then a mechanism for the transfer should have been included in the patent.

Passive Two axes trackers -

Many single axis trackers can be turned into full tracking types by providing independent means to turn about a second axis perpendicular to the first one. In fact, manual mobile types use this approach to orient the panel. The second axis for these cases is almost always vertical. An obvious problem is the additional cost and complexity for the expected energy gains. The single axis W-E tracking will have improved yields by 20 - 30% (Bekker, 2007; Rabinowitz, 2011; Kanyarusoke et al. 2012a, b; Sobamowo et al., 2012). The additional 5 to 10 percentage points may not easily be justified. This is particularly true in the tropics where the sun's noon zenith angle cannot exceed 47° and therefore the additional gain is at the lower end. The closer to the equator, the smaller will be the necessity to double track. Because of these limitations, the literature does not show many passive double trackers. For example, a June 2013 Google scholar search with Two axes passive solar tracking yielded only 235 results – most of which were not about tracking in the context here. However, three recent patents came up. Of these, only one is suitable for smaller domestic systems. It is similar to an 'improved' Zomeworks'. Djeu (2004) patented a passive full tracker for a solar concentrator that could be visualised as shown in Figure 5.6. A reflecting/refracting system focuses radiation onto a fixed collector. The energy receiving sub system is mirrored about a central plane for balancing purposes. One Gimbal rotates about an N-S axis and carries the optical system - with its balancing subsystem. The other rotates about an E-W axis. The fixed energy collection surface contains the point of intersection of the two axes. Refrigerant is held in shaded canisters at either end of the axes. The canisters for each axis are connected by piping as in the Zomeworks system.

The technical issues with this system are mainly to ensure proper balance of the gimbal and the usual 'wake up' and maximum inclination angle problems.

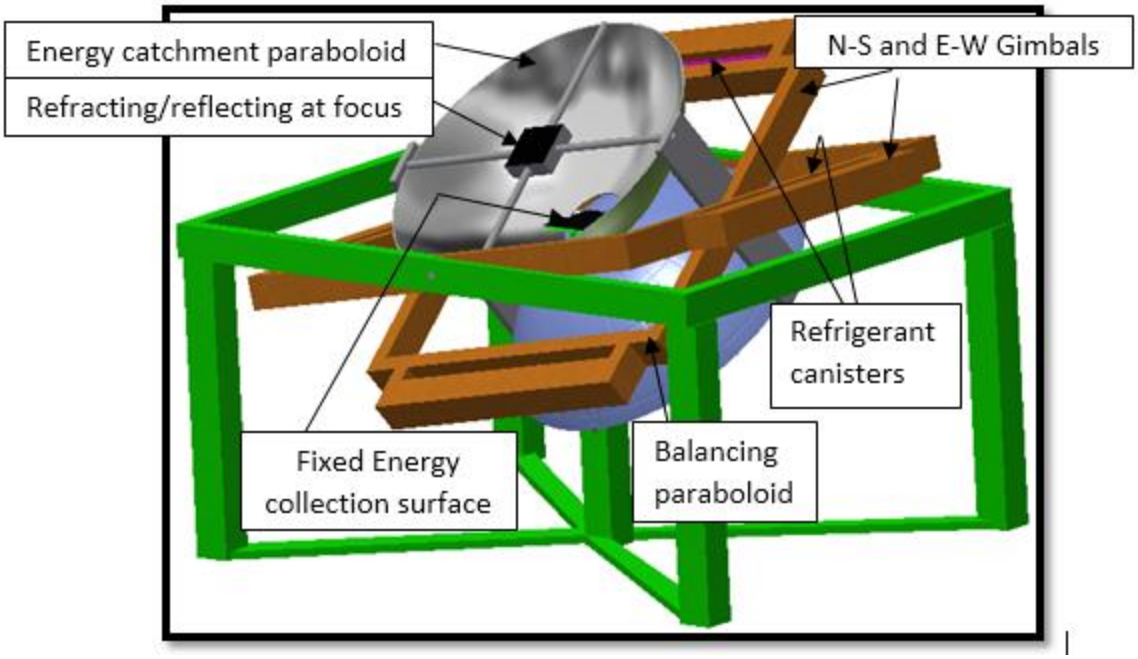

Figure 5.6: A 3-D visualisation of a typical Djeu's 2004 passive full tracker

5.1.3.2 *Active Tracking*

Active trackers use electricity to drive the mechanism. They use any of 3 methods to sense the sun relative position: Light dependent resistors (LDRs), Photo transistors and Photocells. The devices are arranged in pairs to detect differential illumination which is transduced to an amplifiable voltage. The amplified signal is then used in a control circuit to drive a motor rotating the mechanism about an axis of interest. In general, each control axis will have its own sensing-control-motor–drive set up. Thus, single axis tracking has one set while two axes trackers have two sets.

Active Single axis trackers -

There are few active single axis trackers. The following three have been identified in the recent literature. Zerlaut and Heiskell (1977) patented a tracker with a clock override for Desert Sunshine Exposure Tests Inc. The override prevents fooling of the tracker by bright objects in the sky when the sun is occluded. Rizk and Chaiko (2008) designed a unit capable of supporting an 8 kg 75 W panel using simple scrap parts. They reported a material purchase cost of Aus. $ 100 to 150 for the tracker. On a 9 Wp rated panel, they generated 6.3 W against 3.51 W when the panel was horizontal. While this is a substantial gain, it would have been more appropriate to compare yields with those from an inclined panel – since Australia is situated well south of the equator - and the optimal fixed slope panel is not expected to be zero. The tracker consumed 48 mW under no load conditions - or less than 1% of total power generated. Whether this justifies tracking or not depends on what power would have been produced in an optimally inclined fixed position.

Ciobanu *et al*. (2010) discussed kinematics of cam linkages coupled to parabolic mirrors. These mechanisms require less complicated control circuitry, can resist

disturbance loads more robustly but add to the number of moving parts and consequential drive power losses. A typical mechanism is shown in Figure 5.7.

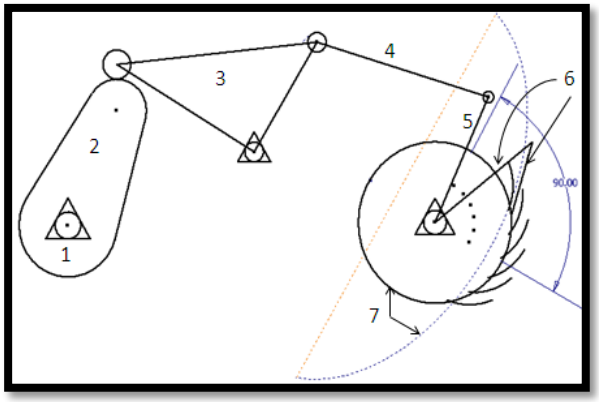

Figure 5.7: Example of one of Ciobanu *et al.*'s linkages

1-Frame; 2- Disc cam; 3- Oscillating follower; 4- Transmission link; 5- Rocker; 6- Ratchet locking link; 7- Ratchet and Parabolic mirror

Active Two axes trackers -

Most active trackers are of the two axes type. Hence, there are many variants in the literature. Here, we cite some of those reported after 2005. Bakos (2006) reports use of 2 sets of LDRs as sensors to drive a 1370 rpm, 0.37 kW motor on the W-E axis and a 930 rpm, 0.75 kW one on the vertical. It is an electromechanical drive employing 4 relays and 2 electronic circuits connected to a computer with suitable software. A 46.46% energy gain when compared to a fixed 40^{o} slope panel is reported. Louchene et al. (2007) report use of fuzzy logic in generation of command signals to the drive motors.

Barsoum and Vasant (2010) report the design of a simplified full axes tracking system shown in Figure 5.8. It uses LDRs and varies the panel's azimuth and slope.

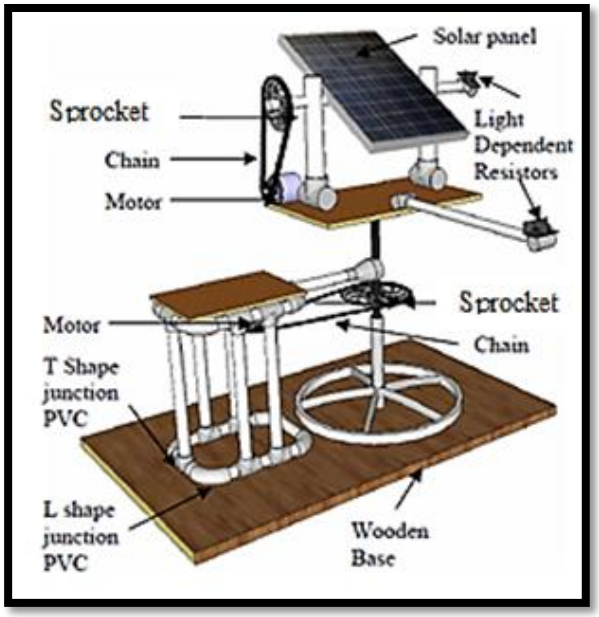

Figure 5.8: Barsoum and Vasant's Solar Tracking Prototype: (with permission from: Global Journal on Technology and Optimisation Vol. 1, 2010 pp38-45)

Meyer (2010) patented a unit using lead screws driven by stepper motors to adjust the collection surface at two places for Solid Tech Inc. The surface was supported on spherical bearings at a third point. Martinez (2010) reports a bigger variant of linear positioning control. Hydraulic actuators in two orthogonal directions do the positioning. It is not suitable rural African home requirements.

Sobolewski *et al*. (2011) patented a roof mounted PV tracker for Rutgers, The State University of New Jersey, US. The tracker is mounted at the apex of an East-West roof to maximise tracking angles in these directions. Figure 5.9 gives the arrangement and the reported limit angles.

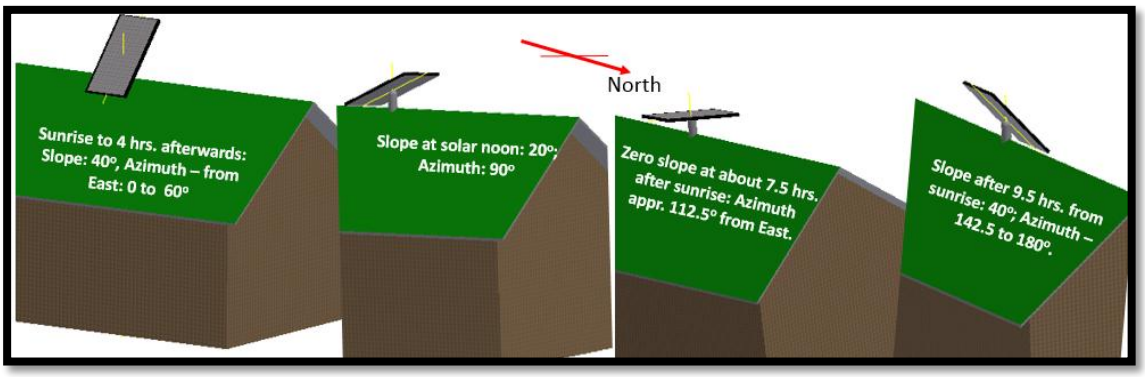

Figure 5.9: Sobolewski *et al*.'s roof apex mounted full tracker and the tracking angles progression across the day.

While this is an improvement on other roof mounted systems, it still leaves a big fraction of hours under non optimal tracking conditions.

5.1.4 *The technologies and relevance in tropical Africa's context*

Research on tracking technology developments in tropical Africa presents problems because internationally available documented outputs in this region are far in between. As is evident in the above survey, it is mainly Nigeria and Kenya showing some limited activity on the international scene. Others might be doing research in the area but are probably localised in publication. It could be argued that this makes sense since Technology – unlike Science – is society specific. Never the less, fairly recent work in other developing countries was looked at – to see if some of it can be adopted in tropical Africa's conditions of low incomes, scarce technical skills and sparse population density.

In particular, from China, work by Wu Chun –Sheng *et al*. (2008) on automatic sun tracking and that by Chia-Yen Lee *et al*. (2009) on general tracking mechanisms were reviewed. In the Middle East, Arafat *et al*. (2010) work was also looked at. Quite earlier in the history of solar thermal electricity technology, Mill's global review was studied (Mill, 2004). So was Tomson's simplified two position tracker (Tomson, 2008). This latter work is of interest to the authors because it is related to their earlier findings and recommendations on adopting two-slopes fixed panels (Kanyarusoke *et al*., 2012a). Recent work by Slama and Combarnous (2011) on orange peels drying in Tunisia can help improve performance of crop dryers in solar thermal systems.

The following works between 2012 and early 2013 were also reviewed: Kelly and Gibson (2012) patented a cloudy-conditions tracker for General Motors Global Technology Operations on 24th Jan 2012. It automatically changes to a horizontal slope when the sun is occluded. This maximises diffuse radiation capture. In China, He *et al*. (2012) used a parallel links mechanism to track on two axes. They report motor power consumption reduction of up to 70%. Ghazali and Rahman (2012) investigated performance of amorphous, poly and mono crystalline solar panels under tracking conditions in Malaysia. They found that polycrystalline panels did best. Finally in Bangladesh, Rahman *et al*. (2013) used LDRs and two amplifiers to demonstrate a gain of 52.78% energy yield between fixed slope and two axes tracking.

These technologies are yet to be fully adopted in Tropical Africa. The low level of modern solar energy harnessing aside, there are problems with the technologies. We now turn to these hereunder.

5.1.4.1 *Problems with the Technologies*

From tropical Africa's perspective, Table 5.1 summarises possible pertinent technology issues under the headings of energy sourcing; sensing and actuation.

5.1.5 *Conclusions*

In this paper, the more recent tracking technologies were reviewed. It was found that current technologies have many issues to resolve before adoption at a domestic level in rural Africa. Functionality, legality, security, operability and maintainability were some of the issues encountered. In absence of empirical long term tracker performance data in the region, it is difficult to give definitive recommendations on type(s) of trackers which will be most successful. A particular tracker's acceptance elsewhere is not a guarantor of its success in the region. This is because the art of tracking can theoretically be implemented by many competing low level technologies as described in parts of the survey above. Never

the less, single axis trackers showed that clock controlled passive trackers with weights of either solids or non-polluting liquids could possibly stand better chances of acceptability in the region.

Table 5.1: Summary of key issues in surveyed solar tracking mechanisms

Area	Alternatives	Issues
Energy source	Manual	Not viable
	Weights	Counter weights for balancing and control Frequent reloading
	Solar thermal	Speed of response Availability in case of cloud cover Evening and morning collection effectiveness
	Hydraulic	Pressure head source Needs reliable working fluid supply
	Springs	Frequent re energising
	Electricity	Needs electric source Complex control system
Sensory system	Clock	Insensitive to diffuse radiation effects
	Shading	Affected by sky objects
	Photo sensor	Needs electronic circuitry Unequal ageing of sensors
System Actuation	Manual	Tedious
	Clock	Separate programming
	Bimetallic strips	Low thermal efficiency Low tracking angle range 'Wake up' and evening return problems
	Shape Memory Alloys (SMAs)	Low tracking angle
	Vapour pressure	Use of refrigerants 'Wake up' and evening return problems
	Electric motors	Cost Maintenance of attendant control & drive elements
	Linkages	Power losses Bulk and maintenance issues
	Hydraulic	Pressurised liquid reservoir Size and maintenance issues

Acknowledgement

This research is being funded by the Cape Peninsula University of Technology – to whom we are grateful.

References

Abdulrahim A.T., Diso I.S. and El-Jummah A.M. (2010). Solar concentrators' developments in Nigeria: a review, *Cont. J. Eng. Sci*. 5 (2010) 38-45.

ADB *see* Africa Development Bank.

Africa Development Bank, The Middle of the Pyramid: Dynamics of the Middle Class in Africa. http://www.afdb.org/fileadmin/uploads/afdb/Documents/Publications/The%20Middle%20of%20the%20Pyramid_The%20Middle%20of%20the%20Pyramid.pdf [14th July 2011].

Ahmed M.B. (2001). Design, Fabrication and Performance evaluation of an improved solar concentrating collector using slat-mirrors, Unpublished MSc. Eng. Thesis,.Mech. Eng. Dept. Ahmed Bello University, Zaria Nigeria, 2001.

Ajiya M. (1995). Design and Construction of a parabolic solar cooker, Unpublished B Eng project. Mech. Eng. Dept. University of Maiduguri, Nigeria, 1995.

Anonymous. (2011). Canadian Teen Makes Cheaper, More Efficient Solar Tech., Altern. Energy Afr. 6th June 2011.

Arafat K.Md.T. Shahrear T.S.M., Rifat R., and Shafiul A.S.M. (2010). Design and Construction of an Automatic Solar Tracking System. ICECE, 2010. 326 – 329. eeexplore.org/stamp/Stamp.jsp?tp=&arnumber=5700694 [23 Feb 2013].

Bakos C.G. (2006). Design and Construction of a two –axis sun tracking system for parabolic trough collector (PTC) efficiency improvement, Renew. Energy. 31 (2006) 2411-2421.

Barsoum N., and Vasant P. (2010). Simplified solar tracking prototype, Glob. J. on Technol. & Optim. 1 (2010) 38-45.

Bekker B. (2007). Irradiation and PV array energy output, cost, and optimal positioning estimation for South Africa, J. Energy in S. Afr. 18 (2) (2007) 16-25.

Bennett, L. (2008). Assets under Attack: Metal Theft, the Built Environment and the Dark Side of the Global Recycling Market. Environmental law and Management. 20(2008) 176-183.

Beringer S., Schilke H., Lohse I., and Seckmeyer G. (2011). Case study showing the tilt angle of PV plants is nearly irrelevant. Sol. Energy. 85 (2011) 470-476.

Brent, A. C. and Rogers, D. E. (2010). Renewable Rural Electrification: Sustainability Assessment of Mini-Hybrid off-grid Technological Systems in the African context. Renewable Energy. 35(2010) 257–265

Brew-Hammond, A & Kemausuor, F. (2009). Energy for all in Africa—to be or not to be?! Environmental Sustainability, 1 (2009) 83–88.

Budynas R. G., and Nisbett J. K. (2015). Shigley's Mechanical Engineering Design 10th ed. (SI units), McGraw-Hill, Asia.

Bugaje, I.M. (2006). Renewable Energy for Sustainable Development in Africa: A Review. Renewable and Sustainable Reviews. 10 (2006) 603–612. Available from Science Direct [2014, July 3].

Chia – Yen Lee, Po – Cheng Chon, Che – Ming Chiang, and Chiu – Feng Liu. (2009). Sun Tracking systems: A review, Sensors 2009, 9 3875 – 3890; doi: 10.3390/S90503875. www.mdpi.com/journal/sensors [23 Feb 2013].

Chong K.K. and Wong S.W. (2009). General formula for on axis sun-tracking system and its application in improving tracking accuracy of solar collector, Sol.Energy. 83 (2009) 298 – 305.

Christopher M. 2016. Logistics & Supply Chain Management. 5ed. Pearson UK.

Ciobanu D., Visa I., Jaliu C., and Burduhos B.G. (2010). Tracking system type linkage mechanisms. Annals of DAAAM for 2010 and proceedings of the 21st International DAAM symposium, 21 (1) ISSN 1726-9679, ISBN 978-3-901509-73-5. Ed. Kantalimo, DAAAM International, Vienna, Austria, EU 2010.

Clifford M.J. and Eastwood D. (2004). Design of a novel passive solar tracker, Sol. Energy. 77 (2004) 269–280.

Djeu D. (2004). Passive Solar Tracker for a Solar Concentrator, US Patent application. 20040112373, 2004. patents.com/us-20040112373.html – Cached [3rd April 2011].

Ellegard, Arvidson, A., Nordstro¨ma, Mattias,Kalumiana, O, S., and Mwanza, C. (2004). Rural People Pay for Solar: Experiences from the Zambia PV-ESCO Project. Renewable Energy. 29 (8) (2004) 1251–1263.

Elmer Z.K.G. (2006). Optimising solar tracking systems for solar cells, 4th Serbian – Hungarian Joint symposium on intelligent systems. SISY (2006) 167-180.

Eveleens I. E. Africa's first solar-panel plant supports Kenya's clean energy push, AlertNet, 23rd Nov 2011.

Fluri T P. (2009). The Potential of Concentrating Solar Power in South Africa. Energy Policy, 37(2009) 5075–5080.

Fthenakis, V. M. (2000). End-of-life management and recycling of PV modules. Energy Policy, 28 (14) (2000) 1051-1058.

Full E. (2010). Appropriate Technologies in Mpala Village, Kenya: Solar, Water and Bamboo, [PPT] presentation, www.princeton.edu/grandchallenges/health/...2010/Full_Eden_SOL.pptx [4th July 2011].

Ghazali A. M. and Rahman A. M. A. (2012). The performance of three different solar panels for solar electricity applying solar tracking device under the Malaysian climate condition, Energy and Environment Research, 2 (1) (2012) 235 -243.

He X., Wang B., Huang F., Zhu W. and Gao C. (2012). Solar Automatic tracker based on parallel mechanism, J. Mech. & Elec. Eng, (01) (2012).

Helwa N.H., Bahgat A.B.G., El Shafee A.M.R. and El Shenawy E.T. (2000). Maximum collectable energy by different solar tracking

systems, Energy Sources, 22 (2000) 23-34.

Hernandez C. (2011). The 19-year-old innovator revolutionizing solar energy systems. http://www.smartplanet.com/blog/pure-genius/the-19-year-old-innovator-revolutionizing-solar-energy-systems/6436 [4th July 2011].

Hitchcock. R.D. (1976). Passive solar tracking system for steerable Fresnal elements, US Patent. 3986021, 1976. www.patentstorm.us/patents/3986021/description. html – Cached [3rd April 2011].

IEA see International Energy Agency. International Energy Agency, Renewables and Waste in Africa in 2008. http://www.iea.org/stats/renewdata.asp?COUNTRYCODE=11 [30th June 2011].

International Energy Agency IEA (2011). Energy for all: Financing access for the poor. World Energy Outlook, (2011) 11.

Kalogirou S. (2007). Recent patents in solar energy collectors and applications, Recent Pat. on Eng. 1(1) (2007) 23-33.

Kalogirou S. (2009). Thermal Performance, economic and environment life cycle analysis of thermo syphon solar water heaters. Solar Energy. 83 (1) (2009) 39-48.

Kanyarusoke, K. E. (1997). Developing new products with a Standards Bureau in mind. Presentation at a Uganda National Bureau of Standards (UNBS) seminar for industry, September 1997, Kampala, Uganda.

Kanyarusoke, K.E., Gryzagoridis, J. and Oliver, G. (2012a). Issues in solar tracking for sub-Sahara Africa, 1st Southern African Solar Energy Conference (SASEC), Stellenbosch, South Africa 21st-23rd May 2012.

Kanyarusoke, K.E., Gryzagoridis, J. and Oliver, G. (2012b) Annual Energy Yields Prediction from Manufacturers' Photovoltaic Panel Specifications for Sub-Sahara Africa, Proceedings of International Journal of Energy in Southern Africa • Vol 26 No 1 • February 2015 93 Conference on Engineering and Applied Science 2012 (ICEAS 2012), 24th-27th July 2012. Beijing China. pp. 223-235.

Kapur K. C. (1996). Techniques for estimating Reliability at Design stage, In Ireson, Coombs and Yates, *Handbook of Reliability Engineering and Management*, 2ed. McGraw Hill, NY pp. 24-1 – 24-23.

Karekezi S. (2002). Renewables in Africa – Meeting the Energy Needs of the Poor. Energy Policy. 30 (2002) 1059 -1069.

Kelly N.A. and Gibson T.L. (2010). Optimizing the Photovoltaic Solar Energy Capture on Sunny and Cloudy Days Using a Solar Tracking System. http://www.cormusa.org/uploads/CORM_2010_presentation_Nelson_Kelly_Optimizing_the_Photovoltaic_Solar_Energy.pdf [30th June 2011].

Kelly N.A. and Gibson T.L. (2012). Solar Photovoltaic output for cloudy conditions with a solar tracking system, US patent No. US 8,101,848B2 of Jan 24, 2012.

Kraak, A. (2005). Human Resources Development and the Skills Crisis in South Africa: The Need for a Multi-Pronged Strategy. Journal of Education and Work. 18(1) (2005) 57-83.

Lambert D. M. and Cooper M. C. (2000). Issues in supply chain management. Industrial Marketing Management Vol. 29, pp. 65-83.

Louchene A., Benmakhlouf A. and Chagai. (2007). Solar tracking system with Fuzzy reasoning applied to crisp sets, Revue des Energies Renouvelables. 10 (2) (2007) 231-240.

Markvart T. (ed.). (2000). Solar Electricity 2nd ed. John Wiley & Sons, Chichester 2000.

Martinez C.M.C. (2010). Bidirectional solar tracker, US Patent. 2010/0095955, 22nd April 2010.

Meyer S.M. (2010). Two Axes solar tracking system, http://www.freepatentsonline.com/y 2010/02880 62.html [15th June 2012].

Mills D. (2004). Advances in Solar thermal electricity Technology, Sol Energy. 76 (2004) 19 – 31.

Mousazadeh H., Keyhani A., Javadi A., Mobli H., Abrinia K., and Sharifi A. (2009). A review of principle and sun-tracking methods for maximizing solar systems output, J. Renew. & Sustain. Energy Rev. 13 (2009) 1800 –1818.

Mshelbwala S.A. (1996). Experimental investigation of a parabolic solar cooking device, Unpublished BEng. Project. Mech. Eng. Dept. University of Maiduguri, Nigeria, 1996.

Mulugetta, Y., Nheteb T. and Jacksona T. (2000). Photovoltaics in Zimbabwe: Lessons from the GEF Solar Project. Energy Policy. 28 (140) (2000) 1069–1080

Murphy J.T. (2001). Making the energy transition in East Africa: Is Leapfrogging an alternative? Technol. Forecast. & Soc. change. 68 (2001) 173-193.

Musa U., Sambo A.S. and Bala E.J. (1992). Design, Construction and Performance test of a parabolic concentrator cooker, Paper presented at the 1992 National Energy Forum, Sokoto.

Mwithiga G. and Kigo S.N. (2006). Performance of a solar dryer with limited sun tracking capability, J.Food Eng. 74 (2006) 247–252.

Oyetunji S.O., Sawhney R.I. and Aro I.O. (1989). Design, Construction and Estimation of performance of composite conical concentration, Directory of Renewable Energy Research and Development activities in Nigeria, SERC Sokoto. 1:12.

Pauw, K., Oosthuizen, M., & Westhuizen, c. Van der. (2008). Graduate Unemployment in the Face of Skills Shortages: A Labour Market Paradox. South African Journal of Economics. 76 (2008) 1.

Pegels, A. (2010). Renewable Energy in South Africa: Potentials, Barriers and Options for Support. Energy Policy. 38 (2010) 4945–4954.

Pelemo D.A., Fasasi M.K., Owolabi S.A. and Shaniyi J.A. (2002a). Design, Construction and Performance of focusing type solar cooker, Niger. J. Phys., 4 (2) (2002) 109-112.

Pelemo D.A., Fasasi M.K., Owolabi S.A. and Shaniyi J.A. (2002b). Effective utilisation of solar energy for cooking, Nig. J. Eng. Manag. (NJEM), 3 (1) (2002) 13-18.

Pelemo D.A., Fasasi M.K., Owolabi S.A. and Shaniyi J.A. (2003). Application of solar concentrator for water boiling and distillation, Niger. J. Sol. Energy, 14 (2003) 51-54.

Peter, P. and Donnelly Jr., J. H. (2009). Marketing Management 9th ed. McGraw Hill, New York (2009).

Poulek V. (1994). New low cost tracker, Sol. Energy Mater. & Sol. Cells, 33 (1994) 287-291.

Rabinowitz M. (2011). Tracking and focusing adjustable fresnel lens array solar collector, US Patent. 7960641B2. www.uspto.gov/web/patents/patog/../US07960641-20110614.html – Cached [2nd August 2011].

Rahman S., Ferdaus R. A., Mannan M. A. and Mohammed M. A. (2013). Design and Implementation of a dual axis solar tracking system. Am. Acad. & Scholarly Res. J. 5 (1) (2013) 47 – 54.

Rizk J. and Chaiko Y. Solar Tracking system. (2008). More efficient use of solar panels, World Acad. Of Sci. and Techno, 28 (28) (2008) 313-315.

Seme S., Stumberger G. and Vorsic J. (2011). Maximum efficiency trajectories of a two – axis sun tracking system determined considering tracking system consumption, IEE Transactions on Power Electronics, 26(4) (2011) 1280 – 1290.

Slama R.B. and Combarnous M. (2011). Study of Orange peels drying kinetics and development of a solar dryer by forced convection, Sol. Energy. 85 (2011) 570-578.

Sobamowo M.G., Kamiyo O.M, Ojolo S. J. and Ogundeko I.A. (2012). Design and Development of a Photovoltaic-Powered DC Refrigerator System with an Incorporated Solar Tracker, 1st Southern African Solar Energy Conference (SASEC), Stellenbosch, South Africa 21st-23rd May 2012.

Sobolewski. (2011). Roof mounted double axis tracker, US Patent. 20110120447, 26th May 2011.

Solar Buzz (2012). Solar Energy Market Growth. http://www.solarbuzz.com/facts-and-figures/marketsgrowth/market-growth [7th April 2012].

Sovacool B. K., D'Agostino A. D. and Bambawale, M. J. (2011). The Socio-technical Barriers to Solar Home Systems (SHS) in Papua New Guinea: "Choosing pigs, prostitutes, and poker chips over panels. Energy Policy. 39 (3) (2011) 1532–1542.

Suleiman A.K., Bajpai A.C. and Sulaiman A.T. (1989). Design, Fabrication and Testing of a low-cost cylindrical collector for steam generation, Directory of Renewable Energy Research and Development Activities in Nigeria, SERC, Sokoto, 1989, pp. 1-13.

Tina G.M. and Gagliano S. (2011). Probabilistic modelling of hybrid solar/wind power with solar tracking system, Renew. Energy, 36 (2011) 1719 –1727.

Tomson T. (2008). Discrete two positional tracking of solar collectors, Renewable Energy. 33 (2008) 400 – 405.

Ulrich K. T. & Eppinger S. D. (2016). Product Design and Development 6th ed. McGraw-Hill, NY.

United Nations Energy Agency. (2007). Energy for Sustainable Development: Policy Options for Africa. Vol. 2008.

United Nations (2014). Division for Sustainable Development. Department of Economic and Social Affairs. A Survey of International Activities in Rural Energy Access and Electrification.

United Nations Economic Commission for Africa. (2006). African Regional Implementation review for the 14th Session of the Commission on Sustainable Development (CSD-14) (2006). Report on "Energy for Sustainable Development". United Nations Economic Commission on behalf of the Joint Secretariat UNECA, UNEP, UNIDO, UNDP, ADB and NEPAD Secretariat.

Vanek F. M., Albright L. D. and Angenent L.T. (2012). Energy Systems Engineering: Evaluation and Implementation 2nd ed. New York, McGraw Hill, (2012) 49-71.

Winston R. (2001). Solar concentrators, In Gordon, J. (ed.) Solar Energy: The state of the art – ISES position papers. James and James Science Publishers, London, 2001, pp. 357-436.

Wu Chun-Sheng, Wang Yi-Bo, Liu Si-yang, Peng Yan – Chang, and Xu Hong – Hua. (2008). Study on Automatic Sun-Tracking technology in PV Generation. DRPT 2008, 6-9 April 2008, Nanjing, China. IEEEXplore 2586 – 2591.

Yi J-H. and Hwang W-C. (2009). Solar tracking device with springs, US Patent. 7607427 B2, 2009. www.wikipatents.com/...Patent-7607427/solar-tracking-device-with-... – Cached) [3rd April 2011].

Zerlaut G.A. and Heiskell R.F. (1977). Solar Tracking device, US Patent. 4031385, 21st June 1977.

Zomeworks. (n.d.). PV trackers. http://zomeworks.com/products/pv-trackers/howtrackers-work [3rd April 2011].

5.2 Concluding the chapter

This chapter deviated from the previous one in that it sought more radical ways of improving energy yields from existing flat plate collectors. On the premise that energy yield gains might be substantial compared to those of chapter 4 if the collectors track the sun, the more recent tracking technologies were reviewed. It was found that current technologies have many issues to resolve before adoption at rural domestic level in Africa. The overriding issues were affordability and availability. Functionality, legality, security, operability and maintainability were some of the other issues encountered. If most of these could be resolved, the market could be seeded and grown.

CHAPTER SIX:

FOURTH ARTICLE:

"MODELING ANNUAL YIELDS OF A SOLAR-TRACKING SOLAR SYPHON USING ASHRAE'S WEATHER DATA FOR TROPICAL AFRICA"

KANYARUSOKE, Kant E; GRYZAGORIDIS, Jasson; OLIVER, Graeme

DE-13-C024; ASHRAE Transactions, 2013, Vol. 119 Issue 2, p1-8: May 2013

Also online at: http://www.thefreelibrary.com/Modeling+annual+yields+of+a+solar-tracking+solar+syphon+using...-a0371285197

6.0 Introducing the paper

As far as flat collectors are concerned, the solar tracker survey done in the previous chapter revealed an established bias towards tracking PV systems. Part of the literature survey in chapter 2 showed that at the rural domestic home level, ST systems would perhaps be more popular if they addressed cooking needs. Later, in chapter 5, attempts at addressing these needs were noticed, especially in Nigeria. Most of those attempts focused on concentrating solar radiation using concentrated power collectors (CPCs) so as to produce a sufficiently high temperature to cook food. Even the single reported incidence of de-novo mechanised solar tracking design (Abdulrahim, 2008) was concerned with focusing the radiation using paraboloids. Both on the continent and elsewhere, the literature does not reveal interest in tracking flat collectors for cooking purposes.

Cooking food aside, the literature survey of chapter 2 and some efforts in chapter 5 reveal areas which could benefit from a solar tracking flat heating surface. Air and water heating and/or preheating; crop and fruit drying, etc. are examples of such areas. In this paper, focus is on water heating using solar siphons. To be more useful in homes, water does not always have to be heated to boiling point. Most hygiene applications of water are actually required at temperatures in the 40-60°C range. Therefore, a solar tracking device which exposes the water heating surface longer to beam radiation, (and therefore sustains these temperatures longer) could be of value in these applications.

This paper was written and published largely for an American audience much earlier than the others. Its symbols and nomenclature are slightly different from those of other papers. They are listed here for clarity.

6.1 Symbols and Nomenclature for the ASHRAE paper

A	Area (m^2)
C	Heat capacity (J/K)
F	Perez empirical sky brightness function
H	Hydraulic head at riser inlet (m)
I	Irradiance on surface (W/m^2)
L	Latitude angle (°)
M	Mass of stored fluid (kg)
P	Pressure (Pa or N/m^2)
R_b	Ratio of incident beam radiation on panel to that on horizontal surface
T	Absolute temperature (K)
U	Heat transfer coefficient ($W/m^2.K$)
a	Perez parameter dependent on incidence angle
b	Perez parameter dependent on zenith angle
c	Specific heat capacity (J/kg.K)
d	Diameter (m)
h	Convection coefficient (W/m2.K); Specific enthalpy (J/kg)
k	Thermal conductivity (W/m.K)
l	Distance (m)
m	Mass of flowing fluid
n	Number of riser tubes in solar syphon
q	Heat transfer per unit area (J/m^2)
t	Time since day-break (hours); Thickness of heat transfer medium (m)
v	Speed (m/s)
w	Width of riser-plate bond (m)
Gr	Grashof Number
Pr	Prandtl Number
Ra	Rayleigh Number
rl	Length of riser tube (m)

α	Sun elevation angle (°); Thermal diffusivity (m^2/s)
β	Panel/collector slope (°)
γ	Angle (^{o})
ζ	Angle (°)
ε	Emmissivity
η	Efficiency
θ	Angle (^{o})
μ	Dynamic viscosity (Pas)
ρ	Density (kg/m^3); Reflectivity
σ	Stephan-Boltmann constant ($W/m^2.K^4$)
ϕ	Angle (°)
ω	Humidity ratio

6.2 The Journal paper

Modeling Annual Yields of a Solar-tracking Solar syphon using ASHRAE's Weather Data for Tropical Africa.

Kant E Kanyarusoke, MSc. Jasson Gryzagoridis, PhD Graeme Oliver, PhD

TRACKING OF SOLAR SYPHONS

This work is a follow on to previous ones on solar tracking in Tropical Africa by the authors. While the first work showed the necessity to replace current fixed panels/collectors with two slope fixed installations at prescribed angles and times, the second established the need for - and determined the constraining techno-economic factors of tracking photovoltaic panels in rural Africa. This paper covers the introductory part of tracking passive flat collectors as would be applied in hot water cylinders (domestic water geysers) in these areas.

INTRODUCTION

In general, solar syphon flat collectors as used in domestic installations for geysers or hot water cylinders are installed not to track the sun. One reason is that they are able to utilize diffuse radiation quite effectively. The other could be the complexity in water connections both at inlet and outlet from the collector. Uncritical use of special fittings and/or of flexible hoses at these points could cause high pressure drops and flow reversal in some tubes during tracking – thus compromising net flow rates and attendant energy yields. This is a problem because it does not give any economic and technical benefits to rotate the tank and its inlet/outlet pipes in a bid for the collector to track the sun.

One possible answer to this problem is to mount the collector on fixed bearings supporting the pipes. This is viable provided good water sealing can be used at the connection to the headers. By 'good' we mean: low friction – to allow easy rotation – but tight enough to prevent leakage. Flow into and out of the collector needs to be collinear to minimize head losses in the said pipes. Figure 6.1 illustrates the design scheme adopted in the work being reported.

The flow in risers is uneven because the headers are not horizontal and the flow paths between them are now of different lengths. This problem has not been adequately addressed in the literature - perhaps because flat plate collectors have almost universally been installed as fixed slope systems. (Duffie and Beckman, 2006:238). Buoyancy driven collectors have the additional issue of low hydraulic heads – thus compromising flow rates. We lay out a theoretical framework for investigating these issues in this paper.

Previous work on Passive collectors

Rehm and Baun (1978) derived approximate equations for buoyant flow in non-adiabatic gases – as occur in fires. They showed that when the heat generation rate is low, the Boussinesq condition of isochoric flow and heat transfer is approximated. Pressure waves were generated as well. In a thermo syphon, we can use the Boussinesq relation – as is standard in current CFD software. But what happens to wave generation? Du *et al*. (1994) investigated hydrodynamic instability in water thermo syphons. But they concluded that because of extremely low heat generation (by solar), and the high friction coefficients in pipes, it was not possible for their model to predict instability. Earlier, Bhargava and Argarwal (1979) had done a mathematical analysis of fully developed natural convection in a circular pipe. Their analysis however was for one pipe using a density distribution parameter that had been used by Sastri and Vajravelu (1977) on vertical walls. The problem of heated inclined multi pipes connecting two *inclined* headers may well be different. Aicher and Martin (1997) presented empirical correlations on mixed and turbulent natural and forced convection in vertical tubes. Their correlations reportedly yielded accuracies of within ±20% of experimental data.

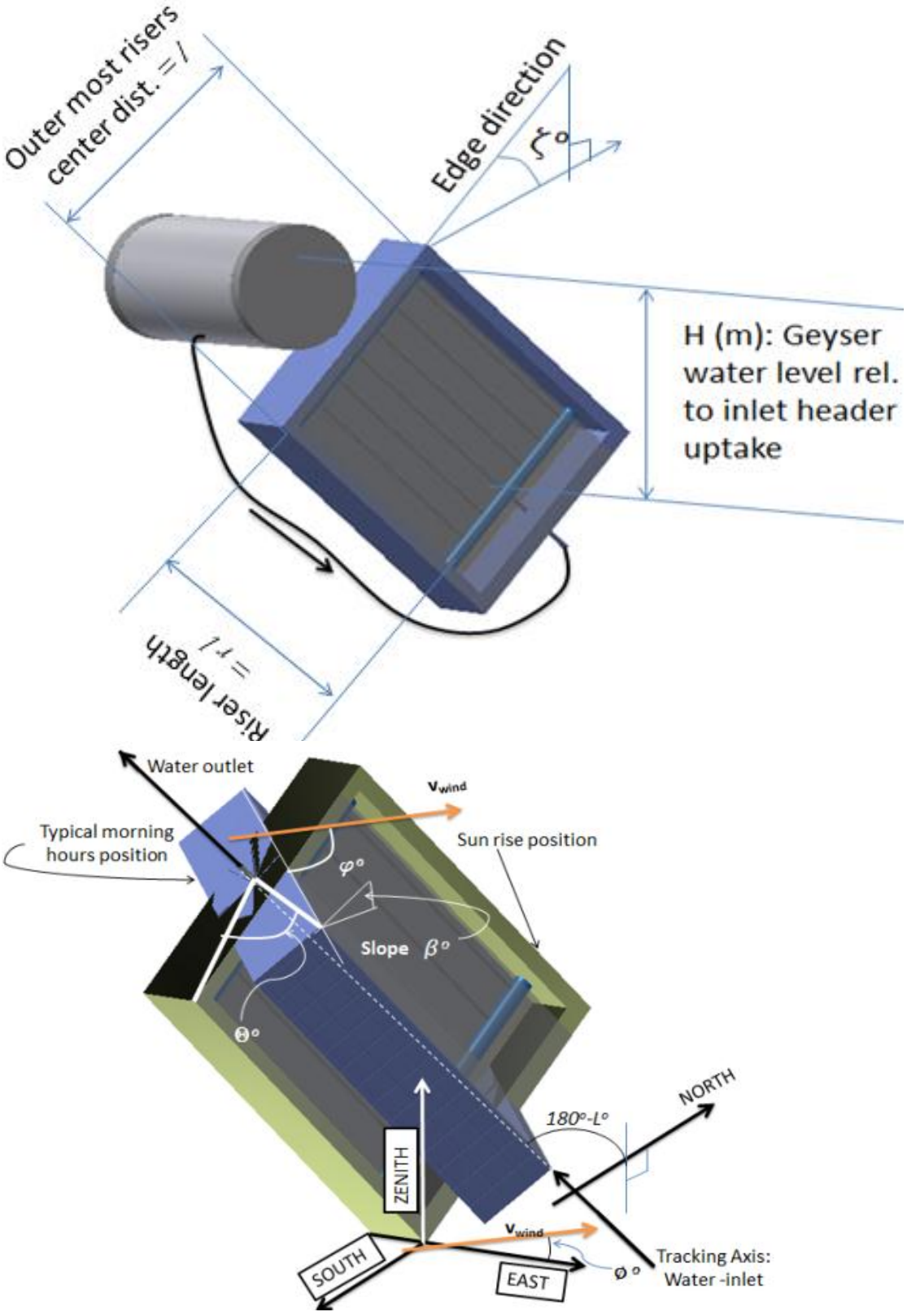

Figure 6.1 (a) Passive Solar tracking collector-Geyser system and (b) Basis of geometrical relationships.

The problem of flow through headers and risers as occurs in thermo syphon collectors received much attention from McPhedran *et al*. (1983), Norton *et al*. (1992) and many others. The 1983 studies showed that when pressure drops across a header exceeded 16 kPa, flow reversal in tubes was more likely. Further, that the outlet header conditions were more critical

in determining flow reversal. Hence, the recommendation that: where possible, the outlet header diameter should exceed that of the inlet. More recently, Prayagi and Thombre (2011) studied the flow in inclined tubes and established working relationships for natural convection heat transfer and buoyancy induced flow rates. It is these that we will later use in the modeling of flow in riser tubes.

But solar thermo syphon problems extend beyond fluid flow and heat transfer. The energy source and environment are constantly varying. So are the water usage and supply rates. In this work, we also impose a varying collector slope and azimuth in different regions of Africa. Past and present investigators individually focused on a few of these variables at a time. (e.g. Morrison and Braun (1985), Yamamoto *et al*. (2004), Fung *et al*. (2008), Nizami *et al*. (2013), etc.). Even the TRNSYS software does not give the detail we require for this work. Hence we collate relevant data and findings of these and other researchers and use them in one integrated project to establish trackability of solar thermal flat collectors for rural Africa. This is part of our work on design of purpose built trackers for the region.

SOLAR SYPHON MODELING

Geometry

Referring to Figure 6.1b, with the origin at the day break vertex shown, vector algebra gives the slope β^{o} at the typical morning position as:

$$\cos(\beta^{o}) = \sin(\theta^{o})\cos(L^{o}) \tag{1}$$

The wind intercepts the collector header axes at an angle φ^{o} given by:

$$\cos(\varphi^{o}) = \cos(\phi^{o})\sin(\theta^{o}) + \sin(\phi^{o})\cos(\theta^{o})\sin(L^{o}) \tag{2}$$

Energy Harvest

For glazing and back heat transfers ($q_{rg}+q_{hg}$) and ($q_{rb}+q_{hb}$) we apply the 1st law of Thermodynamics to the collector system, with some notation from Figure 6.2a to obtain the rate of energy harvest per square meter of collector area as:

$$\dot{q}_{w} = \left[\left(1-\rho_{g}\right)I_{panel} - \left(\dot{q}_{rg} + \dot{q}_{hg}\right) - \left(\dot{q}_{rb} + \dot{q}_{hb}\right) - \left(C_{g}\dot{T}_{gm} + C_{pl}\dot{T}_{p} + C_{b}\dot{T}_{bm}\right)\right]^{+} \tag{3}$$

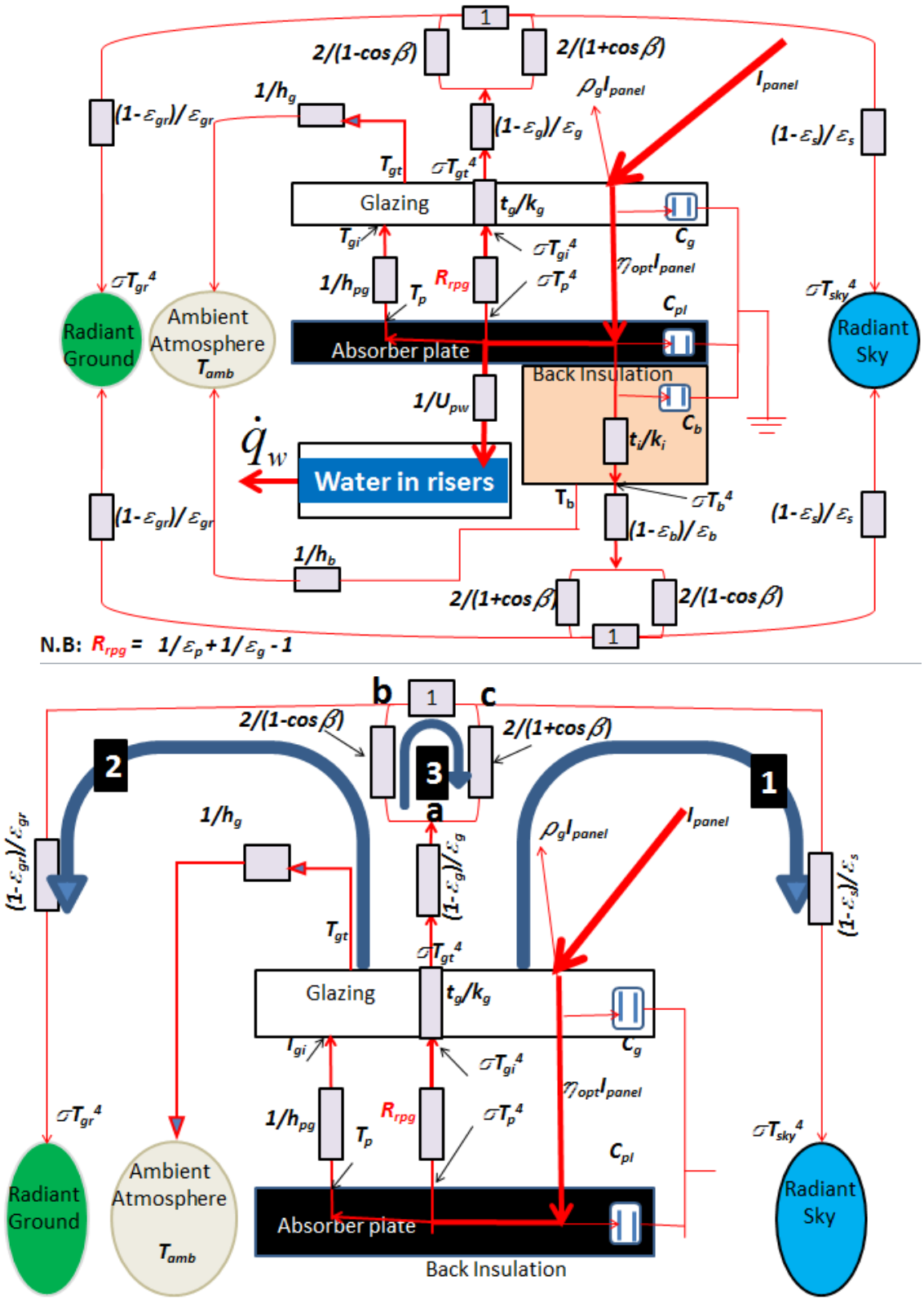

Figure 6.2: (a) Thermal circuitry for entire collector assembly and (b) Energy balancing on glazing.

The + sign in equation 3 indicates harvest is possible only when the incident radiation I_{panel} is at such an angle and of such a magnitude that a critical level is exceeded to begin generating sufficient head to cause positive circulation in the circuit. I_{panel} was determined in our previous work (Kanyarusoke et al, 2012), basing on ASHRAE weather data and the

Perez et al. (1990) model:

$$\mathbf{I_{panel} = I_{bh} R_b + I_d(1 - F_1)\left(\frac{1 + \cos\beta^\circ}{2}\right) + I_d F_1 \frac{a}{b} + I_d F_2 \sin\beta^\circ + I_h \rho_g \left(\frac{1 - \cos\beta^\circ}{2}\right)} \quad (4)$$

The present work examines each of the loss terms in equation 3. It also expands the gain term, $\dot{q}_w$ - subjecting it to cylinder stratification and water circuit pipeline pressure drop conditions. We treat the entire system as constantly unsteady. On convection, we delink radiation terms completely from convection coefficients. This is unlike in the literature where the two get mathematically linked to transfer heat to ambient air. We found that such mathematical treatment *was at variance* with the Physics of transfer when there is internal capacitance and at times when ambient temperature equaled collector surface temperature. For example, in the latter case, one gets *zero* heat transfer by the contemporary approach: Yet actually there is heat transfer to the sky - which is almost always at a different temperature. The relaxations we make are that the tank and the entire pipeline can be insulated enough to make heat losses through them negligible. Also, we suppose that hot water withdrawal is done late in evenings and recharge is done at night.

Loss through glazing $\dot{q}_g = \dot{q}_{rg} + \dot{q}_{hg}$: Referring to Figure 6.2b, for the top surface of the glazing, the radiation term $\dot{q}_{rg}$ can be deduced from a solution of 6 equations for nodes a, b, c and loops 1, 2, and 3 respectively. In matrix form, they are given by equation 5.

$$\begin{bmatrix} 1 & 0 & 0 & -1 & 0 & -1 \\ 0 & 0 & -1 & 0 & -1 & 0 \\ 0 & -1 & 0 & 0 & 1 & 1 \\ \frac{1-\varepsilon_g}{\varepsilon_g} & \frac{1-\varepsilon_s}{\varepsilon_s} & 0 & 0 & 0 & \frac{2}{1+\cos\beta^o} \\ \frac{1-\varepsilon_g}{\varepsilon_g} & 0 & \frac{1-\varepsilon_{gr}}{\varepsilon_{gr}} & \frac{2}{1-\cos\beta^o} & 0 & 0 \\ 0 & \frac{1-\varepsilon_s}{\varepsilon_s} & -\frac{1-\varepsilon_{gr}}{\varepsilon_{gr}} & 0 & 1 & 0 \end{bmatrix} \begin{bmatrix} \dot{q}_{rg} \\ \dot{q}_{rts} \\ \dot{q}_{rtgr} \\ \dot{q}_{rggr} \\ \dot{q}_{rtgrs} \\ \dot{q}_{rgs} \end{bmatrix} = \begin{bmatrix} 0 \\ 0 \\ 0 \\ \sigma T_{gt}^{\ 4} - \sigma T_s^{\ 4} \\ \sigma T_{gt}^{\ 4} - \sigma T_{gr}^{\ 4} \\ 0 \end{bmatrix} \quad (5)$$

The temperature of the ground is assumed equal to that of ambient air while the sky temperature – in Kelvin - is estimated from the Berdahl and Martin equation (1984) as cited by Duffie and Beckman (2006:148). For a local atmosphere ambient temperature T_{amb} (K) and with a dew point T'_{dp} (°C), clear sky temperature T_s (K) at *t* hours from midnight is:

$$T_s = T_{amb}(0.711 + 0.0056T'_{dp} + 0.000073T'^{\,2}_{dp} + 0.0013\cos(15t^o))^{0.25} \quad (5a)$$

In IP units – with T_s, T_{amb} in °R, and T_{dp} in °*F* - use the same equation but with T'_{dp} replaced by $0.5556T'_{dp} - 17.7778$.

The sky emissivity is approximated as 1 because the sky can be modeled as a big object surrounding small ones. ASHRAE (2009) guidelines recommend Pepper's (1988) equation for the dew point temperature T'_{dp} (°C):

$$T'_{dp} = 6.54 + 14.526\alpha + 0.7389\alpha^2 + 0.09486\alpha^3 + 0.4569(P_w/1000)^{0.1984} \quad (5b)$$

Where α is the natural logarithm of the water vapor partial kPa pressure (P_w /1000) in the air, itself a function of ambient dry and wet bulb temperatures. The partial pressure P_w (Pa) and air humidity ratio ω are related to atmospheric pressure P_{at} and temperatures as:

$$P_w = P_{at}\,\omega/(0.6219+\omega) \text{ and } \omega = \frac{(2501 - 2.326T'_{wb})\omega_{Twb} - 1.006(T'_{amb} - T'_{wb})}{2501 + 1.86T'_{amb} - 4.186T'_{wb}}. \quad (5c \text{ and } 5d)$$

$\boldsymbol{\omega_{Twb}}$ in this case is the saturation humidity ratio at the wet bulb temperature. To determine it, a relation between saturation temperature and pressure is required. Several are available. Here, the simpler ASHRAE 2009 recommendation is used:

$$\ln P_{ws} = -(5.8002/T)X10^3 + 1.3915 - 4.864X10^{-2}T + 4.1765X10^{-5}T^2 - 1.4452X10^{-8}T^3 + 6.54597\ln T \quad (5e)$$

When IP units are used, (i.e. replace ˚C by ˚F and kPa by psia) the ordered numerical coefficients in the above equations are:

(5b): 100.45, 33.193, 2.319, 0.17074, 1.2063; 1.

(5d): Numerator -: 1093; -0.556; -0.24. Denomenator-: 1093; 0.444; -1. (5e): -1.044 X 10^4; -11.295; -0.02702; 1.289 X 10^{-5}; -2.478 X 10^{-9}; 6.54597.

With molecular masses of 18 and 28.96 for water and dry air respectively, ω_{Twb} is now computable from a variant of (5c) with $P_w = P_{sat@Twb}$.

The convection term $\dot{q}_{hg}$ is determined from equation (6) below. In the computations, this is the most complicated term. At each collector position $\boldsymbol{\theta}^\circ$ in Figure 1b, the wind speed and direction have to be noted. Then, a characteristic length has to be computed from geometry. This partly depends on the angle ϕ° of equation (2) but also on the Physics of the transfer. Then it has to be decided whether the transfer is 'natural', mixed or 'forced'. Within each of the major categories, a decision on lamina or turbulent flow is made. Jaffer (2012) has provided substantial recommendations on handling heat transfer to/from isothermal flat plates. But the collector surfaces in bright sunlight may rather be treated as constant flux plates within the short time intervals of the simulation. This is what was done – and therefore some of Jaffer's recommendations were modified to cater for this.

$$\dot{q}_{hg} = h_g\left(T_{gt} - T_{amb}\right) \quad (6)$$

Loss through the back $\dot{q}_b = \dot{q}_{rb} + \dot{q}_{hb}$: The equations for the back losses are similar. The difference on the radiation term $\dot{q}_{rb}$ is on interchange of resistances $\frac{2}{1+\cos(\beta^\circ)}$ and $\frac{2}{1-\cos(\beta^\circ)}$ in the thermal resistance matrix. It is also assumed that since the heat loss through the back is normally small, the back surface is very nearly isothermal within the simulation time intervals. Hence the coefficients in the forced convection Nusselt number expressions during the day are those of Jaffer, (2012). Natural convection terms differ from those of the

glazing because heat transfer is then downward from the collector. The losses through the back and the glazing form a combined total loss to the environment U_L given by equation 6a:

$$U_L = \left(\dot{q}_b + \dot{q}_g\right) \Big/ \left(T_p - T_{amb}\right) \quad (6a)$$

In both back and glazing losses relations, air is treated as an ideal gas whose transport properties are temperature dependent. With all properties in primary SI units the following equations were programmed to output a 'film' properties vector in the simulations.

$$\rho_{air} = \frac{P_{atm}}{287 T_{amb}};\ \mu_{air} = \left(1.512 X 10^{-6}\right)\frac{T^{1.5}}{120 + T};\ \mathrm{Pr}_{air} = \frac{\mu_{air} c_{pair}}{k_{air}};\ \alpha_{air} = \frac{\rho_{air} k_{air}}{c_{pair}};$$

(6b – 6e)

$$k_{air} = -0.000393 + 1.0184 X 10^{-4} T - 4.8574 X 10^{-8} T^2 + 1.5207 X 10^{-11} T^3 \quad (6f)$$

$$c_{p_{air}} = 1.9327 X 10^{-10} T^4 - 7.9999 X 10^{-7} T^3 + 1.1407 X 10^{-3} T^2 - 0.4489 T + 1057.5 \quad (6g)$$

For IP units (T in $^{\circ}$R and time in hr), the ordered constants in the respective equations would be: (6b): 53.35 ft.lbf/lb.$^{\circ}$R; (6c): 0.2726X10^{-2} lbm/ft.hr.$^{\circ}$R$^{1/2}$ and 216 $^{\circ}$R; (6f): -0.000227Btu/h.ft.$^{\circ}$R, 0.3269X10^{-4}, -0.8663X10^{-8} and 0.1507X10^{-11}; (6g): 4.3974X10^{-15}; -3.2763X10^{-11}; 8.4090X10^{-8}; -5.9566X10^{-5} and 0.2526 Btu/lbm.$^{\circ}$R.

Capacitance effects, $C_g \dot{T}_{gm} + C_p \dot{T}_p + C_b \dot{T}_{bm}$**.** The capacitances C are evaluated from the masses of the materials per unit area and the specific heat capacities. It is assumed the latter do not vary much with temperature in the range of normal operation. The temperatures are approximated from: $T_{gm} \approx 0.5(T_{gt}+T_{gi})$; $T_{bm} \approx 0.5(T_b+T_p)$; T_p is a driving variable to be determined by the simulation.

Internal heat balances:

For the glazing:

$$\left[1 - \rho_g - \eta_{opt}\right] I_{panel} + \sigma\left(T_p{}^4 - T_{gi}{}^4\right) \Big/ R_{rpg} + \left(T_p - T_{gi}\right) h_{pg} - 0.5 C_g \left(\dot{T}_{gt} + \dot{T}_{gi}\right) - \dot{q}_{rg} - \dot{q}_{hg} = 0 \quad (7)$$

Also, for conduction in the glazing, $\dot{q}_{rg} + \dot{q}_{hg} = \dfrac{T_{gi} - T_{gt}}{t_g / k_g}$ (7a)

The convection coefficient h_{pg} - according to Hollands et al. (1976) as cited by Duffie and Beckman, 2006:151 – is given by:

$$h_{pg} = \frac{k}{x_{gap}}\left[1 + 1.44\left(1 - \frac{1.708\left(\sin(1.8\beta^o)\right)^{1.6}}{Ra_{xgap}\cos(\beta^o)}\right)\left(1 - \frac{1708}{Ra_{xgap}\cos(\beta^o)}\right)^{+} + \left[\left(\frac{Ra_{xgap}\cos\beta^o}{5830}\right)^{1/3} - 1\right]\right]^{+}$$

(7b)

For radiation between plate and glazing; $\dot{q}_{rpg} = \sigma\left(T_p{}^4 - T_{gi}{}^4\right) \Big/ R_{r\,pg}$ (7c)

For the thin, highly conductive - and hence lumped analysis - absorber plate:

$$\eta_{opt} I_{panel} - \sigma\left(T_p^{\,4} - T_{gi}^{\,4}\right) \Big/ R_{rpg} + \left(T_p - T_{gi}\right) h_{pg} - C_{pl}\dot{T}_p - U_{pw}\left(T_p - T_{w-mean}\right) - \dot{q}_{pb} = 0 \quad (8)$$

For the back insulation:

$$\dot{q}_{pb} - \dot{q}_{hb} - \dot{q}_{rb} - 0.5C_b\left(\dot{T}_p + \dot{T}_b\right) = \dot{q}_{pb} - \left(T_p - T_b\right) \Big/ \left(t_b / k_b\right) - 0.5C_b\left(\dot{T}_p + \dot{T}_b\right) = 0 \quad (9)$$

For water in the risers:

For one (out of n) riser i, $\dot{q}_i = \dot{m}_i c_w \left(T_{out-i} - T_{in}\right)$ (10)

So that:

$$\dot{q}_w = U_{p-w}\left(T_p - T_{w-mean}\right) = \frac{\dot{m}_w c_w}{A}\left(T_{out-mean} - T_{in}\right) = \frac{c_w}{A}\sum_{i=1}^{n} \dot{m}_i \left(T_{out-i} - T_{in}\right) \quad (10a)$$

From which we deduce: $T_{out-mean} = \sum_{i=1}^{n} \dot{m}_i T_{out-i} \Big/ \sum_{i=1}^{n} \dot{m}_i$ and $\dot{m}_w = \sum_{i=1}^{n} \dot{m}_i$ (10b)

The Duffie and Beckman, 2006:264 outflow temperature equation – when adopted for one riser i, gives T_{out-i} as:

$$T_{out-i} = T_{amb} + \frac{\eta_{opt} I_{panel}}{U_L} + \left(T_{in} - T_{amb} - \frac{\eta_{opt} I_{panel}}{U_L}\right) \exp\left(-U_L \frac{A \eta_{fc}}{n \dot{m}_i c_w}\right) \quad (10c)$$

Where the collector efficiency factor η_{fc} is worked out from the riser – plate bonding and is also dependent on flow conditions as given by:

$$\eta_{fc} = \left(w\left[\frac{1}{d_o + \left(w - d_o\right)\eta_{fin}} + U_L\left(\frac{t_{bond}}{k_{bond} w_{bond}} + \frac{1}{\pi d_i h_i} \right) \right] \right)^{-1} \quad (10d)$$

The fin efficiency η_{fin} of the plate-riser connection can be deduced from formulae – derived in standard Heat Transfer textbooks. It is:

$$\eta_{fin} = \left(\tanh\left(w - 0.5 d_o\right) \sqrt{\frac{U_L}{k_p t_p}} \right) \Big/ \left(\left(w - 0.5 d_o\right) \sqrt{\frac{U_L}{k_p t_p}} \right) \quad (10e)$$

The mass flow rate $\dot{m}_i$ and the internal convection coefficient h_i are each related to conditions of flow in the riser. The literature does not give much information on natural convection correlations for *Nu* in inclined pipes. A recent modeling and experimentation with water in tubes of different lengths, diameters and at various slopes is by Prayagi and Thombre (2011). For a modified Grashoff number below 106, they give the correlations:

$$h_i = 0.005 \frac{k_w}{d_i} \left(Ra_d \sin(L^o)\right)^{0.5}; \ \mathrm{Re} = 0.02 \left(\frac{Gr*}{\mathrm{Pr}} \frac{rl \sin(L^o)}{d_i} \right)^{0.5}; \text{ where } 48 \le \mathrm{Re} \le 180 \text{ and}$$

$$50 \le \left(\frac{Gr*}{\mathrm{Pr}} \frac{rl \sin(L^o)}{d_i} \right) \le 2X10^7 \quad (10f \text{ and } 10g)$$

If the inlet header temperature T_{in} and the loss coefficient U_L are known for a given collector, equations (10) to (10g) can be solved for $\dot{m}_w$ and $T_{out-mean}$ provided there is a way of

distributing the flow to the n inclined risers.

Distributing flow to risers: Because current flat collectors do not track the sun, they are intended to be installed with horizontal distributor header axes. This tends to equalize flows in the risers – assuming other factors (e.g. shading) are similar.

In non-equatorial regions, polar tracking about an axis of symmetry however, would offset these distributions in all but the solar noon position. The authors consider the possibility that the static pressure head at entry of an individual riser could contribute to the flow apportionment to that riser. This would mean risers at the bottom get more flow than those at the top. The effect would then be to have a higher temperature rise in the top tubes, which in turn would lead to an offsetting increment of flow rate. But the high temperature water would probably find more resistance to enter the axial pipe leaving the outlet header because of density differences. Similarly, the 'high' flow rate from below would not easily rise against the lighter water from mid-section risers. Is it then possible that flow from the outer risers could stagnate and even reverse? This is not likely for the lower risers because stagnation would lead to heating up above the outlet temperatures of the mid-section – causing positive flow. That danger however, exists for the upper risers. To partially address the concern, the outlet header could be slightly curved upward on the surface where the risers enter it – allowing the center risers to heat up slightly more than the outer ones, and hence causing probably greater fluid mixing before entry into the exit pipe. Distributing the flow according to the total static head at riser inlet, for a riser *i* from the lowest (*I* = 1), using Figure 1a, we can show:

$$\dot{m}_i = \dot{m}_1\left[1-\frac{i-1}{n-1}\frac{l\sin(\xi^o)}{\left[H+0.5l\sin(\xi^o)\right]}\right] \text{ and } \dot{m}_1 = \frac{\dot{m}_w}{n}\left[1+\frac{l\sin(\xi^o)}{2H}\right] \qquad \text{(11 and 11a)}$$

With the distribution assumed, the collector modeling is complete. However, to determine the actual flow rates, temperatures - and hence energy yields, it is necessary to look at the circulation in the collector-storage tank circuit.

Collector-Tank circuit:

We suppose that the collector is a pump circulating the water at a rate $\dot{m}_w$ by virtue of its Boussinesq buoyant pressure $(\rho_{\text{in}}\text{-}\rho_{\text{out-mean}})g(\rho l)\sin(L^\circ)$. In the inlet and outlet headers, average properties as given by equations 12 to 15 below are assumed. In line with the Boussinesq model however, properties in the 'pump' are approximated as constant - at inlet header values.

Key Property relations for water: [ρ (kg/m^3); *T*' (^{o}C); *T* (K); μ (Pas); *k* (W/m.K); and *c* (kJ/kg.K); *h* (kJ/kg)]

Kell (1975) gave an equation for density (kg/m^3) variation with degree centigrade

temperature (T'):

$$\rho = \frac{999.84 + 16.94518T' - 798.7X10^{-5}T'^{2} - 461.7X10^{-7}T'^{3} + 105.56X10^{-9}T'^{4} - 280.54X10^{-13}T'^{5}}{1 + 0.01687985T'} \quad (12)$$

The dynamic viscosity and conductivity vary according to: (T now in K)

$$\mu_w = 2.414X10^{-5}X10^{\frac{247.8}{T-140}} \;;\; k_w = -0.900 + 0.008387T - 1.118X10^{-5}T^2 \quad (13 \text{ and } 14)$$

And the specific heat capacity at 1.01325 bar pressure and enthalpy are approximated by: (T' in ^{o}C)

$$c_w = 4.21744 - 0.0056182T' + 0.00129925T'^{1.5} - 0.0001153535T'^{2} + 4.14964X10^{-6}T'^{2.5} \quad (15)$$

$$h_w = -0.0284 + 4.212T' - 1.017X10^{-3}T'^{2} + 1.311X10^{-5}T'^{3} - 6.756X10^{-8}T'^{4} + 1.724X10^{-10}T'^{5} \quad (15a)$$

In IP units, with *T'* in $^{\circ}$F and *T* in $^{\circ}$*R*, the same equations can be used when T is replaced by 0.5556T, *T'* by *0.5556T' -17.7778* and the resulting properties values adjusted as follows: (12): divide by 16.0185 to get ρ in lbm/ft^3; (13): Multiply by 2419.082 to get μ_w in lbm/ft.hr; (14): divide by 1.7306 to get k_w in Btu/h.ft.$^{\circ}$F; (15): divide by 4.186 to get c_w in Btu/lbm.$^{\circ}$R; (15a): divide by 2.326 to get h_w in Btu/lbm.

Like for air, these thermal physical properties are scripted so that a properties vector at any trial temperature and condition is readily available to the simulations. The pressure head supplied by the 'pump' – and used in recirculation is then expended in circuitry friction and 'minor' losses including: hot water cylinder entry and exit: headers entry and exit. We include a special term we call a 'Headers losses'. We have taken it as 50% of the associated entry (for inlet header) and exit (for outlet header) minor loss. Losses due to bends and fittings in the pipeline are considered negligible

Many researchers – including the already cited McPhedran et al. (1983) have grappled with the problem of flow in manifolds and headers to no final and definitive recommendation. A solar tracking flat plate collector is only now being proposed. One of the issues to study in detail later is the head loss associated with the headers at various slopes and how to reduce it. For the stated conditions, we derived equation (16).

$$\left(\frac{1.25}{\rho_{in}A_{in}^{\;2}} + \frac{0.875}{\rho_{out}A_{out}^{\;2}}\right)\dot{m}_w^{\;2} + 8\pi\left(\frac{\mu_{in}l_{in}}{\rho_{in}A_{in}^{\;2}} + \frac{\mu_{out}l_{out}}{\rho_{out}A_{out}^{\;2}}\right)\dot{m}_w - (\rho_{in} - \rho_{out})g(rl)\sin(L^o) = 0 \quad (16)$$

Where, l_{in} and l_{out} are pipeline lengths while (rl) is the riser length. A_{in} and A_{out} are the collector inlet and outlet pipe flow areas. This completes the modeling. It is required to solve the above equations for each collector angular position.

SOLUTION PROCEDURE

The varying collector water inlet temperature, - along with solar irradiance - and weather

conditions drive the system. ASHRAE weather data provide the latter. For the inlet temperatures, consider the schematic of a horizontal cylindrical 100 liter payload tank in Figure 3. We stratify it into 4 zones – not primarily defined by temperatures but by operational requirements. The uppermost 124.2 mm segment is a vapor section venting to the atmosphere, ensuring safety and keeping all internal pressures at positive gauge. The second 120.3 mm section receives water from the collector through the 'delivery' pipe alluded to earlier. The next 120.3 mm section is the payload zone, from and through which, a target 100 liters of water can be withdrawn per day. This means the total design volume of segments 1 and 2 is 100 liters. The bottom 124.2 mm segment is the in feed zone into which cold water can be supplied, and out of which, the 'pump suction' pipe draws supply to the collector inlet header. The design volume of water in this zone is 33.5 liters.

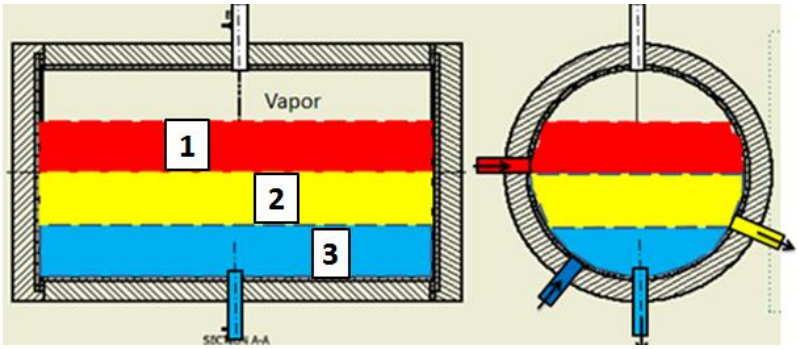

Figure 6.3: Geyser stratification

Analysis:

When heated water enters the tank, it is assumed to settle in zone 1. During a given small time interval t_1 to t_2, a mass $\Delta m_2 = \int_{t_1}^{t_2} m_w dt$ settles in the upper segment with its collector-added enthalpy. A similar mass but with lower specific enthalpy, h_{w1} leaves and enters zone 2. Thus the temperature of zone 1 increases by an amount:

$$\Delta T_{2,1} = \Delta m_2 \left(h_{w-out2} - h_{w1,1}\right) / M_{w1} c_{w1} .$$

In like manner, the temperature gain of zone 2 is:

$$\Delta T_{2,2} = \Delta m_2 \left(h_{w1,1} - h_{w2,1}\right) / M w_2 c_{w2}$$

And that for zone 3 together with the suction pipeline and inlet header is:

$$\Delta T_{2,3} = \Delta m_2 \left(h_{w2,1} - h_{w3,1}\right) / M_{w3} c_{w3} .$$

This gives a way of determining inlet header temperatures throughout the day. Now all equations 3 to 16 are solvable for a given single glazing flat plate collector at a given location and subject to the above assumptions throughout the year.

Solution Procedure summary:

Here, we only outline the procedure. Details are in a subsequent publication. Beginning at

daybreak, assume the collector to be at one uniform temperature T_0 - since it will have had a long non-heating period overnight. From weather data, compute T_{s0}. Then balance convection and radiation energy transfer on surfaces to obtain T_0. Then, initial loss coefficient U_{L0}, is computed. For each successive interval, equation (3) is integrated with respect to time. The method we adopted was to change T_{gt} by a small trial amount, solve for T_p, and T_{gi}; Then for this trial, make another guess for T_b so that we could enter the risers with a U_L. Find whether the trial T_b gives an overall heat balance for its parent T_{gt}. If not, make another 'informed' trial for T_b until parent T_{gt} is satisfied. If so, we checked, the flow conditions in equation (16). Satisfying (16) means both parent T_{gt} and child T_b are 'correct' – and therefore, all other values of variables associated with them are listed as the solutions at that stage. The process continues until the end of the day – and the cumulative energy gains and final temperature distribution in the hot water cylinder (geyser) are deduced.

CONCLUSIONS

In this paper, we have modeled energy gain and temperature attainment in a complete solar syphon system. What is different in our treatment is the delinking of radiation heat transfer from convection. We have also made the inclination variable and thus, introduced 'man-made' perturbations in the collector's natural convection and flow. In this, we suggested a way to distribute the flow to the risers – based on static pressure levels at entry. While we cannot at this stage verify the validity of the suggestion, it is a way of obtaining an indicative guide as to whether solar tracking for passive geysers might after all be meaningful. Much work still lies ahead in areas of flow distribution control in heated inclined risers and in their headers. This is in spite of significant efforts by previous and current researchers in the area.

ACKNOWLEDGMENTS

We are grateful to the Cape Peninsula University of Technology Research Fund for the sponsorship.

REFERENCES

Aicher, T. and Martin, H. 1997. New correlations for mixed turbulent natural and forced convection heat transfer in vertical tubes. Int. J. Heat and Mass Transfer. 40(15):3617-3626).

ASHRAE. 2009. ASHRAE Handbook-Fundamentals. Atlanta: American Society of Heating Refrigeration and Air Conditioning Engineers, Inc.

Bhargava, R., and Agarwal, R.S. 1979. Fully Developed Free Convection Flow in a Circular pipe. Indian J. Pure and Applied Math. , 10(3):357-365.

Du, S.C., Huang, B.J., and Yan, R.H. 1994. Hydrodynamic Instability of Solar Thermo syphon Water Heaters. Solar Energy Engineering, 116:53-62

Duffie, J.A., and Beckman, W.A. 2006. Solar Engineering of Thermal Processes. 3rd Ed. John Wiley and Sons, Inc. Hoboken, NJ.

Fang, L., Yong-hao, L., and Shi-ming, Y. 2008. Analytical and Experimental Investigation of Flow Distribution in Manifolds for Heat Exchangers. J. Hydrodynamics, 20(2):179-185.

Jaffer, A. 2012. Convection From a Rectangular Plate. http://people.csail.mit.edu/jaffer/SimRoof/Convection [5 Dec 2012]

Kanyarusoke, K.E., Gryzagoridis, J., and Oliver, G. 2012. Annual Energy Yields Prediction from Manufacturers' Photovoltaic Panel Specifications for Sub-Sahara Africa. ICEAS Proceedings, 2012: 223-255.

Kell, G.S. 1975. Density, Thermal Expansivity, and Compressibility of Liquid Water from 0" to 150°C: Correlations and Tables for Atmospheric Pressure and Saturation Reviewed and Expressed on 1968 Temperature Scale. J. Chem. and Eng. Data, 20(1):97-105.

McPhedran, R.C., Mackay, D.J.M., and McKenzie, D.R., and Collins, R.E. 1983. Flow Distribution in Parallel Connected Manifolds for Evacuated Tubular Solar Collectors. Aus. J. Phys., 1983(36):197-219.

Morrison, G.L., and Braun, J.E. 1985. System Modeling and Operation Characteristics of Thermo syphon Solar water heaters. Solar Energy, 34:389-405.

Nizami, D,J., Lightstone, M.F., Harrison, S.J., and Cruickshank, C.A. 2013. Negative buoyant plume model for solar domestic hot water tank systems incorporating a vertical inlet. Solar Energy, 87(2013): 53-63.

Norton, B., Edmonds, J.E.J., and Kovolos, E. 1992. Dynamic Simulation of Indirect Thermo syphon Solar Energy Water Heaters. Renewable Energy, 2(3): 283 – 297.

Perez, R., Ineichen, P., Seals, R., Michalsky, J., and Stewart, R. 1990. Modeling Daylight Availability and Irradiance Components From Direct and Global Irradiance. Solar Energy, 44(5):271-289.

Prayagi, S.V., and Thombre, S.B. 2011. Parametric Studies on Buoyancy Induced Flow through Circular Pipes in Solar water heating system. IJEST, 3(1):616-626.

Rehm, R.G., and Baum, H.R. 1978. The Equations of Motion for Thermally Driven, Buoyant Flows. J.Res. National Bureau of Standards, 83(3):297-307.

Sastri, K.S., and Vajravelu, K. 1977. Fully developed laminar free convection flow between two parallel vertical walls. Int. J. Heat and Mass Transfer, 20, 655.

Yamamoto, S.,Niiyama, D., and Shin, B.R. 2004. A numerical method for natural convection and heat conduction around and in a horizontal circular pipe. Int.J. Heat and Mass Transfer, 47(2004):5781-5792.

6.3 Concluding the chapter

This chapter was devoted to a fairly new area: that of tracking solar siphons. It was mainly mathematical in outlook, providing a model that could be used to predict the performance of a system if the weather data were known. However a working prototype of solar tracking solar siphon was built as described in this paper – i.e. about an inclined axis (Figure 6.4) but it still has flow reversal problems alluded to in chapter 1 of this thesis (see Figure 1.3).

Figure 6.4: The Researcher and the inclined axis solar tracking solar syphon

CHAPTER SEVEN:

FIFTH ARTICLE:

"THE NEW HYDRO-MECHANICAL SOLAR TRACKER: PERFORMANCE TESTING WITH A P-V PANEL"

Kant E Kanyarusoke kanyarusokek@cput.ac.za; and **Jasson Gryzagoridis** gryzagoridisj@cput.ac.za; *Mechanical Engineering Department, Cape Peninsula University of Technology, Bellville (7535) Cape Town South Africa.*

2016 International Conference on the Domestic Use of Energy (DUE), 30 – 31 Mar 2016, Cape Town, pp. 178-185. Online Publication by IEEE. DOI. 10.1109/DUE.2016.7466720
http://ieeeplore.ieee.org/stamp.jsp?tp=&arnumber=7466720

7.0 Introducing the chapter

In this penultimate chapter, a summary of the design process of a new solar tracking device adaptable to sub-Saharan Africa's conditions of bi-hemispherical location, low technology base (and low incomes and credit) is given first. Because the product is patented for the university, only details necessary to follow the performance testing described in the paper are disclosed.

7.1 A summary of the design process

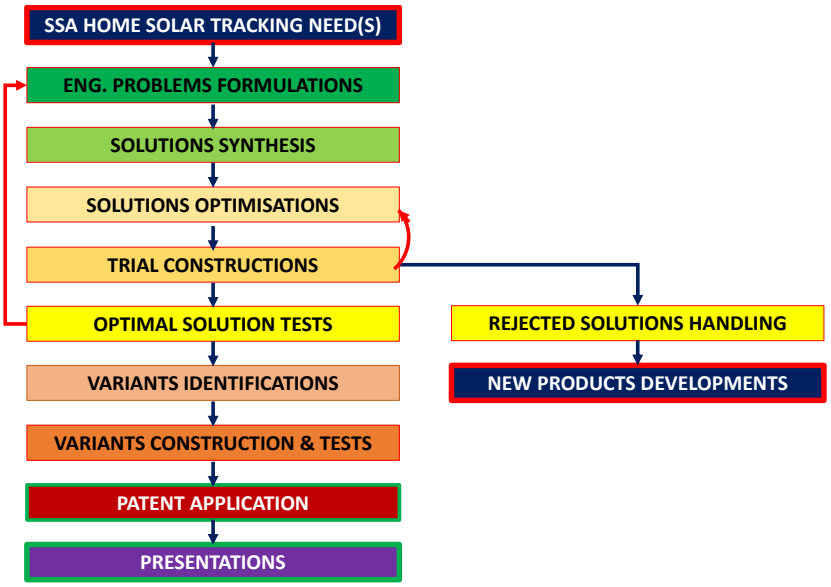

Figure 7.1: The Design process for the novel solar tracker

Figure 7.1 shows the design process that was followed. The needs which drove the process arose from findings of chapter 5. They are summarised as:

Required: -

"A novel, almost technical maintenance-free, cost effective mechanical energy driven solar tracking device that can be used on both PV and ST home systems and is deployable any where in the tropics without need for internal readjustments for optimal performance."

After many iterations - as implied in the figure - a day time gravity driven, single axis solar tracking device was prototyped and patented in 3 variants: a fully automatic system, able to self return at night almost indefinitely; a semi automatic version that needs manual intervention about once a month (refilling a raised water supply tank); and a mannual system requiring human intervention (simple turning on and off of a water valve) only at day-break.

Figure 7.2 shows the general layout. In the auto and semi automatic versions, a small dc - powered 10 W, 4 m head pump (50) is required for less than one minute a day. In the manual and semi auto versions, tank (60) is required. In the manual variant, one way valve (54) is replaced by a simple tap and connected directly to (60). Appendix A5.2 on the DVD disk gives videos of the mechanism in operation.

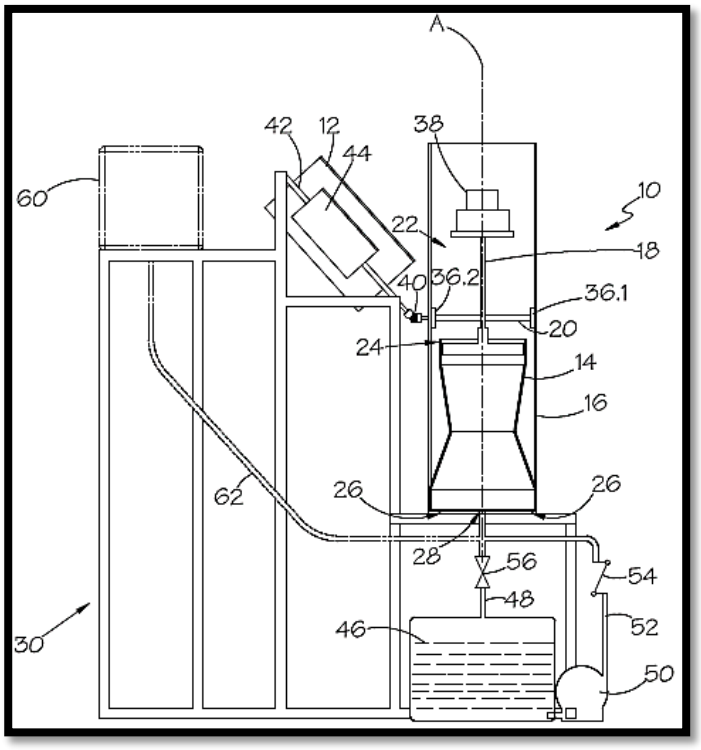

Figure 7.2: Simple layout of the solar tracker: Key elements are: 12 – solar panel/collector; 14 – bladder; 18 – double rack; 38 – Drive weights; 40 – Hooke joint

7.2 Introducing the published paper

The paper introduces the invention in the form of theoretical modelling and experimental testing of the prototype. It determines the %age energy gains: first – reaching the surface, and second, being converted to electricity by a PV panel. In addition to yields, the chapter gives an indication of the effects of environmental conditions on performance and measurements of overall energy utilisation of the prototype. From the former, it is possible to make 'intelligent' expectations of performance in different climatic regions of SSA. And from results of the latter, queries on mechanical energy consumption within the mechanism itself can be made for future product reengineering.

7.3 The paper

The new hydro-mechanical solar tracker: performance testing with a P-V panel

Kant E Kanyarusoke kanyarusokek@cput.ac.za; and **Jasson Gryzagoridis** gryzagoridisj@cput.ac.za; *Mechanical Engineering Department, Cape Peninsula University of Technology, Bellville (7535) Cape Town South Africa.*

Abstract— This paper describes work carried out to test the performance of a newly invented solar tracker. It is a gravity driven, bladder-flow controlled, Hooke coupled inclined non polar axis solar tracker. The performance of the tracker when coupled with a PV panel was first modelled in MATLAB® using the Perez anisotropic diffuse radiation and the King cell temperature models. Experiments with two identical 90 Wp panels were done over a 40 day period in outdoor conditions. One PV panel was fixed on optimised slope, the other, was driven by the tracker about a similarly sloped axis. Weather data consisting of total and diffuse radiation, ambient temperature and wind speed was also collected using a Campbell Scientific weather station adjacent the panels. This data was used to simulate performances of the panels in the MATLAB® model. TRNSYS simulations were also done for the two panels. The three sets of results were compared. It was found that the tracked panel yielded 34% more energy than the fixed one and that the experimental results correlated more closely with the MATLAB® models than with TRNSYS ones. Results also indicated that the efficacy of the tracking device could be influenced by the timing of cloudiness during the day and by wind speed.

***Index Terms*— MATLAB, PV panel, Single axis tracker, Solar energy, Solar Tracking, TRNSYS.**

7.3.1 *INTRODUCTION*

Previous work in [1] indicated that most of the existing solar tracking devices were either unsuitable or unavailable for domestic home use in sub-Sahara Africa. Therefore, a new device, designed with the region's conditions of low skill base, bi-hemispherical tropical location and low disposable incomes in mind, was invented by the authors. It is described in a patent application by Cape Peninsula University of Technology (CPUT) [2]. A line sketch of the tracker is shown in Fig. 7.3. Its photograph is given later in the experimental section of this paper.

Work by other inventors and researchers (e.g. [3] – [7]) shows that energy gains between 15 and 49% are possible when using different trackers, depending on whether the tracking is on single or on double axis. The work in this paper aimed to find out how much electrical energy gain could be obtained from using the invented device at the Bellville campus of CPUT – coordinates: 33.935°S, 18.644°E, 68.5 m. In addition, we wanted to know how predictions by TRNSYS simulation and by a MATLAB® based code using actual weather data, compared to actual energy yields.

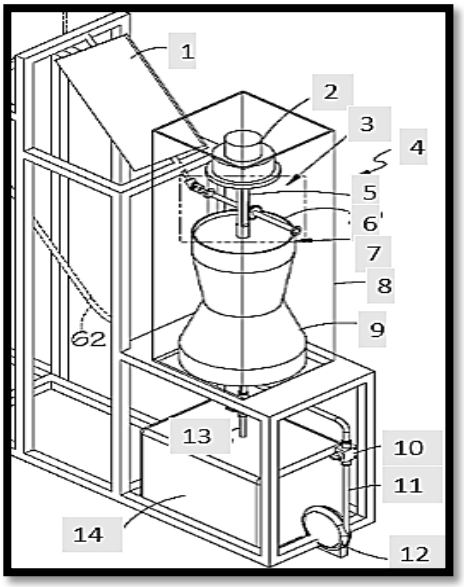

1 PV panel
2 Drive weight
3 Gear rack assembly
4 Tracker assembly
5 Rack
6 Gear shaft
7 Piston
8 Mechanism housing
9 Bladder
10 One way valve
11 Bladder feed pipe
12 Pump
13 Solenoid valve
14 Water tank

Fig. 7.3: The prototype solar tracker

7.3.2 *THEORETICAL MODELLING*

In this section, the incident energy on an inclined photovoltaic (PV) panel – which is described by Duffie and Beckman [8] is summarised first. The panel's parameters at the manufacturer test conditions are also deduced. A method for analytically determining electrical energy yield from the PV panels is given.

7.3.2.1 *Incident energy on an inclined panel*

Fig. 7.4 illustrates the important angles and incident energy terms on a southern hemisphere panel sloped at angle $\beta°$ and with azimuth $\psi°$. Beam and circumsolar radiation reach the panel at a variable angle of incidence $i°$. At this instant, the sun is viewed at an azimuth angle $\psi_s°$, and either an elevation $\alpha°$ or a zenith angle $z°$. Perez *et al.* [9] give an expression for total incident radiation on the panel G_{panel} as in equation (1) – with terms defined as in equations (2-4) [8].

$$G_{panel} = G_{bh}R_b + G_d(1 - F_1)\left(\frac{1+\cos(\beta)^\circ}{2}\right) + G_d F_1 \frac{a}{b} + G_d F_2 \sin(\beta^\circ) + G_h \rho_g \left(\frac{1-\cos(\beta^\circ)}{2}\right) \quad (1)$$

$$R_b = \frac{G_{bpanel}}{G_{bh}} = \cos(i^\circ)\sec(z^\circ) \quad (2)$$

Where: G_h is total radiation on a horizontal surface – consisting of the beam/circumsolar part, G_{bh} and the diffuse part; G_d. Ground reflectivity is denoted as ρ_g. F_1 and F_2 are empirical circumsolar and horizon brightness functions of z and sky brightness determined according to the Perez model instructions [9]. Parameters a, and b are given by equations 3 and 4 respectively [8].

$$a = \max(0, \cos(i^\circ)) \, ; \, b = \max(\cos(85^\circ), \cos(z^\circ)) \quad (3, 4)$$

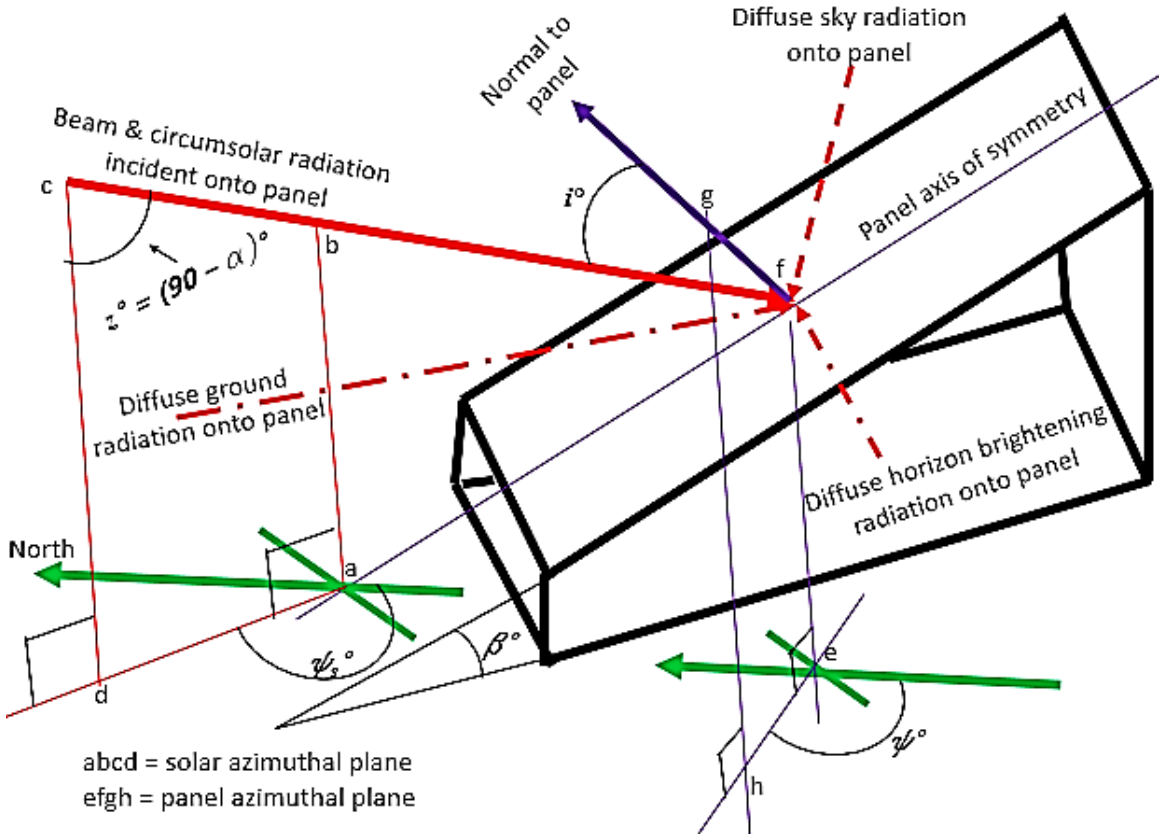

Fig. 7.4: Important angles and incident energy components onto an inclined panel

For a given panel slope β and azimuth ψ, the angles ***i***, $\psi_s°$ and z (or α) depend on latitude ***L***°, day of year ***n***, and time from solar noon, ***t***. Expressions for these are available in standard solar energy engineering text books such as [8], [10] and [11].

When either the panel's slope or azimuth is made to vary (as in many solar tracking systems), vector algebra can be used to determine the new direction of the surface's normal, and hence, the angle of incidence. In the experiments of section 4 for example, one of the panels tracks about a fixed axis (β_{axis} = 30°). In that case if the panel rotates an angle $\phi°$ from a start position of β = 90°, ψ = 270° (i.e. facing East), the algebra gives its slope and azimuth as in equations (5) and (6) respectively.

$$\beta = \cos^{-1}\left(\cos\beta_{axis}\sin\phi\right) \qquad (5)$$

Before Solar noon:

$$\psi = 180 + \cos^{-1}\sqrt{1 - \frac{1}{1+\tan^2\phi\sin^2\beta_{axis}}} \qquad (6a)$$

After solar noon:

$$\psi = 180 - \cos^{-1}\sqrt{1 - \frac{1}{1+\tan^2\phi\sin^2\beta_{axis}}} \qquad (6b)$$

7.3.2.2 *The PV panel and its characteristics*

Although [8] uses a 5 parameter model for PV panels, TRNSYS simulation recommends a 4 parameter (I_L, I_0, R & n) model for mono-crystalline silicon cells [12]. Since the work here aimed to compare results with TRNSYS predictions, the latter model was used in the MATLAB® formulation. The characteristic equation relating current ***I*** to voltage ***V*** is then given as:

$$\begin{aligned} I &= I_L - I_0\left[\exp\left(q(V+IR)/nkT_cN_s\right) - 1\right] \\ &\approx I_L - I_0\left[\exp\left(q(V+IR)/nkT_cN_s\right)\right] \end{aligned} \qquad (7)$$

Where: ***q*** is the electron charge, 1.602E-19 C and ***k*** is Boltzmann's constant, 1.381E-23 J/K. For the panels used, N_s = 36 cells.

Fig. 7.5 is a graphical representation of the equation – and it shows how to geometrically locate the operating point for maximum power generation ($d(IV) = 0$) using a straight edge. The slope of the edge is varied until its tangency to the characteristic curve is exactly half way between edge intercepts on the two axes.

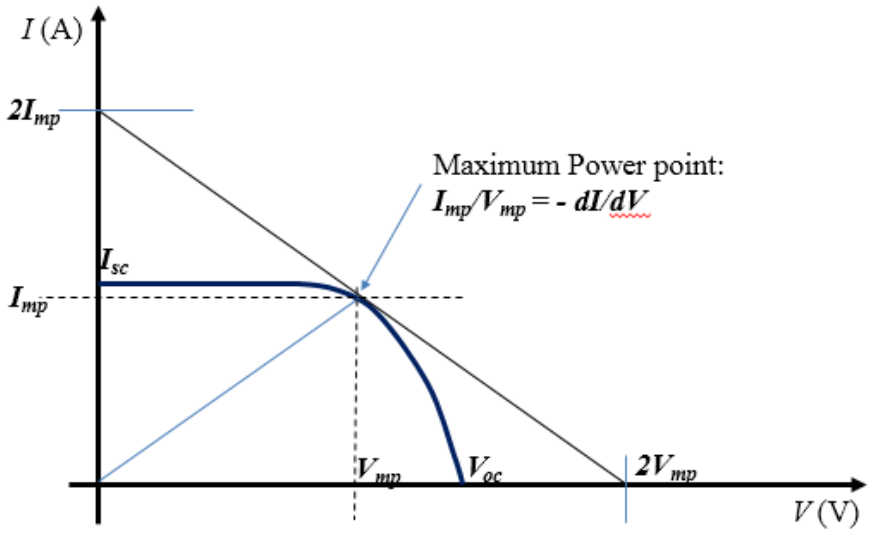

Fig. 7.5: The 4-parameter model characteristic for a PV panel

Manufacturer panel specifications give short circuit current I_{sc}, open circuit voltage V_{oc}, maximum power current and voltage I_{mp} and V_{mp} based on standard conditions of G_{std} = 1000 W/m^2; $T_{ambient}$ = 25°C = 298.15 K; v_{wind} = 1 m/s; and optical air mass m_{air} = 1.5 at sea level. The four parameters at those conditions ($I_{L\text{-}std}$, $I_{0\text{-}std}$, ***R and n***) can be determined by solving the given 3 instances of equation (7) and its differential at maximum power using suitable software. In the present case, the standard parameters were computed using a MATLAB® script and are given in Table I.

Table I. The test panels: key specifications and standard test parameters

Manufacturer's specifications	*Standard conditions parameters*
I_{sc} = 5.50 A	$I_{L\text{-}std}$ = 5.5 A
V_{oc} = 22.4 V	$I_{0\text{-}std}$ = 1.721E-10 A
I_{mp} = 4.90 A	***R*** = 0.1001 Ω
V_{mp} = 18.4 V	***n*** = 1.001
α_{isc} = +1.55 mA/K	G_{std} = 1000 W/m^2 (given)
α_{voc} = -79.2 mV/K	**NOCT** = 45°C = 318.15 K (given)
α_W = - 0.46%/K	

Operating conditions characteristics -

Operating conditions differ from those during tests – and therefore parameter values in Table I do not reflect actuals in practice except for the 'ideality' factor ***n*** and the internal module resistance ***R***. In earlier work [13], equations (8) to (10) from [8] and [14] were used to relate panel currents to incident radiation and module cell temperatures. The same equations are applicable here.

$$I_L = \frac{G_{panel}}{G_{std}}\left[I_{L-std} + \alpha_{isc}\left(T_c - 298.15\right)\right] \quad (8)$$

$$I_0 = I_{0-std}\left(\frac{T_c}{298.15}\right)^3 \exp\left(47.04822 - \frac{14027.427}{T_c}\right) \quad (9)$$

$$T_c = T_{back} + \frac{G_{panel}}{G_{std}}\Delta T \quad (10a)$$

$$T_{back} = T_a + G_{panel}\exp(a' + b' v_w) \quad (10b)$$

Where T_{back} and T_a are panel backside and ambient temperatures; ***a'***, ***b'*** and ΔT are respectively -3.56, -0.075 and +3 for a glass-cell-

polymer sheet open rack mounting used in the experiments below.

Equations (8) – (10) are used along with the fixed values of $\boldsymbol{R}$ and $\boldsymbol{n}$ in Table I to determine the characteristics of the panel at any given instant.

Energy yield from a PV panel -

Parameters in equation (1) were evaluated for the recorded actual values of G_h and G_d in MATLAB®. Hence, G_{panel} was computed for each instant. Consequently, all terms in the characteristic curve equation (7) could be determined. In the experiments below, Maximum Power Point Trackers (MPPTs) were used – and therefore, instantaneous power generated could be computed by locating the point of maximum power in Figure 3 – as represented by the approximation in equation (11).

$$\frac{dI}{dV} + \frac{I}{V} = 0 \approx \frac{\delta I}{\delta V} + \frac{I}{V} \qquad (11)$$

Incremental values of $0.01\boldsymbol{I_L}$ for $\boldsymbol{I}$ between $0.30\boldsymbol{I_L}$ and $0.98\boldsymbol{I_L}$ in MATLAB® were used to check satsfaction of this condition, and hence, to determine the maximum power point, $(\boldsymbol{I_{mp}}, \boldsymbol{V_{mp}})$. By recording these $\boldsymbol{I_{mp}}$ and $\boldsymbol{V_{mp}}$ values across each day during the period of interest, the maximum possible total electrical energy yield from the panels was determined by numerical integration.

7.3.3 *TRNSYS MODELLING*

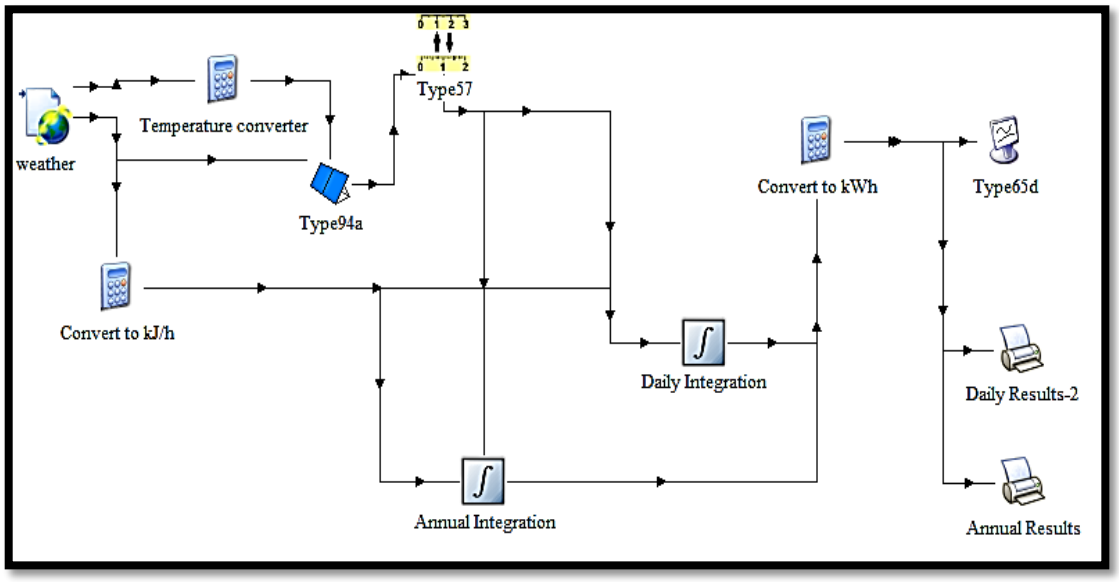

Fig. 7.6. The TRNSYS model for determining PV energy yield.

In Fig. 7.6, the type 94a PV panel was configured for both fixed and single inclined axis tracking to get two sets of results.

7.3.4 *EXPERIMENTAL INVESTIGATIONS*

7.3.4.1 *Tools and Equipment*

- 1 - Prototype gravity driven, bladder flow controlled hydro-mechanism adopted for solar tracking.
- 2 – Mono crystalline silicon Solar panels: as specified in Table I. Manufacturer: SetSolar, Cape Town.
- 2 – MPPT charge controllers 10 A from SetSolar.
- 2 – Batteries: Deep cycle lead-acid; 12 V; 105 Ah.
- 2 – Bulbs MR-16 dichroic halogen lamp; 50 W, 3000 hours.
- Weather station – Campbell Scientific. Consisting of: 1 Kipp Zonen CMP06 Pyranometer, ISO First class; 2 SP LITE

silicon Pyranometers (with one shaded to measure diffuse radiation), a 03101 R.M Young anemometer and an ambient dry bulb temperature probe.

- 1 - 32 channel Campbell Scientific measurement and control data logger.
- Three weather proof enclosures: two for the batteries and charge controllers, the other for the electric bulbs.

7.3.4.2 *Set up and Procedure*

- One 90 Wp solar panel was set up facing true north, sloped at 30° from the horizontal (the TRNSYS derived optimal slope for the site). The mount for the panel had been designed with an adjustable mechanism to vary the angle – which was measured using a smart phone with a protractor application installed - and crosschecked by trigonometric computations. Parallel to this, but offset southward, a stand for the tracking panel and tracking mechanism was erected. The southward offset was to ensure that the tracking PV panel did not shade the fixed one during operation.
- A shaft inclined at 30°, supported on the stand with self-aligning ball bearings, was connected to the new tracker's Hooke coupling. The PV panel was centrally attached to this shaft using suitably designed brackets. A counter weight was centrally attached to the shaft on the backside of the PV panel, thus ensuring stability.
- The panels, batteries, charge controllers, bulbs, data logger and the tracking mechanism were wired up as in Fig. 7.7. The system was run for the planned 40 day period: 15 Nov – 24 Dec 2015. Occasionally during the period, readings of panels' voltage and current were taken manually using a hand held voltmeter and clamp ammeter. This was only meant to randomly cross check with the automatically recorded 15 minute data in the logger. The bulbs were left on during the entire period to ensure the batteries always started in a minimum charge condition – thus causing the panels to generate maximum power during the day.
- Weather data: i.e. horizontal surface total irradiance, G_h (W/m^2), diffuse irradiance G_d (W/m^2), ambient temperature, T_a (°C) and wind speed v_w (m/s) were recorded in the logger. The data acquisition and processing circuitry had been configured to sample every 2 s, totalise the data, and store the average values over each 15 minute interval.
- Similarly, interval average voltages and currents from both panels were recorded in the logger at 15 minute intervals.

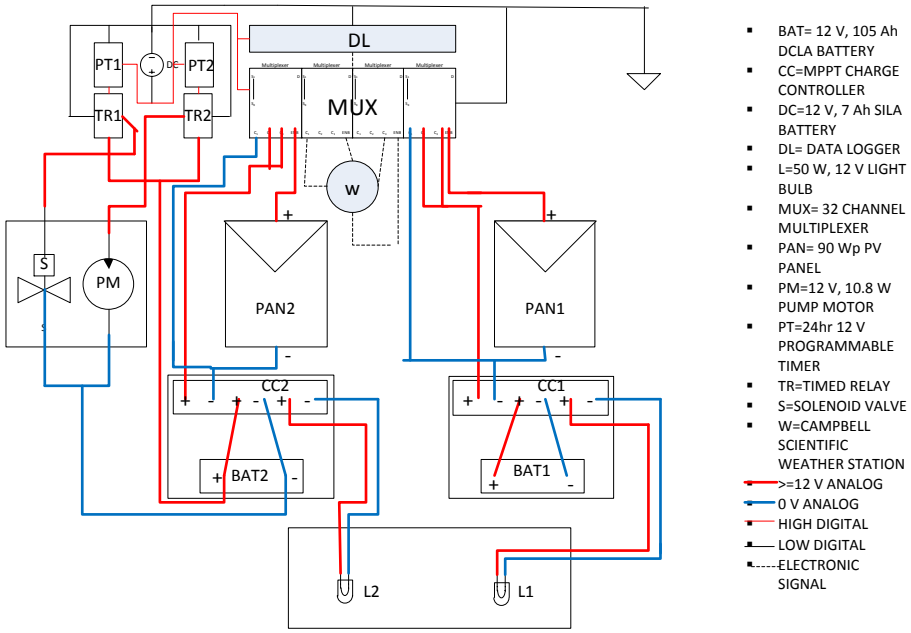

a) Wiring diagram

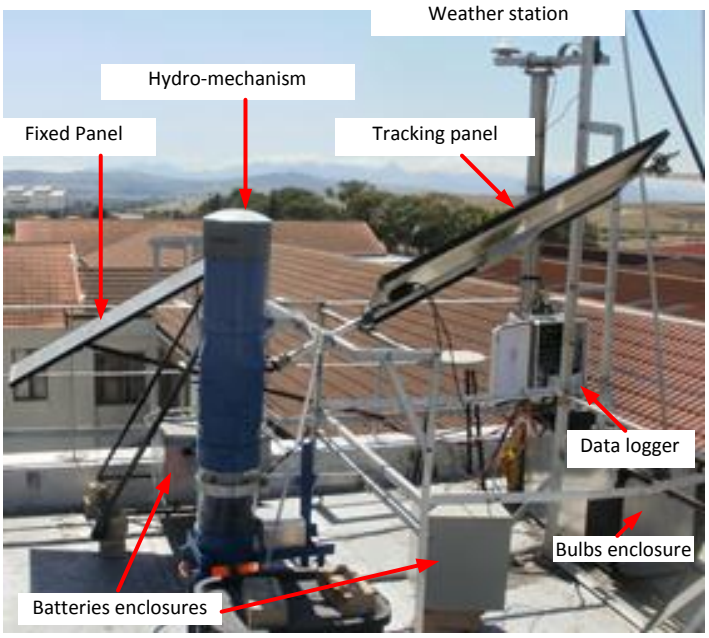

b) Actual Layout

Fig. 7.7. Experimental set-up

7.3.4.3 *Analysis*

The analysis involved two approaches: one was the use of the raw weather data in the models to derive or predict the performance for each of the panels. The other approach was the extraction of actual measured power in order to deduce daily electrical energy output which could be compared with predictions from TRNSYS simulations and from the MATLAB® model.

Using Weather data -

Solar radiation data from the logger was reconfigured in two MATLAB® scripts using equations (1) – (6) to derive 15 minute incident solar power on each panel, $W_{inc\text{-}panel}$. The ground reflectivity ρ_g (roof and faroff ground objects) was assumed to be 0.2. Data for ambient temperature and wind speed were used in the second part of the scripts to determine panel cell temperatures, T_c in accordance with equations (10). Then, equations (8), (9) and (11) were programmed to give the maximum power point, and hence, the peak power generation every 15 minutes for each panel, $W_{out\text{-}panel}$. The third part of the scripts totalised (i.e. integrated power), compared daily output energy with input incident energy and graphed the panels' performances.

Using Measured Voltage and Current data -

Daily electrical energy production from each panel was found by numerical integration of the power data. The trapezium approximation was used because of its simplicity. In total, there were up to 62 time intervals in a day ranging from 5 am to 8 30 pm. The energy data was transferred to MS EXCEL spreadsheets for comparison with the outputs from the TRNSYS simulation and the MATLAB® model.

7.3.4.4 *Results*

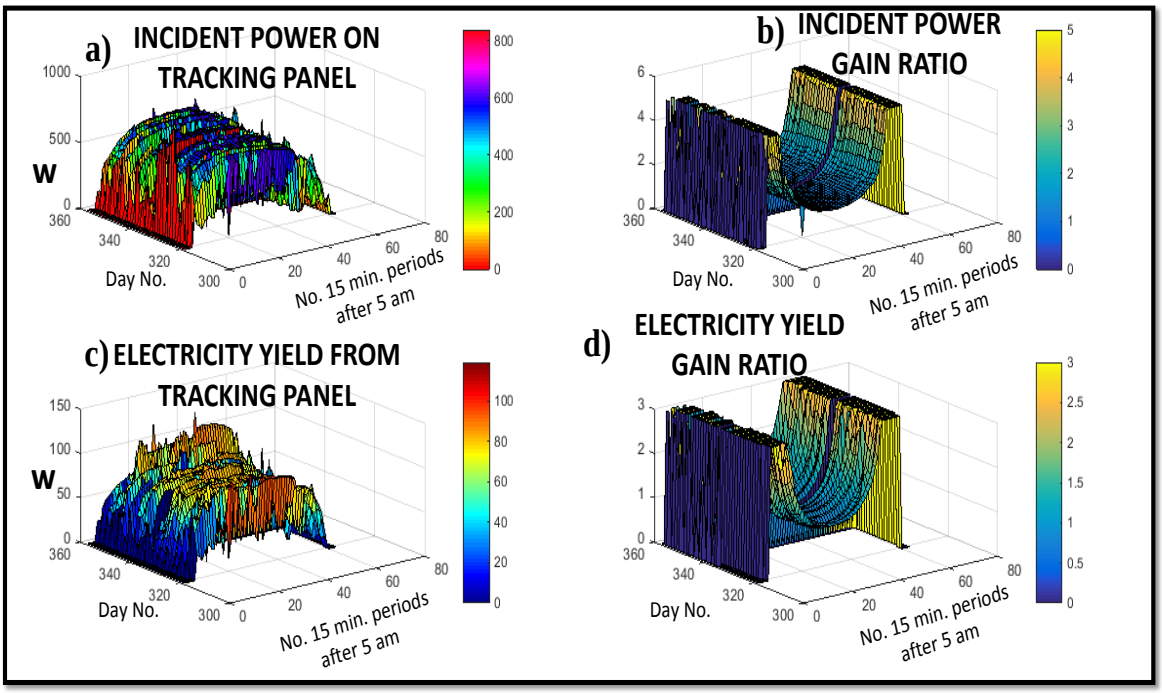

Fig. 7.8. Summary of experimental data for period: 15 Nov-24 Dec 2015: a) Incident solar radiation power on solar tracking panel; b) Ratio of incident power on tracking to that on non tracking panel; c) Measured electrical power output of the solar tracking panel d) Ratio of measured power from tracking to that from the non-tracking panel.

Of the targeted 40 days, there were full data for 39 days. Data for day no. 339 (5th Dec 2015) was incomplete because the data logger battery had to be recharged for most part of the day. Data for this day is therefore excluded from the report.

Overview -

Fig. 7.8 gives a graphical overview of the results. In a) the quarter hourly incident power on the tracking panel as computed in section 7.1.4.3 is depicted. Rather than present a similar one for the non-tracking panel, Fig. 7.8b) gives the ratio between the two amounts of incident power. It was found that very early morning and late evening, the ratios were very high - due to the Perez horizon brightening effect in equation (1). Hence, to get a scalable figure, the depicted ratios at these times were capped to 5 although actual values were left intact in the primary data for other computations. Fig. 7.8c) gives the tracking panel's actual computed output power from section 7.3.4.3. Fig. 7.8d) gives the output power gain ratio computed from actual measurements. Like in b), it is capped, but this time at 3.

Observations during experiments -

During the course of experiments, three phenomena were observed: effect of windy conditions; effect of clouds/rain; and propensity of fixed panel to get dirty/dusty (and difficulty to clean it) relative to the tracking one.

Windy conditions stronger than gentle breezes ($v_w \geq 3.5$ m/s) tended to affect the tracking mechanism through reduction of panel rotary speed between intended start-stop positions. This led to tracking errors, especially in mid-morning hours – since the travel time was fixed.

Power and energy computations at the end of each day showed that clouds and rain tended to affect the day's tracking energy gain ratio depending on which times of the day were cloudy/rainy – with late mornings and early afternoons being less consequential than mid-mornings and late afternoons.

Besides a tendency for dust to settle and remain on the fixed panel, it was noticed that birds preferred its upper edge to that of the tracking panel as a resting place (or was it for surveillance purposes?). Consequently, in addition to dust,

bird droppings were more common on the fixed panel, making it more involving to clean and maintain.

The overall effects of the first two observations led to a qualitative two dimensional performance possibility space depending on tracking accuracy (low average wind speeds) and extent of beam radiation (i.e. absence of cloudiness) during the day. The descriptive statistics for the 39 days were consequently reconfigured in 4 performance quadrants as in Table II. Performances on typical days in each quadrant are illustrated in Fig. 7.9.

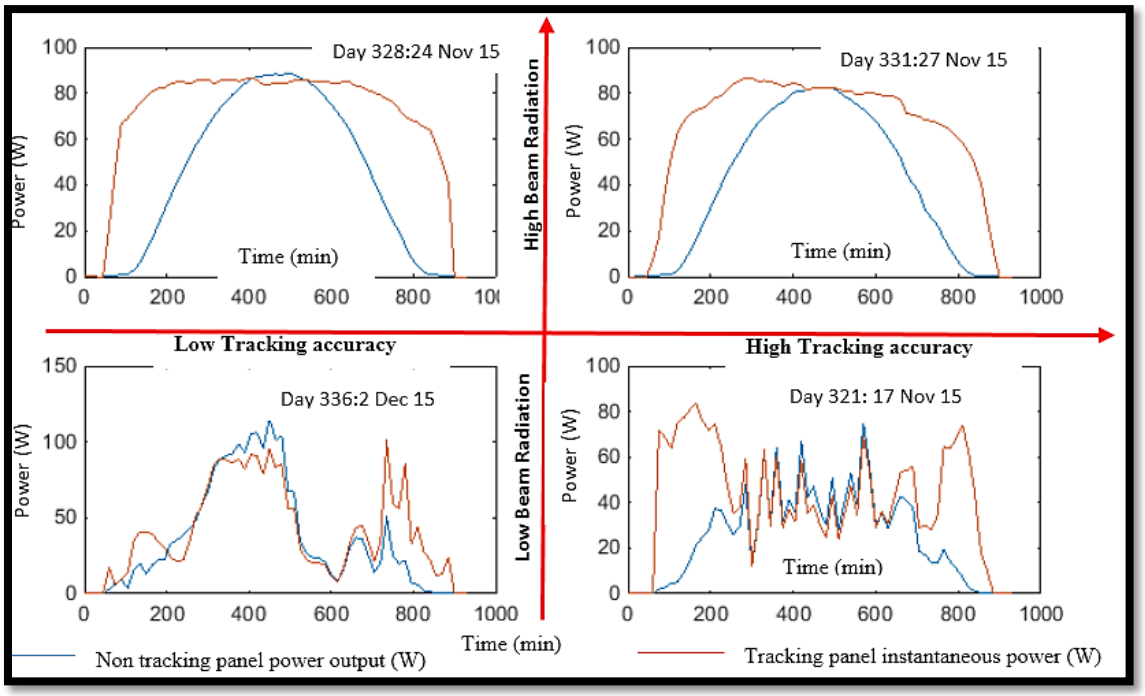

Fig. 7.9: Representative days in performance quadrants: 1st quadrant: High beam radiation with high tracking accuracy; 2nd quadrant: High beam radiation with some tracking errors; 3rd quadrant: Low beam radiation with tracking errors; 4th quadrant: Low beam radiation with high tracking accuracy.

Comparison of performances -

Figure 7.10 gives the comparative performances of fixed and tracking panels. In meeting the other objectives of this work, it compares actual energy yield with each of the models' predictions.

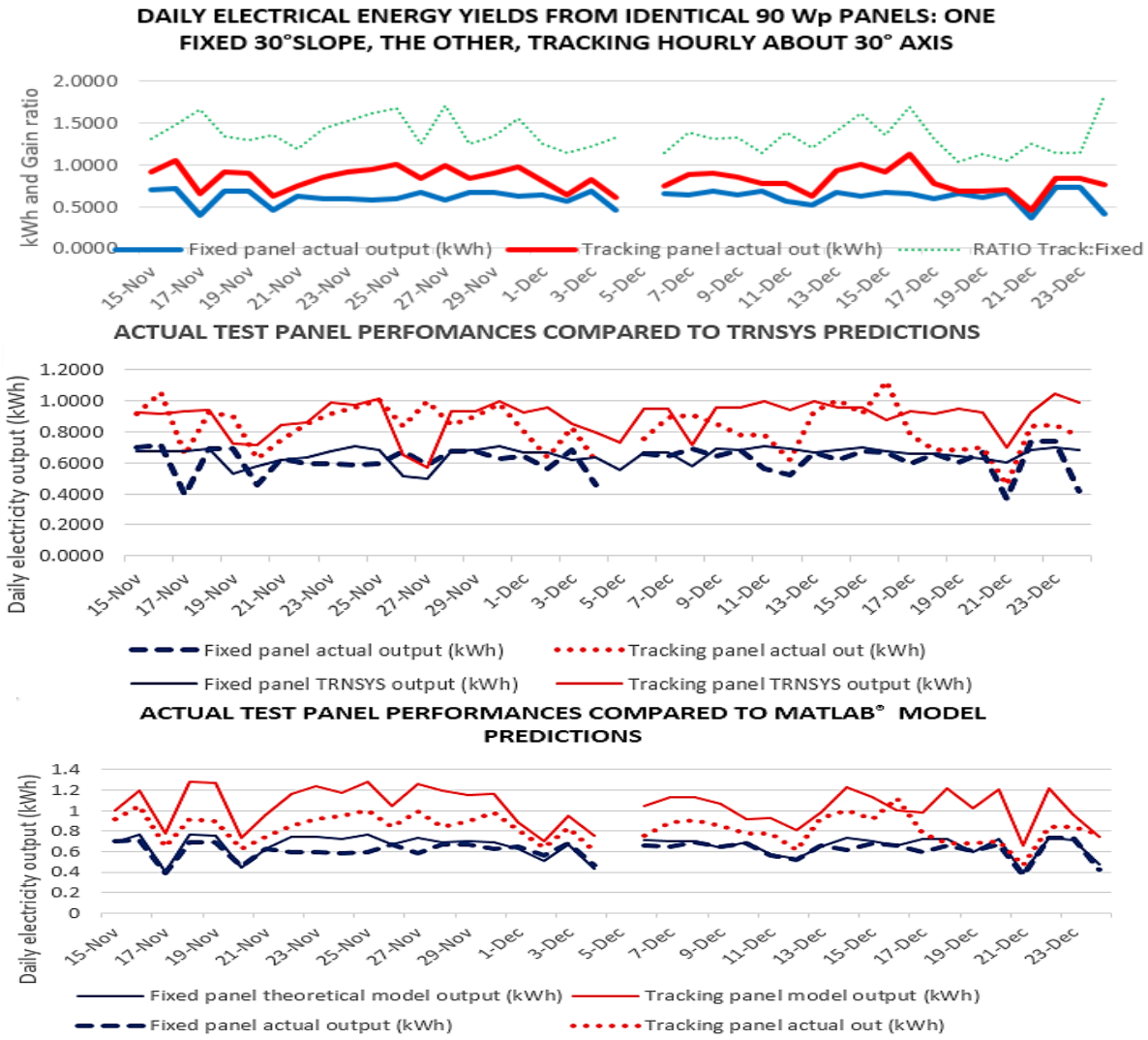

Fig. 7.10. Actual daily energy outputs compared with TRNSYS and MATLAB® predictions

7.3.5 *RESULTS DISCUSSION*

In this section the results arrived at during this work are interpreted and explained. Where appropriate, implications on possible applications of the tracking mechanism are deduced.

7.3.5.1 *General observations (Figure 7.8)*

Incident radiation -

The tracking panel generally received more radiation on it in spite of fluctuations throughout the day. For the entire period, the incident energy gain ratio was found to be 1.53. Whereas this seems to be a relatively high value, it is different from – and actually - does not necessarily reflect energy output ratios from devices run by the tracker – as evidenced by a 1.34 ratio for the latter in this case. Fig. 7.8b shows that, most relative gains were made in the hours between daybreak and about 9 am (240 min) and then much later in the day, between 5 pm and 7 pm (720-840 min). This is as expected because the difference in angles of incidence for the two panels is greatest at these times. The practical implication of this result is that the tracker would be most useful in systems seeking to extend solar energy harnessing to these times.

Output electrical energy -

Electricity yield approximately followed the pattern of incident energy on each panel. There was limited energy gain from tracking between mid-mornings and early afternoons, with 20 of the 39 days indicating gain ratios of just below 1 in the solar noon hours (ranging between 450 and 540 min). Whereas theory indicates that the outputs in these hours should always be equal, giving a ratio of 1, random tracking errors occasioned by the open loop control design of

the tracker [2] led to this variation. Even with these errors however, the overall electrical energy gain ratio for the period, remained relatively high at 1.34 - as pointed out above.

Thermodynamic efficiencies of the panels -
Efficiency is generally defined as a ratio of an output of what is desired to the total input in similar units of measure. For the fixed panel in the period, this simplifies to the ratio of output electrical energy to the incident solar energy on panel cells. It worked out as 16.7% (or 23.078 kWh/149.882 kWh). This was approximately in line with the manufacturer's claim of 17%. A similar ratio for the tracking panel was 14.66% (or 33.609 kWh/229.3 kWh). This latter value however, is not the exact efficiency of the tracking system. The system consumed electrical energy to operate it. Each of the electronics circuits for the pump and solenoid ran full time at 20 mA, 12 V from the data logger battery. The 5 W solenoid valve ran 12 times a day for 6 s each time. The 10.8 W pump ran once a day for 55s. This gave a total combined consumption of 0.0104 kWh from the battery being charged by the tracking panel. Consequently, the tracking system overall energy efficiency η_{track} was 14.62%.

It is seen that although the electrical energy output is increased significantly by the solar tracker, the energy efficiency is remarkably reduced. This could be explained from cell temperature considerations. Tracking increases photocell exposure to beam radiation which in turn increases both numbers of electron-hole pairs generated and their velocities. This increases average kinetic energy at the cell junctions, and hence, thermodynamic temperature T_c. Light current I_L increases from increased properly directed electron-hole pairs (thermodynamic work) but so does the reverse diode current I_o – from misdirected ones - at an even higher rate. The combined effect of these is to increase useful power while at the same time increasing the proportion of incident energy converted to thermal. Hence, the negative power coefficient (α_W) quoted by the manufacturer (see Table I).

7.3.5.2 *Detailed performance (Fig. 7.9)*
Table II shows that about half of the days were in the 2nd and 3rd quadrants of Figure 7.7. The tracking accuracy therefore has room for improvement. This could be done either by adjusting the solenoid valve timing from 6 s or by adopting a closed loop control system. While the former affects overall gain ratios, the latter - for technical reasons - was considered inappropriate in the market for which the tracker is intended.

Table II: Descriptive statistics of tracking panel performances

Quadrant Number	Description	Number of days
1	*Clear sky:* $v_w < 3.5$	11
2	*Clear sky;* $v_w \geq 3.5$	11
3	*Cloudy:* $v_w \geq 3.5$	9
4	*Cloudy;* $v_w < 3.5$	8

Perhaps the most important result in Figure 7.9 is the one that shows effects of diffuse radiation on energy gain ratios. This is manifested in the 3rd and 4th performance quadrants – where there was a total of 17 days. The combined ratio in these quadrants was found to be 1.30 as opposed to 1.37 for the 22 days of high beam radiation in the 1st and 2nd. On its own, this result shows that clear skies - tend to favour tracking. But there is more: The daily gain ratios for the 17 days ranged between a minimum of 1.1247 on day 353 and a maximum of 1.6627 on day 321 (see Fig. 7.9 for the latter) - depending on times during the day when the sky was cloudy. If in mid mornings or late afternoons, the gain ratio was low. It was higher if cloudiness was experienced around late morning to early afternoon. The issue here is the unpredictability of when skies will be clear, and therefore, the stochastic nature of tracking reliability in such circumstances.

7.3.5.3 *Modelling efficacy comparisons (Fig. 7.10)*
To determine the efficacy of the model in section 7.1.2 and of TRNSYS simulation, bivariate correlation analyses were done on fixed and

tracking panel electric output results using SPSS software. This yielded 6 Pearson correlation coefficients for the 3 possible combinations of: MATLAB®, TRNSYS and Experimental. The results are summarised in Table III.

Table III: Pearson correlation coefficients for daily electrical energy outputs using different methods: N = 39: significant at the 0.01 level, 2 tailed.

	EXPT.	TRNSYS	MATLAB	
EXPT.		0.546	0.718	FIXED
TRNSYS	0.525		0.648	PANEL
MATLAB	0.672	0.575		
	TRACKING PANEL			

These statistics together with the graphs of Figure 7.10 show that while there was significant positive correlation for all pairs, the MATLAB® model agreed most closely with the experimental work on fixed panel results. The closer agreement than TRNSYS in both fixed and tracking could be attributed to the MATLAB® model's use of actual weather data – while TRNSYS uses historical statistical data. There was a slight drop in the MATLAB®'s model agreement with experimental results when it came to tracking (0.718 to 0.672). This could be attributed to tracking errors – since the model assumed exact 15° hourly tracking. In summary therefore, it could be said that where actual weather data is known with a high degree of certainty, the MATLAB® model would be the preferred analysis tool to estimate PV electrical energy yield when the latter are connected to operate at maximum power points. Short of actual weather data, however, TRNSYS would still remain a fairly reliable tool.

7.3.6 CONCLUSIONS

This paper has described testing of a newly invented - solar tracking device. The device powered a PV panel tracking about a non polar inclined axis. The axis slope corresponded to a TRNSYS optimised value for a fixed PV installation at the site. The testing was done against three reference settings: a real identical panel at the optimised fixed slope; a virtual identical panel, tracking the sun about an identical axis in TRNSYS simulation; and a virtual identical panel tracking the sun about the same axis, in exactly identical weather conditions but in a MATLAB® simulation environment.

During development of these tests, a simple graphical method to locate the maximum power point on the characteristic of a PV panel was explained. A MATLAB® script to deduce manufacturer standard characteristic parameters was written as a precursor to developing a new model that would use real time weather data to predict panel performance.

Experiments were done over a period of 40 days, registering 2457 valid sets of readings out of a possible total 2520 (i.e. 97.5%). Each set recorded: day, time, 4 pieces of data on weather and 4 others on the 2 panels' outputs. Virtual panels performance data for the new MATLAB® based model was derived from the real weather data so that 4 additional pieces of data were added to each of the above sets. Thus, 34398 data pieces were available for reconfiguration and comparison with TRNSYS simulation results for the two panels.

From the resulting information, the following key performance indicators and ratios were deduced:

- The new tracking device improved daily electrical energy yields by variable ratios over the period ranging from 1.03 to 1.84. In total however, a 34% gain over the fixed panel yield was obtained for the entire period.
- On about 50% of the days, the new tracking device was slightly inaccurate owing to wind disturbances.
- The new MATLAB® model correlated better with experimental data when compared with the TRNSYS's model by factors of 1.11 and 1.28 for a fixed and a tracking panel respectively.

Considering that this tracker was designed for domestic use in sub-Sahara Africa, the results seem to suggest that it would be most appropriate in the southern mid tropical areas where according to [15] – [17], skies are most clear and wind speeds are low. In the great lakes subregion - with convectional rainfall in mid afternoons - chances are that it would also be valuable since

most of its energy gains are made in mid morning and late afternoons. At this stage however, it is not clear how useful the tracker would be in the windy and dusty Sahel subregion of west and mid northern Africa. This tracker would perhaps be least useful in the equatorial rain forests of Congo river basin. All said, further experimentation in the said subregions would be most appropriate before adoption on a mass scale.

References

[1] K. E. Kanyarusoke, J. Gryzagoridis and G. Oliver, "Are solar tracking technologies feasible for domestic applications in rural tropical Africa?" *JESA*, vol. *26*, no. *1*, pp. 86-95, 2015.

[2] K. E. Kanyarusoke and J. Gryzagoridis, "A hydraulic mechanism. Solar Tracker," South Africa Patent application P72557Z - 2015/09278P00, Dec, 21, 2015.

[3] M. J. Clifford and D. Eastwood. (July, 2004). Design of a novel passive solar tracker. Solar Energy. [Online]. 77, pp. 269–280. Available: http://ac.els-cdn.com/S0038092X04001483/1-s2.0-S0038092X04001483-main.pdf?_tid=62b42852-c9a4-11e5-bcc5-00000aab0f26&acdnat=1454414537_c97ff18104b23154870a11e6a4969981

[4] F. J. G. Gil, M. D. Martín, J. P. Vara and J. R. Calvo, "A review of solar tracker patents in Spain," in *Proc.3rd WSEAS Int. Conf. on Renewable energy sources*, Spain, 2009, pp. 292-297.

[5] B-J. Huang, Y-C. Huang, G-Y. Chen, P-c. Hsu and K. Li. "Improving solar PV system efficiency using one-axis 3-position sun tracking," *Energy Procedia*, vol. 33, pp. 280-287, 2013.

[6] S.Bazyari, R. Keypour, S. Farhangi, A. Ghaedi and K. Bazyari. "A study on the effects of solar tracking systems on the performance of photovoltaic power plants," *JPEE*, vol. 2, pp. 718 -728, 2014.

[7] J. R. B. del Rosario, R. C. Gustilo and E. P. Dadios, "Optimisation of a small scale dual-axis solar tracking system using nanowatt technology," *JOACE*, vol. 2 no.2, pp. 134-137, 2014.

[8] J. A. Duffie and W. A. Beckman, *Solar Engineering of Thermal Processes*. 4th ed. Solar Energy Laboratory, University of Wisconsin-Madison, USA, Wiley, 2013, pp. 91-97.

[9] R. Perez, P. Ineichen, S. J. Michalsky and R. Stewart, "Modelling daylight availability and irradiance components from direct and global irradiance," *Solar Energy*, vol. 44 no.5, pp. 271-289, 1990.

[10] G. N. Tiwari, *Solar Energy: Fundamentals, Design, Modelling and Applications*, New Delhi India, Narosa, 2002 pp.16-40.

[11] S. A. Kalogirou, *Solar Energy Engineering Processes and Systems*. 2nd ed. Oxford, UK, Elsevier Inc., 2014, pp.51-106.

[12] S. A. Klein, J. A. Duffie, J. C. Mitchell, J. P. Kummer, J. W. Thornton, E. Bradley, D. A. Arias, W. A. Beckman, N. A. Duffie, J. E. Braun, *et al*. *TRNSYS 17 A transient system simulation program.* Madison, USA: Solar Energy Laboratory, University of Wisconsin, 2012.

[13] K. E. Kanyarusoke, J. Gryzagoridis and G. Oliver, "Predicting photovoltaic panel yields in sub-Sahara Africa," in *Proc. ICEAS*, Beijing, China, 2012, pp. 223-255.

[14] D. L. King, W. E. Boyson and J. A, Kratochvill, (2004, Dec.). Photovoltaic Array Performance Model. SANDIA Report SAND2004-3535, Sandia National Laboratories, Albuqurque, New Mexico.[Online] Available: http://prod.sandia.gov/techlib/access-control.cgi/2004/043535.pdf

[15] A. Hoscilo, H. Balzter, E. Bartholomé, M. Boschetti, P. A. Brivio, A. Brink and M. Clerici, (2015). A conceptual model for assessing rainfall and vegetation trends in sub-Saharan Africa from satellite data. *Int. Journal of Climatology* [on line], 35, pp. 3582-3592 Available: Onlinelibrary.wiley.com/doi/10.1002/joc.4231/epdf

[16] M. Haile, (2005). Weather patterns, food security and humanitarian response in sub-Saharan Africa. *Philosophical Transactions of The Royal Society B: Biological Sciences*, 360(1463), 2169 - 2182. http://doi.org/10.1098/rstb.2005.1746.

[17] L. Guertin, (nd). *Earth 105: Environments of Africa – Geology and climate history*. Penn. State College of Earth and Mineral Sciences, [Online]. Available: http://courseware.e-education.psu.edu/courses/earth105new/content/home.html

AUTHORS BIOS AND PHOTOGRAPHS

Kant E. Kanyarusoke received his 1st class honours BSc. Eng. degree from Makerere University, Uganda in 1982, a MSc. (Mech. Eng.) from University of Lagos, Nigeria in 1985 and a cum laude PG HDHET from CPUT in 2009. He is now a doctoral candidate in Mechanical Engineering at CPUT. A member of ASHRAE, he has about 20 years industrial experience in Chemicals, Foods and Beverages factories and in small scale industrial setups in several sub-Sahara African countries. He has an almost equal number of years in university teaching and engineering education. He now lectures Machine Design and Thermodynamics and supervises PG solar engineering students at CPUT.

Jasson Gryzagoridis Pr. Eng. BSc, MSc, PhD is a registered professional engineer, and holds degrees from Lamar University, Texas A&M University and the University of Cape Town respectively. He is an Adjunct Professor acting as post graduate student's mentor at the Mech. Eng. Department at Cape Peninsula University of Technology (CPUT).

Presenting author: Kant E. Kanyarusoke

7.4 Concluding the chapter

This chapter presented the functionality of the designed, constructed - and now patented - solar tracking device. Within the limitations of experimental work and conditions at one site within the target SSA region, it also attempted to guess how functional the device would be in some of the other areas. The overall energy consumption in the fully automatic version of the device in these experiments was small at 3.7% of the gain. This is 1.26% of the fixed panel's yield and 0.94% of the tracking panel's. However, it would appear that in other seasons - such as rainy winter – the consumption might be above 1%.. Similarly, in some regions of the continent such as the Congo basin or along the West African coastline, it is highly likely that consumption will exceed 1% of production from a 90 Wp panel. The energy consumption therefore needs closer scrutiny - especially under windy and cloudy conditions before commercialisation. For now, the product works 'well' and has been in operation since July 2015. In the next – and concluding - chapter of the thesis, an indication of development costs is given.

CHAPTER EIGHT

THESIS CONCLUSIONS

8.0 Introduction

This chapter starts with a quick summary of the work reported. A description of achievements follows in section 8.2, where engineering and technical achievements can satisfactorily be supported with concrete evidence. Subsequent developments of the work could be expected to yield benefits in the socio-economic area. An attempt to predict economic and commercial benefits from development materials and processes cost data in the work is made in sections 8.3 and 8.4. The penultimate section outlines further R & D work necessary to build on what is in this report so as to almost fully address SSA's rural home energy needs using solar energy.

8.1 Work reported

This work was motivated by observation of energy poverty in a region with a rapidly growing population (2.6% annual growth rate) and an expanding middle class. The energy problem was more to do with conversion, transmission and distribution to largely rural and dispersed population areas (forming over 80% in most countries of the region). These factors combine in some countries to make universal access to electric grid supply a virtual impossibility now and in the near future.

However, there is an abundant solar resource throughout the year, owing to tropical location either side of the equator. Within the region, the lowest recorded annual resource level on a horizontal surface is about 1500 kWh/m^2 in parts of the Congo River basin while most of the rest receives well in excess of 2100 kWh/m^2. To the researcher, this availability and reliability motivated efforts to attempt to simplify and enhance solar energy harnessing with an expectation that 'modern energy' access could more easily be achieved throughout the region.

The work scope was delimited to a manageable level allocated for part time doctoral studies: i.e. covering small distributed standalone PV and SS systems. Consequently, the following areas were investigated and acted upon.

8.1.1 *Solar resource estimation*

After reviewing various estimation methods, the traditional ASHRAE method was used in a conference paper (Kanyarusoke et al. 2012) to do a preliminary study. Later, the versatile TRNSYS – was used to estimate both the resource availability and the PV panel yields in the region.

8.1.2 *Innovations*

A series of technical innovations for flat plate panels/collectors were developed. These included the two azimuths installation for tropical areas – and their associated changeover dates

guidelines; the optimised panel slopes and pictorial equipment selection guides to meet the most basic energy requirements by homes starting to emerge from energy poverty in the region. The most important innovation in this work was the invention of a hydro mechanism that was deployed in a novel, inclined non polar axis solar tracking device.

8.2 Achievements of the work

The accomplishments of this work can be grouped into 3 categories: *Direct Engineering/Technical*: *Purely academic*; and *By-products* of the work. They are summarised as follows:

8.2.1 *Direct Engineering/Technical achievements*

- Introduction of a two azimuths installation for flat collectors in tropical areas. Traditionally, it had been that fixed slope installations on one side of the equator were effected to face the equator. This study found that this arrangement does not maximise annual energy yields in tropical areas. Rather, more energy could be harnessed from the sun if at certain times of the year, the panel/collector was made to face away from the equator. This led to a two azimuths installation. Two methods of achieving this installation were suggested. Moreover, throughout the tropical region, the changeover dates were computed and presented on maps.
- Introduction of optimised PV equipment selection guides for energy poor homesteads for the whole of SSA. Basic energy requirements for such homes were scientifically analysed. It was determined that each rural mid-class home required about 500 Wh or 42 Ah at 12 V mainly to meet the standardised needs of lighting. Equipment selection guides were presented in map form because these were considered easier and more convenient to use by the target audience, than alpha-numeric presentations.
- A novel gravity-operated and hydro-mechanically regulated inclined axis solar tracker. A review of available solar trackers found that they were largely unsuitable for domestic applications in SSA. Therefore, a solar tracker – in manual, semi and fully automatic versions was designed, constructed, tested and patented for the university. The fully automatic unit increased energy yield by 34% had an energy consumption of 0.94% of that generated when running a 90 Wp PV panel in Cape Town's summer conditions. This meant that just below 4% of the gain accorded by the tracker was self-consumed.

8.2.2 *Purely Academic achievements*

These were in form of: a patent, journal papers and conference papers as lead author and/or presenter.

- Patent – **1** South African provisional patent (January 2016)
- Journal papers – **4** journal papers as follows: 4 published (2013, 2015a, 2015b, 2016a).

- Conference papers – 5 conference papers as follows: 2 published internationally (2012b, 2016b); 2 presented - and presentations published (2012a, 2014); 1 presented internationally (2015c).

8.2.3 *By-products from the work*

These were mainly in the form of both Masters Students' projects and some solar energy engineering products.

- Masters projects – 3 MTech. Students' projects as follows: 1 graduated (Mbadinga, 2015) - Solar assisted rural water purifier. 1 completed and marked: to graduate cum laude, September 2016 (Obiang, 2016); 1 in progress (Alkelani, 2016) – Solar assisted high temperature refrigeration for a small rural fruit farmer.
- Other products – A solar crop dryer as a byproduct of 'rejected solutions' in Figure 7.1.

8.3 Cost considerations and commercial aspects of the work

This section outlines non-technical benefits that could possibly accrue if the innovations in this work were taken up on a large scale. In terms of costs, it is not possible to tell with certainty what will happen after adoption. However, the development materials that went directly into the products are given only as a first step in illustrating how total costing would be evaluated if other data were available.

8.3.1 *Example baseline costing of a fixed slope PV system in the region*

In this section, costs of a newly installed fixed slope system in Kyegegwa, Uganda (nearest weather station – Mbarara: June 2016) are given. Although the panel, LED bulbs, and charge controller were sourced from South Africa (freight was free of cost), local availability of solar panels and other components even at district level made delivered costs comparable irrespective of source. Table 8.1 gives the cost breakdown while Figure 8.2 shows the installation in progress.

Table 8.1: Capital costs of a 200 Wp PV system at Kyegegwa: near Mbarara: 637020, Uganda

Item	Description	Quantity	Unit cost (US$ Equiv.)*	Amount (US$ Equiv.)	Comment
PV Panel - 200 Wp; 12 V polycrystalline silicon panel		1	141.60	141.60	From South Africa
Charge Controller - 15 A MPPT		1	120.00	120.00	From South Africa
LED Bulbs - 5.5 W, 12 V LED bulbs; 480 Lumen		12	7.00	84.00	From South Africa
Battery - 12 V; 105 Ah deep cycle with min. allowable charge of 30%		2	121.21	242.42	From Uganda
Wires/switches/isolators etc. - Assorted lot		1	67.00	67.00	From South Africa
Installation labour				30.00	Labour - self with 2 assistants but here valued at market rate
Total installed cost (US$ Equiv.)				**685.02**	

* Prices differ from those in chapter 4 because of time differences. These are June 2016 prices when 1 US$ ≈15.00 ZAR ≈ 3300 UShs.

PUTTING UP THE 200 Wp PANEL | PANEL AT 5 DEG SLOPE, 0 DEG AZIMUTH | WORKING INSIDE NEWLY CONSTRUCTED ROOF

Figure 8.2: Typical rural village house trying to emerge from energy poverty using work of chapter 4.

This demonstrates that it is possible to implement recommendations of chapter 4 on fixed slope units within US$ 700 for a 200 Wp system in Uganda. This cost is US$ 100 lower than the 2012 estimate of US$ 800. (Kanyarusoke et al., 2012:223-255).

8.3.2 *Capital cost of solar tracking*

In this section, a summary of direct costs incurred in construction of the invented solar tracker is given in its 3 variants. Table 8.2 on page 154 gives the detailed costs.

In summary, the materials in the 3 variants cost about US$ 270, 240 and 200 for the fully automatic, semiautomatic and fully manual. These direct material costs could be reduced in reengineered products for commercial purposes. It is not meaningful at this stage to comment on other costs – as those would vary from country to country and from one business organisation to another.

8.3.3 *Life cycle costing comparisons between fixed and tracking PV panel systems using the Net Present Value (NPV) method*

Using actual costs of the fixed slope installation in Table 8.1 and the development direct material costs of Table 8.2, a ‘pointer’ towards the relative unit energy cost of the two systems might be made. Appendix A4 developes the ‘pointer’ for a place in Uganda which used the materials of Table 8.1 in Figure 8.2. Table 8.3 gives the summary of the costs from the appendix.

These values show that the unit energy cost from a fixed panel might be lower than that from a smaller but equivalent solar tracking panel even before non material costs are added for the tracking units. A question therefore arises on whether tracking is worth the additional effort and cost. To satisfactorily answer this question, one needs to examine the detailed hourly energy yields in chapter 7. This is discussed among ‘potential benefits’ in the next section.

Table 8.2: Direct material costs for development of 3 variants of the gravity driven hydro-mechanical solar tracker

			Fully Automatic Variant		Semi-automatic Variant		Manual Variant	
	ITEM DESCRIPTION	UNIT COST (US$) Equiv.	Qty.	Amount (US$ Equiv.)	Qty.	Amount (US$ Equiv.)	Qty.	Amount (US$ Equiv.)
1	Bladder 1 mm latex	12.57	1	12.57	1	12.57	1	12.57
2	Hooke coupling - 25 mm	5.83	1	5.83	1	5.83	1	5.83
3	Shaft - 2 m X 25 mm X 2 mm Al. piping	5.56	1	5.56	1	5.56	1	5.56
4	Shaft bearings - SKF 6205	4.75	2	9.50	2	9.50	2	9.50
5	Gear - Steel spur, 3 mm module X 30 teeth X15 mm	4.75	1	4.75	1	4.75	1	4.75
6	Rack - Steel spur, 3 mm module X 30mm wide X 330 X mm long	4.75	1	4.75	1	4.75	1	4.75
7	Piston & piston rod - PVC 160 mmØ X 200 mm	27.50	1	27.50	1	27.50	1	27.50
8	Piston rod bearings – SKF 6205	4.75	4	19.00	4	19.00	4	19.00
9	Housing - PVC piping 200mm Ø X 990 mm	8.33	1	8.33	1	8.33	1	8.33
10	Pump 12 V DC 10.8 W 4 m head	83.33	1	83.33	0	0.00	0	0.00
11	Solenoid valve - 5 A 19 mm Ø	14.25	1	14.25	2	28.50	0	0.00
12	1-way valve - 20 mm PVC	5.83	1	5.83	1	5.83	0	0.00
13	Manual valve - 20 mm PVC	1.67	0	0.00	0	0.00	1	1.67
14	Timers	5.13	2	10.27	2	10.27	0	0.00
15	Lot of Fittings & Consumables	25.00	1	25.00	1	25.00	1	25.00
16	Discharge tank – 10 litre PVC	4.00	1	4.00	1	4.00	1	4.00
17	Elevated tank – 100 litre PVC	10.00	0	0.00	1	10.00	1	10.00
18	Mechanism Stand – Steel frame 200 mm high	6.67	1	6.67	1	6.67	1	6.67
19	Elevated tank stand - Steel frame 3.5 m high	33.33	0	0.00	1	33.33	1	33.33
20	Capillary tube/ Orifice	5.20	0	0.00	0	0.00	1	5.20
	Subtotal			**247.13**		**221.39**		**183.66**
	Other costs (Misc.)			24.71		22.13		18.37
	Grand total delivered cost (US$)			**271.85**		**243.53**		**202.02**

Table 8.3: Approximate energy cost comparisons between Fixed and Tracking panel using different versions of the solar tracker (see Appendix A4 for full development)

	FIXED SLOPE	MANUAL TRACK	SEMI AUTO	FULLY AUTO
SOLAR PANEL REQUIRED (Wp)	200	150	150	150
TOTAL 'POSSIBLE' ELECTRICITY IN 25 YEARS (kWh)	6568	6600	6600	6600
CAPITAL COST (excluding non material tracker costs) (US$)	**685.02**	**856.64**	**903.15**	**931.47**
PRESENT VALUE 25 YEAR OPERATING COST (US$)	527.58	527.58	527.58	527.58
PRESENT VALUE 25 YEAR MAINTENANCE COST (US$)	406.12	507.87	535.45	552.24
PRESENT VALUE RUNNING UNIT ENERGY COST (US$/kWh)	**0.14**	**0.16**	**0.16**	**0.16**
PRESENT VALUE TOTAL UNIT ENERGY COST (US$/kWh)	**0.25**	**0.29**	**0.30**	**0.30**

8.4 Potential benefits from the work

There are non-cost related benefits of the work. In PV systems, they include ability to harness solar energy at times it may be most useful for some day applications; similarly in solar thermal systems, extended solar energy harnessing times to mornings and evenings mean greater usability of the total system; social-economic benefits could include commercialisation, local manufacture and concomitant employment creation for both skilled and unskilled labour.

8.4.1 *Electric energy yield improvement from solar tracking when most needed*

In Figure 7.8 of the last chapter, it is seen that gain ratios in mornings and evenings far exceed the averaged 1.34 for the entire period, by factors of up to 3 in some periods. This means simply increasing the fixed panel capacity by 34% - though increasing annual yields by a similar ratio – does not provide the necessary energy output for activities that may be required in the said times. Examples of these activities can include morning and late afternoon water pumping for watering plants and animals in dry seasons. Direct connection to the PV panel (i.e. bypassing the charge control system) in a smaller solar tracked system would improve the system capacity utilisation ratio as discussed in section 4.4.4.2 with little to no impact on the night energy requirements.

It is also important to note that for a system already in place, such as an old 150 Wp panel in this case, adding a new 50 Wp panel does not necessarily give the expected 200 W at the cost of the extra panel. This is because of at least two reasons. First, the 150 Wp panel will have deteriorated in performance depending on its age and on environmental factors. Secondly, because the panels are of different ratings, they may not be connected in parallel – meaning that the new one will need its own charge controller, and probably additional battery storage. Hence, the additional costs to get to 200 Wp equivalent cannot simply be that of the new panel. A series connection between the panels may not even be contemplated because that changes the input voltage at the charge controller and also increases the probability of system failure. Both of these problems are avoided with use of a tracker. A look at Figure 7.9 shows that the tracker increases energy yield without affecting either the day's peak voltage or peak current. Hence, there is no need to change the controller in that case.

In summary therefore, it may be said that although Table 8.3 is indicative of a more costly tracking option, that may be true for completely new systems. When energy demands on an existing system increase by modest amounts (in this case up to 34%) it may be worthwhile not to dismiss tracking as a means to meeting the extra demand.

8.4.2 *Improvements in ST gains and utilisation*

Whereas the foregoing discussions have been on PV systems, the situation would be different for ST systems. Addition of energy collection area for these in lieu of tracking would

necessarily have to involve work on the energy storage system as well (e.g. more tubes on the collector mean longer horizontal tank). This significantly increases the effective cost of the additional area, increasing the likelihood that a smaller solar tracking unit will be more cost effective. Together with ability to harness the energy for much longer times, this would make the solar tracking alternative much more attractive from energy cost, quality and quantity points of view.

8.4.3 *Socio-Economic benefits*

The materials and processes used in manufacture and assembly of the innovation units are simple and readily available in most countries. Moreover, they could be suitably substituted by local alternatives as follows:

- Aluminium parts and frame – steel/galvanised iron, suitably treated timber.
- Gear materials – plastic, timber.
- Latex for the bladder – papaya latex, plastic film, suitably treated canvas, suitably treated leather or even in extreme cases, suitably treated slaughtered animal bladders.

Skills employed would include:

- Mechanical fitting and machining
- Simple dc electrical wiring
- Tailoring

Non specialist skilled workers would be involved in making of bladders by straightforward painting on a pattern – as was done in this project.

8.5 Closure

This thesis looked at the energy paradox in SSA: where there were plenty of different energy resources, yet minimal per capita accessibility to modern energy forms. The researcher argued the case that to tackle this paradox in an urgent and feasible way, it was necessary to exploit a universally available energy resource at home level. This resource was solar energy; it required simple technologies to harness; it was safe; it needed no transmission/distribution; it had no legal or social issues; it needed permission from no one – and as at now in the region, it is by far more viable to acquire at home level than grid supply or any other form. That aside, it is clean; it improves health in homesteads and has a positive impact on the environment - as less plant material is harvested for firewood and charcoal.

Obvious as the above advantages of solar energy harnessing may be, the issue in the thesis was to suggest region-appropriate improved means of harnessing the resource. Thus, innovations in collection and solar tracking were made and tested.

APPENDICES

A1: TRNSYS FILES FOR CAPE TOWN AND MBARARA (CHAPTERS 3, 4, 8 & 9)

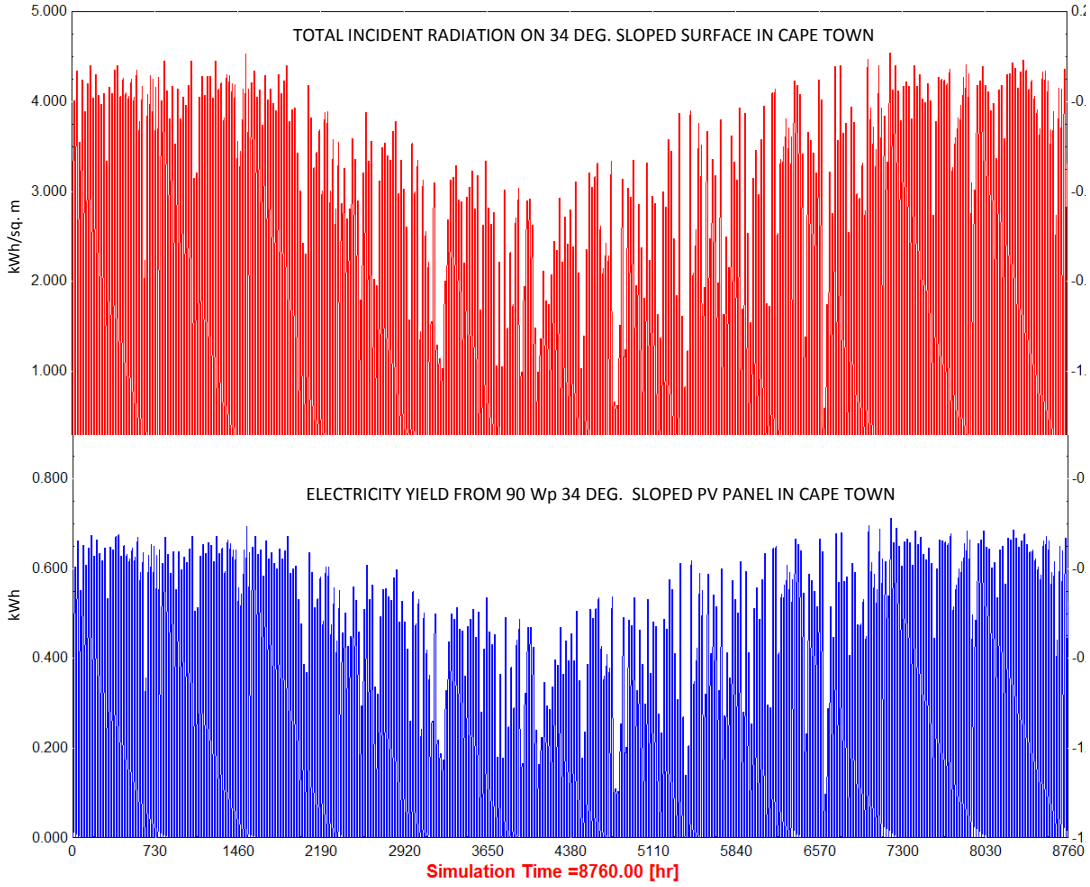

Figure A1.1: TRNSYS Source file results for Figure 3.5

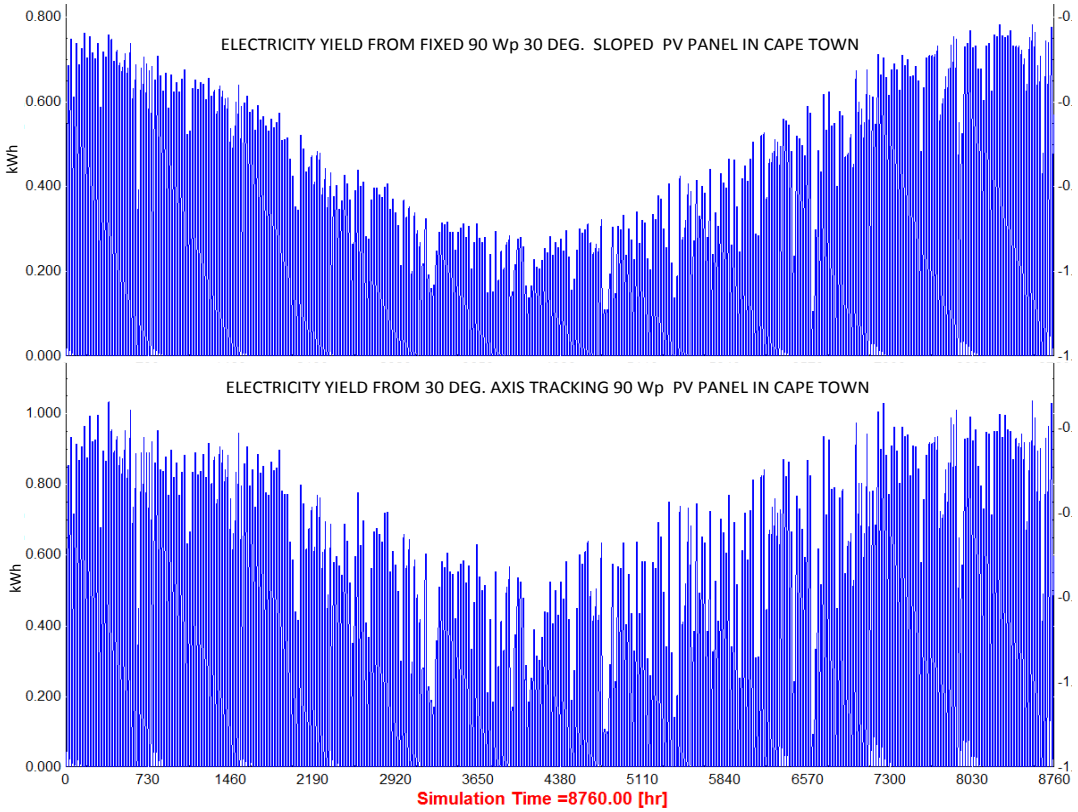

Figure A1.2: TRNSYS Source file results for Figure 7.10

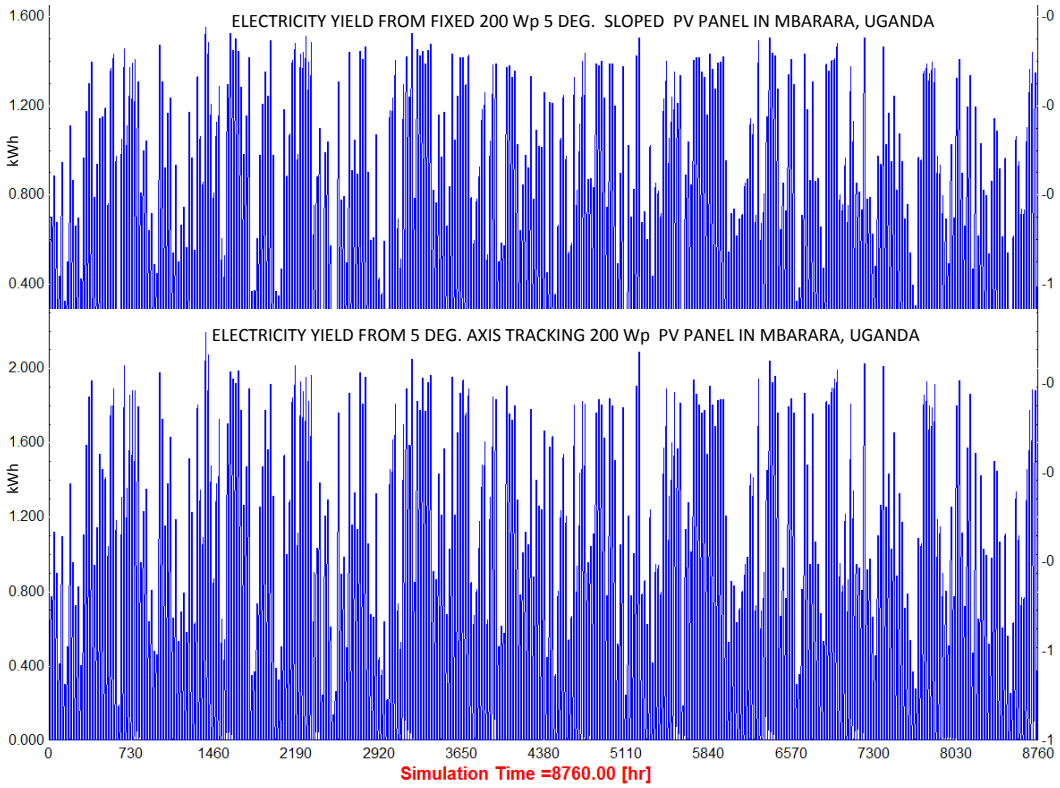

Figure A1.3: TRNSYS Source file results for Figure 4.5 & Section 8.3.3

A2: MATLAB® PROGRAMS (CHAPTER 7)

A2.1 *Script for determining the 4 standard parameters of a PV panel from its manufacturer's specification* (TABLE I ch.7): (This script gives n, R_1 and I_{Lstd} directly but I_{0std} has to be estimated separately from an EXCEL spread sheet because of its small value).

```
Vo=22.4; Is=5.5; Im=4.9; Vm=18.4; % These are manufacturer specs at
reference conditions
f1=Is/Im; f3=Im/Vm;
Ns=36; %This is the number of cells connected in series in the panel
a=0.926; err1=1; diff2=1;
while ((abs(diff2)>0.15)||(abs(err1)>0.15))&&(a<2)
a=a+0.0001; R1=0.100; diff1=1;eo=exp(Vo/a);
while (abs(diff1)>0.15)&&(R1<0.8200)
    R1=R1+0.0001;em=exp((Vm+Im*R1)/a);es=exp(Is*R1/a);
    f2=(1-em/eo)/(1-es/eo);
    diff1=f1-f2;
end
err1=diff1;
f4=Im/((a*eo/em-1)+Im*R1);
diff2=f3-f4;
end
if ((abs(diff1)>0.15)+(abs(diff2)>0.15))>0
    disp('No solution');
else
    ILm=Im/(1-em/eo); ILs=Is/(1-es/eo);
    IL=[ILm ILs];Io=IL/eo;
    n=a*11600/(Ns*298.13);
    disp([n R1 ILm ILs])
end
```

A2.2 *Function to use in computing the optical efficiency through a panel glazing (will be useful in A2.3 and A2.4)*

```
function y=opteff1(in,K,x,ref) %function definition
% opteff1(in,K,x,ref)     helps work out the multiplier for incident
%                       radiation in the process of computing the
% optical efficiency of a glazing defined by a characteristic
% extinction rate 'Kx', a refractive index 'ref' when the angle of
% incidence is 'in' degrees. First it computes the refraction angle
% 'r' from Snell's law. Then it computes the effect of glazing
% thickness and extinction coefficient. This is influenced by the
% angle r. So we get exp -Kxsecr. Finally, the incident angle effect
% is computed by the sin and tangent functions of r and in.
r=asind(sind(in)/ref);a=2.72.^(-K*0.001*x*secd(r)); b=(sind(r-
in)).^2./(sind(r+in+(sind(r+in)==0)*0.0001).^2);
c=(tand(r-in)).^2./(tand(r+in+(tand(r+in)==0)*0.0001).^2); y=a.*(1-
0.5*(b+c));
```

A2.3 *Script for PV energy yield from fixed panel using actual weather data* (SECTION 7.3.4.3: 'Using the weather data')

```
rhog=0.20;% Ground reflectivity; can be varied depending on
conditions
geog=[-33.932 -18 68.5 -15];
L=geog(1); Long=geog(2); h=geog(3);
Longt=geog(4);MJdayh=zeros(40,1);MJdayn=zeros(40,1);
```

```
Ren=[];
k=sum(Ren(:,1)>0);%This gives the day's results (Ren)from the data
logger and the number of daylight readings, k.
n=Ren(:,1);time=Ren(:,2);Gh=Ren(:,3);Gd=Ren(:,4); Ta=Ren(:,5);
vw=Ren(:,6); mfix=Ren(:,8);
dayminutes=15*k;t=time-0.5*dayminutes;
delta=23.45*sin(2*pi*(284+n)/365); %declination angle in degrees
Bdeg=360*(n-1)/365; %Spencer's correction angle due to variable earth
orbital speed
G0=1367*(1.000110+0.034221*cos(pi*Bdeg/180)+0.001280*sin(pi*Bdeg/180)
+0.000719*cos(pi*Bdeg/90)+0.000077*sin(pi*Bdeg/90));
%Extraterrestrial radiation in kW/m2
E=229.2*(0.000075+0.001868*cos(pi*Bdeg/180)-
0.032077*sin(pi*Bdeg/180)-0.014615*cos(pi*Bdeg/90)-
0.04089*sin(pi*Bdeg/90)); %Equation of time in min. due to earth
orbit perturbations

alpha=asind(cos(pi*L/180)*cos(pi*delta/180).*cos(pi*t/720)+sin(pi*L/1
80)*sin(pi*delta/180));% Defines solar altitude
z=90-alpha;cosine=cos(pi*z/180)+(cos(pi*z/180)==0)*0.0001;%This
avoids dividing by zero at z=90deg.
mair=(exp(-0.0001184*h))./((cosine+0.50572*(96.07995-
z.*(z<96.07995)).^(-1.6364))); %This gives the apparent air mass
accounting for altitude as well
Gbh=Gh-Gd; Gbn=Gbh./cosine;
e=1+Gbn./(Gd.*(1+5.535*10^(-6).*z.^3));% This is the Perez clearness
parameter at a given time
del=mair.*Gd./G0; %This is the Perez brightness parameter at a given
time;
if e<1.065, f=[-0.008 0.588 -0.062; -0.060 0.072 -0.022];
elseif e<1.230, f=[0.130 0.683 -0.151; -0.019 0.066 -0.029];
elseif e<1.500, f=[0.330 0.487 -0.221; 0.055 -0.064 -0.026];
elseif e<1.950, f=[0.568 0.187 -0.295; 0.109 -0.152 0.014];
elseif e<2.800, f=[0.873 -0.392 -0.362; 0.226 -0.462 0.001];
elseif e<4.500, f= [1.132 -1.237 -0.412; 0.288 -0.823 0.056];
elseif e<6.200, f=[1.060 -1.600 -0.359; 0.264 -1.127 0.131];
else f=[0.678 -0.327 -0.250; 0.156 -1.377 0.251];
end; % These are the Perez brightness coefficients for an anisotropic
sky
F1=max(0,(f(1)+del*f(1,2)+z*pi*f(1,3)/180));
F2=f(2)+del*f(2,2)+z*pi*f(2,3)/180;
gamas=sign(t).*abs(acosd((cosine*sin(pi*L/180)-
sin(pi*delta/180))./(sin(pi*z/180)*cos(pi*L/180))));
beta1=30;
iangle=acosd((cosine.*cos(pi*beta1/180)+sin(pi*z/180)*sin(pi*beta1/18
0).*cos(pi*(180-gamas)/180)));
% incidence angle in terms of solar azimuth, gamas and inclination
angle beta for fixed well installed panel
% with panel azimuth, gama = 0 or 180 if north facing.
a=max(0,cos(pi*iangle/180)); b=max(cos(pi*85/180),cosine);%a and b
define effects of cone circumsolar
%incidence angles on inclined panel and horizontal plane
respectively.
Rb=(cosd(iangle).*(iangle<90))./cosine;
Gpanel=max(Gbh.*Rb+Gd.*(1-
F1)*0.5*(1+cos(pi*beta1/180))+Gd.*F1.*a./b+Gd.*F2*sin(pi*beta1/180)+G
h*rhog*0.5*(1-cos(pi*beta1/180)),0);


panel=[3.2, 1.0, 0.84, 0.845, 0.035, 3.93, 1.526];
```

```
xg=panel(1); kg=panel(2);eg=panel(3); trg=panel(4); ag=panel(5);
Kg=panel(6);refg=panel(7);
%These 7 inputs define the characteristics of the panel top cover
glazing.
%Next we input the cell characteristics
cell=[0.935823, 0.054289, -0.008677, 0.000527,-0.000011];
c0=cell(1); c1=cell(2); c2=cell(3); c3=cell(4); c4=cell(5);
mountm=[-3.47    -0.0594     3
       -2.98     -0.0471     1
       -3.56     -0.075      3
        -2.81    -0.0455     0
       -3.58     -113        3
       -3.23     -130        13];
mount=mountm(3,:);
aprime=mount(1); bprime=mount(2); delT=mount(3);
% Now enter panel dimensions:
Pdims=[1.207, 0.541];
Len=Pdims(1); Wid=Pdims(2); Lc=2*Len*Wid/(Len+Wid);
%Next we enter the manufacturer's data.
%First state or enter the panel electrical specs:(max power at cell
temp.
%of 25; size of individual cell (m square); No. of cells; negative
max. power efficiency temp. coeff; and reference optical efficiency
and panel irradiance during factory tests.

 Vmp25 = 18.4; Imp25 = 4.90; celsize = 0.125; Ns =36; amp = 0.0046;
opteff25 = 0.92; Gpanel25 = 1000;
Apanel=Ns*celsize^2; W25 = Vmp25*Imp25; Isc25 = 5.50; Voc25 = 22.4;
av = -0.079; ai = 0.00155;
% The above is data given by the manufacturer. Below is the derived
data for the panel's characteristic equation at 25oC.
I025 = 1.721e-10; IL25 = 5.5; R1 = 0.1001; na = 1.001; an25 =
na*0.92527;
%The following are the dynamic variables of the panel installation:
%namely, ambient, back and cell temperatures; incident radiation in
its various forms - beam, circumsolar, sky or isotropic diffuse,
ground reflected and horizon brightening especially at sunrise and
sunset.


Tb=Ta+Gpanel.*exp(aprime+bprime.*vw)/1000;Tc=Tb+273.15+Gpanel*delT/10
00;
%back and cell temperatures of panel
Mprime=c0+c1*mair+c2*mair.^2+c3*mair.^3+c4*mair.^4;
isk=59.7-0.1388*abs(beta1)+0.001497*beta1^2; ig=90-
0.5788*abs(beta1)+0.002693*beta1^2;
Gc1=max(Mprime.*(Gbh.*Rb+Gd.*F1.*a./b).*opteff1(iangle,Kg,xg,refg),0)
;
Gc2=max(Mprime.*(Gd.*(1-
F1)*0.5*(1+cos(pi*beta1/180))+Gd.*F2*sin(abs(pi*beta1/180))).*opteff1
(isk,Kg,xg,refg),0);
Gc3=max(Mprime.*Gh.*rhog*0.5*(1-
cos(pi*beta1/180)),0).*opteff1(ig,Kg,xg,refg);
opticleff=min((Gc1+Gc2+Gc3)./(Gpanel+(Gpanel==0).*((Gc1+Gc2+Gc3))),1)
;%Eliminate division by zero and efficienies higher than 1.

%Now compute the efficiencies and anticipated max. power output from
the panel per square metre.

Eff25 = W25/(Gpanel25*Apanel*opteff25);
```

```
I0Tc = I025*(Tc/298.15).^3.*exp(47.04822-14027.427./Tc);
    IL = (opticleff.*Gpanel).*(IL25+ai.*(Tc-298.15))/(1000*opteff25);
    an = an25*Tc/298.15;
WTime=zeros(k,1); opticleffTime=zeros(k,1);EffTime=zeros(k,1);
    s=0;
for Time=1:k,
    s=s+1;
    mult=mfix(s);

ILTime=IL(s);I0TcTime=I0Tc(s);anTime=an(s);opticleffTime=opticleff(s)
;
    GpanelTime=Gpanel(s);TcTime=Tc(s);     treemax=50;% Search for
maximum power point between 0.30IL(s) and 0.98IL(s)
voltage=zeros(treemax,1);Watts=zeros(treemax,1);current=zeros(treemax
,1);
I=0.30*ILTime;
for tree=1:treemax,
    I=I+0.01*ILTime;
    V=anTime*log((ILTime-
I+0.00001*(ILTime==0))/(I0TcTime+0.00001*(I0TcTime==0)))-I*R1;
    current(tree)=I;
    voltage(tree)=V;
    Watts=current.*voltage;
    Power=[current, voltage, Watts];
end;
WTime(s)=max(Power(:,3))*mult;
EffTime(s)=WTime(s)/(opticleffTime.*GpanelTime*Apanel+0.00001*((optic
leffTime*GpanelTime)==0));
out=[WTime, EffTime];
end
Dayout=[n time Gpanel Tb WTime EffTime];
Wpanel=Gpanel*Apanel;
MJdaypanel=0.06*Apanel*trapz(time,Gpanel);
MJdayelectric=0.06*trapz(time,WTime);
dayeff=MJdayelectric/MJdaypanel;
Dayperf=[MJdaypanel/3.6 MJdayelectric/3.6];
disp(Wpanel)
plot(time,Gpanel*Apanel,time,WTime)
```

A2.4 *Script for PV energy yield from inclined axis solar tracking panel using actual weather data* (SECTION 7.3.4.3: 'Using the weather data')

```
rhog=0.20;% Ground reflectivity; can be varied depending on
conditions
geog=[-33.932 -18 68.5 -15];% These are the geographic coordinates of
the site and its standard time correction longitude
L=geog(1); Long=geog(2); h=geog(3;
Longt=geog(4);MJdayh=zeros(40,1);MJdayn=zeros(40,1);
Ren=[];% This is a matrix of daily results from the data logger
k=sum(Ren(:,1)>0);%This gives the day's results (Ren)from the data
logger and the number of daylight readings, k.
n=Ren(:,1);time=Ren(:,2);Gh=Ren(:,3);Gd=Ren(:,4); Ta=Ren(:,5);
vw=Ren(:,6); phi=Ren(:,7); mtrack=Ren(:,9);
dayminutes=15*k;t=time-0.5*dayminutes;
delta=23.45*sin(2*pi*(284+n)/365); %declination angle in degrees
Bdeg=360*(n-1)/365; %Spencer's correction angle due to variable earth
orbital speed
G0=1367*(1.000110+0.034221*cos(pi*Bdeg/180)+0.001280*sin(pi*Bdeg/180)
+0.000719*cos(pi*Bdeg/90)+0.000077*sin(pi*Bdeg/90));%Extraterrestrial
radiation in kW/m2
```

```
E=229.2*(0.000075+0.001868*cos(pi*Bdeg/180)-
0.032077*sin(pi*Bdeg/180)-0.014615*cos(pi*Bdeg/90)-
0.04089*sin(pi*Bdeg/90)); %Equation of time in min. due to earth
orbit perturbations

alpha=asind(cos(pi*L/180)*cos(pi*delta/180).*cos(pi*t/720)+sin(pi*L/1
80)*sin(pi*delta/180));% Defines solar altitude
z=90-alpha;cosine=cos(pi*z/180)+(cos(pi*z/180)==0)*0.0001;%This
avoids dividing by zero at z=90deg.
mair=(exp(-0.0001184*h))./((cosine+0.50572*(96.07995-
z.*(z<96.07995)).^(-1.6364))); %This gives the apparent air mass
accounting for altitude as well
Gbh=Gh-Gd; Gbn=Gbh./cosine;
e=1+Gbn./(Gd.*(1+5.535*10^(-6).*z.^3));% This is the Perez clearness
parameter at a given time
del=mair.*Gd./G0; %This is the Perez brightness parameter at a given
time;
if e<1.065
    f=[-0.008 0.588 -0.062; -0.060 0.072 -0.022];
elseif e<1.230
    f=[0.130 0.683 -0.151; -0.019 0.066 -0.029];
elseif e<1.500
    f=[0.330 0.487 -0.221; 0.055 -0.064 -0.026];
elseif e<1.950
    f=[0.568 0.187 -0.295; 0.109 -0.152 0.014];
elseif e<2.800
    f=[0.873 -0.392 -0.362; 0.226 -0.462 0.001];
elseif e<4.500
    f= [1.132 -1.237 -0.412; 0.288 -0.823 0.056];
elseif e<6.200
    f=[1.060 -1.600 -0.359; 0.264 -1.127 0.131];
else
    f=[0.678 -0.327 -0.250; 0.156 -1.377 0.251];
end; % These are the Perez brightness coefficients for an anisotropic
sky
F1=max(0,(f(1)+del*f(1,2)+z*pi*f(1,3)/180));
F2=f(2)+del*f(2,2)+z*pi*f(2,3)/180;
gamas=sign(t).*abs(acosd((cosine*sin(pi*L/180)-
sin(pi*delta/180))./(sin(pi*z/180)*cos(pi*L/180))));

AxiSlope=30;AxiAzimuth=0;
beta=acosd(cosd(AxiSlope)*sind(phi));%This gives the slope of the
panel surface at any position if its axis of rotation is in the
meridian plane
%i.e zero axis azimuth.
tan=1+(tand(phi-0.001*(phi==90)).*sind(AxiSlope)).^2;
%This avoids infinity at phi=90 deg.

gama=(180+acosd((1-1./tan).^0.5)).*(t<=0)+(180-acosd((1-
1./tan).^0.5)).*(t>0);

iangle=acosd((cosine.*cosd(beta)+sind(z).*sind(beta).*cosd(gama-
gamas)));
% incidence angle in terms of solar azimuth, gamas and panel oslope
beta
%and azimuth gama.

a=max(0,cosd(iangle)); b=max(cosd(85),cosine);%a and b define
%effects of cone circumsolar incidence angles on inclined panel and
%horizontal plane respectively.
```

```
Rb=(cosd(iangle).*(iangle<90))./cosine;
Gpanel=max(Gbh.*Rb+0.5*Gd.*(1-
F1).*(1+cosd(beta))+Gd.*F1.*a./b+Gd.*F2.*sind(beta)+0.5*rhog*Gh.*(1-
cosd(beta)),0);


panel=[3.2, 1.0, 0.84, 0.845, 0.035, 3.93, 1.526];
xg=panel(1); kg=panel(2);eg=panel(3); trg=panel(4); ag=panel(5);
Kg=panel(6);refg=panel(7);
%These 7 inputs define the characteristics of the panel top cover
glazing.
%Next we input the cell
cell=[0.935823, 0.054289, -0.008677, 0.000527,-0.000011];
c0=cell(1); c1=cell(2); c2=cell(3); c3=cell(4); c4=cell(5);
mountm=[-3.47    -0.0594     3
       -2.98     -0.0471     1
       -3.56     -0.075      3
        -2.81    -0.0455     0
       -3.58     -113        3
       -3.23     -130        13];
mount=mountm(3,:);
aprime=mount(1); bprime=mount(2); delT=mount(3);
% Now enter panel dimensions and orientation:
Pdims=[1.207, 0.541];
Len=Pdims(1); Wid=Pdims(2); Lc=2*Len*Wid/(Len+Wid);


%Next we enter the manufacturer's data.
%First state or enter the panel electrical specs:(max power at cell
temp. of 25 deg. C; size of individual cell (m squared); No. of
cells; negative max. power efficiency temp. coeff; and reference
optical efficiency and panel irradiance during factory tests.

 Vmp25 = 18.4; Imp25 = 4.90; celsize = 0.125; Ns =36; amp = 0.0046;
opteff25 = 0.92; Gpanel25 = 1000;
Apanel=Ns*celsize^2; W25 = Vmp25*Imp25; Isc25 = 5.50; Voc25 = 22.4;
av = -0.079; ai = 0.00155;
% The above is data given by the manufacturer. Below is the derived
data
% for the panel's characteristic equation at 25oC.
I025 = 1.721e-10; IL25 = 5.5; R1 = 0.1001; na = 1.001; an25 =
na*0.92527;
%The following are the dynamic variables of the panel installation:
%namely, ambient, back and cell temperatures; incident radiation in
its various forms - beam, circumsolar, sky or isotropic diffuse,
ground reflected and horizon brightening especially at sunrise and
sunset.


Tb=Ta+Gpanel.*exp(aprime+bprime.*vw)/1000;Tc=Tb+273.15+Gpanel*delT/10
00;
%back and cell temperatures of panel
Mprime=c0+c1*mair+c2*mair.^2+c3*mair.^3+c4*mair.^4;
isk=59.7-0.1388*abs(beta)+0.001497*beta.^2; ig=90-
0.5788*abs(beta)+0.002693*beta.^2;
Gc1=max(Mprime.*(Gbh.*Rb+Gd.*F1.*a./b).*opteff1(iangle,Kg,xg,refg),0)
;
Gc2=max(0.5*Mprime.*(Gd.*(1-
F1).*(1+cosd(beta))+Gd.*F2.*sin(abs(beta))).*opteff1(isk,Kg,xg,refg),
0);
```

```
Gc3=max(0.5*rhog*Mprime.*Gh.*(1-
cosd(beta)),0).*opteff1(ig,Kg,xg,refg);
opticleff=min((Gc1+Gc2+Gc3)./(Gpanel+(Gpanel==0).*((Gc1+Gc2+Gc3))),1)
;%Eliminate division by zero and efficienies higher than 1.

%Now compute the efficiencies and anticipated max. power output from
the panel per square metre.

Eff25 = W25/(Gpanel25*Apanel*opteff25);
I0Tc = I025*(Tc/298.15).^3.*exp(47.04822-14027.427./Tc);
    IL = (opticleff.*Gpanel).*(IL25+ai.*(Tc-298.15))/(1000*opteff25);
    an = an25*Tc/298.15;
WTime=zeros(k,1); opticleffTime=zeros(k,1);EffTime=zeros(k,1);
    s=0;
for Time=1:k,
    s=s+1;
    mult=mtrack(s);

ILTime=IL(s);I0TcTime=I0Tc(s);anTime=an(s);opticleffTime=opticleff(s)
;
    GpanelTime=Gpanel(s);TcTime=Tc(s);     treemax=50;% Search for
maximum power point between 0.30IL(s) and 0.98IL(s)
voltage=zeros(treemax,1);Watts=zeros(treemax,1);current=zeros(treemax
,1);
I=0.30*ILTime;
for tree=1:treemax,
    I=I+0.01*ILTime;
    V=anTime*log((ILTime-
I+0.00001*(ILTime==0))/(I0TcTime+0.00001*(I0TcTime==0)))-I*R1;
    current(tree)=I;
    voltage(tree)=V;
    Watts=current.*voltage;
    Power=[current, voltage, Watts];
end;

WTime(s)=max(Power(:,3))*mult;
EffTime(s)=WTime(s)/(opticleffTime.*GpanelTime*Apanel+0.00001*((optic
leffTime*GpanelTime)==0));
out=[WTime, EffTime];
end
Dayout=[n time Gpanel Tb WTime EffTime];
Wpanel=Gpanel*Apanel;
MJdaypanel=0.06*Apanel*trapz(time,Gpanel);
MJdayelectric=0.06*trapz(time,WTime);
dayeff=MJdayelectric/MJdaypanel;
Dayperf=[MJdaypanel/3.6 MJdayelectric/3.6];
disp(Wpanel)
plot(time,Gpanel*Apanel,time,WTime)
```

A3: THE PATENT AND OTHER AUTHORED PAPERS

A3.1 The Patent documentation

COPY OF PROVISIONAL SPECIFICATION

Application No.	2015/09278
Filing Date	21 December 2015
Your Ref	
Our Ref	P72557ZP00
Name of Applicant(s)	CAPE PENINSULA UNIVERSITY OF TECHNOLOGY
Name of Inventor(s)	KANYARUSOKE, Kant Eliab GRYZAGORIDIS, Jasson
Title of Invention	A HYDRAULIC DRIVE MECHANISM
Completion Date	21 December 2016

A DRIVE MECHANISM

A & A Ref No: **P72557ZP00**

ADAMS & ADAMS
PATENT ATTORNEYS
PRETORIA

FORM P6

REPUBLIC OF SOUTH AFRICA
Patents Act, 1978

PROVISIONAL SPECIFICATION
(Section 30 (1) - Regulation 27)

21	01	OFFICIAL APPLICATION NO	22	LODGING DATE
				21 December 2015

71	FULL NAME(S) OF APPLICANT(S)

CAPE PENINSULA UNIVERSITY OF TECHNOLOGY

72	FULL NAME(S) OF INVENTOR(S)

1) KANYARUSOKE, Kant Eliab
2) GRYZAGORIDIS, Jasson

54	TITLE OF INVENTION

A HYDRAULIC DRIVE MECHANISM

FIELD OF INVENTION

This invention relates to a drive mechanism. It relates particularly, but is not necessarily limited to, a drive mechanism for displacing a solar collector device for solar tracking.

A3.2 Other peer reviewed papers (i.e. not included in this thesis)

A3.2.1 Conference papers

1. Kanyarusoke K. E., Gryzagoridis J., and Oliver G. (2012a). Issues in solar tracking for sub-Sahara Africa. *Proceedings of Southern African Solar Energy Conference.* Stellenbosch South Africa, 21-23 May 2012. (Presentation available on line: www.slideserve.com/nairi/issues-in-solar-tracking-for-sub-sahara-africa)
2. Kanyarusoke K. E., Gryzagoridis J., and Oliver G. (2012b). Predicting photovoltaic panel yields in sub-Sahara Africa. *Proceedings of International Conference on Engineering and Applied Science 2012* Beijing, China. pp. 223-255.
3. Kanyarusoke K. E., Gryzagoridis J., and Oliver G. (2014). Solar lighting and water preheating in Tropical African homes: What sustainable possibilities? Ontario International Conference on Sustainable Development, Richards Bay, South Africa 2nd-3rd December 2014. Presentation available online: https://www.youtube.com/watch?v=IQIANmDjsIE

A4: COMPUTATION OF ENERGY COSTS: AN APPROXIMATION

A4.1: DEVELOPMENT OF COSTING

The cost of electricity from the systems in this thesis – namely the optimised fixed slope 200 Wp panel and its equivalent inclined axis solar tracking 150 Wp panel – is estimated for a rural home near the equator in Uganda. Actual June 2016 prices of components are used in the estimates. The other data on the economy used is as follows:

General inflation rate i_r = 6% (based on long term value over the past 20 years)

Bank interst rate over inflation, i_b = 10% (based on a savings interest rate of 16% from Bank of Uganda)

Special item inflation rates over and above general rate were assumed as follows (ipdct):

Maintenance labour:	=	5%	Maint. cost rate	=	4% of initial capital
Batteries:	=	2.5%	Life	=	5 years
Charge controllers:	=	5%		=	15 years
LED bulbs:	=	-2.5%		=	15 years
System life expectancy	=	25 years;	Maintenance	=	1 year

For an item costing an amount ***C*** today, the present value cost after ***n*** years is given by the equation: (Blank & Tarquin 2012: 367-374).

$$C_n = C\left[\frac{1+i_r+i_{pdct}}{1+i_r+i_b}\right]^n \qquad \text{(A1)}$$

Also, the present value $\boldsymbol{E_n}$ of total annual expense ***E*** growing at a rate $\boldsymbol{r_p}$ over and above general inflation after ***n*** years is given as:

$$E_n = E\left[\frac{1+i_r+r_p}{r_p-i_b}\right]\left[\left[\frac{1+i_r+r_p}{1+i_r+i_b}\right]^n - 1\right] \qquad \text{(A2)}$$

For the data of Tables 8.1 and 8.2, equations (A1) and (A2) were laid out in an Excel spreadsheet and present day costs evaluated as given in A4.2.

Different data can be in-put into the grey-shaded cells to reflect given economic conditions and/or prices but all unshaded cells are automatically computed.

A4.2: ENERGY COSTING FOR FIXED SLOPE 200 Wp AND 150 Wp TRACKING PANELS

Capital costs:					**Fixed slope**	**Manual Track**	**Semi auto**	**Auto track**
	SIZE	LOCAL PURCH. PRICE (US$)	QTY.	LOCAL TRANSPORT	DELIVERED COST	150 Wp panel	150 Wp panel	150 Wp panel
Solar Panel	200 Wp	141.6	1	0	141.60	106.20	106.20	106.20
Batteries	105 Ah	121.21	2	0	242.42	242.42	242.42	242.42
Charge Controller	15 A	120	1	0	120.00	120.00	120.00	120.00
Bulbs (LED)	11 W	7	12	0	84.00	84.00	84.00	84.00
Installation Materials	Lot	67	1	0	67.00	67.00	67.00	67.00
Sub Total basics					655.02	619.62	619.62	619.62
Installation labour					30.00	35.00	40.00	40.00
Solar Tracker (materials only)					0	202.02	243.53	271.85
Total capital costs					685.02	856.64	903.15	931.47

Running costs:								
System expected lifespan: years	25							
Expected charger lifespan: years	15							
Expected LED Bulbs Lifespan: years	15							
Expected Battery Lifespan: years	5							
Anticipated general annual inflation rate(%)	6							
Excess alternative investment return rate relative to inflation on general items: e.g. Bank saving interest rates over and above inflation (%)	10							
Annual Maintenance charge as % of initial capital	4	**Running costs**			**System Maintenance costs**			
Anticipated excess price inflation over and above that of general items (%)		**Batteries**	**LED Bulbs**	**Charger**				
		2.5	**-2.5**	**5**	**5**			
	Repl. No.							
Number of replacements expected over entire life time		4	1	1	25			
Present worth of Operational expenses for 1st replacement (US$)	1	173.55	15.2	61.97				
Present worth of Operational expenses for 2nd replacement (US$)	2	124.25	0.00	0.00				
Present worth of Operational expenses for 3rd replacement (US$)	3	88.95	0.00	0.00				
Present worth of Operational expenses for 4th replacement (US$)	4	63.68	0.00	0.00				
Present worth of Operational Expenses: US$		**450.43**	**15.2**	**61.97**	**406.12**	**507.87**	**535.45**	**552.24**
Total Present Worth Capital + Running costs (US$)					**1618.73**	**1892.1**	**1966.2**	**2011.3**
Total Present Worth Running costs (US$)					**933.71**	**1035..5**	**1063.0**	**1079.8**
Total useful energy produced over lifecycle: kWh					**6568.00**	**6600**	**6600**	**6600**
Present worth Running unit energy cost: US$/kWh					**0.14**	**0.16**	**0.16**	**0.16**
Present worth Capital unit energy cost: US$/kWh					**0.10**	**0.13**	**0.14**	**0.14**
Present worth Total unit energy cost: US$/kWh					**0.25**	**0.29**	**0.30**	**0.30**

A5: LARGE FILES: SOFT COPIES ON DISK

A5.1 EXCEL *FILES*

A5.1.1. Weather data for Chapter 3

A5.1.2. Primary data for Chapter 7

A5.2 VIDEO *FILES*

A5.2.1. Some stepped rotations of East to West solar tracking

A5.2.2. Night return of the tracker